MANCHESTER 1824

The University of Manchester

CHARACTERISATION OF THE CHEMICAL PROPERTIES AND BEHAVIOUR OF AEROSOLS IN THE URBAN ENVIRONMENT

A THESIS SUBMITTED TO THE UNIVERSITY OF MANCHESTER
FOR THE DEGREE OF DOCTOR OF PHILOSOPHY
IN THE FACULTY OF ENGINEERING AND PHYSICAL SCIENCES

2014

Dominique E. Young
School of Earth, Atmospheric and Environmental Sciences

Contents

Word Count: 57446

Abstract

CHARACTERISATION OF THE CHEMICAL PROPERTIES AND BEHAVIOUR OF AEROSOLS IN THE URBAN ENVIRONMENT

Dominique E. Young

A thesis submitted to the University of Manchester
for the degree of Doctor of Philosophy, 2014

Atmospheric aerosols have adverse effects on human health, air quality, and visibility and frequently result in severe pollution events, particularly in urban areas. However, the sources of aerosols and the processes governing their behaviour in the atmosphere, including those which lead to high concentrations, are not well understood thus limit our ability to accurately assess and forecast air quality.

Presented here are the first long-term chemical composition measurements from an urban environment using an Aerodyne compact Time-of-Flight Aerosol Mass Spectrometer (cToF-AMS). Organic aerosols (OA) were observed to account for a significant fraction (44%) of the total non-refractory submicron mass during 2012 at the urban background site in North Kensington, London, followed by nitrate (28%), sulphate (14%), ammonium (13%), and chloride (1%). The sources and components of OA were determined using Positive Matrix Factorisation (PMF) and attributed as hydrocarbon-like OA (HOA), cooking OA (COA), solid fuel OA (SFOA), type 1 oxygenated OA (OOA1), and type 2 oxygenated OA (OOA2), where HOA, COA, and SFOA were observed to be of equal importance across the year. The concentration of secondary OA increased during the summer yet the extent of oxidation, as defined by the oxygen content, showed no variability during the year.

The main factors governing the diurnal, monthly, and seasonal trends observed in all organic and inorganic species were meteorological conditions, specific nature of the sources, and availability of precursors. Regional and transboundary pollution influenced total aerosol concentrations and high concentration events were observed to be governed by different factors depending on season. High-Resolution ToF-AMS measurements were used to further probe OA behaviour, where two SFOA factors were derived from PMF analysis in winter, which likely represent differences in burn conditions. In the summer an OA factor was identified, likely of primary origin, which was observed to be strongly associated with organic nitrates and anthropogenic emissions.

This work uses instruments and techniques that have not previously been used in this way in an urban environment, where the results further the understanding of the chemical components of urban aerosols. Aerosol sources are likely to change in the future with increases in solid fuel burning as vehicular emissions decrease, with significant implications on air quality and health. Thus it is important to understand aerosol sources and behaviour in order to develop effective pollution abatement strategies.

Declaration

Candidate Name: Dominique E. Young

Faculty: Engineering and Physical Sciences

Thesis Title: Characterisation of the Chemical Properties and Behaviour of Aerosols in the Urban Environment

I declare that no portion of this work referred to in this thesis has been submitted in support of an application for another degree or qualification of this or any other university or other institute of learning.

Copyright

Acknowledgements

Firstly, I would like to thank my supervisors, Hugh Coe and James Allan, for their guidance, support, and encouragement throughout my PhD. I am incredibly grateful for their time and enthusiasm and could not ask for better supervisors. Despite there only being 24 hours in the day, too few for most and especially for Hugh, he always found time to discuss my work and provided much appreciated advice about my future. I'm eternally grateful to James for so many things including keeping me sane on fieldwork, providing me with much food for thought regarding my work, and teaching me not to be afraid of a bit of DIY.

I would also like to thank the funding bodies that enabled me to do my research over the last four years. This work, including field projects, was funded by the Natural Environment Research Council (NERC) in several ways including my studentship (NE/I528142/1) and the ClearfLo project (NE/H008136/1). I am very grateful for the additional funding provided by Defra for the long-term aerosol measurements.

Many thanks go to everyone from Manchester and beyond who was involved in the fieldwork and various aspects of data analysis including Paul Williams, Dave Green, Michael Flynn, Will Morgan, the CIMS boys, and the York crew. Thanks to everyone from the field and the department both past and present who have become great friends as well as colleagues. There are too many people to list but you know who you are; you have made my time at Manchester a lot of fun and I will always look back on my PhD experience with fond memories.

Special thanks must go to my friends who have stuck by me through the good times and the bad, reminding me it is just as important to relax and play hard as it is to work. I am eternally grateful to Corinne Fay, without whom I probably would not have made it as far as I have during the 8 years since we first met; your friendship means so much.

Finally but definitely not least, I would like to thank my family for always believing in me, for being supportive and caring, and for encouraging me to follow my dreams. Mum, Dad, and Steph: I really would not be where I am today without you.

Chapter 1

Introduction

1.1 Motivation

The association between ambient aerosols and adverse effects on human health has long been recognised (Pope and Dockery, 2006 and references therein). However, the mechanisms by which the effects occur are not well understood owing to the complex nature of atmospheric aerosols. Particulate matter (PM) consists of many different components with a range of chemical compositions, which originate from a large range of sources (Seinfeld and Pandis, 2006). The components of PM therefore exhibit different behaviours and have different impacts. Once emitted into the atmosphere aerosols undergo various physical and chemical transformations resulting in the highly variable concentration, size, and composition of ambient aerosols, both temporally and spatially (Pöschl, 2005). Exposure to particulate pollution is ubiquitous and although the concentration, size, and chemical composition of aerosol particles are all important parameters in determining the health effects (Pöschl, 2005) it is unclear which aspect of aerosols is responsible for the observed adverse health effects (Harrison and Yin, 2000).

In addition to impacts on health, elevated aerosol concentrations are known to contribute to poor visibility and air quality (Watson, 2002; AQEG, 2012), especially in urban areas during the winter due to a combination of meteorological conditions and emissions from anthropogenic activities (e.g. Zhang et al., 2007; Martin et al., 2011). Furthermore, atmospheric hazes frequently affect cities especially in the summer owing to increased photochemistry (Goldstein et al., 2009). Levels of anthropogenic aerosols have been increasing since the Industrial Revolution leading to numerous episodes of severe air pollution including the Great Smog of 1952 in London, which

resulted in approximately 4000 excess deaths (Brunekreef and Holgate, 2002). Several legislative measures have been implemented across local and European regions to reduce emissions with an aim to improve air quality and protect human health. Despite various improvements, poor air quality continues to persist in developed countries and could even be deteriorating (Harrison et al., 2012). A significant proportion of Europe's population currently live in urban areas (EEA, 2010) and as more people are expected to live in cities in the future it is important to understand the sources and properties of aerosols and how they change temporally and spatially to better inform pollution abatement strategies and air quality models.

The Aerodyne Aerosol Mass Spectrometer (AMS) can quantitatively measure size-resolved chemical composition of non-refractory submicron particulates with high time resolution (Jayne et al., 2000; Canagaratna et al., 2007). The AMS has demonstrated its versatility across the world in a range of environments, from rural and remote to urban areas (Zhang et al., 2007) with significant advancements made over the last two decades meaning the AMS is a powerful tool for investigating aerosols and aerosol sources. London suffers from substantial air quality problems (AQEG, 2012) owing to the high emissions from anthropogenic activities from its 8.4 million inhabitants (ONS, 2014). The measurements presented here therefore elucidate the importance of the different components of PM in contributing to air pollution in an area with a high population density. The measurements will concentrate upon the behaviour of aerosols in London including seasonal changes in chemical composition, contribution to the total aerosol burden, as well as the importance of local and transported pollution.

1.2 Atmospheric aerosol properties and life cycle

Atmospheric aerosols are defined as an assembly of solid or liquid particles suspended in a gaseous medium (Seinfeld and Pandis, 2006). Aerosols have both anthropogenic and biogenic sources and are either emitted directly into the atmosphere, termed primary aerosols, or form by gas-to-particle conversion processes in the atmosphere, termed secondary aerosols (Seinfeld and Pandis, 2006). Aerosols are further classified by their chemical composition, whether organic or inorganic. Aerosols have many sources and each aerosol particle possesses different combinations of chemical, microphysical, and optical properties to the next aerosol particle. Consequently, aerosols have a complex nature where a further complicating aspect arises from the fact that aerosols may be present in the atmosphere at a range of concentrations. The effects

aerosols have once emitted into the atmosphere are dependent on their various properties, so the exact impacts of aerosols and the mechanisms by which they occur are not well understood. Furthermore, aerosols transform once emitted into the atmosphere through various atmospheric processes including oxidation, photolysis, and hydrolysis, which result in changes in the properties of aerosols. In order to better understand the potential impacts of aerosols and their severity, each of the properties needs to be considered individually and viewed holistically.

1.2.1 Aerosol sources

In addition to the grouping of aerosols according to whether they are directly emitted or formed in the atmosphere, aerosols can also be classified by origin. Aerosols are emitted from both natural and anthropogenic sources where natural primary aerosols include wind-blown mineral dust from arid land and sea salt particles emitted from the ocean surface as sea spray. Other natural primary aerosols include particulate emissions from volcanoes and biological materials such as pollen (Monks et al., 2009). The primary sources of anthropogenic aerosols include biomass burning, cooking, and the incomplete combustion of fossil fuels (Seinfeld and Pandis, 2006; Jimenez et al., 2009). Primary anthropogenic aerosols can also be emitted as a result of mechanical processes such as the wearing down of vehicle tyres (Thorpe and Harrison, 2008). In addition, vehicle brake lining wear, construction dust, and fragments of road surfaces in urban environments can result in the emission of primary aerosols.

Secondary aerosols are formed from the nucleation and condensation of both biogenic and anthropogenic gaseous precursors in the atmosphere. Such precursor gases include nitrogen oxides (NO_x) from combustion of fossil fuels, sulphur dioxide (SO_2) predominantly from solid fuel combustion, and dimethyl sulphide (DMS) from phytoplankton emissions. Secondary organic aerosols also form from the condensation of volatile organic compounds (VOCs) which have both biogenic and anthropogenic sources such as vegetation and combustion, respectively.

1.2.2 Particle sizes and mode classifications

In the atmosphere, the size distributions of aerosol particles span several orders of magnitude although they can be crudely split into three groups: ultrafine particles with a diameter less than 100 nm; fine particles with a diameter less than 2.5 μm and coarse particles with a diameter greater than 2.5 μm. Particles of various sizes frequently

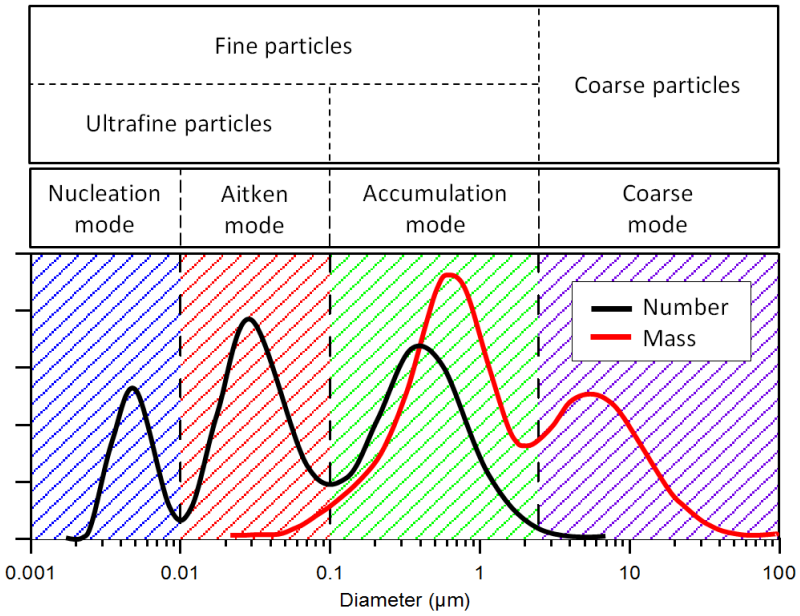

Figure 1.1: An illustration of particle number and mass distributions for the different particle sizes and modes. Figure adapted from Heintzenberg et al. (2003) and Seinfeld and Pandis (2006).

form discrete modes in the atmosphere. Consequently, these groups can be further classified by four modes where fine particles encompass three of these modes (Figure 1.1). Particles with a diameter less than 0.01 μm are referred to as 'nucleation mode' particles, the 'Aitken mode' includes particles with a diameter between 0.01 - 0.1 μm, and the 'accumulation mode' includes particles with a diameter between about 0.1 - 2.5 μm. Finally, the coarse mode includes particles with a diameter greater than 2.5 μm (Heintzenberg et al., 2003; Seinfeld and Pandis, 2006). Although this grouping is relatively simple, the distinction between the modes is important due to the varying origination of the aerosols, their transformations, mode of deposition, chemical composition, optical properties, and therefore the different impacts they have on both climate and human health (Seinfeld and Pandis, 2006).

Particles in the nucleation mode are formed as a result of gases having recently undergone nucleation (Heintzenberg et al., 2003) where fresh particles are formed from the nucleation of atmospheric species (Seinfeld and Pandis, 2006). Coagulation with larger particles causes the majority of losses of nucleation mode particles from the troposphere.

Aitken mode particles are formed as a result of the coagulation of nucleation mode

particles. They can also be formed from primary emissions during combustion processes. In general, when the Aitken and nucleation modes are grouped together it is typically found that they include the majority of the number of particles in the atmosphere. However, their contribution to the total mass of airborne particles is minor due to their small size.

Accumulation mode particles are formed as a result of the growth of existing nucleation and Aitken mode particles, which occurs due to condensation onto these particles (Seinfeld and Pandis, 2006). Coagulation of smaller particles also results in the formation of accumulation mode particles. Chemical reactions in cloud droplets form particle mass and thus contribute to the accumulation mode particles (Heintzenberg et al., 2003). Accumulation mode particles tend to remain in this mode as they are not removed from the atmosphere as efficiently as other modes and growth to larger particle sizes is slow. Therefore, the lifetime of particles in the accumulation mode in the atmosphere is significantly longer than those in other modes. A significant proportion of the number distribution in the atmosphere is accounted for by particles in the accumulation mode.

Coarse mode particles are generally formed as a result of mechanical processes such as the mechanical break-up of bulk material. Although coarse mode particles account for a significant proportion of the total aerosol mass, such particles are present in the atmosphere in very low numbers. Furthermore, due to their size, and therefore large sedimentation velocities, coarse mode particles settle out of the atmosphere over a short timescale of a few hours to days. Examples of particles that exist in the coarse mode include anthropogenic aerosols and natural dust particles (Seinfeld and Pandis, 2006).

Particulate matter (PM) is a mass-based metric predominantly used in air quality studies. PM is categorised using the aerodynamic diameter, which describes the aerodynamic behaviour of the particle as if it were a unit-density sphere with an equal diameter as that of the particle of interest (WHO, 2005). PM_{10} is used to describe particles with a diameter less than 10 μm and $PM_{2.5}$ represents those particles with a diameter less than 2.5 μm. PM_1 is also sometimes used, however in most health policies and guidelines PM_{10} and $PM_{2.5}$ are used as the main indicators for certain sized particles.

The aerodynamic diameter is used as the associated properties determine how far the particle travels, how it is removed from the atmosphere, and how far it penetrates

human respiratory tracts (WHO, 2005). Ambient PM pollution levels deemed acceptable are generally based on the PM_{10} and $PM_{2.5}$ indicators (Pope and Dockery, 2006). PM_{10} is used to indicate those particles which are of a size that can be inhaled and penetrate the thoracic region of the lung; thoracic coarse particles fall between $PM_{10-2.5}$ and fine particles fall into the $PM_{2.5}$ category.

The overall contribution each of these size fractions has to airborne particle mass differs. The air quality guidelines produced by WHO (2005) state that the chemical composition, source, and physical characteristics of these fractions also all differ, where the source of the pollutants determines the chemical composition.

1.2.3 Aerosol chemical composition

Aerosols can be further classified by their chemical composition and are broadly categorised as being inorganic or organic. Organic aerosols are those which contain carbon whereas those which do not contain carbon are the inorganic aerosols. A recent overview by Monks et al. (2009) stated that PM predominantly comprises organic compounds, black or elemental carbon, nitrate, sulphate, ammonium, mineral species (mostly desert dust) and sea salt. It is estimated that, on average, the total particle mass concentrations range between 1 and 100 μg m^{-3} where each of the chemical compounds contribute approximately 10-30% to this total mass loading (Monks et al., 2009). The dominant components of the submicron particulate mass are inorganic aerosols including nitrate, sulphate, and ammonium and various organic species.

1.2.3.1 Inorganic aerosols

Both nitrate and sulphate are secondary inorganic species as they are formed in the atmosphere from the oxidation of gaseous precursors. The exceptions to this for sulphate are emissions of sea salt containing sulphate and emissions from construction activities involving gypsum (Monks et al., 2009).

Sulphate aerosols are formed from both natural and anthropogenic precursor gases where sulphur dioxide (SO_2) is the dominant anthropogenic precursor from fossil fuel and biomass burning emissions. Natural precursors include SO_2 emitted from volcanoes and dimethyl sulphide (DMS) emitted from biogenic sources such as marine phytoplankton. The oxidation of SO_2 involves hydroxyl radicals (OH) producing sulphuric acid droplets (H_2SO_4) which are subsequently neutralised to form ammonium bisulphate ($(NH_4)HSO_4$) by ammonia. Ammonium bisulphate can be further neutralised

to form ammonium sulphate ($(NH_4)_2SO_4$) depending on the availability of ammonia. Sulphuric acid is preferentially found in the particle phase as it has a very low saturation vapour pressure where the dependency on ammonia availability results in partial or full neutralisation of sulphuric acid particles. Thus sulphate aerosols are present as liquid droplets or in a partly crystallised form (Forster et al., 2007). Sulphate aerosols can also form via aqueous phase reactions within cloud droplets and via condensational growth onto pre-existing particles.

The oxidation of nitrogen oxides (NO_x) in the atmosphere forms nitric acid (HNO_3), where NO_x is emitted from high temperature combustion, as well as from soils, and lightning. Nitric acid is formed during the day when NO_x is oxidised by OH radicals and can also be formed during the night in the absence of solar radiation from nitrate radicals (NO_3), which are formed from the oxidation of nitrogen dioxide (NO_2) by ozone (O_3). Nitrate radicals are also important in forming nitric acid via other heterogeneous reactions such as those involving the uptake of dinitrogen pentoxide (N_2O_5) in cloud water or on particle surfaces (Abdalmogith and Harrison, 2006). Nitric acid tends to remain in the gas phase when there is limited ammonia availability as sulphuric acid is preferentially neutralised. However, if sufficient ammonia is available nitric acid reacts with the excess ammonia to form ammonium nitrate (NH_4NO_3, Equation 1.1), a semi-volatile inorganic salt.

$$NH_3(g) + HNO_3(aq) \rightleftharpoons NH_4NO_3(s) \tag{1.1}$$

Owing to the high saturation vapour pressure of nitric acid, the partitioning from the gas phase to the particle phase is strongly dependent on the availability of the precursor gases ammonia and NO_x as well as the ambient conditions, namely relative humidity and temperature (Ansari and Pandis, 1998). Nitrate aerosols are preferentially found in the particulate phase when temperatures are low and relative humidity is high (Stelson and Seinfeld, 1982). Other forms of nitrate are also present in the atmosphere such as sodium nitrate, formed from the deposition of nitric acid onto sea salt and mineral dust particles, which are typically found in the coarse mode.

Although less abundant in the atmosphere, ammonium chloride is another form of secondary inorganic aerosol which is formed from the reaction of ammonia with hydrochloric acid, which is primarily from the combustion of coal. Similar to ammonium nitrate, ammonium chloride is also semi-volatile. In addition to ammonium chloride, chloride salts are present in the atmosphere, mainly arising from sea salt, where sodium chloride (NaCl) is the major constituent by weight (85%).

1.2.3.2 Carbonaceous species

The carbonaceous fraction of atmospheric aerosols comprises black carbon (BC) and organic carbon where BC is a primary aerosol emitted during incomplete combustion processes and is the light-absorbing component of soot (e.g. Schwarz et al., 2008). The terminology of these particles varies in the literature depending on the measurement techniques used, where definitions are based on particle morphology, optical properties, sources, and chemical composition. Black carbon, elemental carbon, and soot are terms that are frequently used interchangeably although the most commonly used term is BC and is similar to soot carbon in terms of composition and optical properties (Andreae and Gelencsér, 2006).

Organic carbon is a collective term for the other components of the carbonaceous fraction (Quincey et al., 2009) and is a complex mixture of hundreds of carbon-containing compounds. Organic species have both biogenic and anthropogenic sources and can be grouped into primary and secondary organic aerosols (POA and SOA, respectively). In an urban environment, sources of POA typically include cooking, vehicular transport, and solid fuel burning. SOA form from the gas-to-particle conversion of atmospheric oxidation products of volatile organic compounds (VOCs). Goldstein and Galbally (2007) estimate that 10 000-100 000 different VOCs have been measured in the atmosphere and many more may be present. These gas phase organic compounds have a variety of biogenic and anthropogenic sources, leading to a range of properties, including volatility and reactivity, and therefore different propensities to generate SOA.

1.2.4 Aerosol lifetimes and sinks

Once emitted into the atmosphere, aerosols undergo several transformation processes, causing the properties of the aerosol to change. The particle size and composition can alter through chemical reactions, by mixing with each other, through the condensation of vapour species, and by coagulation. Atmospheric aerosols can either be removed from the atmosphere by wet or dry deposition where particle size is an important factor in controlling the lifetime of the aerosol in the atmosphere. Larger particles such as 100 μm sized sea salt particles tend to be removed from the atmosphere relatively quickly through gravitational settling (WHO, 2005). Similarly, mineral dust is also removed through gravitational settling and wet deposition but can have a lifetime of up to two weeks depending on wind speed and can be transported large distances (Seinfeld

and Pandis, 2006).

Wet deposition includes those processes involving precipitation. For example, particles can be scavenged through the formation and removal of cloud condensation nuclei (CCN) whereby the particle is activated in the cloud before being rained out. Activated raindrops can promote diffusion scavenging and larger raindrops can intercept cloud droplets when falling (Kanakidou et al., 2005). The latter process is known as washout whereby atmospheric hydrometeors (airborne water particles) such as rain, snow, cloud and fog drops, scavenge material and transport it to the Earth's surface thus removing it from the atmosphere (Seinfeld and Pandis, 2006). Scavenging can occur both in cloud and below cloud.

Dry deposition is the removal process where aerosols impact with the Earth's surface and is a process which is significant close to the ground. The size of the particle controls the dry deposition velocity of aerosols. For large particles the aerosol mass density is also a factor in determining the deposition velocity. The most efficient removal processes for very small particles are turbulent transport and Brownian diffusion (Kanakidou et al., 2005).

The layer of the atmosphere into which the aerosols are emitted will also determine the residence time of an aerosol; the stratosphere is a much more stable layer of the atmosphere than the troposphere so aerosols have a longer residence time in the stratosphere (one to two years) than in the troposphere (about a week) (Crutzen, 2006). Tropospheric aerosols have relatively short lifetimes due to the two modes of deposition.

1.3 Aerosol effects

Atmospheric aerosols are important constituents of the atmosphere, influencing the biosphere, air quality, human health, and climate. Furthermore, aerosols play significant roles in various chemical and physical processes within the atmosphere. The Earth's climate, various ecosystems, and the hydrological cycle are all known to be affected by atmospheric aerosols through altering the Earth's radiative balance, the deposition of nutrients, toxins, acids, and other material onto soils and crops and into aquatic systems, and through providing surfaces for cloud droplets. As aerosol sources are not uniformly distributed geographically, the atmospheric distribution of aerosols is fairly inhomogeneous meaning these aerosols can have both global and regional effects on climate.

For the first time in history, more than half of the world's population live in an urban area (WHO, 2014). By 2050, it is predicted that 70% of the total population will live in a city (WHO, 2010). In Europe, 80% of the population are predicted to live in a city by 2020 (EEA, 2010). The adverse effects of aerosols on air quality and visibility as well as human health are therefore of principal concern in urban areas, particularly as both the emission rates of aerosols and the number of people exposed to urban pollution are likely to increase into the future.

1.3.1 Air quality and visibility

Air quality describes the state of air pollution and is defined as being the degree to which the air is free of pollutants. In general, the degree to which anthropogenic pollutants perturb the atmosphere is indicated by the state of air quality. However, interactions between anthropogenic and natural emissions including those of biogenic origin also need to be considered as these may have feedbacks with the composition of the atmosphere (Monks et al., 2009). Air quality is assessed through various measurements where poor air quality indicates a high concentration of pollutants, which include both gaseous species and particulate matter. Qualitative assessments of air quality are often made by members of the general public by way of visibility. Visibility impairment is a well understood effect of air pollution whereby the physical and chemical mechanisms leading to the removal of light from a sight path due to the interaction of light with pollutants in the atmosphere have been long established (Watson, 2002). Reduced visibility is associated with atmospheric hazes where the clarity and colour of the air changes depending on the concentration of the pollutants. Furthermore, depending on the properties of the particles some light is scattered and some is absorbed; sulphate aerosols typically scatter light and black carbon absorbs light. However, the exact effects of pollutants from specific sources on air quality are not very well understood.

Some natural events lead to low visibility and poor air quality such as wind-blown dust storms, wildfires, and volcanic eruptions. However, these are episodic so are difficult to include in emissions estimates which are used to predict air quality. However, it is anthropogenic emissions that typically result in the majority of observed haze events.

There has been a long history of air pollution and air quality problems at many locations across the world (Jacobson, 2002). In the 19th and 20th centuries London suffered from many air quality problems but it was only after the Great Smog of 1952 that these issues were addressed through changes in practices and regulations which

included the introduction of the 1956 Clean Air Act. The smogs in London were typically a result of high concentrations of sulphur dioxide and smoke particles (Monks et al., 2009). Smoke Control Areas were introduced across the country where only smokeless fuels are permitted to be burned. Also as part of the Act, the heights of chimneys on power stations were increased, with many power stations being relocated away from cities. In contrast, the smogs in Los Angeles, USA, are often a result of photochemical reactions of primary pollutants emitted from vehicles. The concentration of the formed secondary pollutants is further increased due to temperature inversions which trap pollution within the Los Angeles basin.

The dominating air pollutants in the urban atmosphere changed between the start of the 20th and the 21st centuries, following the change in dominant anthropogenic activity. At the start of the 20th century the burning of coal meant that smoke and sulphur dioxide heavily polluted the atmosphere in urban areas. In the 21st century these pollutants were replaced by the products of fossil-fuelled vehicles (Brimblecombe, 2009). Emissions from vehicles include NO_x, carbon monoxide (CO), VOCs, and PM, which can affect air quality in the source areas (usually urban areas) as well as further afield as these pollutants can undergo long-range transport. In addition, the smaller particles, such as $PM_{2.5}$, are more likely to be transported over longer distances than larger particles (Wilson and Suh, 1997). Consequently, pollution formed in one country may influence the air quality in another. However, their episodic nature and numerous sources means it is difficult to include imported pollution in emissions inventories. Due to increasing urbanisation in more recent times urban air pollution can no longer be considered a local problem as long-range transport now largely determines pollution levels (Fenger, 1999). Thus the limits set as part of European and American air quality standards (Tables 1.1 and 1.2) are likely to be exceeded because of transboundary pollution events.

Despite various improvements, air quality is still an issue in developed countries in Europe and North America, and is a particular problem in less developed countries (Harrison et al., 2012). Pollution levels in China can be several orders of magnitude greater than those experienced by the UK and other European countries, and frequently exceed values in air quality guidelines (Tao et al., 2014). In western Europe, PM_{10} concentrations have changed little since the start of the century (Harrison et al., 2008) despite stricter controls on many anthropogenic emissions. The reasons for this are not fully understood, although it could be that there is a shift in the concentrations of individual atmospheric components as emission standards become progressively

more strict. For example, coincident with reductions in the concentration of $PM_{2.5}$ in London between 1998 and 2005, $PM_{2.5-10}$ concentrations increased, which Carslaw et al. (2006) suggest was a consequence of the congestion charge that was introduced in February 2003 as the number of buses increased at this time. Consequently, the limits set as part of European air quality standards for PM_{10} concentrations may not be met despite the reductions in $PM_{2.5}$ concentrations, which are more detrimental to health.

1.3.2 Human health

> "Clean air is considered to be a basic requirement of human health" (WHO, 2005)

The association between adverse health effects and ambient particles has long been recognised (e.g. Pope and Dockery, 2006); for over a century various epidemiological studies have linked air pollution with increasing morbidity and mortality, with substantial progress made since the 1990s. WHO (2005) report that as exposure to PM is ubiquitous considerable health effects from air pollution will be expected to occur in all urban areas and therefore the impact of urban air pollution on human health is of principal concern.

Therefore, in order to protect human health and improve air quality, governments and international organisations have set standards for ambient air quality. For example, the European Union's (EU) Air Quality Directive (2008/50/EC) has set limit and target values of various pollutants, which are set out in Table 1.1. Similarly, the United Sates Environmental Protection Agency has set air quality standards for principal pollutants, where details of the standards for particulates are listed in Table 1.2. Legislation to reduce particle emissions from key sectors such as industry and vehicular transport are also in place. However, in Europe and the USA most official regulations on particulate pollution are based on the mass-based metrics such as PM_{10} and, more recently, $PM_{2.5}$, which refer to PM with aerodynamic dynamic diameters less than 10 μm and 2.5 μm respectively (European Union, 2008). In Europe, the annual mean value for PM_{10} is 40 μg m^{-3} with a daily mean value of 50 μg m^{-3}, which must not be exceeded more than 35 times in a year. Currently, only an annual mean exists for $PM_{2.5}$, which is 25 μg m^{-3} with specific targets to reduce concentrations by 15% at urban background locations across the UK. There are also limits for other pollutants such as NO_2, O_3, and CO with specific objectives for NO_x, SO_2, and O_3 for the protection of vegetation

and ecosystems.

In 2010, the Committee on the Medical Effects of Air Pollutants (COMEAP) reported that life expectancy from birth would increase by 20 days with a reduction in annual average concentration of $PM_{2.5}$ by 1 μg m^{-3}. Furthermore, COMEAP (2010) estimated that life expectancy in the UK would increase by six months if all anthropogenic particulate matter contributing to air pollution was removed. An eight year-long study performed by Schwartz et al. (1996) in six eastern US cities found $PM_{2.5}$ to have the most significant association with increased daily mortality. A 1.5% increase in total daily mortality was found with an increase in two-day mean $PM_{2.5}$ concentration of only 10 μg m^{-3}. The authors did not find any relationship between what they defined as being coarse mass ($PM_{2.5}$-PM_{10}) and mortality. Nawrot et al. (2007) found that the associations between air pollution and adverse health effects are temperature and seasonally dependent with stronger associations in the summer than winter.

WHO (2005) emphasise that the length of time an individual is exposed to air pollution, environmental conditions, as well as personal characteristics determines the susceptibility to air pollution. It is thought that long-term exposure to particles could result in the most severe health effects with the most susceptible groups in the population to the effects of air pollution being those with pre-existing medical conditions as well as the elderly and young (Wichmann and Peters, 2000; AQEG, 2005). Respiratory and cardiovascular effects from both short- and long-term exposures are the primary focus in many studies even though the less severe health effects are likely to dominate the total impact of air pollution on the population (WHO, 2005). Increased cardiovascular mortality has been associated with long- and short-term PM exposure (Pope and Dockery, 2006) where stroke mortality and myocardial infarctions are also associated with short-term exposures. It has been estimated that in the UK 6,500 deaths and 6,400 hospital emissions were brought forward as a result of short-term exposure to PM_{10} levels in 2002 (AQEG, 2005).

Along with $PM_{2.5}$, PM_1 (PM with an aerodynamic diameter less than 1 μm) is receiving greater attention from the air quality and medical communities as these particles can penetrate more deeply in to the lungs where they can remain for long periods of time. Ramgolam et al. (2009) recommended that particular attention should be paid to PM_1 in future regulations due to their potential to cause inflammation. Ibald-Mulli et al. (2002) examined evidence from various studies and concluded that the health effects of fine and ultrafine particles (UFPs) might be independent of each other.

Pollutant	Applies	Objective	Concentration measured as	Date to be achieved by and maintained thereafter	European obligations	Date to be achieved by and maintained thereafter
Particles (PM_{10})	UK	50 μg m^{-3} not to be exceeded more than 35 times a year	24 hour mean	31 December 2004	50 μg m^{-3} not to be exceeded more than 35 times a year	1 January 2005
	UK	40 μg m^{-3}	annual mean	31 December 2004	40 μg m^{-3}	1 January 2005
	Scotland	50 μg m^{-3} not to be exceeded more than 7 times a year	24 hour mean	31 December 2010		
	Scotland	18 μg m^{-3}	annual mean	31 December 2010		
Particles ($PM_{2.5}$) Exposure Reduction	UK (except Scotland)	25 μg m^{-3}	annual mean	2020	Target value 25 μg m^{-3}	2010
	Scotland	12 μg m^{-3}		2020	Limit value 25 μg m^{-3}	2015
	UK urban areas	Target of 15% reduction in concentrations at urban background		Between 2010 and 2020	Target of 20% reduction in concentrations at urban background	Between 2010 and 2020

Table 1.1: Table of National air quality objectives and the European Union's Air Quality Directive limit and target values for the protection of human health.

Pollutant	Primary/Secondary	Averaging Time	Level	Form
PM_{10}	Primary and secondary	24-hour	150 μg m^{-3}	Not to be exceeded more than once per year on average over 3 years
$PM_{2.5}$	Primary	Annual	12 μg m^{-3}	Annual mean, averaged over 3 years
	Secondary	Annual	15 μg m^{-3}	Annual mean, averaged over 3 years
	Primary and secondary	24-hour	35 μg m^{-3}	98th percentile, averaged over 3 years

Table 1.2: Table of National Ambient Air Quality Standards set by the United States Environmental Protection Agency.

Small particles may reach the alveoli within the lungs where they can disrupt the gas-exchange processes, potentially enter the blood stream and subsequently can be distributed throughout the body, causing further damage such as cardiovascular disease (Oberdörster et al., 2005). In addition, Oberdörster et al. (2004) suggest that UFPs are translocated to the central nervous system (CNS) without having entered the blood stream. Instead, the authors propose UFPs are deposited in the respiratory tract and reach the brain via the olfactory nerve, which carries the sensory information for the sense of smell. UFPs may also act as catalysts for reactions with cells due to their large surface area relative to mass (Oberdörster, 2000).

Few epidemiological studies specifically investigate the effects of PM_1 but rather the focus of most studies is on either the fine or ultrafine fractions (commonly defined as $PM_{2.5}$ and $PM_{0.1}$, respectively). Therefore there are currently no standards for PM_1 concentrations for air quality or health. Furthermore, as current legislation focuses on reducing the mass of particle emissions there may be little effect on health outcomes as it is likely that average particle size will reduce as a result of reduced mass, with little effect on the number of particles (Harrison and Yin, 2000).

The size of the particle is not the only property of aerosols that is of concern in relation to health but also the chemical composition. Particle toxicity varies greatly with chemical composition whereby particles comprising heavy metals, organics, and secondary inorganics are toxic when inhaled or ingested (Donaldson et al., 2003). Furthermore, smaller particles are typically composed of these constituents thus are likely to be most detrimental to human health. In particular, UFPs could carry large amounts of adsorbed or condensed toxic pollutants into the body (Oberdörster, 2000). Despite the large geographical variations in the concentration and chemical composition of PM in urban areas around the world there appears to be little spatial variation in the exposure-response functions (Harrison and Yin, 2000).

PM air pollution is a heterogeneous mixture of particles, making research into risks of and exposure to PM difficult. Once emitted into the atmosphere both primary and

secondary forms of PM undergo several chemical physical transformations. Therefore, due to the complexity of fine particles and the ways in which they can be measured the effects on health and the mechanisms by which they occur are not well understood. Furthermore, linking health effects to specific PM characteristics is difficult whereby Harrison and Yin (2000) concluded that there was little evidence for the adverse health effects resulting from a single aerosol property. There is currently no safe level for particulate matter below which no adverse health effects are likely. It could be that a threshold concentration may not exist as health effects are evident even at very low levels of exposure (Brunekreef and Holgate, 2002). Neverthelss, WHO (2005) recommend that exposure of populations to air pollution need to continue to be minimised and air quality needs to continue to be improved. These gaps in scientific knowledge have motivated further research for health, medical, and scientific reasons (Pope and Dockery, 2006).

1.4 Thesis overview

The previous sections have highlighted the importance of pollution, especially due to particulate matter, where the effects of aerosol particles on health and air quality in urban areas are of principal concern. With increasing urbanisation, emissions and thus exposure to pollution are expected to increase and air quality is likely to deteriorate. In order to design and develop cost-effective pollution abatement strategies a greater understanding of the sources and behaviours of the different chemical components of urban pollution is required.

This thesis will utilise both short- and long-term in-situ measurements from an urban background location in the UK to explore the constituents of ambient submicron aerosol. An overview of the instrumentation and techniques used in this thesis, namely the Aerosol Mass Spectrometer (AMS) and Positive Matrix Factorisation (PMF), are described in Chapter 2. Many previous studies have sought to investigate the chemical composition of particulate matter including identifying major components, their sources, trends, and contributions to total mass as well as to pollution events. Such studies have been performed using a number of instruments and techniques, including the AMS and PMF, in a variety of site types at numerous locations across the world for a range of durations. The results and major findings from these measurements are presented in Chapter 3, providing an overview of the current state of knowledge and highlighting the gaps in scientific knowledge. This thesis aims to fill some of

these gaps and address the remaining questions regarding urban pollution, where the results from the ambient measurements performed as part of the Clean Air for London (ClearfLo) project in London are presented in Chapter 4. The sources and behaviour of the different chemical constituents of London's aerosol and resulting impacts on air quality and health are discussed in Chapter 5. In addition, the implications for developing air quality policies through improved measurements and parametrisation of aerosols in numerical models are also highlighted.

Chapter 2

Instrumentation and analysis techniques

The Aerodyne Aerosol Mass Spectrometer (AMS) can quantitatively measure size-resolved chemical composition of non-refractory submicron particulates with high-time resolution, where the particles have a variety of volatilities (Jayne et al., 2000; Allan et al., 2003b; Jimenez et al., 2003; Canagaratna et al., 2007). The AMS is an on-line instrument and has several advantages over many of the traditional methods used to measure the chemical composition of particulate matter (PM) as information on diurnal variability and chemical history or source can be gleaned from measurements. The AMS has demonstrated its versatility in a range of environments across the world (Zhang et al., 2007) as part of several field and aircraft measurement campaigns as well as laboratory studies (e.g. Ng et al., 2010 and references therein). The AMS is therefore well suited to measurements investigating some of the aerosol properties known to have adverse effects on health, air quality, and climate, where significant advancements made over the last two decades mean the AMS is a powerful tool for investigating aerosols and aerosol sources. Several different versions of the AMS have been developed, which predominantly differ by the type of mass spectrometer employed, where each version aims to further improve the sensitivity and time resolution of the AMS. The original AMS uses a quadrupole mass spectrometer (Q), producing ensemble average data of the sampled aerosol, whereas time-of-flight (ToF) mass spectrometers are used in later versions, producing complete mass spectral data for each extraction. The three main versions of the AMS currently in use are the Quadrupole AMS (Q-AMS, Jayne et al., 2000), the compact Time-of-Flight AMS (cToF-AMS, Drewnick et al., 2005) and the High-Resolution Time-of-Flight AMS (HR-ToF-AMS, DeCarlo et al.,

2006), where the basic instrument design and mode of operation are the same for all three. The following sections will describe the instrument design and operation, which is common to all three versions. As this work uses data measured by the cToF-AMS and HR-ToF-AMS versions, the technical aspects of these versions will be described and the data analysis techniques will be discussed.

2.1 Instrument design, description, and modes of operation

The AMS comprises three main sections as illustrated in Figure 2.1: the particle beam generation stage, the aerodynamic sizing chamber, and the detection region, which is where the mass spectrometer is located and the particle composition is determined.

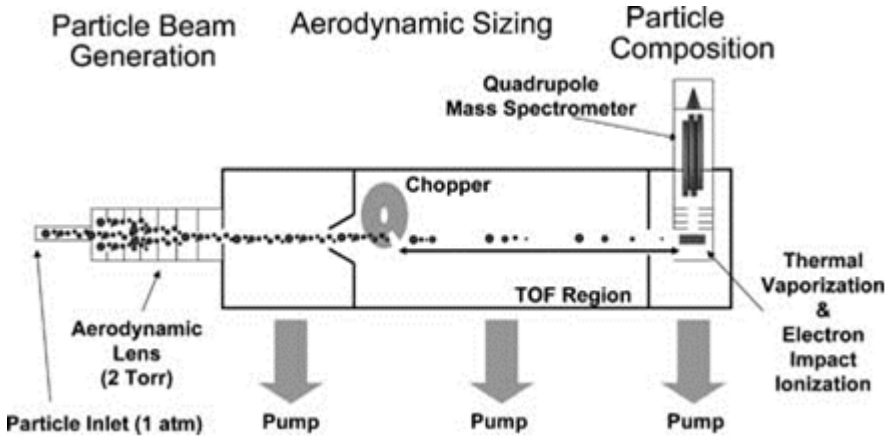

Figure 2.1: Schematic of the Q-AMS, illustrating the three main sections of all versions of the AMS. Reprinted with permission from Canagaratna et al. (2007). Copyright 2007.

In the particle beam generation stage of the AMS, submicron particles are sampled from ambient air by the particle inlet and enter the AMS through the aerodynamic lens, where the particle beam is focused. The flow rate into the AMS is controlled via a critical orifice which is incorporated within the inlet. A critical orifice with a diameter of either 100 μm or 120 μm is typically used depending on the intended use of the instrument, resulting in flow rates of 1.5 cm^3 s^{-1} and 2.0 cm^3 s^{-1}, respectively (Allan et al., 2003b). The critical orifice also acts to reduce the ambient pressure to approximately 267 Pa. An aerodynamic lens system focuses the sampled air into a narrow particle beam though a series of apertures of decreasing diameter (Liu et al.,

1995a,b; Zhang et al., 2002). A combination of passing through each of the apertures and entering the differentially pumped vacuum chamber upon exiting the lens system results in the divergence of the gas phase molecules. The majority of the gas is removed from the sample flow at this stage by a skimmer cone. Consequently, the sampled particles have been focused into a tightly collimated beam which is enriched by a factor of approximately 10^7 compared to the ambient air. However, the gas phase still dominates the mass of the beam rather than the particle phase.

Particles with aerodynamic diameters between 70 nm and 500 nm have been shown by computational fluid dynamic simulations of the inlet system to be transmitted to the detection region with 100% efficiency (Jayne et al., 2000; Zhang et al., 2002, 2004). Furthermore, particles in the ranges 30-70 nm and 500-2500 nm have substantial transmission efficiency where particles smaller than the 30 nm cut-off follow the gas streamlines in the lens system and larger particles are lost to the interior of the lens system. Such transmission efficiencies have been based on the assumption that the particles are spherical, where experimental verification has shown that some non-spherical particles are also well focused by the lens. However, chain agglomerates such as black carbon (BC) and other highly non-spherical particles are unlikely to be focused as efficiently (Liu et al., 1995b). For particles with aerodynamic diameters of 1 μm, the transmission efficiency is approximately 50% in the AMS (Canagaratna et al., 2007).

Once focused into a beam, the particles enter the aerodynamic sizing region of the AMS, which is a vacuum chamber comprising a mechanical chopper. The chopper wheel is a rotating disc with two radial slits positioned 180° apart and is used to modulate the particle beam by being operated in one of three positions. The 'open' position allows particles to pass freely through to the detection region whereas the 'blocked' position completely blocks the beam and is used for background measurements. Finally, the 'chopped' position allows small packets of the particle beam to pass through at a rate of 100-150 cycles per second, which is defined by the user. The chopped position is used to determine the particle's time of flight, which can be related to particle size. Upon exiting the aerodynamic lens, the particles expand into the vacuum chamber where the velocity they acquire is directly related to their vacuum aerodynamic diameter. The time taken for a packet of material to travel between the chopper and the detection region is used to determine the particle velocities. This chamber is therefore also known as the particle time-of-flight section of the AMS (Figure 2.1), where the length of the chamber differs between versions of the AMS. However, for both the cToF-AMS and HR-ToF-AMS used in this study, the chamber length is 0.395 m.

Finally, in the particle composition section of the AMS, where the pressure is less than 10^{-7} Torr, the particles impact upon a resistively heated surface that is typically made from porous tungsten (Figure 2.2). The heater is operated at a temperature of approximately 600 °C, where the non-refractory components of the particle beam flash vapourise on impact. The refractory components, such as black carbon and sea salt, are not measured by standard configurations of the AMS although the Soot Particle AMS (SP-AMS, Onasch et al., 2012), which uses laser vaporisation, has been developed to enable black carbon containing particles to be measured. The tungsten heater is shaped into an inverted cone to also reduce the number of particles that are not vaporised due to rebounding off the heater. The resultant vapour is ionised by 70 eV electron impact (EI) and where significant fragmentation of the molecules can also occur during ionisation due to the high energy of the electrons. However, under vacuum conditions, EI is a reproducible and linear technique for the ionisation of gas phase molecules. Therefore, this fragmentation can be accounted for in the analysis of the data (see Section 2.3.1).

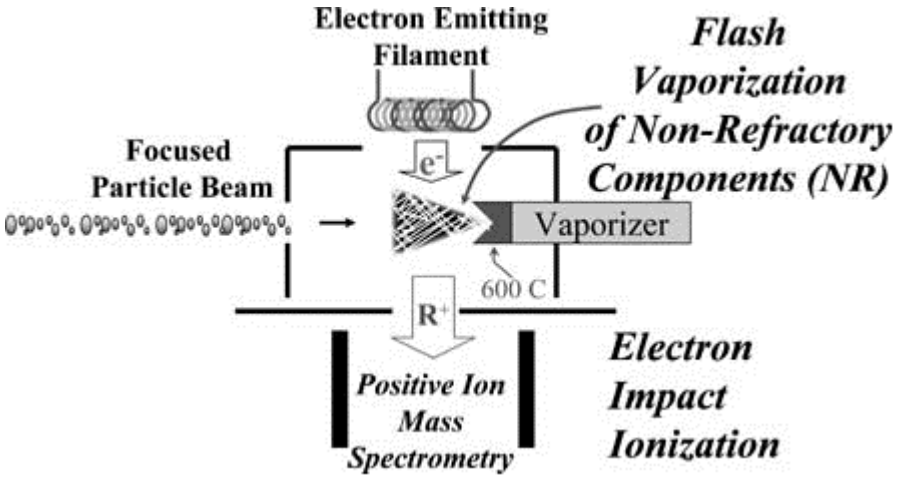

Figure 2.2: Schematic of the AMS detection scheme. Reprinted with permission from Canagaratna et al. (2007). Copyright 2007.

The AMS has two modes of operation: the Mass Spectrum (MS) and Particle Time-of-Flight (PToF) modes (Jimenez et al., 2003). When operated in MS mode, the chopper is alternated between its open and blocked positions. An ensemble averaged MS of the entire sample, including both particle and gas phase species, is obtained when the chopper is in the open position and the background MS is obtained when the chopper is in the closed position. Any contribution from background gases is therefore removed by subtracting the average MS acquired when the chopped is in the blocked position

from the average MS acquired when the chopper is in the open position. The resulting MS can be used to derive quantitative ambient mass concentrations of chemical species. When operated in PToF mode, the chopper is set to the chopped position and averaged size distribution data for an ensemble of particles is obtained. The time at which the aerosol beam passes through the slit in the chopper is recorded using an optical sensor positioned on the chopper mount, which detects when the slit in the chopper is positioned to allow the aerosol beam to pass through. The particle time of flight is the delay time between the aerosol beam passing through the slit in the chopper and its detection in the mass spectrometer. Size resolved chemical distributions are generated from averaging the signals obtained over many chopped cycles using the vacuum aerodynamic diameter (d_{va}) of the particles.

In addition, a third data acquisition mode has been implemented to measure single-particle events. This mode is called the 'Brute Force Single Particle (BFSP) mode', and is similar to the PToF mode except that the multiple chopper cycles are not averaged (DeCarlo et al., 2006). Instead, a single chopper cycle is captured and transferred to the computer. Consequently, there are large amounts of data transferred resulting in a low duty cycle (approximately 3%) thus this mode is typically used for ionisation efficiency calibrations (see Section 2.3.2) rather than ambient measurements.

2.2 Versions of the Aerosol Mass Spectrometer

2.2.1 Compact Time-of-Flight Aerosol Mass Spectrometer

The compact Time-of-Flight Aerosol Mass Spectrometer (cToF-AMS) comprises the three main sections of the AMS as described above, where the air sample enters the instrument and is focused into a collimated particle beam, which is then aerodynamically sized, and finally vaporised and ionised before entering the detection region. A time-of-flight mass spectrometer developed by Tofwerk AG (Thun, Switzerland) is utilised in this version of the AMS. The ions are transported into a time-of-flight extractor after they are vaporised and ionised, where they are then orthogonally extracted by a pulsed high voltage into the time-of-flight section. The time taken between extractions is dependent on the m/z of the ions, where the ion duty cycle increases with the square root of the mass. Each extraction yields a complete mass spectrum as a function of size for individual particles as the extractor is pulsed several times during each particle vaporisation event so has the capability to provide size distributions for all m/z. As the

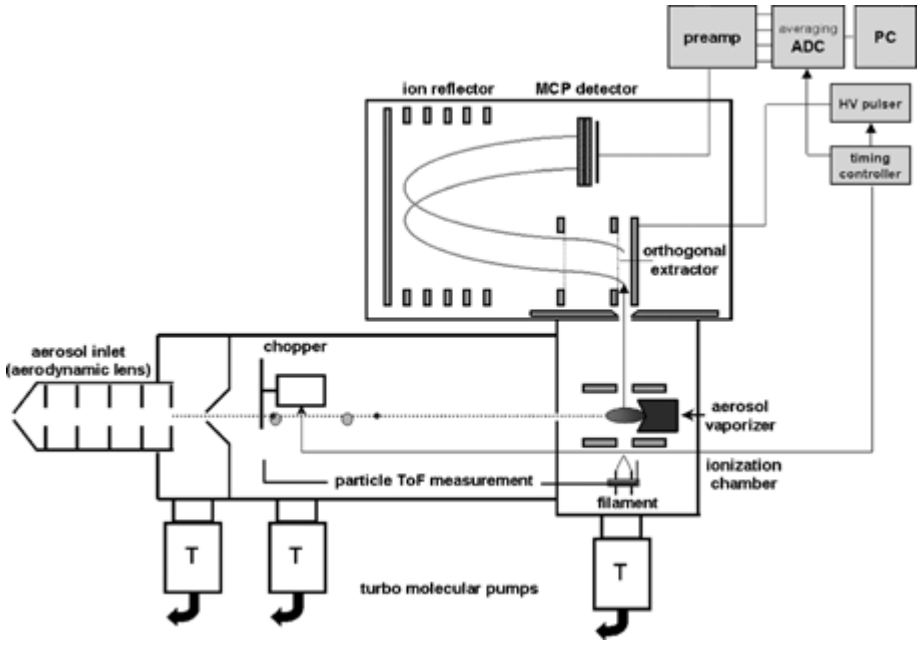

Figure 2.3: Schematic of the cToF-AMS, illustrating the 'C' shaped ion flight path. Reprinted with permission from Drewnick et al. (2005). Copyright 2005.

extraction period is typically 12 μs, approximately 83 300 complete mass spectra can be generated per second. The time-of-flight mass spectrometer has an effective flight path of 430 mm due to it comprising a two-stage gridded ion reflector. The shape of the flight path therefore resembles a 'C' as illustrated in Figure 2.3. The long flight path within the cToF-AMS results in large temporal separation and therefore improves the time resolution and sensitivity of the instrument compared to the earlier version of the AMS, the Q-AMS (Drewnick et al., 2005). Finally, the ions are collected by the electron multiplier detector, which is a multichannel plate (MCP) detector, where the output signal is detected by a data acquisition card and transferred to a personal computer at a rate of 1 GHz.

2.2.2 High-Resolution Time-of-Flight Aerosol Mass Spectrometer

Recently, the High-Resolution Time-of-Flight Aerosol Mass Spectrometer (HR-ToF-AMS) has been developed to further improve the resolution of the AMS (DeCarlo et al., 2006) whereby ions at the same nominal m/z are separated into their specific elemental compositions. The HR-ToF-AMS is the first real-time AMS which is capable of separating inorganic and organic species at the same unit mass as well as quantifying different organic fragments. This is possible due to the fact that the different ions

that contribute to each unit mass peak have small differences in mass defect, where the mass defect is the difference between the exact mass and the nominal mass. As the HR-ToF-AMS has a high time resolution and is field-deployable, it is suitable for studies requiring detailed insight into elemental composition of ambient air with high time resolution.

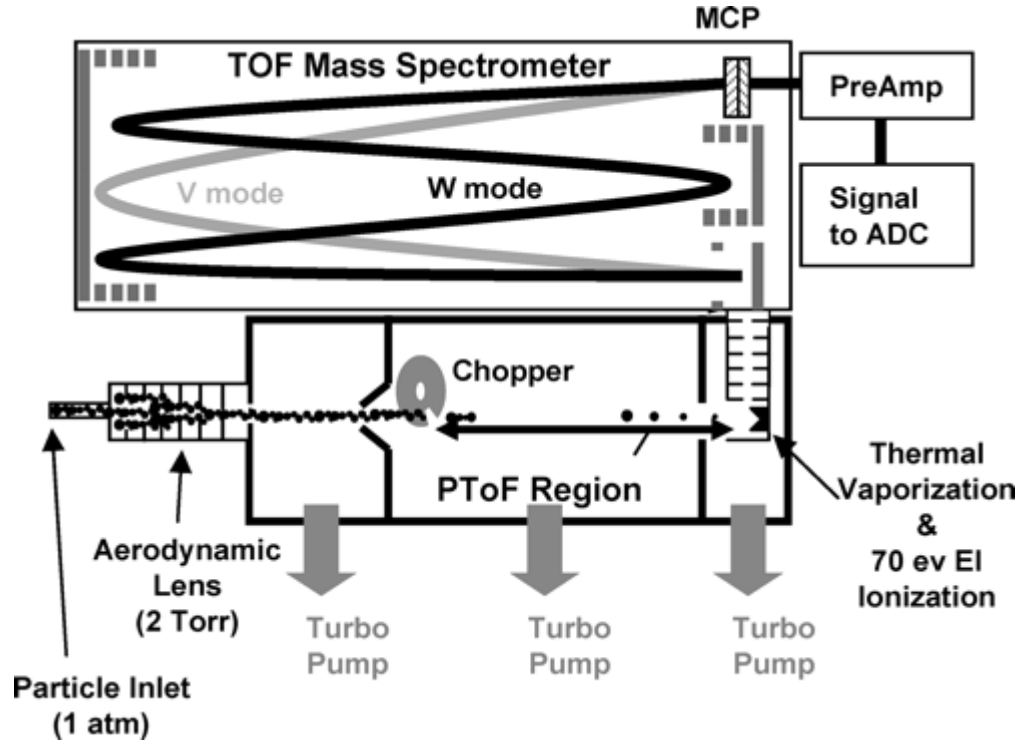

Figure 2.4: Schematic of the HR-ToF-AMS, illustrating the 'V' and 'W' ion flight paths. Reprinted with permission from DeCarlo et al. (2006). Copyright 2006 American Chemical Society.

The HR-ToF-AMS comprises the three main beam generation, particle sizing, and composition regions as the cToF-AMS and uses the same principal modes of operation, which are the MS and PToF modes. The main difference between the HR-ToF-AMS and the cToF-AMS is the length of the effective ion flight path as the former has two ion optical modes offering different sensitivities and resolving power. In 'V' mode, the instrument has a high sensitivity but low resolving power as the ions follow a traditional reflection path from the extraction region with only a single reflection within the mass spectrometer to the MCP detector (Figure 2.4). In contrast, 'W' mode offers a higher resolving power with lower sensitivity due to its two-reflectron configuration where ions are reflected three times by an ion mirror (hard mirror) within the spectrometer thus increasing the effective flight path. The effective ion flight path is 1.3 m

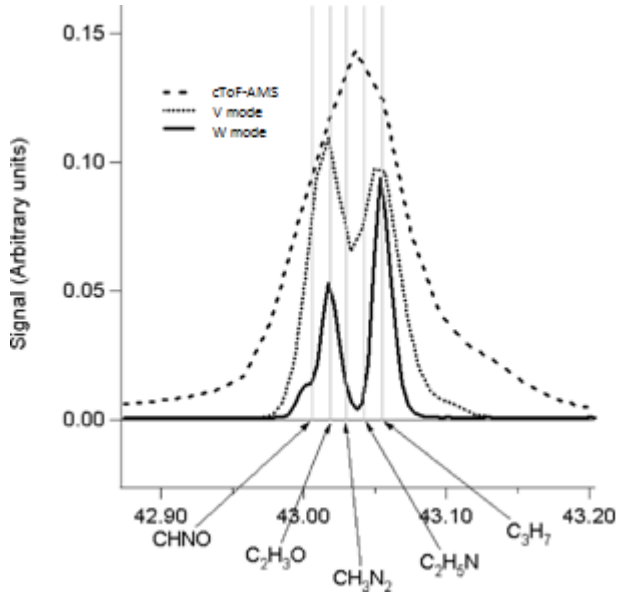

Figure 2.5: Illustration of the resolving power of the cToF-AMS and the two modes of the HR-ToF-AMS, 'V' and 'W', through comparison of the mass spectral signal observed at m/z 43, a common organic fragment. The resolving power increases from the cToF-AMS up to 'W' mode of the HR-ToF-AMS. Figure adapted by Canagaratna et al. (2007) and reprinted with permission from DeCarlo et al. (2006). Copyright 2006 American Chemical Society.

in 'V' mode and 2.9 m in 'W' mode, which is approximately 3 and 6 times longer, respectively, than the path length in the cToF-AMS. The reduction in sensitivity with increasing path length (resolution) results from the lateral broadening of the ions thus fewer ions reach the detector and the total signal is reduced. Consequently there is a trade-off between increased resolution and decreased sensitivity. In comparison to the cToF-AMS which has a resolution of approximately 1000, the resolving power of the HR-ToF-AMS ranges between 2100 and 4300 depending on whether the instrument is operated in 'V' or 'W' mode, respectively (DeCarlo et al., 2006). The resolving power of the cToF-AMS and the 'V' and 'W' modes of the HR-ToF-AMS are compared in Figure 2.5 by way of the different mass spectral signatures from each of the instruments observed at m/z 43, which is a common organic fragment.

2.3 Data quantification

2.3.1 Aerosol chemical composition

The mass spectra of ambient samples consist of both gas and particle phase species, where at any particular m/z there can be contributions from different ions. Furthermore, the thermal energy obtained during vaporisation often results in fragmentation (Allan et al., 2004b), whereby the particles separate out into their constituent ions. Some species such as nitrate have simple fragmentation patterns enabling them to be readily identified in mass spectra (Canagaratna et al., 2007). Table 2.1 summarises some of the key ion fragments and their corresponding masses used to identify aerosol species from AMS spectra, where the chemical species listed are typically detected in ambient aerosol (Allan et al., 2004b). However, as ambient particles are often composed of many individual chemical species which are not separated out prior to being vaporised and ionised, the process of determining the chemical composition of the particles is complex.

Group	Molecule/Species	Ion Fragments	Mass Fragments
Water	H_2O	$\mathbf{H_2O^+}$, HO^+, O^+	**18**,17,16
Ammonium	NH_3	NH_3^+, $\mathbf{NH_2^+}$, NH^+	17, **16**,15
Nitrate	NO_3	HNO_3^+, $\mathbf{NO_2^+}$, NO^+	63, **46**,30
Sulphate	H_2SO_4	$H_2SO_4^+$, HSO_3^+, SO_3^+ $\mathbf{SO_2^+}$, $\mathbf{SO^+}$	98, 81, 80 **64**, **48**
Organic (*oxygenated*)	$C_nH_mO_y$	H_2O^+, CO^+, $\mathbf{CO_2^+}$, $\mathbf{H_3C_2O^+}$, HCO_2^+, $C_nH_m^+$	18, 28, **44**, **43**, 45, ...
Organic (*hydrocarbon*)	C_nH_m	$C_nH_m^+$	27, 29, **41**, **43**, **55**, **57**, 69, 71, ...

Table 2.1: Main inorganic and organic ion fragments used to identify different aerosol species in AMS spectra. The bold text highlights the most useful fragments for identifying such species. Table reproduced and adapted with permission from Canagaratna et al. (2007). Copyright 2007.

Allan et al. (2004b) developed the fragmentation table, which is used in the AMS analysis toolkit software to extract species specific mass spectra. The fragmentation table is a user-defined list containing the contribution of each chemical species at any

given m/z. The table has been constructed using the reproducible dependencies between the relative sizes of the mass spectrum fragments as defined in laboratory experiments. Using this technique, the ensemble mass spectra can be broken up according to the different chemical species, which can be coloured in the mass spectral plots using the toolkit to aid interpretation. Furthermore, this technique has enabled the development of a consistent method across the AMS community for analysing ambient data, which is more thorough and systematic. In addition, other chemical types such as polycyclic aromatic hydrocarbons (PAHs) and chemical markers for combustion sources have been able to be probed and identified as a result of this technique (e.g. Alfarra et al., 2007; Dzepina et al., 2007). Results from various laboratory studies across the AMS community are used to continually update and expand the tables.

2.3.2 Chemically speciated mass concentration

An important aspect of the AMS is the ability to provide quantitative information on ambient aerosols. The following section describes the steps and methodologies used to derive mass concentrations of chemical species from detected ion signals from the mass spectrometer. The various calibrations performed during instrument operation and the processes that need to be accounted for in the calculations are also discussed.

Voltage outputs from the preamplifier ('preamp' in Figures 2.3 and 2.4) are the data acquired by the logging computer and are proportional to the electrical current outputs of the MCP (Figures 2.3 and 2.4). The detected ion rates are derived by dividing the electrical current outputs by the average single ion strength. The single ion strength is determined as part of the daily calibrations performed during measurement campaigns whereby the particle beam is blocked by setting the chopper into the appropriate position, allowing single ions to be distinguished from the background gas phase material and measured. The peaks from the individual ions are averaged to give the average single ion strength, which depends on the gain of the MCP as well as the preamplifier. The gain of the MCP deteriorates with use, where the sensitivity is assessed during the daily calibrations allowing the MCP voltage to be adjusted when necessary to maintain an appropriate level of gain.

The following formula, presented by Jimenez et al. (2003) is used to convert the detected ion rates (I, in Hz) into ambient mass concentrations (C, in μg m^{-3}):

$$C = I.\frac{1}{IE}\frac{1}{Q}\frac{MW}{N_A}.10^{12} \tag{2.1}$$

where MW is the molecular weight of the parent species (in g mol^{-1}), IE is the ionisation efficiency, Q is the volumetric flow rate into the instrument (in cm^3 s^{-1}), N_A is Avogadro's number (6.023×10^{23} mol^{-1}), and the factor of 10^{12} is used to convert from g cm^{-3} in to μg m^{-3}. Equation 2.1 is used to calculate the mass concentration at a specific m/z. In order to calculate the total mass concentration for species that produces multiple ions at multiple m/z's, the ion signals for each of mass fragment are summed as follows:

$$C_s = \left(I.\frac{1}{IE_s}\frac{1}{Q}\frac{MW_s}{N_A}\sum_{alli} I_{s,i} \right).10^{12} \tag{2.2}$$

where the subscript i denotes the mass fragments of the specific species, s. The ionisation efficiency (IE) is a species specific dimensionless quantity defined as the number of ions detected by the MCP per molecule of the parent species (e.g. Allan et al., 2003b). The IE reflects the probability that a sample particle is ionised, efficiently transmitted through the mass spectrometer and detected by the MCP.

Aerosol particles are complex, meaning that IE quantification is very difficult due to it being species specific. Furthermore, as there are a huge number of species present in the atmosphere, especially molecular organic species, it is not possible to calibrate the IE_s for every single species. As nitrate (NO_3) is efficiently volatilised (close to 100%) upon impact with the vaporiser, the IE of nitrate is calculated and is therefore used as a reference framework for other molecules. IE_{NO_3} is regularly calculated during AMS operation from routine calibrations using a well-tested experimental methodology (e.g. Jayne et al., 2000; Allan et al., 2003b; Jimenez et al., 2003). Ammonium nitrate (NH_4NO_3) particles are generated from a nebulizer from a solution of ammonium nitrate salt dissolved in deionized water, which are then dried. The resulting particles are subsequently size selected by being passed through a Vienna design differential mobility analyser (DMA, Winklmayr et al., 1991). A mobility diameter of 350 nm is usually selected as ions of this size are reliably distinguished and counted. As the diameter of the calibration particles has been pre-selected, and the density (1.725 g cm^{-3}) and Jayne shape factor (0.8, Jayne et al., 2000) for ammonium nitrate are known, the average mass of the particles entering the AMS can be determined and the number of parent molecules can therefore be estimated. The number of ions detected by the MCP is obtained by averaging the integrated signal pulse produced by single particles in the instrument, where the majority of the nitrate signal is produced at m/z's 30 and 46. The IE of nitrate can then be calculated by comparing the

number of ions detected with the number of molecules in the calibration sample and the efficiency of particle transmission in the AMS is verified through comparison with a condensation particle counter (CPC, e.g. Wiedensohlet et al., 1997). By running the AMS in PToF mode, particles with aerodynamic diameters that are too large can be rejected during post processing of the calibration as these are likely multiply charged particles and are to be removed from the analysis.

Assuming that the ionisation cross section of the parent molecules is proportional to the number of molecules present and that the ionisation cross section is proportional to the molecular weight (MW_s) of the species (Jimenez et al., 2003), the ionisation efficiency of a particular chemical species can be determined (IE_s). The IE of these other chemical species is derived using the IE_{NO_3} calculated by the described calibration method in the following calculation:

$$\frac{IE_s}{MW_s} = RIE_s \frac{IE_{NO_3}}{MW_{NO_3}} \tag{2.3}$$

where RIE_s is defined as the relative ionisation efficiency of a specific species, s, relative to nitrate (Alfarra et al., 2004). The RIE is determined by laboratory experiments or from individual IE calibrations of specific species. Finally, substituting Equation 2.3 into Equation 2.2 results in the generalised method for calculating mass loadings:

$$C_s = \left(\frac{1}{RIE_s} \frac{MW_{NO_3}}{IE_{NO_3} Q N_A} \sum_{alli} I_{s,i} \right) .10^{12} \tag{2.4}$$

The RIE values typically used in AMS calculations to determine ambient concentrations of organic molecules, and NO_3, sulphate (SO_4), and ammonium (NH_4) moieties are 1.4, 1.1, 1.2, and 4, respectively. The RIE for nitrate is not equal to 1, as may be expected, due to additional nitrate ions such as m/z 14 for nitrogen and m/z 63 for nitric acid which are not included in the calculations described above as m/z 30 and m/z 46 produce the largest signals. Recently, the RIE for SO_4 has been identified as being less stable than originally thought. The stability of the default RIE value for organic molecules is also currently under investigation. Therefore ammonium sulphate calibrations are becoming standard practise along with ammonium nitrate calibrations during measurement campaigns in the field and laboratory. Ammonium sulphate calibrations are performed using the same methodology as that for ammonium nitrate, where the sulphate RIE is calculated using molar ratios of SO_4 and NH_4. The NH_4 RIE also varies depending on the instrument (Canagaratna et al., 2007) as well as ambient

conditions thus can be adjusted accordingly following ammonium nitrate calibrations by comparing the molar ratios of ammonium and nitrate.

The MCP degrades over time, resulting in a reduced signal from the detected ions. As the IE depends on the MCP gain, it is therefore important to correct for the MCP degradation, especially when viewing time series of the data. This is done by way of an airbeam correction in the post processing analysis of AMS data based on the assumption that the degradation for all parent species present in the sample should be uniform (Allan et al., 2003b). If the magnitude of the ion signal did not decrease with time, the signals of m/z's 28 and 32 would be constant in ambient air, so any reduction in their signal strength results from changes in instrumental performance. These signals correspond to the mass spectrum peaks of nitrogen (N_2^+) and oxygen (O_2^+), respectively and are the largest signals within the air beam. Using the signals of these two ions, a time dependent correction factor can be calculated and applied to the data. The flow rate of the airbeam into the instrument also changes due to changes in ambient temperature and partial blockages of the pinhole so is included in the correction.

An additional factor that needs to be taken into account when quantifying the aerosol mass loadings as measured by the AMS is that only a fraction of the particles which enter the instrument are successfully transmitted through the instrument, vaporised, and detected. The collection efficiency (CE) of the AMS can be evaluated to describe the efficiency to which the particles entering the instrument are detected. Particles which do not reach the vaporiser are lost in the instrument through deposition in the interior of the aerodynamic lens or due to divergence of the aerosol beam. Furthermore, some particles bounce off the vaporiser itself. The CE accounts for all the detection losses within the instrument and for a given particle size and type is expressed as

$$CE(d_{va}) = E_L(d_{va}).E_s(d_{va}).E_b(d_{va}) \tag{2.5}$$

where E_L is the transmission efficiency of the inlet and aerodynamic lens for spherical particles, E_s accounts for the broadening of the particle beam due to irregular shaped particles, and E_b accounts for losses at the vaporiser surface due to bouncing, thus describes the detection efficiency of the particles which impact upon the vapouriser (Huffman et al., 2005). Particle size, design of the lens, operating pressure, and particle phase have been shown to be factors that influence the CE, where particle non-sphericity only results in small losses (Huffman et al., 2005; Quinn et al.,

2006; Salcedo et al., 2007). Various measurements have suggested that the CE is significantly affected by particle phase, where the degree to which a particle bounces upon impact with the vaporiser is a function of the particle phase (Allan et al., 2004a; Matthew et al., 2008). The relative humidity of the sampling line, organic liquid and ammonium nitrate contents, as well as the acidity/neutralisation of the sulphate content can influence the particle phase in the AMS (Allan et al., 2004a; Quinn et al., 2006; Weimer et al., 2006; Crosier et al., 2007; Matthew et al., 2008; Middlebrook et al., 2012).

When CE is included in the calculations to determine mass, Equation 2.4 becomes

$$C_s = \left(\frac{1}{RIE_s} \frac{MW_{NO_3}}{IE_{NO_3} QN_A} \sum_{alli} I_{s,i} \right) . \frac{10^{12}}{CE_s} \tag{2.6}$$

Although applying an average CE of 0.5 to whole datasets has been deemed valid for measurements from most ambient environments, a composition- and time-dependent CE has been found to be more appropriate when characterising individual pollution events. Middlebrook et al. (2012) therefore created an algorithm to estimate the CE of the AMS which improved the quantification of mass concentrations compared to when the default value was used. Significant improvements in the mass concentrations were therefore found if the composition-dependent CE was applied to the datasets when particles were believed to be acidic or contain large amounts of nitrate.

The CE is validated by comparison with external measurements, where the AMS volume concentration is typically compared to that of size distribution instruments such as the differential mobility particle sizer (DMPS, e.g. Williams, 1999; Williams et al., 2007) or scanning mobility particle sizer (SMPS e.g. Wang and Flagan, 1990). The volume concentration of the AMS is estimated using the assumed bulk densities for organic and inorganic species reported by Cross et al. (2007) of 1.27 g cm^{-3} and 1.77 g cm^{-3}, respectively. The mass loadings can therefore be calculated by including the inverse of the CE in Equation 2.4.

2.3.3 Particle size

In addition to knowing the chemical composition mass of particles, it is useful to know how the mass is distributed as a function of aerodynamic diameter. The aerodynamic diameter is defined as the diameter of a sphere of unit density (1 g cm^{-3}) that would reach the same terminal velocity during sizing as the particle of interest. In order to determine size distributions, a velocity calibration must be performed that relates the

particle velocities determined in the PToF region of the AMS to their aerodynamic diameter in the following formula:

$$v_p = \frac{L_c}{t_p} \tag{2.7}$$

where v_p is the particle velocity, L_c is the length of the particle flight chamber, and t_p is the time of flight of the particle. The particle velocity prior to the acceleration through the nozzle is included in this equation to account for the majority of the acceleration occurring at the nozzle. Therefore Equation 2.7 becomes

$$v_p = \frac{L_c}{t_p} = \frac{v_g - v_l}{1 + \left(\frac{D_{va}}{D^*}\right)^b} + v_l \tag{2.8}$$

where v_g is the velocity of the gas upon leaving the nozzle, v_l is the velocity of the gas within the aerodynamic lens, and D^* and b are constants determined during the calibration. The calibration procedure is described in Jayne et al. (2000) and is performed using polystyrene latex spheres (PSLs), which are standard calibration particles of accurately known size, density, and shape. A range of PSLs are typically used to calibrate for the range of particle sizes measured by the AMS, where the calibrations are performed at least once during measurement campaigns. The size distributions can then be determined by inputting the variables from Equation 2.8 into the data acquisition software, where the size distributions are mass-weighted (dM/dlogd_{va}) as the AMS signal is proportional to particle mass.

2.4 Positive Matrix Factorisation

The Positive Matrix Factorisation (PMF) model was first developed by Paatero and Tapper (1994) and later refined by Paatero (1997). PMF is applied to measured data in order to further probe the chemical constituents and investigate potential sources. PMF is based on mass conservation and is classed as a receptor-only factorisation model as no a priori information regarding factor profiles or time trends is required in order to derive a solution. The measured dataset which PMF is applied to is assumed to comprise a linear combination of factors with constant profiles, where the contributions of the factors vary across the time of the dataset. For AMS data the constant source profiles are the mass spectra and the contributions are the derived time series. The profiles and contributions are constrained to have positive values within PMF so that

the derived solution is physically meaningful. Lanz et al. (2007) first applied PMF to aerosol mass spectra where Ulbrich et al. (2009) further standardised the technique of the application of the PMF model to organic AMS data.

In index notation, the bilinear unmixing model is defined as:

$$x_{ij} = \sum_{p} g_{ip} f_{pj} + e_{ij} \tag{2.9}$$

where i refers to the row and j refers to the column indices in the matrix of the measured data set and p is the number of factors in the solution. x_{ij} is the signal of the ion fragment j at time step i, g_{ip} is the concentration of factor p at time step i, and f_{pj} is the fractional contribution of ion fragment j in the mass spectrum of factor p. e_{ij} describes the residuals. The time series of a factor (g_p) is represented by a column vector and the row vector represents the mass spectrum for that factor (f_p).

In matrix form, Equation 2.9 can be written as:

$$\mathbf{X} = \mathbf{GF} + \mathbf{E} \tag{2.10}$$

where $\mathbf{X}$ is the measured data set, $\mathbf{G}$ is the matrix of the contributions of each of the factors, $\mathbf{F}$ is the matrix of constant profiles (mass spectra), and $\mathbf{E}$ is a matrix of the residuals. For AMS data, $\mathbf{X}$ is a $m \times n$ matrix where m are rows of ensemble average mass spectra and n are columns of the time series of each m/z sampled. $\mathbf{G}$ is a $m \times p$ matrix where p are the factor time series and $\mathbf{F}$ is a $p \times n$ matrix where n are the mass spectra of the factors. As each of the AMS mass spectra are normalised to 1, the time series have units of mass concentration which is usually μg m^{-3}. $\mathbf{E}$ is an $m \times n$ matrix, which contains the residuals for each experimental data point which were not fit by the model so that **E=X-GF**. The smallest residuals signify that a greater proportion of the measured data set has been explained by the factors derived through PMF analysis. The model uses a least-squares algorithm to iteratively fit the values of $\mathbf{G}$ and $\mathbf{F}$ to the data. This acts to minimize the quality of fit parameter, Q, which is defined as:

$$Q = \sum_{i=1}^{m} \sum_{j=1}^{n} (e_{ij}/\sigma_{ij})^2 \tag{2.11}$$

where σ_{ij} is an element of the $m \times n$ matrix of estimated errors, in the form of standard deviations, of the points in the data matrix, $\mathbf{X}$. Q is used to determine the quality of fit of the PMF solution for the chosen number of factors to the data. The number of free parameters fitted to the data subtracted from the number of data values

is represented by expected Q (Q_{exp}) and can be described as representing the degrees of freedom of the fitted data (Paatero et al., 2002) such that

$$Q_{exp} = (nm) - p(n+m) \tag{2.12}$$

If the value of Q/Q_{exp} is 1 then the model is appropriate and the estimation of the data uncertainties is accurate thus the solution set accounts for the variance associated with random errors. Q_{exp} is therefore approximately equal to nm i.e. the number of data values in the matrix (Ulbrich et al., 2009). An underestimation of the errors in the data i.e. variance unaccounted for by the solution set, is indicated by values of Q/Q_{exp} greater than 1. Conversely, values less than 1 indicate an overestimation of the errors of the input data. As the degrees of freedom increase when the number of factors is increased, Q is expected to decrease as more of the data should be able to be fitted.

As the number of factors, p, in the real dataset are unknown, several criteria are used to select the appropriate number of factors from the model. This is the most subjective part of PMF analysis and is the most critical decision in order to fully interpret the results. In order to choose the best modelled number of factors there are diagnostics within the PMF analysis toolkit, which can be used to assess the quality and suitability of a solution set. For example, the mathematical criterion Q can be used to choose the solution set based on the assumption that significantly more of the variation in the data is likely to have been explained when another factor has been considered and coincides with a large decrease in Q. However, there may be several local minima in the Q value so additional solution sets have to be explored. The stability of a solution set can be explored by starting PMF analysis using different random initial values, or seeds. The most stable solution is one in which the factors derived from PMF do not vary significantly with seed in terms of their contribution so the results do not depend on the starting value.

An additional aspect that must be borne in mind when exploring the solution sets is that there may be linear transformations or "rotations" of the solution (Paatero et al., 2002). In such circumstances, the PMF solutions are non-unique whereby different combinations of factor time series and mass spectra result in an identical fit to the data. In such circumstances,

$$\mathbf{GF} = \mathbf{GTT}^{-1}\mathbf{F} \tag{2.13}$$

where $\mathbf{T}$ is a transformation matrix and $\mathbf{T}^{-1}$ is the inverse of the transformation matrix. An infinite number of rotations may exist and yet the constraint of non-negativity could still be met, which can significantly complicate the process of identifying the most suitable solution. The fPeak parameter can therefore be used to explore ambiguity in a solution due to such rotational freedom whereby throughout the iteration process, rotations are imposed on the emerging solutions. This results in alternative solutions which also satisfy the convergence criteria but may also produce a higher value of Q. Variation of the solutions demonstrated through use of fPeak parameter can indicate the amount of rotational ambiguity present (Paatero et al., 2002). Positive fPeak values result in variations in the mass spectra of the solutions whereas variations in the time series result from using negative fPeak values. However, Paatero et al. (2002) do not recommend the use of non-zero values of fPeak for environmental data as the solution at fPeak of zero is most likely to be physically meaningful.

The true, or best, solution cannot be determined explicitly from using the fPeak parameter or the other metrics described above, particularly as the solution set that is atmospherically realistic and the solution set with the number of factors resulting in a value of Q/Q_{exp} closest to unity may not be the same. Therefore, the solution is validated with external parameters, both reference mass spectra and other measurement parameters.

Chapter 3

Previous aerosol composition measurements

Aerosol particles are ubiquitous in the atmosphere yet their sources are not fully understood. It is therefore important that ambient aerosols are correctly apportioned into their sources and components, particularly as accurate source apportionment of particulate matter (PM) is fundamental to the development of effective schemes to reduce pollution. This is especially true in locations where limit values for PM mass concentration set in air quality legislation are frequently exceeded.

The majority of the information used to design aerosol emission abatement strategies and assess the state of air quality comes from measurements obtained at various sites within monitoring networks. Several air quality programmes and monitoring networks are currently in operation in the United States (e.g. the Interagency Monitoring of Protected Visual Environments (IMPROVE) programme and the State and Local Air Monitoring Stations (SLAMS) network) and Europe (e.g. the European Monitoring and Evaluation Programme (EMEP) and the Aerosols, Clouds, and Trace gases Research Infrastructure (ACTRIS) network). Various aerosol properties are measured as part of the IMPROVE and EMEP programmes at sites that are representative of the regional background (Collaud Coen et al., 2013). Localised networks also exist within these larger programmes such as the Automatic Urban and Rural Network (AURN) introduced in 1992, which is the UK's largest automatic monitoring network, and National Air Monitoring Stations (NAMS), which are part of SLAMS. Several different air pollutants and meteorological parameters are monitored at these sites such as carbon monoxide (CO), nitrogen dioxide (NO_2), sulphur dioxide (SO_2), ozone (O_3), PM,

temperature, wind speed, and wind direction. However, the instrumentation and analysis techniques used at the various stations are highly variable although there have been increased efforts to provide standardised instruments to allow comparisons between the sites. Measurements of the mass-based regulated parameters, PM_{10} and $PM_{2.5}$, are standardised, which allows reliable comparison of the data between different sites. Data from the AURN sites, for example, are used for compliance reporting against the European Union's (EU) Air Quality Directives. However, as discussed in Chapter 1 it is important to understand other aerosol properties, such as particle number and chemical composition, in addition to mass to determine their effects on health and air quality. During the last decade there have been significant advances in the development of instrumentation and techniques to measure the chemical composition of aerosols (e.g. Laj et al., 2009). Therefore, chemical composition data are increasingly becoming available where the United States Environmental Protection Agency have a Chemical Speciation programme and dedicated networks have been introduced to improve the understanding of the composition of PM such as the Particle Numbers and Concentrations Network in the UK. In Europe, secondary inorganic aerosol (SIA) concentrations and trends are monitored and assessed as part of the EMEP programme (Aas et al., 2012).

Aerosols can be classified by chemical composition and whether they are emitted into or formed in the atmosphere, where in-situ measurements enable these properties and processes to be determined. Previous studies highlight the variation in chemical composition with location due to a combination of meteorological conditions and sources. Therefore, long-term measurement campaigns are required to fully characterise aerosols by way of chemical composition, formation processes, behaviour, and subsequent impacts. Such measurements are important for identifying temporal trends both on a short-term basis to identify aerosol characteristics during a particular time period, season, or event and on a longer time basis to observe any effects due to changes in emissions from mitigation strategies, which aim to reduce emissions, or behavioural changes such as urban expansion, which likely results in increased emissions.

The following sections will present an overview of the main chemical components of ambient PM, with a discussion of the methods used to identify components of PM. Chemical composition measurements from long-term studies using various instruments and analysis techniques will be presented. In addition, results from studies which specifically employ the Aerosol Mass Spectrometer (AMS) will be discussed in order to inform and contrast with the work presented in this thesis where the focus is

on AMS measurements. Chemical composition studies have been performed at various sites across the world including urban, urban downwind, and remote locations, with a predominance of campaigns occurring in the Northern Hemisphere. The focus of the following sections however will be on those studies from urban and urban background locations. Finally, the current state of knowledge will be identified and the gaps will frame the themes of the work in this thesis.

3.1 Methods to identify ambient aerosol components

As discussed in Section 1.2.3, aerosols comprise inorganic and organic components, where the focus of many studies is the identification and estimation of the contributions of the constituents of each of these major aerosol species, such as sulphate, nitrate, and primary and secondary organic aerosols.

Many instruments can directly measure individual inorganic components through chemical analyses on filter measurements or from on-line instruments such as the URG Ambient Ion Monitor, the MARGA system, and the AMS. Organic aerosols (OA) comprise many primary and secondary organic species from multiple biogenic and anthropogenic sources thus various methods are employed to separate the different components of OA. For example, filter samples have been used to estimate primary and secondary OA from the elemental carbon and organic carbon ratio (EC/OC) (Turpin and Huntzicker, 1991). Many techniques use the carbon radioisotope ^{14}C to apportion the contributions of fossil and modern carbon sources to PM (Heal, 2014) where Szidat et al. (2006) used $^{14}C/^{12}C$ ratios determined from EC measurements to apportion anthropogenic and biogenic OA.

Over the past decade, several on-line analysis techniques have evolved to complement off-line techniques thus increase the information yielded from laboratory and ambient measurements of aerosols. Real-time instruments based on mass spectrometry or ion chromatography which measure aerosol chemical composition sampling can produce data with reduced sampling artefacts compared to filter measurements (e.g. Laj et al., 2009). Examples of these on-line instruments include single-particle mass spectrometers such as the aerosol time-of-flight mass spectrometer (ATOFMS) and particle analysis by laser mass spectrometry (PALMS) as well as the thermal desorption aerosol gas chromatograph-mass spectrometer (TAG). Lambe et al. (2010) compared the results from filter-based techniques and TAG, finding that despite known issues with both techniques, good agreement was found between most species measured.

In order to determine the sources of PM, techniques such as cluster analysis are employed or measured data are input into various models for further analysis. For example, cluster analysis can be used to identify possible aerosol sources of data measured by single-particle mass spectrometer instruments (e.g. Murphy et al., 2003). Several different methods are used for source apportionment of PM using models, which can broadly be categorised into chemical transport models (CTMs), which are source orientated, and receptor-orientated models (RMs), including source-receptor and receptor-only methods. Russell and Dennis (2000) present a review of air quality models, including a discussion on the models themselves and the modelling process. The receptor models currently used for source apportionment of PM in Europe are discussed in a review by Belis et al. (2013).

The main difference between CTMs and RMs are that the former use emission rates of pollutants and meteorological data to simulate atmospheric transport and chemical reactions (e.g. Pandis et al., 1992; Russell and Dennis, 2000) whereas the latter use statistical analyses of measured pollutant concentrations from a sampling site to determine potential sources and estimate their concentrations (Belis et al., 2013 and references therein). Ambient measurements are input into RMs to perform source apportionment rather than detailed emission inventory data, which are used in CTMs. RMs include approaches based on incremental concentrations, enrichment factors and tracers, as well as mass conservation models such as the Chemical Mass Balance (CMB) model and principal component analysis (PCA). Factor analysis (FA) methods such as Positive Matrix Factorisation (PMF) and hybrid methods are also used. Solving the mass balance problem (Equation 2.9) is common to all multivariate RMs, although the assumptions and data input differ between the methods. For example, CMB depends on the constancy of the source profiles whereas FA methods depend on a uniform variation in the source profiles and other methods assume the source profiles are relatively constant with time. In addition, there are several differences between the RMs in terms of the nature of the input data; atmospheric concentrations of chemical species are reconstructed in CMB using source profiles (Friedlander, 1973), which must be known a priori. OA extracted from filters can be apportioned using molecular markers or trace elements in the CMB model (Watson et al., 1984; Schauer et al., 1996). In contrast, PMF requires no a prior information about time trends or source profiles.

3.2 Main chemical components of atmospheric aerosols

Sulphate is a significant component of the aerosol mass at a number of locations across the world (Zhang et al., 2007) and can contribute more than 25% to the total submicron mass at remote sites as well as some urban locations. This is a result of the activities occurring at those locations, where for example, in China the burning of coal in industry results in large emissions of precursors such as sulphur dioxide (SO_2) and thus high concentrations of sulphate aerosol. In Europe, ammonium nitrate is a significant component of the total aerosol mass, particularly in North-Western Europe under polluted conditions (e.g. Schaap et al., 2002; Putaud et al., 2004; Abdalmogith and Harrison, 2005; Koelemeijer et al., 2006). The difference in dominant species depending on location mainly arises because of the changes in emissions due to various legislative measures and changes in activities/practices in these locations. In addition, the prevailing winds and timescale for formation of the various components also leads to spatial differences in the chemical composition of ambient aerosols.

SIA are typically formed from anthropogenic precursors, most of which are well understood. Reductions in road transport and combustion emissions from power generation because of EU control measures led to a decline in nitrogen dioxide (NO_x) emissions between 1980 and 2009 by 57% (Passant et al., 2011). Over the same period, SO_2 fell by 92% due to reductions in power plant emissions and ammonia (NH_3) emissions declined by 21% (Passant et al., 2011). Between 1990 and 2000, emission reductions of NO_x and SO_2 decreased in Europe, with less pronounced decreases observed in the United States and increases in emissions in Eastern Asia (Monks et al., 2009). In terms of PM concentrations, a comparison of the results from the study by Harrison et al. (2004) with those from a similar urban environment in the UK 20 years earlier suggest the concentrations of sulphate particles have decreased significantly. This is consistent with the reductions in SO_2 emissions. The contributions of sulphate and nitrate aerosols to total mass were subsequently found to be very similar. Future annual projections suggest NO_x and SO_2 will continue to decline towards 2030 but at a slower rate than the previous three decades (Misra et al., 2012) whereas NH_3 does not appear to show any particular future trend. However, in terms of molar units, the data from Misra et al. (2012) indicate NH_3 will be the most abundant SIA precursor by 2020 in the UK. This has important implications for SIA formation whereby reductions in SO_2 emissions ultimately result in greater availability of NH_3 to form particulate ammonium nitrate. In addition, NH_3 emissions vary both temporally and spatially due to the dominant source being agriculture and farming activities (Passant

et al., 2011; NAEI, 2014) and NH_3 emission rates depending on conditions such as temperature and pH (Skjøth et al., 2011). However, the concentrations of SIA respond in a non-linear way to changes in precursor emissions (AQEG, 2012), thus the impacts on SIA formation from changes in precursor emissions, both temporally and spatially, are uncertain and are yet to be fully evaluated (Megaritis et al., 2013).

Organic aerosols (OA) are of particular interest as they can often represent a substantial fraction, and up to 90%, of the total fine particulate mass depending on location (Kanakidou et al., 2005). OA also transform as they undergo atmospheric processing, where for example, increased oxidation and photochemistry can result in the ageing of OA. Organic species can be classified by the way they are emitted, as with all aerosols, whereby primary organic aerosol (POA) is emitted directly into the atmosphere whereas secondary OA (SOA) are formed from the gas-phase oxidation of a number of volatile organic compounds (VOCs) in the atmosphere (e.g. Goldstein and Galbally, 2007). Due to their different origins and formation via different microphysical pathways the chemical composition and the microphysical properties of POA and SOA are different. Furthermore, POA and SOA result in increases in total aerosol mass and number concentrations at different particle size ranges, where POA are of smaller particle size thus are of more concern in terms of health effects. Separation of the organic fraction into its component factors can improve the temporal and spatial characterisation of organic species and OA evolution thus various studies focus on the apportionment of the carbonaceous fraction of PM using various factorisation methods. However, separation of OA into its different components can prove difficult due to the complex nature of OA.

Measurement studies have shown that at various types of sites there is a predominance of SOA over POA (Zhang et al., 2005b, 2007; Lanz et al., 2007). However, there are complications in deriving the contributions of POA and SOA from measurements including the techniques used to estimate the concentrations (e.g. Trivitayanurak and Adams, 2014) where the concentrations between the total OA mass and POA is frequently inferred to be SOA (Castro et al., 1999; Strader et al., 1999; Cabada et al., 2002; Harrison and Yin, 2008). Furthermore, concentrations vary depending on location and season where POA typically dominates the total OA mass during the winter in urban areas (e.g. Allan et al., 2010).

The concentrations and variability of OA observed in the atmosphere have generally been unsuccessfully reproduced in models (de Gouw et al., 2005; Heald et al., 2005; Johnson et al., 2006; Volkamer et al., 2006; Capes et al., 2009) where a greater

contribution from POA to total OA is predicted by some models (Volkamer et al., 2006 and references therein). However, large uncertainty exists surrounding the SOA budget (Kanakidou et al., 2005; Goldstein and Galbally, 2007; Hallquist et al., 2009; Spracklen et al., 2011). Part of this uncertainty arises from the importance of biogenic and anthropogenic precursors where SOA production from biogenic VOCs (BVOCs) was found to be greater than that from anthropogenic VOCs (AVOCs) in some models (Tsigaridis and Kanakidou, 2003). Furthermore, the presence of both anthropogenic and biogenic VOC sources could result in SOA formation from a mixture of the two and potentially influence the total mass produced (Weber et al., 2007) with more mass in polluted regions. However, variations in the sectors emitting anthropogenic VOCs as well as seasonal and speciation changes result in large uncertainties regarding emissions inventories for anthropogenic VOCs (Monks et al., 2009). Similarly, emission rates from sources of biogenic SOA precursors depend on many factors; variations in land use and vegetation type combined with changes in meteorological conditions results in the spatial variation of biogenic VOC emissions across Europe (Guenther et al., 1995; Monks et al., 2009). Discrepancies between measurements and models when estimating the relative contributions of POA and SOA to total OA as well as SOA production highlight the need to better understand the sources, formation, and evolution of the components of OA if we are to accurately predict the concentrations, evolution, and impact of OA on human health, air quality, and climate.

3.3 Previous chemical composition studies

3.3.1 Long-term chemical composition studies

In addition to identifying sources of PM, it is also important to understand the temporal variability in air pollutants in order to inform pollution abatement strategies and assess the effects of air quality on human health. Several factors are known to govern long-term temporal variations in air pollutants such as meteorological conditions and seasonality of emissions. On shorter time scales, anthropogenic activities and transported pollution events (regional or transboundary) can influence the temporal patterns. The importance of these factors will vary spatially as well as temporally.

Ambient measurements from monitoring stations are used to inform air quality policies along with data from specific long-term term studies performed at various sites across the world. As stated in Section 1.3 both the emission rates and the number

of people exposed to urban pollution are likely to increase as we look into the future. Therefore the following section will discuss some of the long-term field measurements which have been performed in urban areas, with a focus on Europe where a summary of the studies are detailed in Table 3.1.

Putaud et al. (2004) present a synthesis of chemical characteristics of PM at a range of sites across Europe over a 10-year period where organic matter (OM) was found to be the major component of both PM_{10} and $PM_{2.5}$, particularly at the kerbside and urban sites. In addition to carbonaceous particles, secondary inorganic particles (nitrate and sulphate) are frequently observed to be dominant components of PM (e.g. Yin et al., 2010; Bressi et al., 2013). Multiple source apportionment models have been applied to long-term datasets to investigate the components of ambient PM. For example, Harrison et al. (2004) used a mass closure method to determine the major components of PM at the urban background sites in Birmingham and London in the UK, finding particles were composed of carbonaceous species, secondary sulphates and nitrates, sodium chloride, and coarse dusts. The sources of these particles were likely combustion, regional transport, soils, building activities, and road traffic. In contrast, Mazzei et al. (2008) performed PMF analysis on a year of daily PM_1 filter samples from an urban background site in Genoa, Italy, in order to characterize local PM. The main components of PM identified from PMF analysis were attributed to soil, secondary compounds, heavy oil combustion, and traffic. Amato et al. (2009) applied PMF and ME-2 to two years of PM_{10}, $PM_{2.5}$, and PM_1 filter samples from an urban background site in Barcelona, Spain. Vehicle exhaust as well as secondary sulphate and nitrate were identified as the dominant components of PM_1 mass from both models. Fuel oil combustion and industrial emissions also influenced concentrations although the exact contributions and compositions of these two factors were uncertain. Other factors were either only identified in larger size fractions or only in one of the models. Comparisons of the results from each of the models can indicate the applicability of such models to datasets of this type, where Amato et al. (2009) comment on the suitability of using multilinear models only when full knowledge of sources is unknown.

Bressi et al. (2013) presented a comprehensive chemical characterisation of $PM_{2.5}$ in Paris, including the temporal behaviour, at both suburban and urban sites between 2009 and 2010. The chemical composition and behaviour at both sites were very similar, where the highest concentrations of $PM_{2.5}$ occurred from late autumn through to early spring with the lowest concentrations in the summer, which were attributable to variations in OM and nitrate concentrations. Although performed over a relatively

Location	Site type	Time period	Duration	Sampling method/ instrumentation	Apportionment technique	Reference
London and Birmingham, UK	Four paired roadside and urban background sites	April 2000 - January 2002	Various within total 21 months	PM_{10} and $PM_{2.5}$ filters	Pragmatic mass closure	Harrison et al. (2004)
Birmingham, UK	Urban background and rural	May 2007 - April 2008	1 year	$PM_{2.5}$ filters	CMB	Yin et al. (2010)
Paris, France	5 sites covering urban, suburban, rural background	September 2009 - September 2010	1 year	$PM_{2.5}$ filters	Chemical mass closure	Bressi et al. (2013)
Lens, France	Urban background	March 2011 - March 2012	1 year	PM_{10} filters	PMF	Waked et al. (2014)
Genoa, Italy	4 sites covering urban traffic, heavy traffic, industrial, and urban background	May 2002 - July 2005	Various within total 3 years	PM_{10}, $PM_{2.5}$, and PM_1	PMF	Mazzei et al. (2008)
Barcelona, Spain	Urban background	2005-2007	2 years	PM_{10}, $PM_{2.5}$, and PM_1 filters	PMF and ME-2	Amato et al. (2009)
Berlin, Germany	Three urban sites with different vegetation influences	February - October 2010	9 months	PM_{10} and $PM_{2.5}$ filters	Tracers and PMF	Wagener et al. (2012b,a)
Helsinki, Finland	Urban background	March 2006 - February 2007	1 year	PM_1 filters	PMF	Saarikoski et al. (2008)
Europe	Kerbside, urban, rural, and background	1991 - 2001	10 years	PM_{10} and $PM_{2.5}$ filters	N/A	Putaud et al. (2004)

Table 3.1: Table of long-term chemical composition studies in urban locations.

short time period of 9 months, Wagener et al. (2012b) determined the seasonal variations of biogenic tracers in Berlin. The combustion product, levoglucosan, was found to exhibit higher concentrations during the months with lower temperatures whereas higher concentrations of secondary compounds occurred during the warmer months. Waked et al. (2014) performed the first source apportionment study in France where PM_{10} inorganic and organic species were combined. Similarly to other northwestern European cities, PM_{10} concentrations were observed to be dominated by OM, nitrates, and sulphates where nine main sources were identified from PMF analysis with a significant influence from biogenic emissions. Secondary nitrate and mineral dust concentrations were found to increase during spring, whereas biomass burning increased during winter and primary biogenic emissions increased during summer.

More recently, studies have sought to further apportion the organic fraction of PM and investigate temporal characteristics as there are many sources yet to be identified and characterised. For example, Yin et al. (2010) used the CMB model to apportion carbonaceous particles at an urban background site in Birmingham, UK. SOA was suggested to be a significant component of OA, as was road traffic. Smaller contributions to total OA mass were from other primary OA sources such as wood smoke, natural gas, coal, vegetative detritus and dust/soil. Organic compounds in Berlin were apportioned using PMF where six sources were identified: combustion fossil, biomass burning, bio/urban primary, bio primary, isoprene-derived SOA, and α-pinene-derived SOA (Wagener et al., 2012a). Biomass burning exhibited seasonal variations, dominating the organic fraction during the cooler months, whereas both SOA factors exhibited a dependence on temperatures. Wagener et al. (2012a) highlighted the implications for adverse health effects, including allergies, from PM concentrations in densely populated urban areas where OA is significantly influenced by biogenic emissions and biomass burning. Similarly, Saarikoski et al. (2008) also identified biomass combustion, traffic, secondary production, and long-range transport as influencing organic carbon concentrations in Helsinki, Finland, from PMF analysis where SOA dominated in summer and biomass burning dominated in winter. The importance of long-range transport in contributing to total PM concentrations in an urban environment as well as to organic carbon concentrations was highlighted in this study.

Long-term measurements also enable temporal variations in the composition of high concentration events to be investigated. In the UK, high pollution events were observed to be governed by increases in secondary particles, carbonaceous particles from traffic, and iron-rich dust concentrations, where nitrate concentrations increased

significantly on days where PM_{10} was in excess of 50 μg m^{-3} (Harrison et al., 2004). Furthermore, Putaud et al. (2004) observed that nitrate concentrations were found to be greater than the concentrations of OM when PM_{10} exceeded 50 μg m^{-3}, where high concentration events frequently occurred during cold periods. Similar observations were made in France (Waked et al., 2014), where large contributions from nitrate and organic matter characterise exceedences and biomass burning, secondary nitrate, and sulphate were important during the cold periods. Furthermore, Bressi et al. (2013) highlight the importance of transported pollution, particularly in contributing to pollution events, which were primarily composed of OM and SIA in Paris. Moreover, Waked et al. (2014) suggest long-range transport may contribute to exceedences where associations between high concentration events in France and continental air masses were observed. Designing efficient emission abatement strategies therefore requires the need to collaborate with neighbouring countries.

Despite the different locations and approaches in the studies discussed and detailed in Table 3.1, the major findings of all the studies show that the main constituents of ambient aerosol are organic or carbonaceous species and SIA, predominantly nitrate and sulphate. Furthermore, the different apportionment models utilised result in the identification of similar sources, with influences from SIA, SOA, and other primary organic sources including traffic, biomass burning, and fossil fuel combustion. Differences in sources identified arise due to influences from local sources, which are specific to the measurement location, the size fraction examined, or the methodologies used including both the instrumentation and factorisation model. SIA precursors are not very well represented in many RMs so can lead to overestimations of the contributions from these components (Belis et al., 2013). Furthermore, the applicability of some measurement techniques is limited as dominant OA components, for example, are often uncharacterised due to the methodology employed (e.g. Huffman et al., 2009; Lambe et al., 2010). For example, SOA estimated using secondary tracers such as some organic acids including pinic acid (Schauer et al., 2002; Zheng et al., 2002; Fraser et al., 2003; Fine et al., 2004; Yin et al., 2014) in the CMB model are not very accurate as only sources with unique markers are successfully identified using this method as CMB depends on the availability of source profiles, thus estimations of POA contributions are more accurate (e.g. Ulbrich et al., 2009; Belis et al., 2013). Furthermore, filter measurements suffer from artefacts and low time resolution as samples are typically collected over 12-24 hour periods. Schaap et al. (2011) indicate the benefits of sampling with high time resolution, such as hourly measurements compared to daily

measurements, which is the standard sampling period for long-term monitoring.

Following a meta-analysis of 243 data sets of different sampling durations, methods, and approaches in Europe, Belis et al. (2013) suggest the uncertainties surrounding estimated source contributions need to be better constrained. Furthermore, more long-term chemical composition measurements are required, particularly in urban areas, to develop and improve the results obtained from studies using RMs for source apportionment. Moreover, source profiles need to be better constrained and understood, which can be achieved through additional measurements.

3.3.2 Aerosol Mass Spectrometer studies

The use of aerosol mass spectrometry techniques developed with the introduction of the Aerodyne Aerosol Mass Spectrometer (AMS) into the scientific community in 2000 (Jayne et al., 2000). As described in Chapter 2, several different versions of the AMS are currently in use, providing invaluable information with high-time resolution on aerosol composition, allowing the formation and evolution of aerosols in the atmosphere to be further investigated. The AMS has been deployed during many experimental campaigns at a variety of site types, in different locations across the world, for different durations and during different seasons (e.g. Zhang et al., 2007). In addition, measurements have been made on mobile platforms such as research aircraft and ships. However, as the work in this thesis is based on in-situ measurements, the following discussion will focus on measurements from ground sites.

AMS studies have enabled the temporal variations in chemical composition to be examined with high-time resolution. For example, Martin et al. (2011) assessed temporal variations of the chemical composition of submicron aerosols in Manchester using seven AMS datasets obtained during different seasons over the course of seven years. Wind direction and season were identified as the main factors governing mass concentrations, where easterly conditions resulted in high sulphate and OM concentrations, particularly in the summer, whereas westerly conditions led to low concentrations of all species during most seasons. Nitrate and organic aerosol concentrations were found to be especially high during the winter due to low temperatures and reduced boundary layer height.

Organic aerosols comprise many different components and are typically classified as being either primary or secondary in nature and yet actually separating measured ambient aerosols into POA and SOA is challenging. The components and evolution of OA in the atmosphere have been investigated in many studies and continue to be

the focus of laboratory and field experiments to further scientific understanding and better characterise OA in regional and climate models. As the AMS measures the whole organic fraction it is a very good instrument for extracting information on the sources and components of OA, where several OA deconvolution techniques have already been successfully applied to ambient datasets. OA data from the AMS were first deconvolved using a receptor-only method by Zhang et al. (2005a) where a custom version of the principal component analysis (PCA) technique was utilised whereby the organic mass concentration measured in Pittsburgh during 2002 was separated into hydrocarbon-like OA (HOA) and oxygenated OA (OOA). These factors were interpreted as POA and SOA, respectively, due to their strong associations; HOA and OOA are now generally used as surrogates for POA and SOA. In order to apportion OA into more than two factors Zhang et al. (2007) developed the Multiple Component Analysis (MCA) technique, an expanded version of the custom PCA, and applied it to numerous ambient measurements from the Northern Hemisphere. In this study, the chemical composition of ambient aerosols were investigated using AMS measurements from 37 field campaigns from different site types. The dominant component of the total non-refractory submicron particle mass (NR-PM_1) was OA at most locations, with significant contributions from sulphate and nitrate, although this was not the case at all locations. Ammonium and chloride also contributed to the total submicron mass. OA was deconvolved into HOA and several types of OOA through the application of the MCA method.

As discussed in Section 2.4, PMF (Paatero and Tapper, 1994; Paatero, 1997; Lanz et al., 2007; Ulbrich et al., 2009) has recently become a useful tool for source apportionment where different primary and secondary sources can be probed. PMF is one of the most commonly used source apportionment techniques used in the atmospheric research community, where there have been many advances regarding the quantitative factorisation of OA, predominantly through the application of techniques such as PMF. Lanz et al. (2007) first used PMF in conjunction with organic data obtained by an AMS in an urban environment. This technique has since been used at a variety of locations across the world allowing the evolution of organic aerosols in the atmosphere to be investigated. For example, Ng et al. (2010) provided a holistic overview of the components of OA in the Northern Hemisphere, where it was possible to separate OA into OOA and HOA at most sites through PMF analysis with additional factors such as biomass burning OA (BBOA) identified at some sites. Similarly, Jimenez et al. (2009) used PMF to further probe the organic fraction of NR-PM_1 from the studies in Zhang

et al. (2007), identifying HOA, semi-volatile oxygenated OA (SV-OOA), low volatility oxygenated OA (LV-OOA), as well as other primary OA components including BBOA. This was the first study to use PMF on organic data in UK cities.

Identification of key organic components can also be achieved by using the related multilinear engine ME-2 (Lanz et al., 2008). The ME-2 model is another bilinear numerical method, where a priori knowledge by way of factor profiles and/or time series is required. This method has been found to produce more representative results in some circumstances (e.g. Lanz et al., 2008), particularly when temporal co-variation of factors arises. A toolkit for the application of ME-2 to AMS data was developed by Canonaco et al. (2013) and has been used to test the solutions derived from PMF and CMB analyses. Furthermore, Crippa et al. (2014) successfully applied the ME-2 model to 25 AMS datasets and produced a standardised procedure for source apportionment of data from any location as well as for long-term data retrieved from instruments such as the Aerosol Chemical Speciation Monitor (ACSM, Ng et al., 2011b). However, unconstrained PMF analysis is used to obtain a factorisation without a priori assumption and thus as a first stage in any further analyses.

Some of the important studies utilising AMS measurements and the PMF model to probe the different OA components which have been performed since those analysed and discussed in Zhang et al. (2007) and Jimenez et al. (2009) will be presented in the following section with an overview of the main findings. Details of the individual studies can be found in Table 3.2.

During the cooler months, the primary fraction of OA is expected to be prominent whereas secondary components are prominent during the summer when photochemistry and precursors emissions are greater. In order to further investigate the components of POA, Allan et al. (2010) performed three measurement periods during autumn and winter in London and Manchester. Emissions from traffic, cooking, and solid fuel burning were identified as significant sources of POA at the different locations. However, due to warmer temperatures during one of the measurement campaigns in London, only traffic and cooking were identified as components of the primary fraction of OA. Solid fuel OA (SFOA) was likely present in quantities too small to be detected as warmer temperatures mean space heating is less likely to be required. A local and unique factor was determined from measurements in Cork, Ireland, which was attributed to peat and coal burning (Dall'Osto et al., 2013). This factor contributed 21% to the total OA mass and was distinctly different to the wood burning BBOA factor, which was suggested to be due to differences in atmospheric processing the two factors

Location	Site type	Time period	Duration	AMS version	Project	Reference
Manchester and London, UK	Urban background	Manchester: January 2007 - February 2007 London: October 2006, October 2007 - November 2007	3-4 weeks	Manchester: cToF-AMS London: cToF-AMS and HR-ToF-AMS	REPARTEE	Allan et al. (2010)
Cork, Ireland	Urban	February 2009	3 weeks	HR-ToF-AMS		Dall'Osto et al. (2013)
Barcelona, Spain	Urban background	March 2009	1 month	cToF-AMS and HR-ToF-AMS	DAURE	Mohr et al. (2012)
Paris, France	3 sites representing 1 urban and 2 urban background	July 2009	1 month	cToF-AMS and HR-ToF-AMS	MEGAPOLI	Freutel et al. (2013)
Paris, France	3 sites representing 1 urban and 2 urban background	January 2010 - February 2010	1 month	cToF-AMS and HR-ToF-AMS	MEGAPOLI	Crippa et al. (2013b)
Europe	17 sites, covering urban, rural, remote, and high altitude	April 2008 - April 2009	Various within 1 year	Q-AMS, cToF-AMS, and HR-ToF-AMS	EUCAARI and EMEP	Crippa et al. (2014)
Beijing, China	Urban	July - September 2008	2 months	HR-ToF-AMS	CAREBeijing -2008	Huang et al. (2010)

Table 3.2: Table of AMS studies in urban locations using the PMF model, except for Crippa et al. (2014) where ME-2 is used to apportion the organic aerosols.

undergo. This study therefore highlights the importance of local sources in contributing to total OA mass and PM_1 as well as the variability in the behaviour of the OA components. Several other studies have identified local factors as components of OA, which are predominantly of primary origin, where the nature and behaviour vary depending on the specific sources and meteorology at each of the locations (e.g. Aiken et al., 2009; Sun et al., 2012; Hayes et al., 2013).

Mohr et al. (2012) separated the organic fraction into five components using PMF conducted on both compact Time-of-Flight AMS (cToF-AMS) and High-Resolution Time-of-Flight AMS (HR-ToF-AMS) data collected at an urban background site in Barcelona, Spain, for a month at the beginning of spring. Three primary components were identified as HOA, cooking OA (COA), and BBOA, and attributed to traffic emissions, cooking, and agricultural biomass burning activities or domestic heating, respectively. The non-negligible contribution of emissions from cooking activities to episodes of poor air quality was highlighted in this study. The importance of cooking emissions at urban locations has also been emphasised in other studies (Huang et al., 2010; Crippa et al., 2014). Crippa et al. (2014) presented a source apportionment procedure applied to 25 datasets, from various locations across Europe including two urban sites, where HOA, BBOA, SV-OOA, and LV-OOA were determined from ME-2 analysis of the organic fraction at both urban sites. However, COA was only identified at the Barcelona site and not at any of the other sites analysed. Similar sources were identified for organic aerosols in Paris during winter (Crippa et al., 2013b), although differences were found between two urban background sites. Four factors were identified at both sites where HOA, BBOA, and OOA were common to both. The fourth component at one site was COA and at the other site a secondary organic factor termed OOA_2-BBOA was identified. A hypothesis for these differences was due to the distance from primary sources, which makes clear separation of the the organic components by PMF analysis difficult due to the similarity of the temporal variations of the factors. However, different versions of the AMS were also used at the two sites: a High-Resolution Time-of-Flight AMS (HR-ToF-AMS) was used at the site where COA was identified whereas a compact Time-of-Flight AMS (cToF-AMS) was used at the site where the OOA_2-BBOA factor was identified. Measurements were also obtained at an additional site in the city centre using a HR-ToF-AMS where all five factors were derived from PMF analysis. Source apportionment at different sites indicated that regional factors dominate particulate pollution in Paris, where there is little effect of emissions from the city itself on the surrounding areas. As part of the

same project, Freutel et al. (2013) investigated the aerosol chemical composition during summer in Paris, finding significant influences from meteorology and air mass origin. In particular, HOA concentrations were influenced by local meteorology whereas concentrations of OOA, as well as the other secondary species sulphate (SO_4), nitrate (NO_3), and ammonium (NH_4), were influenced by air mass origin, especially when air masses advected from Central Europe.

The two subtypes of OOA are used to describe the degree to which the OOA has been atmospherically processed, whereby SV-OOA represents fresh SOA which becomes increasingly oxidized and less volatile through additional processing resulting in LV-OOA (Jimenez et al., 2009). However, it is not always possible to separate OOA into its two subtypes through the application of PMF analysis particularly in winter because of reduced photochemical and meteorological conditions compared to the summer (Jimenez et al., 2009). For example, only a single OOA factor was derived from PMF analysis of organic data from two UK cities during the winter (Allan et al., 2010). Interestingly, a single SOA factor was identified in a study conducted in August in Cork (Dall'Osto et al., 2013), which was observed to be highly oxidised, exhibiting strong correlations with auxiliary measurements and was very similar to LV-OOA identified at other urban locations, thus this factor was deemed to be LV-OOA. Contrastingly, Mohr et al. (2012) derived both LV-OOA and SV-OOA from measurements in Spain during spring, representing regional and aged secondary OA and fresher OA, respectively. Similar to previous findings, the two SOA factors contributed just over half of the total OA mass.

3.4 Current knowledge of organic aerosol components

Many studies that applied PMF to AMS measurements found the main components of POA to be HOA, BBOA, and COA (e.g. Lanz et al., 2007; Zhang et al., 2007; Allan et al., 2010; Mohr et al., 2012; Crippa et al., 2014). However, the contributions to POA from each of these factors vary with location and season due to emissions from local sources (e.g. wood burning activities) and meteorological conditions. Compared to rural areas, HOA will be prominent in urban areas (Zhang et al., 2007) although surprisingly small contributions from HOA have been found, with significant contributions to total OA mass from charbroiling and wood burning (Lanz et al., 2007). Nevertheless, HOA has been identified in multiple studies and is attributed to traffic in urban areas where the diurnal trends in concentration closely follow that of rush hours

(Lanz et al., 2007; Allan et al., 2010; Mohr et al., 2012; Freutel et al., 2013; Crippa et al., 2014). The profile, sources, and variability of HOA are therefore relatively well understood, although the source profiles of HOA can vary due to differences in vehicle fleets with country and continent, where diesel engine light duty vehicles are prevelant in Europe and less so in North America (Yin et al., 2010).

The temporal and spatial variability of other components of OA are much less well constrained. Lanz et al. (2008) hypothesised that wood burning, cooking, and SOA profiles are highly variable, with changes in concentration, both seasonally and regionally. Part of the variability of the wood burning profile can be explained by the burning of different types of biomass and other fuels which contribute to the OA produced from this sector. Therefore the solid fuel OA (SFOA) classification as introduced by Allan et al. (2010) is increasingly being used in the literature. In addition, uncertainty surrounds the origin of biomass burning aerosols i.e. whether they are primary or secondary, particularly the oxidised fraction (Paglione et al., 2014). Characterisation of the behaviour and ageing of biomass burning aerosols has been the focus of many laboratory and field studies (e.g. Weimer et al., 2008; Grieshop et al., 2009; Cubison et al., 2011; Jolleys et al., 2012, 2014). Subsequently, factorisation of OA data from the AMS and other instruments has resulted in several different terms being used in the literature if a source has been characterised in more detail such as the fuel type(s) contributing to the factor identified e.g. BBOA, SFOA, wood burning OA (WBOA, Crippa et al., 2013a), peat and coal OA (PCOA, Dall'Osto et al., 2013), and coal combustion OA (CCOA, Hu et al., 2013; Sun et al., 2013; Zhang et al., 2014). The different terminology assigned to such factors highlights the variability in the sources, profiles, and behaviour of emissions from the burning of biomass and other solid fuels.

Variations in cooking profiles arise from different cooking activities (e.g. frying, charbroiling, grilling) and atmospheric processing. In order to inform and validate factorisation techniques, different types of cooking have been sampled (e.g. Allan et al., 2010; He et al., 2010; Mohr et al., 2012; Abdullahi et al., 2013) and individual cooking species have been photochemically aged in laboratory studies (e.g. Zahardis and Petrucci, 2007). However, profiles that are representative of cooking aerosols which could be identified from bulk OA measurements from the AMS do not currently exist. Mohr et al. (2012) suggest the scarcity of detected and quantified COA in urban environments may be due to the similarity of the HOA and COA profiles when using unit mass resolution data (e.g. from the cToF-AMS). Furthermore, some common signals are shared by the mass spectral profiles of COA and BBOA (e.g. m/z 60). However,

the differences between the mass spectral signatures of emissions from cooking and biomass burning are much larger than the signatures between difference cooking types or biomass burning types (He et al., 2010). Studies to provide profiles and investigate the effects of atmospheric processing on the mass and profiles of cooking organic aerosols are required if we are to better quantify the contributions of COA to total mass loading. Therefore, in order to better inform pollution abatement strategies, the variability of primary organic components such as SFOA and COA requires further investigation and characterisation.

In addition to the uncertainties surrounding SOA and SOA precursors discussed in Section 3.2, difficulties in characterising SOA arise from the fact that once SOA has formed from the gas-phase oxidation of VOCs its properties may change with atmospheric processing. Several metrics and graphical representations of AMS data have therefore been developed to investigate OA evolution; Ng et al. (2010) and Morgan et al. (2010b) presented the f_{44} vs. f_{43} space to describe and explain OA evolution in the atmosphere, which was derived from ground based and airborne measurements, respectively. The degree of oxidation is inferred from the f_{44} value, which is the ratio of the organic signal at m/z 44 to the total organic signal, and the range of precursors is suggested by the f_{43} values, which is the ratio of the organic signal at m/z 43 to the total organic signal. To further investigate OA evolution and the corresponding changes in chemical composition the VK-triangle can be used, which is the f_{44} vs. f_{43} triangle transformed into Van Krevelen space (Ng et al., 2011a), where the Van Krevelen space (Van Krevelen, 1950) is an established method in analytical chemistry (e.g. Kim et al., 2003; Bateman et al., 2009). The use of O:C and H:C ratios in Van Krevelen space can also indicate the likely degree of processing the aerosol has undergone, where changes in functionality can be determined (Heald et al., 2010). The O:C and H:C ratios can also be combined to derive the oxidation state of carbon (Kroll et al., 2011) and thus describe OA chemistry. The metrics described all illustrate that atmospheric processing of fresh OA results in similarly aged and highly oxidised OA, thus the evolution of SOA can be regarded as a continuum of oxidation. The ability to describe the evolution of a complex species, including the oxidation and other key physical and chemical processes OA undergoes in the atmosphere, through the use of such metrics offers the potential to simply represent the chemical evolution of OA in the atmosphere in models as well as to develop simple, predictive models for similarly complex chemical systems (Heald et al., 2010; Kroll et al., 2011). Furthermore, the results gleaned

from these metrics along with other techniques provide useful constraints in models investigating SOA evolution as the processes involved are better parametrised (Ng et al., 2011a) thus improving the characterisation of SOA in models (Pye and Seinfeld, 2010; Jathar et al., 2011).

However, our scientific knowledge is still limited, with regards properties of SOA, their composition and formation mechanisms, despite recent advances in the identification of key anthropogenic and biogenic precursors of SOA (Hallquist et al., 2009) and the improvements of SOA parametrisation in models. Nevertheless, in contrast to SIA, SOA is not well understood owing to the complexity of SOA precursors, the range of atmospheric processing they can undergo, lifetime, and temporal and spatial variability. Such variability presents a major challenge to understanding and characterising SOA and its formation (Goldstein and Galbally, 2007). Consequently, the quantification and accurate prediction of SOA remains limited.

3.5 Summary, remaining questions, and research goals

An overview of the studies investigating the chemical composition of atmospheric aerosols has been presented in this chapter, where substantial progress has been made over the past few decades regarding the identification of components of PM through various measurement techniques and factorisation models. The evidence for the causal link between PM_1 and adverse health effects is therefore increasing, where the chemical composition of submicron and ultrafine aerosols has been identified as playing a key role in the observed toxicological effects from particulate matter. Meteorology, season, air mass origin, and local sources have all been identified as factors that influence ambient aerosol mass concentrations. Therefore, both long-term and intensive measurement periods of higher mass and temporal resolution are important for interpreting and understanding the behaviour of PM. Although numerous studies have already been performed in various sites across the world, they are often only conducted for a short period of time (a month, on average) and have been performed with limited supporting measurements thus provide a narrow view of the temporal characteristics of pollution aerosols. Furthermore, as the number of people living in cities is predicted to continue to increase, such measurements need to take place in urban areas to better understand the roles and contributions of local, regional, and transboundary pollution to PM concentrations if we are to accurately predict levels of pollution and pollution events and thus improve air quality through pollution abatement strategies.

The main gaps identified from the previous sections are that the different sources of PM components are not well understood with uncertainty surrounding the processes governing the formation and evolution of each of the components. The effects of atmospheric aerosols and the mechanisms by which they occur are therefore also not well understood. The contributions of the chemical components to mass and their behaviour vary both temporally and spatially, where the influence of transported pollution in contributing to high concentration events in different areas is uncertain. Consequently, forming predictive measures and effective pollution mitigation strategies remains challenging. There is therefore a need for long-term speciated studies, particularly at higher time resolution than current measurements, in urban areas, and of the smaller particle sizes to apportion the components of atmospheric aerosols. Furthermore, detailed chemical composition measurements are also required to investigate and constrain the specific nature and behaviour of individual PM components, which are typically performed on short timescales. This study will therefore focus on characterising the chemical components of PM_1 in an urban location in the UK through both long-term and short-term measurements as part of the Clean Air for London (ClearfLo) project. The ClearfLo project is the largest measurement campaign to be performed in the UK, where the combination of different measurements and data analysis techniques provides a unique opportunity and very powerful tool to investigate and characterise atmospheric pollution in the urban environment.

In this thesis, the different chemical constituents of atmospheric aerosol will be identified from both short- and long-term measurements of submicron aerosols in London, where the organic fraction will be further separated into its components through factor analysis. The instruments and techniques employed in this work have not previously been used in this way. In particular, this is the first time PMF has been applied to a year of organic aerosol measurements from the AMS in an urban environment. In addition to separating the submicron aerosols into different chemical components, the importance of each in contributing to pollution levels will be assessed and their behaviour in response to different meteorological conditions will be explored in order to capture and understand local and regional/transboundary influences as well as meterological influences on both a short- and long-term basis. The main questions that this study seeks to address are:

- What are the sources and components of submicron aerosols in London and what are their contributions to the total mass loading?
- How do the sources of aerosols and their contribution to total mass vary with

time of year?

Chapter 4

Papers

4.1 Overview of ClearfLo project

The detrimental effects on human health from poor air quality, particularly in urban areas where emissions of pollutants are high, have long been known yet the sources and processes leading to high concentrations of pollutants are not well understood. Detailed measurements are therefore needed to accurately assess and forecast air quality and to inform and evaluate mitigation strategies, particularly in areas such as cities where exposure to pollutants is substantial. Such measurements will enable policy makers to make the best informed decisions regarding the improvement of the general population's health and well-being.

The work in this study focuses on the data collected as part of the UK Natural Environment Research Council (NERC) funded Clean Air for London research project (ClearfLo, www.clearflo.ac.uk, Bohnenstengel et al., 2014). ClearfLo is a large, multi-institutional collaborative scientific project based in the UK, which provides integrated and detailed measurements of the meteorology, composition and loading of both the gas and particulate phases of the urban atmosphere in London with the aim of better understanding the processes underlying poor air quality and subsequently improve the capability to predict air quality. The ClearfLo project will build upon the observations made and further probe the findings from the REPARTEE project (Harrison et al., 2012), which was performed at various sites in London during 2006 and 2007.

The ClearfLo project provides the opportunity to explore the interactions between gas phase chemistry, particulates, and meteorology in London as well as to evaluate air quality and weather forecast models by combining long-term measurements between 2011 and 2013 from a new and unique infrastructure installed at various sites across

London with high-resolution simulations from several models, including the UK Met Office's Numerical Atmospheric-dispersion Modelling Environment (NAME). This combined approach is used to investigate and understand seasonal variations in the composition and meteorology as well as the processes governing such variations. Furthermore, the processes controlling the evolution, particle size, and composition of particulate matter, the vertical structure and evolution of the urban boundary layer, and the chemical controls on nitrogen dioxide and ozone production can be investigated through analysis of more detailed measurements of aerosols, gases, radicals and meteorological parameters from two major intensive observation periods (IOPs) during the winter and summer of 2012 at a number of sites in and near London. In addition to the North Kensington, Marylebone Road, and BT tower sites used in REPARTEE, measurements were also performed during the ClearfLo winter IOP at rural sites to the north-west (Harwell) and south-east (Detling) of London, providing spatial coverage for investigating the urban increment of pollutants.

The overarching aim of the ClearfLo project is to investigate boundary layer pollution across London in order to improve the predictive capability for air quality. The work presented in this thesis focuses on investigating the chemical composition and behaviour of particulates in London from a ground-based urban background site (North Kensington). Long-term measurements from the compact Time-of-Flight Aerosol Mass Spectrometer (cToF-AMS) are used to understand the temporal behaviour of aerosols as well as to identify the importance of different components in contributing to pollution events during different seasons. In addition, London's aerosols are further investigated using High-Resolution Time-of-Flight AMS (HR-ToF-AMS) measurements from the two ClearfLo IOPs. Gas phase and meteorological measurements as well as NAME model outputs are used in conjunction with aerosol measurements to enhance the interpretation of observed variations in aerosol composition and behaviour in the urban environment.

4.2 Paper I: Investigating the annual behaviour of submicron secondary inorganic and organic aerosols in London

Dominique E. Young, James D. Allan, Paul I. Williams, David C. Green, Michael J. Flynn, Roy M. Harrison, Jianxin Yin, Martin W. Gallagher, and Hugh Coe.

The following manuscript has been published in the journal of Atmospheric Chemistry and Physics Discussions (www.atmos-chem-phys-discuss.net/14/18739/2014/, doi:10.5194/acpd-14-18739-2014) and is currently under review for Atmospheric Chemistry and Physics.

Supplementary information is available in Appendix A.1.

Overview

Long-term aerosol chemical composition measurements from the compact Time-of-Flight Aerosol Mass Spectrometer (cToF-AMS) at the urban background site in North Kensington, London, are presented in this paper. The behaviour of non-refractory inorganic and organic submicron particulate through an entire annual cycle was investigated where the sources and components of the organic fraction were identified through the application of Positive Matrix Factorisation (PMF). This was the first time the AMS had been used for long-term measurements in an urban environment and subsequently the first application of PMF to a year of organic aerosol data measured by the AMS in this environment.

The contributions of all species, including the organic components identified from PMF analysis, to the total annual budget were quantified and secondary inorganic and organic aerosols were observed to account for a significant fraction of the total submicron mass throughout the year. The complexity surrounding predicting ammonium nitrate concentrations was emphasised as a combination of factors were identified as governing the formation of particulate nitrate. Each of the primary organic aerosol sources was observed to be of equal importance throughout the year. The evolution of secondary organic aerosol (SOA) on an annual basis was investigated whereby no variability in the extent of SOA oxidation, as defined by the oxygen content, was observed despite changes in SOA mass, precursor emissions, precursor contributions, and photochemical activity across the year. These findings could therefore make characterisation

of SOA in urban environments more straightforward than may be previously supposed. The importance of local, regional, and transboundary pollution in influencing London's total submicron aerosol burden was also highlighted in this paper, as well as the importance of different factors governing high concentration events, which varied with season. In winter, high concentration events were found to be governed by nitrate formation and primary organic particulate emissions, notably from vehicles, cooking, and solid fuel organic aerosol, whereas during the summer high concentrations were driven by SOA formation. The findings from this work could have significant implications for the effects of atmospheric aerosols on human health and air quality as well as for the development of effective pollution abatement strategies and for modelling of urban air pollution.

Author contributions

Dominique Young performed aerosol measurements, analysed and interpreted the data, and wrote the manuscript. James Allan helped to run instruments in the field and assisted with interpretation of results and preparation of the manuscript. Paul Williams assisted with the aerosol measurements. David Green assisted with the aerosol measurements and provided data from the URG Ambient Ion Monitor. Michael Flynn helped prepare the instrumentation both before and during the field campaigns. Roy Harrison and Jianxin Yin provided levoglucosan and potassium ion data. Martin Gallagher assisted in the planning of the field campaigns. Hugh Coe assisted with the interpretation of the data and preparation of the manuscript.

Atmos. Chem. Phys. Discuss., 14, 18739–18784, 2014
www.atmos-chem-phys-discuss.net/14/18739/2014/
doi:10.5194/acpd-14-18739-2014

Atmospheric Chemistry and Physics Discussions

Investigating the annual behaviour of submicron secondary inorganic and organic aerosols in London

D. E. Young[1], J. D. Allan[1,2], P. I. Williams[1,2], D. C. Green[3], M. J. Flynn[1], R. M. Harrison[4,5], J. Yin[4], M. W. Gallagher[1], and H. Coe[1]

[1]School of Earth, Atmospheric and Environmental Sciences, University of Manchester, Oxford Road, Manchester, M13 9PL, UK
[2]National Centre for Atmospheric Science, University of Manchester, Oxford Road, Manchester, M13 9PL, UK
[3]School of Biomedical and Health Sciences, King's College London, London, UK
[4]School of Geography, Earth and Environmental Sciences, University of Birmingham, Edgbaston, Birmingham, B15 2TT, UK
[5]Department of Environmental Sciences/Center of Excellence in Environmental Studies, King Abdulaziz University, Jeddah, 21589, Saudi Arabia

Received: 17 June 2014 – Accepted: 27 June 2014 – Published: 16 July 2014

Correspondence to: H. Coe (hugh.coe@manchester.ac.uk)

Published by Copernicus Publications on behalf of the European Geosciences Union.

Abstract

For the first time, the behaviour of non-refractory inorganic and organic submicron particulate through an entire annual cycle is investigated using measurements from an Aerodyne compact time-of-flight aerosol mass spectrometer (cToF-AMS) located at a UK urban background site in North Kensington, London. We show secondary aerosols account for a significant fraction of the submicron aerosol burden and that high concentration events are governed by different factors depending on season. Furthermore, we demonstrate that on an annual basis there is no variability in the extent of secondary organic aerosol (SOA) oxidation, as defined by the oxygen content, irrespective of amount. This result is surprising given the changes in precursor emissions and contributions as well as photochemical activity throughout the year; however it may make the characterisation of SOA in urban environments more straightforward than previously supposed.

Organic species, nitrate, sulphate, ammonium, and chloride were measured during 2012 with average concentrations (±one standard deviation) of 4.32 (±4.42), 2.74 (±5.00), 1.39 (±1.34), 1.30 (±1.52) and 0.15 (±0.24) $\mu g\,m^{-3}$, contributing 43, 28, 14, 13 and 2 % to the total submicron mass, respectively. Components of the organic aerosol fraction are determined using positive matrix factorisation (PMF) where five factors are identified and attributed as hydrocarbon-like OA (HOA), cooking OA (COA), solid fuel OA (SFOA), type 1 oxygenated OA (OOA1), and type 2 oxygenated OA (OOA2). OOA1 and OOA2 represent more and less oxygenated OA with average concentrations of 1.27 (±1.49) and 0.14 (±0.29) $\mu g\,m^{-3}$, respectively, where OOA1 dominates the SOA fraction (90 %).

Diurnal, monthly, and seasonal trends are observed in all organic and inorganic species, due to meteorological conditions, specific nature of the aerosols, and availability of precursors. Regional and transboundary pollution as well as other individual pollution events influence London's total submicron aerosol burden. High concentrations of non-refractory submicron aerosols in London are governed by particulate emis-

sions in winter, especially nitrate and SFOA, whereas SOA formation drives the high concentrations during the summer. The findings from this work could have significant implications for modelling of urban air pollution as well as for the effects of atmospheric aerosols on health and climate.

1 Introduction

Atmospheric aerosols have adverse effects on human health (Pope and Dockery, 2006), air quality (AQEG, 2012), visibility (Watson, 2002), and climate (Boucher et al., 2013). Pollution abatement is therefore important, especially in cities, when three-quarters of Europe's population currently live in urban areas, a number that is expected to increase to 80 % by 2020 (EEA, 2010). Regulations on air quality are based on PM_{10} and, more recently, $PM_{2.5}$ (particulate matter with aerodynamic diameters less than 10 µm and 2.5 µm respectively, European Union, 2008). A recent study (Aphekom Summary Report, 2011) reported that life expectancy in London could increase by 2.5 months for persons 30 years of age and older if average annual $PM_{2.5}$ concentrations were decreased in line with the World Health Organization's Air quality guidelines to $10\,\mu g\,m^{-3}$ (WHO, 2005). PM_1 (particulate matter with an aerodynamic diameter less than 1 µm) is beginning to receive greater attention from the air quality community as they are associated with adverse health effects due to the depth within the lungs to which these particles can penetrate and can then enter the blood stream, and cause damage to other parts of the body (Oberdörster et al., 2005).

Primary and secondary aerosols have both natural and anthropogenic sources (Seinfeld and Pandis, 2006), resulting in their diverse chemical composition, size, and concentration (Pöschl, 2005). In urban areas, primary aerosols from transport, cooking, and solid fuel burning are of great significance (Allan et al., 2010), particularly in the winter when meteorological conditions are such that their concentrations are elevated resulting in pollution events (Zhang et al., 2007). In addition, transported air masses frequently influence the UK's atmosphere (Abdalmogith and Harrison, 2005) including

polluted air masses from continental Europe and cleaner westerly conditions. Transported pollution typically comprises secondary aerosols, with season having a strong influence on the chemical composition and concentration (Charron et al., 2007). Previous studies highlight the variability in the contribution of both secondary inorganic and organic aerosol (SIA and SOA, respectively) to the total mass depending on location (Jimenez et al., 2009). Furthermore, chemical composition varies with location due to a combination of local and regional aerosol sources as well as daily and seasonal meteorological conditions.

The precursors and formation processes of SIA are relatively well understood, particularly as anthropogenic emissions dominate although concentrations are significantly influenced by regional and transboundary pollution. For example, Abdalmogith and Harrison (2006) estimated that between 2002 and 2004, 88 % of nitrate and 92 % of sulphate in central London originated from the regional background. Due to the non-linear response of SIA concentrations from reductions in precursor emissions, the impacts on formation from changes in emissions are uncertain (AQEG, 2012). In contrast, the complexity of SOA precursors, including the range of atmospheric processing they can undergo, lifetime, and temporal and spatial variability presents a major challenge to understanding and characterising SOA and its formation (Goldstein and Galbally, 2007). Additional variability of SOA sources and formation results from the long distances over which SOA precursors and the resulting aerosols can be transported as well as dependency on meteorological conditions (Martin et al., 2011). Furthermore, SOA evolves in the atmosphere with properties changing with age (Ng et al., 2010) meaning our ability to quantify and predict SOA remains limited.

The Aerodyne Aerosol Mass Spectrometer (AMS) measures size-resolved chemical composition of non-refractory submicron particulates with high time resolution (Jayne et al., 2000; Canagaratna et al., 2007). The AMS has demonstrated its versatility in a range of environments across the world (Zhang et al., 2007) and has been used to successfully investigate SOA behaviour (e.g. Jimenez et al., 2009; Heald et al., 2010; Ng et al., 2010; Kroll et al., 2011). However, despite its widespread use in such process

studies, the instrument is infrequently used for long-term characterisation of aerosols. Here we present a year-long UK urban background data set collected with a compact time-of-flight AMS (cToF-AMS) including results of positive matrix factorisation (PMF) analysis, which is the first time the AMS has been used in this way in an urban environment. The temporal trends and contributions of urban aerosols to PM_1 are evaluated and their sources are investigated. In this paper we will focus on the secondary aerosols; though primary organic aerosol sources are identified in this paper, the behaviour of primary aerosols from these sources will be discussed in subsequent publications.

In Sect. 2 of the paper, the experimental site, instrumentation, and analysis methods utilised in this study are described. In Sect. 3, an overview of the bulk non-refractory PM_1 (NR-PM_1) components including average mass, diurnal profiles, and seasonality is presented along with a discussion on the factors governing concentrations and temporal trends. In Sect. 4, the components of the organic fraction are investigated using receptor modelling. In Sect. 4.3, we investigate two covarying factors derived from PMF analysis, with the method used to estimate the concentrations of the two factors described in Sect. 4.4. In Sect. 5, the organic components are identified and the results from the previous sections are used to probe the behaviour of urban SOA including temporal trends (Sect. 5.1) and state of oxidation (Sect. 5.2). In Sect. 6, the factors governing pollution events across the year, as well as winter and summer, are assessed through identification of the dominant components of the high concentration events. Finally, Sect. 7 summarizes the conclusions from this study on secondary aerosols in London.

2 Experimental

2.1 Site and instrumentation

The measurements for this study were conducted as part of the NERC funded Clean Air for London (ClearfLo) Project (www.clearflo.ac.uk), a large, multi-institutional collaborative scientific project based in the UK. A suite of state-of-the-art instrumentation, measuring aerosols, gases, radicals and meteorological parameters was deployed for two major intensive observation periods (IOPs) during 2012, with long-term continuous measurements conducted between 2011 and 2013. Measurements were conducted at the ClearfLo urban background site in the grounds of a school in North Kensington (51.521055° N, 0.213432° W), where a permanent DEFRA Automated Urban and Rural Network (AURN, http://uk-air.defra.gov.uk/networks/network-info?view=aurn) monitoring station is located. Situated in a residential area 7 km to the west of Central London, the sampling site is not influenced by heavily trafficked roads and is representative of background air quality (Bigi and Harrison, 2010). Along with the school buildings, a car park and a relatively large playing field are also located at the site with several large trees both on site and lining the surrounding pavements. Further details on the ClearfLo experimental campaigns and locations are described in Bohnenstengel et al. (2014).

Aerosol chemical composition was measured by the cToF-AMS for a full calendar year (11 January 2012–23 January 2013) and by the high-resolution time-of-flight AMS (HR-ToF-AMS) during the two IOPs, which were conducted in the winter (January–February) and summer (July–August) of 2012. The cToF-AMS sampled through a $PM_{2.5}$ inlet, with a bypass flow of 16 L min^{-1} and split using an asymmetric Y-piece. The HR-ToF-AMS was located in a shipping container containing several other aerosol instruments, where aerosols were sub-sampled from a sampling stack with a flow of 30 L min^{-1} via a 3.5 µm cut-off cyclone.

Both AMS instruments operated in the standard configuration and took mass spectra (MS) and particle time of flight (pToF) data. An overview of the AMS can be found in Canagaratna et al. (2007) and detailed descriptions of both the cToF-AMS and HR-

ToF-AMS can be found in Drewnick et al. (2005) and DeCarlo et al. (2006) respectively. The instrument operation and data analysis procedures pertinent to this study have been described elsewhere (e.g. Allan et al., 2010). The HR-ToF-AMS operated in both "V" and "W" ion path modes, offering high sensitivity but low mass resolution, and low sensitivity but high mass resolution, respectively. Only the V mode ambient data are analysed further here due to their better signal-to-noise ratio. The time-resolution of the cToF-AMS was 5 min throughout the measurement period. As the HR-ToF-AMS sampled in an alternating sequence with other black carbon and aerosol volatility measurements using a thermodenuder (Huffman et al., 2008) in the winter, 5 min averaged ambient data in V mode were only obtained every 30 min. In the summer, there were no volatility measurements so average data were obtained every 12 min. Both instruments were calibrated using 350 nm mono-disperse ammonium nitrate particles approximately once a month for the cToF-AMS and weekly during the IOPs for the HR-ToF-AMS. Ammonium sulphate calibrations were also performed where possible. The heater bias of the cToF-AMS was tuned to minimise the signal from surface ionised potassium and the filament was run at a lower value than usual in order to prolong the life of the multi-channel plate (MCP). This configuration results in a reduced signal, which in turn reduces the signal-to-noise ratio (Allan et al., 2003).

2.2 Analysis and quality control of AMS data

CToF-AMS data were analysed within Igor Pro (Wavemetrics) using the standard TOF-AMS analysis toolkit software package, SQUIRREL (SeQUential Igor data RetRiEval) v1.53. The HR-ToF-AMS data were analysed using SQUIRREL v1.52J and PIKA v1.11J (Sueper, 2008). Relative ionisation efficiencies (RIEs) of ammonium, nitrate, and sulphate were estimated based on the molar ratios of each species from the ammonium nitrate calibrations (see Table S1 in the Supplement for the ammonium and sulphate RIE values for the cToF-AMS and HR-ToF-AMS). These were compared to particulate sulphate measurements from the URG-9000B Ambient Ion Monitor (AIM) from North Kensington (AURN and Particle Numbers and Concentrations Network,

http://uk-air.defra.gov.uk/networks/network-info?view=particle) where available (Supplement Fig. S1) and indicated that the default RIE of sulphate of 1.2 may not be appropriate for either instrument. As a sulphate calibration was not performed on the HR-ToF-AMS during the winter IOP the RIE was ambiguous, so concentrations were based on those reported by the cToF-AMS, which was calibrated later during the campaign (see Sect. 2.1 in the Supplement for a comparison of the concentrations between the two instruments for the winter IOP and Sect. 2.2 for the summer IOP). This approach, as opposed to using the default RIE of 1.2, was deemed valid as it resulted in a more consistent volume concentration comparison with that derived from a differential mobility particle sizer (DMPS) from the winter IOP (Supplement Fig. S2) where the volume concentration was estimated using the densities reported by Cross et al. (2007). A time and composition dependent collection efficiency (CE) was applied to the data based on the algorithm by Middlebrook et al. (2012). This was also validated for both AMSs by comparing the volume concentration with that derived from the DMPS measurements from the winter IOP (Supplement Fig. S2a and d).

Inspection of the data revealed step changes in cToF-AMS mass concentrations that coincided with changes in the flowrate, which were mostly due to partial blockages in the pinhole (see Sect. 1.2 in the Supplement). In each case, the pinhole was either manually cleaned (through sonication in deionised water) or the flow returned to its average rate of 1.3 cc s^{-1} without intervention. Data were removed if clear mass changes were observed, with distinct start and end points (e.g. 2 June 2012, Supplement Fig. S3b). Other data were flagged as suspect if the flow was significantly different from its normal rate (less than 1.2 cc s^{-1}) but there were no distinct step changes in mass e.g. 4 September 2012 (Supplement Fig. S3c). The final data set comprised 95 % data that had not been removed or flagged as suspect.

2.3 Levoglucosan measurements

24 h $PM_{2.5}$ samples were collected on quartz fibre filters (Whatman QM-A) at NK during the winter 2012 ClearfLo campaign using a high volume Digitel DHA-80 sampler

at a flow of 500 L min^{-1}. These samples were analysed for wood smoke marker levoglucosan using a slightly modified version of the method of Yin et al. (2010) and Wagener et al. (2012). In brief, one portion of the Digitel filter sample was spiked with an internal standard (IS), methyl-beta-D-xylopyranoside (from Sigma-Aldrich Ltd) and extracted with dichloromethane and methanol under mild sonication at room temperature. The combined extract was filtered and concentrated down to 50 µL. One aliquot of the extract was evaporated to near dryness and derivatised by addition of N,O-bis(trimethylsilyl)trifluoroacetamide plus 1 % trimethylchlorosilane (BSTFA + 1 % TMCS) and pyridine at 70 °C for 1 h, and finally cooled in a desiccator. Quantification was based on the IS and a six point authentic standard calibration curve, using the selected ion monitoring (SIM) mode on an Agilent GC-MS instrument. The ions monitored were 204 and 217 for the IS and 204, 217 and 333 for levoglucosan.

3 Results

The daily averaged time series of NR-PM_1 species, their diurnal patterns, and monthly average contributions to total submicron mass are shown in Fig. 1. On average, PM_1 composition is dominated by the organic fraction (Org, 44 %, Fig. 2) with the remainder of the total mass comprising SIA species. Nitrate (NO_3) is the largest SIA component, comprising 28 % of the total mass. Sulphate (SO_4) and ammonium (NH_4) contribute 14 % and 13 % respectively with a small contribution from non-refractory chloride (Chl, 1 %). The contribution of each species to the total mass varies with time; organics dominate in summer and inorganics dominate in winter, with nitrate contributing up to 45 % of the total mass in spring (Fig. 1c).

Organic species constituted, on average, just under half of the non-refractory submicron mass as measured by the AMS in 2012 (44 %, Fig. 2), with a mean annual concentration (±one standard deviation) of 4.32 (±4.42) µg m^{-3}. During the year, concentrations at times increased up to, and over, an order of magnitude greater than this value with a maximum 5 min concentration of 230 µg m^{-3}, observed on 18 February.

This is likely a locally sourced event lasting approximately 6 h as the maximum daily concentration was 16.97 µg m^{-3}, observed on 25 July (Fig. 1a). The mean organic concentrations and diurnal patterns exhibit little seasonality (Supplement Fig. S6a and b, respectively); a large evening peak is observed in all diurnal profiles but the number of peaks and their timing during the day vary slightly with season. Although the total mass of organic species exhibits little seasonality, the organic fraction of total PM_1 varies with season, being largest in summer and autumn.

The average annual PM_1 nitrate concentration was 2.74 (±5.00) µg m^{-3} with several high concentration episodes occurring throughout the year (Fig. 1a). Peak events occurred mainly during the winter and spring, with a maximum 5 min concentration of 48.35 µg m^{-3} measured on 23 March. Increases in the concentrations of all species are also observed during these high nitrate events. Averaged across the year, nitrate exhibits a pronounced diurnal pattern with an overnight increase in mass, peaking at 08:00 UTC, with a daytime minimum at 16:00 UTC (Fig. 1b). The overall shape of the diurnal pattern varies little with season although it becomes less pronounced in summer and autumn (Supplement Fig. S7b). In contrast, the total nitrate mass varies significantly with season (Supplement Fig. S7a), where the greatest concentrations are observed during the spring, which is also when the diurnal pattern is most pronounced due to a large range of concentrations. The lowest concentrations and smallest diurnal range occur during the summer months.

Submicron sulphate represents approximately 25 % of the inorganic fraction, with a mean concentration of 1.39 (±1.34) µg m^{-3}. The maximum sulphate concentration measured in 2012 was 12.75 µg m^{-3} which occurred on 2 May. In general, increases in sulphate mass are coincident with increases in concentration of other AMS measured species. In contrast to nitrate, sulphate exhibits little seasonality although it dominates SIA mass in summer, with higher mean concentrations occurring in spring and summer compared to autumn and winter (Fig. S8a). Furthermore, sulphate exhibits little diurnal variation for each season as well as for the whole year (Supplement Fig. S8b and Fig. 1b).

Almost a quarter of the inorganic mass fraction is comprised of ammonium, with a mean concentration of 1.30 (±1.52) $\mu g\,m^{-3}$. Averaged across the year, ammonium exhibits a weak diurnal profile (Fig. 1b). However, this pattern varies with season, with a peak in concentration between 08:00 and 10:00 UTC in all but the summer months (Supplement Fig. S9b). The most pronounced diurnal variability occurs in spring, which is also when there is the greatest seasonal mass (Supplement Fig. S9a) and maximum concentration of the year (14.23 $\mu g\,m^{-3}$). The aerosol was found to be neutral throughout the year as the balance between inorganic cationic and anionic charge was maintained.

As the AMS does not detect chloride salts such as sodium chloride, the chloride measured here is primarily ammonium chloride. Although this represents a very small fraction of SIA, with an average concentration of 0.15 (±0.24) $\mu g\,m^{-3}$, some seasonal differences are apparent. Chloride exhibits a weak diurnal pattern with slightly higher concentrations at night compared to during the day (Fig. 1b), which changes with season (Supplement Fig. S10b). The highest chloride concentrations are in the winter with comparatively low concentrations in the summer (Supplement Fig. S10a).

3.1 Behaviour of bulk PM_1 components

3.1.1 Organic aerosols

Weak seasonality of organic aerosols in Paris has been previously suggested (e.g. Freutel et al., 2013) and observed in organic carbon (OC) measurements in Birmingham (Harrison and Yin, 2008). The lack of seasonality arises because of the balance of sources that govern the total concentration of organic species differently during each season (Zhang et al., 2007) rather than the constancy of any particular source. As well as differences in sources with season, increased organic concentrations in winter are due to low temperatures and reduced atmospheric mixing, whereas in summer similar concentrations are due to increased photochemistry (Martin et al., 2011). In contrast to absolute mass, there are differences in the organic fraction of total PM_1 with season, which have been observed in Paris (Crippa et al., 2013a; Freutel et al., 2013), Tokyo (Takegawa et al., 2006), and Zurich (Lanz et al., 2007), and can be attributed to seasonal differences in concentrations of other species such as nitrate. Consistent with previous observations, organics in London exhibit little seasonality both in terms of mass and diurnal profile. Any variations in diurnal pattern across the year are due to both mixing layer height dynamics and the nature of the dominant source. The components of the organic aerosol fraction are discussed in more detail in Sect. 4.

3.1.2 Nitrate

The annual cycle of nitrate mass is significantly influenced by season (Martin et al., 2011), driven by emissions of ammonia, which typically peak in the spring (Schaap et al., 2004), as well as temperature and relative humidity (RH), which both control nitrate partitioning (Stelson and Seinfeld, 1982). The diurnal pattern of nitrate in urban locations (e.g. Cork, Dall'Osto et al., 2013; Paris, Freutel et al., 2013) is also largely governed by the semi-volatile behaviour of ammonium nitrate. However, nitrate formation also strongly depends on availability of precursor gases (Ansari and Pandis, 1998) such as nitrogen oxides (NO_x) and, in particular, ammonia, as emissions in urban environments are small compared to NO_x (NAEI, 2013). Although some non-agricultural sources of ammonia are known (Sutton et al., 2000), their strengths and trends are not well understood. Pollution from continental Europe has also been identified as an important contributor to particulate concentrations in many regions (e.g. Manchester, Martin et al., 2011; Paris, Freutel et al., 2013) with the highest nitrate concentrations occurring over North West Europe during pollution episodes (Morgan et al., 2010).

Consistent with previous UK measurements (Harrison and Yin, 2008; AQEG, 2012), the highest concentrations in this study occurred in spring. Although more pronounced in winter and spring, the overall shape of the diurnal profile does not change with season, indicating the strong semi-volatile behaviour of nitrate. Also consistent with previous studies (e.g. Abdalmogith and Harrison, 2005), increased nitrate concentrations occur in air masses influenced by continental North-Western Europe, indicating the im-

portance of transboundary pollution. Nitrate concentrations are therefore governed by a combination of season, ambient conditions, availability of precursor emissions, and air mass trajectory rather than any one factor. Consequently, it was not possible to establish simple metrics that could be used to predict nitrate concentrations, highlighting the need for detailed modelling of aerosol chemistry and thermodynamics to accurately predict nitrate concentrations.

3.1.3 Sulphate

Sulphate concentrations have been decreasing at both urban and rural UK locations for at least the last 10 years (as summarised in Table 1) due to decreasing SO_2 emissions (Monks et al., 2009). However, sulphate concentrations respond non-linearly to reductions in SO_2 emissions (Megaritis et al., 2013). The mean sulphate concentration (1.39 $\mu g\,m^{-3}$) measured by the AMS in 2012 is comparable to the non-sea salt sulphate (1.21 $\mu g\,m^{-3}$) calculated from AIM measurements also at North Kensington. The 2012 AMS measurements are therefore consistent with the trend of decreasing sulphate concentrations observed at sites at North Kensington and Harwell. Similar to the findings of Harrison et al. (2012) and Abdalmogith and Harrison (2006), sulphate exhibits little seasonality and diurnal variation thus emphasising the importance of regional pollution.

3.1.4 Ammonium

Changes in the diurnal profile and total mass of ammonium with season are very similar to those of nitrate and, to a lesser extent, sulphate (Morgan et al., 2009; Bressi et al., 2013). The springtime peak in concentrations is governed by the greater availability of ammonia and favourable meteorological conditions.

3.1.5 Chloride (non-refractory)

The seasonal variation and diurnal pattern of chloride is attributed to its volatile nature as well as planetary boundary layer dynamics where low concentrations are expected during the summer due to increased mixing depth. The availability of ammonia will also govern the concentration of chloride. In addition, increased chloride concentrations in the winter could be attributable to increased coal combustion during this period (Sun et al., 2013).

4 Positive matrix factorisation analysis

To investigate the components and temporal trends of the organic fraction, positive matrix factorization (PMF) (Paatero and Tapper, 1994; Lanz et al., 2007) was applied to the organic matrix from the year-long cToF-AMS data set, which is the first time PMF has been applied to a data set of this duration from an urban environment. Separating long-term data into seasons before performing factorisation analysis may be used to reduce seasonal phenomena affecting the retrieved factors, such as minimising the influence of variations in photochemistry and also to address known PMF limitations such as mixing between factors. However, splitting the data into seasons is subjective, resulting in a bias of the retrieved factors and loss of information on annual trends of potential OA components.

Identification of key organic components can also be achieved by using the related multilinear engine ME-2, for which a protocol for the AMS is currently available (Canonaco et al., 2013) and has been found to produce more representative results in some circumstances (e.g. Lanz et al., 2008), particularly when temporal co-variation of factors arises. However, a priori knowledge by way of factor profiles and/or time series is required to utilise ME-2, so in principle it is preferable to obtain a factorisation without a priori assumption, which is achieved in this study by way of unconstrained PMF analysis. Furthermore, several of the factorisation problems that ME-2 overcomes when

applied to data from the aerosol chemical speciation monitor (ACSM, Ng et al., 2011a) compared to the AMS are related to the fact that the ACSM has much lower signal-to-noise ratio. We present the results from PMF analysis here to compare with earlier work and as a first stage in any further analysis. Furthermore, as we will show in the data presented, temporal co-variation of factors can be overcome by careful scrutiny of the data as well as from the use and support of associated measurements such as from the HR-ToF-AMS.

4.1 Data preparation

PMF was performed on the organic data matrix for the year-long data set from the cToF-AMS and for the winter and summer periods when the HR-ToF-AMS was operating. The data preparation for all three data sets followed the recommended procedures as described by Ulbrich et al. (2009). However, for the final PMF solution, the summer period was removed from the cToF-AMS data set, as the mass spectrometer was mistakenly re-tuned for this period, which caused problems for the factorisation. The changes in the instrumental settings were evident in the data as the concentrations of several of the factors derived from PMF analysis increased simultaneously with a step change in the heater bias. However, due to the nature of the affected factors and the timing of the instrumental changes, it was not possible to calculate a reliable scaling factor to apply to the data from this period. The reader is directed to Sects. 4.1 and 4.2 in the Supplement for more details regarding the data pre-treatment and quality assurance, including the identification and removal of problematic data around the summer IOP. In addition to the standard methods, isotopes were not included in the HR-ToF-AMS organic matrix. The peaks at m/z 30 and 46 were removed from the matrix, as they were not deemed to have been successfully retrieved using PIKA. APES light v1.05 (Sueper, 2008) was used for the elemental analysis of the HR-PMF factors.

4.2 Factorisation results

A 5-factor solution to the PMF analysis was shown to be optimum for the cToF-AMS data set. The details of the choice of factors and solution criteria can be found in the Supplement, Sect. 4.3. The reader is referred to Sect. 5 in the Supplement for the HR-ToF-AMS PMF (HR-PMF) solution criteria, where 5-factor solutions were chosen for both the winter and summer IOPs (Sects. 5.1 and 5.2 in the Supplement, respectively). The cToF-AMS PMF (cToF-PMF) solution criteria are briefly outlined here.

The 5-factor solution resulted in a better separation of the mass spectral profiles compared to the 4-factor solution, with improvements to diagnostics, such as Q/Q_{expected}, used to assess the quality and suitability of a solution set. The 6-factor solution was discarded due to the similarity of several factors (spectra and time series). The 7-factor solution was also discarded due to its significant dependency on the initialisation seed (unlike the solutions with fewer factors) as well as the production of a factor that did not appear physically meaningful. The "fPeak" parameter was used to explore the rotational ambiguity of the 5-factor solution with the most central solution (fPeak = 0) chosen for further analysis. Additional measurements were used to validate the chosen solution and for attribution of the factors.

Three of the five PMF factors were clearly identifiable: hydrocarbon-like OA (HOA), cooking OA (COA), and type 1 oxygenated OA (OOA1). As the remaining two factors (labelled here as SFOA_{PMF} and OOA2_{PMF}) exhibited similar temporal features, notably the diurnal pattern (Fig. 3) with an evening peak in concentration, they are investigated and addressed in detail in the following sections.

4.3 Identifying PMF limitations

The similarity of the diurnal patterns of SFOA_{PMF} and OOA2_{PMF} is likely due to the nature of the aerosols where SFOA_{PMF} is likely emitted from domestic space heating, an activity that occurs in the evening. OOA2_{PMF} is typically thought to be semi-volatile oxygenated OA (SV-OOA) and will preferentially partition to the particle phase when

temperatures are low and RH is high, again most likely in the evening. Conversely, the temporal co-variation of the PMF solution could result in partial mixing of these two factors (Crippa et al., 2013b) leading to the identification of an OOA2-BBOA factor (Crippa et al., 2013a). However, a clearer separation of such factors was obtained through combined AMS and Proton Transfer Reaction Mass Spectrometry (PTR-MS) PMF analysis (Crippa et al., 2013b).

The mass spectral profiles and time series of the cToF-PMF factors are compared to the winter IOP HR-PMF factors, as factor retrieval from HR-ToF-AMS data is more robust with significantly reduced rotational ambiguity and improved separation of factors as individual ion signals at the same nominal mass-to-charge ratio (m/z) are included (see Sect. 6 in the Supplement for comparisons of the mass spectra and time series from the winter and summer IOPs where available). In general, there is good correlation between most factors from the two instruments (Pearson's r of 0.69–0.90, Table 2). However, the concentration of the combined SFOA factors from the winter HR-PMF dataset is approximately double that of the cToF-PMF $SFOA_{PMF}$ factor. A near equal concentration of SFOA from both AMSs is achieved when the cToF-PMF $OOA2_{PMF}$ is combined with the $SFOA_{PMF}$ and correlated with the sum of HR-PMF SFOA factors. This suggests that some of the $SFOA_{PMF}$ mass measured by the cToF-AMS is being assigned to $OOA2_{PMF}$ in PMF; the total SFOA mass could therefore be a factor of two greater than previously estimated.

If SFOA represents all of levoglucosan and other similar species, we might expect good correlation between SFOA and levoglucosan to exist. As org60 (the organic fraction at m/z 60) has contributions from fatty acids arising from cooking POA emissions (Mohr et al., 2009) and carboxylic acids from SOA (e.g. DeCarlo et al., 2008), it is not expected that org60 and levoglucosan would correlate exactly when compared. $SFOA_{PMF}$ and $SFOA_{PMF} + OOA2_{PMF}$ are compared to 24 h filter measurements of levoglucosan from the winter IOP. $SFOA_{PMF} + OOA2_{PMF}$ correlates better with levoglucosan than $SFOA_{PMF}$ on its own (Pearson's r of 0.74 and 0.71 respectively), suggesting that some of the additional variance is carried by a levoglucosan contribu-

tion to $OOA2_{PMF}$. Furthermore, org60 correlates slightly better with levoglucosan than $SFOA_{PMF}$ (Pearson's $r = 0.73$), again suggesting that $SFOA_{PMF}$ is not capturing all the variability of levoglucosan. However, it is unlikely that this is the full explanation as the m/z 60 signal of $OOA2_{PMF}$ is relatively small.

This is not to suggest that all OOA2 factors contain some contribution of SFOA although, as we have shown, it is possible to estimate the proportion of SFOA convolved with OOA2 with the support of additional measurements. More representative results may be produced in the future from the application of ME-2 to similar data sets, particularly in the absence of supporting measurements, such as those from the ACSM. However, further work is therefore required to better resolve the issues arising from PMF analysis regarding the separation of OA in to its primary and secondary constituents, particularly for long-term data sets.

4.4 Estimating concentrations of convolved factors

We infer from the correlations discussed in Sect. 4.3 that nearly all the $SFOA_{PMF}$ is assigned to $OOA2_{PMF}$ during the winter IOP, where the proportion of $SFOA_{PMF}$ that is convolved with OOA_{PMF} can be determined using the relationship between $SFOA_{PMF}$ and OOA_{PMF} from the winter. Both factors have similar, strong diurnal profiles, the effect of which is reduced by using daily averages of each factor in the following equation:

$$OOA2_{PMF} = a \cdot SFOA_{PMF} + OOA2_{noSF} \quad (1)$$

where a is the gradient of an orthogonal distance regression fit, equal to 0.86, and $OOA2_{noSF}$ is the intercept which indicates the amount of $OOA2_{PMF}$ without a solid fuel signature. The remainder is the $SFOA_{PMF}$ assigned to $OOA2_{PMF}$ during the PMF analysis and is estimated based on the gradient of the fit. The SFOA and OOA2 concentrations, $SFOA_{mod}$ and $OOA2_{mod}$ respectively, can therefore be calculated using the

following equations:

$$SFOA_{mod} = SFOA_{PMF} + (a \cdot SFOA_{PMF}) \quad (2)$$

$$OOA2_{mod} = OOA2_{PMF} - (a \cdot SFOA_{PMF}) \quad (3)$$

The relationship based on the winter correlation does not hold true for the whole year and so the annual estimations are improved by using the relationship derived between the daily averages of $OOA2_{PMF}$ and $SFOA_{PMF}$ from December 2012–January 2013, where a is equal to 0.52. However, instrument maintenance (changes in instrument tuning during the summer and change of the MCP in April) will likely add some variation to these estimates. Therefore, the concentrations up until the summer period are estimated using the relationship from the 2012 winter IOP and the concentrations after the summer are estimated using the December 2012–January 2013 relationship. The estimated concentrations of $OOA2_{mod}$ and $SFOA_{mod}$ are used for further analyses. Figure 4 shows the retrieved $OOA2_{mod}$ is dominated by noise, with an average $OOA2_{mod}$ concentration of $0.12\,\mu g\,m^{-3}$ and standard deviation of $0.46\,\mu g\,m^{-3}$ during the winter IOP. The standard deviation provides a measure of uncertainty in our retrieval of $OOA2_{mod}$ and $SFOA_{mod}$ using this approach.

5 Attribution and contributions of organic components

Attributing the PMF factors to different organic sources and components allows the organic fraction to be split in to primary OA (POA) and secondary OA (SOA) and their contribution to total organic mass to be assessed. The behaviour of urban secondary OA (SOA) can then be investigated. The HOA, COA, and $SFOA_{mod}$ factors identified in the previous sections are grouped as primary OA (POA) and OOA1 and $OOA2_{mod}$ are grouped as secondary OA (SOA). The primary fraction is dominated by $SFOA_{mod}$ 38 % (Fig. 2), with smaller contributions from HOA (32 %) and COA (30 %). The secondary fraction is dominated by OOA1 (90 %) with only a small contribution from $OOA2_{mod}$ (10 %).

The greatest contribution of the organic components to total OA mass is from OOA1 (31 %), followed by $SFOA_{mod}$ (25 %), HOA (21 %), and COA (19 %). The remainder comprises $OOA2_{mod}$ (4 %). During 2012, POA and SOA contributed 65 % and 35 % to total OA, respectively (Fig. 2). However, the contribution of POA and SOA to total OA changes with season where SOA contributes just over 50 % on average during the spring and summer (Fig. 5). The smaller annual contribution from SOA could therefore be partly due to the omitted summer data, where SOA dominates the mass fraction.

5.1 The behaviour of secondary organic aerosol in London background air

The average (±one standard deviation) OOA1 concentration observed was 1.27 (± 1.49) $\mu g\,m^{-3}$, with a maximum 5 min concentration of $19.5\,\mu g\,m^{-3}$ measured on 24 May 2012. OOA1 does not exhibit a discernible diurnal pattern (Fig. 3), where the only change with season is by way of concentration (Fig. 6a), suggestive of aged aerosol of a regional nature. The peak in concentrations occurs in spring, where the average concentration is more than double that of the autumn and winter and 1.7 times greater than the summer (Fig. 6b). This spring time peak is consistent with secondary OC measurements in Birmingham (Harrison and Yin, 2008).

In comparison, the $OOA2_{mod}$ concentration averaged 0.14 (± 0.29) $\mu g\,m^{-3}$ over the year, with maximum daily concentrations occurring in the summer. The seasonal trend of $OOA2_{mod}$ is in keeping with it being secondary in nature with concentrations increasing during the summer (Fig. 6c) when photochemical processes and emissions of biogenic volatile organic compounds (VOCs) (Holmes et al., 2014) are greatest.

Several high concentration events lasting 3–8 days are observed in both OOA1 and $OOA2_{mod}$ time series (Fig. 4) such as in May (peaking on 27 May) and to a lesser extent September (peaking on 8–9 September). The event in May is associated mostly with Easterly conditions, likely the result of imported pollution. The September event is associated with a high-pressure system centred just off the SW UK coast with another high pressure system over continental Europe the following day. This resulted in an

increase in concentrations in a stagnant air mass with additional imported pollution on the 9 September.

5.2 SOA chemistry and oxidation state

SOA forms in the atmosphere from the gas-phase oxidation of a number of VOCs (e.g. Goldstein and Galbally, 2007), which can be anthropogenic or biogenic in origin. SOA comprises a mixture of organic compounds with differing volatilities (Donahue et al., 2012) which partition between the gas and particle phases. SOA therefore exists across a variety of chemical states thus increasing its chemical complexity. As bulk chemical characterization of aerosols can be obtained from the AMS, several metrics and graphical representations of the data are used to investigate OA. The information gleaned from such metrics can be used to better inform models on SOA characteristics to improve the quantification and prediction of SOA.

One such metric for describing and explaining OA evolution in the atmosphere is the f_{44} vs. f_{43} space (Morgan et al., 2010; Ng et al., 2010), where f_{44} and f_{43} are the ratios of the organic signal at m/z 44 and 43 to the total organic signal in the component mass spectrum, respectively. The degree of oxidation is inferred from the f_{44} value and the range of precursors is suggested by the f_{43} values. Other metrics include the use of O : C and H : C ratios in Van Krevelen space which reveals changes in functionality and therefore the likely degree of processing the aerosol has undergone (Heald et al., 2010). Kroll et al. (2011) combined these ratios to derive the oxidation state of carbon and thus describe OA chemistry. Furthermore, the chemical evolution of organic aerosol can be analysed by using the oxidation state along with volatility in the two-dimensional volatility-oxidation space (2-D-VBS, Donahue et al., 2012). Despite their differences, these metrics can all be used to describe the evolution of gas-phase organic compounds through to semi-volatile OA and up to the most oxidised OA with low volatility, concluding that atmospheric processing of fresh OA results in similarly aged and highly oxidised OA.

To characterise Northern Hemispheric OA and its evolution in the atmosphere, Ng et al. (2010) compiled ambient AMS data from numerous urban and rural ground-based measurement campaigns of varying duration (from a few days up to 5 weeks), occurring during different seasons. Morgan et al. (2010) investigated the organic chemical evolution through various airborne measurement campaigns, tracking individual air masses and crossing a range of European sites during different meteorological conditions. Data from both studies exhibited a range of f_{44} and f_{43} values, reflecting the different photochemical ages and sources. However, all data were found to lie within a very well defined triangular region in f_{44} vs. f_{43} space with OOA1 and OOA2 clustering in discrete regions of the triangular space. This indicated that irrespective of source, atmospheric processes result in the convergence of all ambient OA to chemically similar, highly aged SOA. The most processed OA, with high f_{44} values, in both studies were from rural/remote locations and generally occurred during the summer or during periods of elevated temperatures and greater photochemistry. To further investigate OA evolution and the corresponding changes in chemical composition Ng et al. (2011b) transformed the f_{44} vs. f_{43} triangle into the Van Krevelen diagram (so called VK-triangle). The ambient data from Ng et al. (2010) fall within a narrow range within the VK-triangle whereas two urban datasets from different seasons fall in a narrow linear area (El Haddad et al., 2013).

In contrast to the above studies, the measurements in this study are from a single location over the course of a year. In order to investigate trends within the secondary component of OA, the PMF-derived primary components ($SFOA_{mod}$, HOA, and COA) are subtracted from the total organic aerosol matrix with the remainder assumed to be secondary (hereafter termed SOA_{calc}). Furthermore, to assess the degree of oxidation of the SOA in London the contribution of the primary components to m/z 44 and 43 are subtracted, so the ratio of m/z 44 : SOA_{calc} to m/z 43 : SOA_{calc} can be determined. When plotted in f_{44} vs. f_{43} space, the majority of the data in this study falls within the triangular space defined by Ng et al. (2010) with the average value falling in the OOA1 region (Fig. 7). Along with the range of f_{44} values, correlations with temperature

and time can elucidate the extent to which the aerosol is oxidised, where in general, temperatures are elevated and photochemistry is greatest in the summer. Figure 7 illustrates the f_{44} vs. f_{43} space for SOA_{calc} coloured as a function of time (Fig. 7a) and temperature (Fig. 7b). SOA_{calc} exhibits little seasonality, where spring and summer averages have only a slightly higher ratio than autumn and winter, with this variation occurring within a distinct area of the f_{44} vs. f_{43} space. There is also little evidence for a temperature trend (Fig. 7b).

OOA1 and OOA2 are thought to represent end members of OA aging from photochemical processing (Jimenez et al., 2009), where OOA1 is more oxygenated and highly aged compared to the fresher and less-photochemically processed OOA2. The f_{44} and f_{43} for the two OOA components identified from PMF analysis in this study are therefore also plotted within the f_{44} vs. f_{43} space to further constrain the degree of oxidation of London SOA. The two subtypes are found to fall within their respective range of f_{44} values expected for each of the two subtypes, with higher f_{44} and f_{43} for OOA1 than OOA2. Using the relationship between f_{44} and O : C for unit mass resolution data from Aiken et al. (2008), the estimated O : C for the long-term $OOA2_{mod}$ and OOA1 factors are 0.36 and 0.79 respectively. In comparison, for the summer IOP there is only a small difference between the O : C ratio of OOA2 and OOA1 (0.44 and 0.52 respectively) obtained from HR-PMF. Here, OOA1 has a much lower ratio compared to other urban studies (e.g. Sun et al., 2011; Mohr et al., 2012).

While the concentration of SOA varies through the year, the extent of SOA oxidation shows no variability as a function of time of year or temperature and remains within a very narrow range of values. This could be explained, in part, by the geographical position of London, which leads to influences from both local sources and transported air masses from all directions. SOA in London forms from a variety of precursors across the year (Holmes et al., 2014) where the contributions of different precursors will change significantly with season. In addition, the greater photochemistry during the summer results in an increase in SOA mass. However, the fraction of oxygen per molecule does not vary as the increase in locally produced fresh SOA likely masks any

increase in the oxidation of transported material resulting in chemically similar SOA throughout the year. Whether this extends to similar urban background sites in other locations remains to be determined but if so, it makes a characterisation of SOA in urban environments more straightforward than may be previously supposed, as the range of precursors and processes appears to lead to consistent average characteristics.

6 Pollution events in London

Acute and short-term exposures to particulates have been associated with various adverse health effects including cardiovascular mortality as well as exacerbating existing illnesses such as pulmonary disease (Pope and Dockery, 2006 and references therein). It is therefore important to investigate episodic pollution events to better understand their effects on human health. During 2012, the average total $NR\text{-}PM_1$ concentration (±one standard deviation) was 9.91 (±10.39) $\mu g\,m^{-3}$ in London, with slightly higher concentrations in the winter than summer (Fig. 8a). Several pollution events occurred throughout the year where the contributions to the high concentrations differed for each of the $NR\text{-}PM_1$ components depending on the time of year. To determine whether emissions or atmospheric processes are the controlling factor in driving such high concentration events, the contributions of the different species to the top 10th percentile of the total annual concentration are assessed (Fig. 8a and b). Furthermore, the top 10th percentile of the winter and summer periods (Fig. 8c and d, respectively) are also analysed to evaluate any seasonal changes in the dominant species and sources.

Secondary aerosols are found to dominate throughout the year (Fig. 8b), irrespective of season, although the individual contributions from SIA and SOA change between winter and summer (Fig. 8c and d). High concentration events are dominated by nitrate in the winter (39 %), with a greater contribution from POA than SOA to the organic fraction (79 % and 21 %, respectively). Furthermore, $SFOA_{mod}$ is the greatest component of POA (43 %) and total organic fraction (34 %). In contrast, the high concentration events are dominated by organics (54 %), with a significant contribution from SOA

(47 %), although POA is still the dominant component of the organic fraction (53 %). Nevertheless, the largest contribution to the organic fraction is from OOA1 (42 %).

Pollution events in the winter are therefore driven by particulate emissions, especially nitrate and SFOA, whereas in the summer greater photochemistry results in higher concentrations predominantly comprised of SOA. Furthermore, the average mass of the pollution events in the winter is greater than that of the summer, suggesting that the limits for daily average concentrations, set to improve air quality and protect human health, are more likely to be exceeded in the winter than summer. Therefore, moderating sources of particulates is likely to be the most effective way of reducing particulates in the winter, although this does not consider the refractory sources of aerosol, such as black carbon, which contribute to the total PM mass in urban areas (e.g. Liu et al., 2014).

7 Conclusions

A full calendar year of NR-PM_1 chemical composition data were acquired using a cToF-AMS at an urban background site in North Kensington, London, where secondary aerosols comprise approximately 71 % of the total non-refractory submicron mass. Nitrate exhibited strong seasonality, peaking in the spring as a result of favourable local meteorological conditions and a peak in ammonia emissions. Several high nitrate concentration events occurred throughout the year, which were the result of a combination of ambient conditions, availability of precursors, and air mass trajectory. Contrastingly, sulphate concentrations in London are predominantly influenced by regional pollution with few or no local sources and ammonium concentrations are governed by the availability of precursor emissions and meteorological conditions. Non-refractory chloride concentrations peak in the winter, governed by the lower temperatures favouring ammonium chloride partitioning to the aerosol phase.

The organic fraction was separated into five factors using PMF analysis: HOA, COA, $SFOA_{PMF}$, OOA1 and $OOA2_{PMF}$. However, PMF was unable to account for the vari-

ance of two factors across the year, resulting in the assignment of some $SFOA_{PMF}$ mass to OOA_{PMF} as indicated by comparison of the factors derived from cToF-PMF and HR-PMF during the winter IOP. Based on the relationship between $SFOA_{PMF}$ and $OOA2_{PMF}$ from the winter at the start and end of 2012, daily concentrations of $SFOA_{mod}$ and $OOA2_{mod}$ were calculated for the year. OOA1 exhibited characteristics consistent with regional behaviour whereas $OOA2_{mod}$ exhibited a seasonal trend typical of SOA, peaking in the summer when VOC emissions and photochemistry are greatest.

Although there is a substantial change in the concentration of SOA through the year, the extent of oxidation of the SOA, as defined by the oxygen content of organic aerosol mass, shows no variability as a function of time of year, air mass history, or temperature at the site. This suggests that in the urban background of London the range of precursors and chemical processing are insufficiently variable to yield secondary organic aerosol that has been exposed to significantly different levels of chemical processing. This is surprising given the variation in precursors throughout the year and the strong annual cycle in photochemical activity. However, this could make characterisation of SOA in urban environments more straightforward than may be previously supposed, as the range of precursors and processes appears to lead to consistent average characteristics.

Several high concentration events occurred in London during 2012, driven by particulate emissions in the winter and formation of SOA in the summer due to the greater photochemistry. The limits for daily average concentrations set to improve air quality and protect human health are more likely to be exceeded in the winter as the events had a greater average mass than those in summer. Moderating sources of nitrate and POA is likely to be the most effective way of reducing particulates in the winter, and due to the dominance of this season to the annual mean, for the whole year. SFOA, COA, and HOA all make a substantial contribution to the POA fraction; however SFOA, along with COA, are less well characterised than HOA so their variability requires further investigation.

Data availability

Processed data are available through the ClearfLo project archive at the British Atmospheric Data Centre (http://badc.nerc.ac.uk/browse/badc/clearflo). Raw data are archived at the University of Manchester and are available on request.

The Supplement related to this article is available online at doi:10.5194/acpd-14-18739-2014-supplement.

Acknowledgements. This work was supported in part by the UK Natural Environment Research Council (NERC) ClearfLo project (grant ref. NE/H008136/1) and is co-ordinated by the National Centre for Atmospheric Science (NCAS). Additional support for the aerosol measurements was provided by the Department of Environment, Food and Rural Affairs (DEFRA). D. E. Young was supported by a NERC PhD studentship (ref. NE/I528142/1). The authors would like to thank Anja Tremper at King's College London for assisting with instrument maintenance and James Lee from NCAS at the University of York for logistical assistance at the North Kensington supersite during the IOPs. Additional thanks to the Sion Manning School in North Kensington and adjacent community centre.

References

Abdalmogith, S. S. and Harrison, R. M.: The use of trajectory cluster analysis to examine the long-range transport of secondary inorganic aerosol in the UK, Atmos. Environ., 39, 6686–6695, doi:10.1016/j.atmosenv.2005.07.059, 2005.

Abdalmogith, S. S. and Harrison, R. M.: An analysis of spatial and temporal properties of daily sulphate, nitrate and chloride concentrations at UK urban and rural sites, J. Environ. Monitor., 8, 691–699, 2006.

Aiken, A. C., DeCarlo, P. F., Kroll, J. H., Worsnop, D. R., Huffman, J. A., Docherty, K. S., Ulbrich, I. M., Mohr, C., Kimmel, J. R., Sueper, D., Sun, Y., Zhang, Q., Trimborn, A., Northway, M., Ziemann, P. J., Canagaratna, M. R., Onasch, T. B., Alfarra, M. R., Prevot, A. S. H., Dommen, J., Duplissy, J., Metzger, A., Baltensperger, U., and Jimenez, J. L.:

O/C and OM/OC ratios of primary, secondary, and ambient organic aerosols with high resolution time-of-flight aerosol mass spectrometry, Environ. Sci. Technol., 42, 4478–4485, doi:10.1021/es703009q, 2008.

Allan, J. D., Jimenez, J. L., Williams, P. I., Alfarra, M. R., Bower, K. N., Jayne, J. T., Coe, H., and Worsnop, D. R.: Quantitative sampling using an Aerodyne aerosol mass spectrometer: 1. Techniques of data interpretation and error analysis, J. Geophys. Res.-Atmos., 108, 4090, doi:10.1029/2002JD002358, 2003.

Allan, J. D., Williams, P. I., Morgan, W. T., Martin, C. L., Flynn, M. J., Lee, J., Nemitz, E., Phillips, G. J., Gallagher, M. W., and Coe, H.: Contributions from transport, solid fuel burning and cooking to primary organic aerosols in two UK cities, Atmos. Chem. Phys., 10, 647–668, doi:10.5194/acp-10-647-2010, 2010.

Ansari, A. S. and Pandis, S. N.: Response of inorganic PM to precursor concentrations, Environ. Sci. Technol., 32, 2706–2714, 1998.

Aphekom Summary Report: Aphekom – Summary Report of the Aphekom Project 2008–2011, 2011.

AQEG: Fine Particulate Matter ($PM_{2.5}$) in the United Kingdom, Report of the UK Air Quality Expert Group, Prepared for: Department for Environment, Food and Rural Affairs; Scottish Executive; Welsh Government; and Department of the Environment in Northern Ireland, 2012.

Bigi, A. and Harrison, R. M.: Analysis of the air pollution climate at a central urban background site, Atmos. Environ., 44, 2004–2012, 2010.

Bohnenstengel, S. I., Belcher, S. E., Aiken, A. C., Allan, J. D., Allen, G., Bacak, A., Bannan, T. J., Barlow, J. F., Beddows, D. C. S., Bloss, W. J., Booth, A. M., Chemel, C., Coceal, O., Di Marco, C. F., Mavendra, D. K., Faloon, K. H., Fleming, Z., Furger, M., Geitl, J. K., Graves, R. R., Green, D. C., Grimmond, C. S. B., Halios, C., Hamilton, J. F., Harrison, R. M., Heal, M. R., Heard, D. E., Helfter, C., Herndon, S. C., Holmes, R. E., Hopkins, J. R., Jones, A. M., Kelly, F. J., Kotthaus, S., Langford, B., Lee, J. D., Leigh, R. J., Lewis, A. C., Lidster, R. T., Lopez-Hilfiker, F. D., McQuaid, J. B., Mohr, C., Monks, P. S., Nemitz, E., Ng, N. L., Percival, C. J., Prévôt, A. S. H., Ricketts, H. M. A., Sokhi, R., Stone, D., Thornton, J. A., Tremper, A. H., Valach, A. C., Visser, S., Whalley, L. K., Williams, L. R., Xu, L., Young, D. E., and Zotter, P.: Meteorology, air quality and health in London: the ClearfLo project, B. Am. Meteorol. Soc., in press, 2014.

Boucher, O., Randall, D., Artaxo, P., Bretherton, C., Feingold, G., Forster, P., Kerminen, V.-M., Kondo, Y., Liao, H., Lohmann, U., Rasch, P., Satheesh, S. K., Sherwood, S., Stevens, B.

and Zhang, X. Y.: Clouds and aerosols, in: Climate Change 2013: The Physical Science Basis. Contribution of Working Group I to the Fifth Assessment Report of the Intergovernmental Panel on Climate Change, edited by: Stocker, T. F., Qin, D., Plattner, G.-K., Tignor, M., Allen, S. K., Boschung, J., Nauels, A., Xia, Y., Bex, V., and Midgley, P. M., Cambridge University Press, Cambridge, UK and New York, NY, USA, 2013.

Bressi, M., Sciare, J., Ghersi, V., Bonnaire, N., Nicolas, J. B., Petit, J.-E., Moukhtar, S., Rosso, A., Mihalopoulos, N., and Féron, A.: A one-year comprehensive chemical characterisation of fine aerosol ($PM_{2.5}$) at urban, suburban and rural background sites in the region of Paris (France), Atmos. Chem. Phys., 13, 7825–7844, doi:10.5194/acp-13-7825-2013, 2013.

Canagaratna, M. R., Jayne, J. T., Jimenez, J. L., Allan, J. D., Alfarra, M. R., Zhang, Q., Onasch, T. B., Drewnick, F., Coe, H., Middlebrook, A., Delia, A. E., Williams, L. R., Trimborn, A. M., Northway, M. J., Decarlo, P. F., Kolb, C. E., Davidovits, P., and Worsnop, D. R.: Chemical and microphysical characterization of ambient aerosols with the aerodyne aerosol mass spectrometer, Mass Spectrom. Rev., 26, 185–222, doi:10.1002/mas.20115, 2007.

Canonaco, F., Crippa, M., Slowik, J. G., Baltensperger, U., and Prévôt, A. S. H.: SoFi, an Igor based interface for the efficient use of the generalized multilinear engine (ME-2) for source apportionment: application to aerosol mass spectrometer data, Atmos. Meas. Tech. Discuss., 6, 6409–6443, doi:10.5194/amtd-6-6409-2013, 2013.

Charron, A., Harrison, R. M., and Quincey, P.: What are the sources and conditions responsible for exceedences of the 24 h PM_{10} limit value (50 µg m^{-3}) at a heavily trafficked London site?, Atmos. Environ., 41, 1960–1975, 2007.

Crippa, M., DeCarlo, P. F., Slowik, J. G., Mohr, C., Heringa, M. F., Chirico, R., Poulain, L., Freutel, F., Sciare, J., Cozic, J., Di Marco, C. F., Elsasser, M., Nicolas, J. B., Marchand, N., Abidi, E., Wiedensohler, A., Drewnick, F., Schneider, J., Borrmann, S., Nemitz, E., Zimmermann, R., Jaffrezo, J.-L., Prévôt, A. S. H., and Baltensperger, U.: Wintertime aerosol chemical composition and source apportionment of the organic fraction in the metropolitan area of Paris, Atmos. Chem. Phys., 13, 961–981, doi:10.5194/acp-13-961-2013, 2013a.

Crippa, M., Canonaco, F., Slowik, J. G., El Haddad, I., DeCarlo, P. F., Mohr, C., Heringa, M. F., Chirico, R., Marchand, N., Temime-Roussel, B., Abidi, E., Poulain, L., Wiedensohler, A., Baltensperger, U., and Prévôt, A. S. H.: Primary and secondary organic aerosol origin by combined gas-particle phase source apportionment, Atmos. Chem. Phys., 13, 8411–8426, doi:10.5194/acp-13-8411-2013, 2013b.

Cross, E. S., Slowik, J. G., Davidovits, P., Allan, J. D., Worsnop, D. R., Jayne, J. T., Lewis, D. K., Canagaratna, M., and Onasch, T. B.: Laboratory and ambient particle density determinations using light scattering in conjunction with aerosol mass spectrometry, Aerosol Sci. Tech., 41, 343–359, 2007.

Dall'Osto, M., Ovadnevaite, J., Ceburnis, D., Martin, D., Healy, R. M., O'Connor, I. P., Kourtchev, I., Sodeau, J. R., Wenger, J. C., and O'Dowd, C.: Characterization of urban aerosol in Cork city (Ireland) using aerosol mass spectrometry, Atmos. Chem. Phys., 13, 4997–5015, doi:10.5194/acp-13-4997-2013, 2013.

DeCarlo, P. F., Kimmel, J. R., Trimborn, A., Northway, M. J., Jayne, J. T., Aiken, A. C., Gonin, M., Fuhrer, K., Horvath, T., Docherty, K. S., Worsnop, D. R., and Jimenez, J. L.: Field-deployable, high-resolution, time-of-flight aerosol mass spectrometer, Anal. Chem., 78, 8281–8289, doi:10.1021/ac061249n, 2006.

DeCarlo, P. F., Dunlea, E. J., Kimmel, J. R., Aiken, A. C., Sueper, D., Crounse, J., Wennberg, P. O., Emmons, L., Shinozuka, Y., Clarke, A., Zhou, J., Tomlinson, J., Collins, D. R., Knapp, D., Weinheimer, A. J., Montzka, D. D., Campos, T., and Jimenez, J. L.: Fast airborne aerosol size and chemistry measurements above Mexico City and Central Mexico during the MILAGRO campaign, Atmos. Chem. Phys., 8, 4027–4048, doi:10.5194/acp-8-4027-2008, 2008.

Donahue, N. M., Kroll, J. H., Pandis, S. N., and Robinson, A. L.: A two-dimensional volatility basis set – Part 2: Diagnostics of organic-aerosol evolution, Atmos. Chem. Phys., 12, 615–634, doi:10.5194/acp-12-615-2012, 2012.

Drewnick, F., Hings, S. S., Decarlo, P. F., Jayne, J. T., Gonin, M., Fuhrer, K.,Weimer, S., Jimenez, J. L., Demerjian, K. L., Borrmann, S., and Worsnop, D. R.: A new time-of-flight aerosol mass spectrometer (TOF-AMS) – instrument description and first field deployment, Aerosol Sci. Tech., 39, 637–658, doi:10.1080/02786820500182040, 2005.

EEA: The European Environment – State and Outlook 2010: Synthesis, European Environment Agency, Copenhagen, 2010.

European Union: Directive 2008/50/EC of the European parliament and of the council of 21 May 2008 on ambient air quality and cleaner air for Europe, Official Journal of the European Union, L152, 2008.

El Haddad, I., Marchand, N., D'Anna, B., Jaffrezo, J.-L., and Wortham, H.: Functional group composition of organic aerosol from combustion emissions and sec-

ondary processes at two contrasted urban environments, Atmos. Environ., 75, 308–320, doi:10.1016/j.atmosenv.2013.04.019, 2013.

Freutel, F., Schneider, J., Drewnick, F., von der Weiden-Reinmüller, S.-L., Crippa, M., Prévôt, A. S. H., Baltensperger, U., Poulain, L., Wiedensohler, A., Sciare, J., Sarda-Estève, R., Burkhart, J. F., Eckhardt, S., Stohl, A., Gros, V., Colomb, A., Michoud, V., Doussin, J. F., Borbon, A., Haeffelin, M., Morille, Y., Beekmann, M., and Borrmann, S.: Aerosol particle measurements at three stationary sites in the megacity of Paris during summer 2009: meteorology and air mass origin dominate aerosol particle composition and size distribution, Atmos. Chem. Phys., 13, 933–959, doi:10.5194/acp-13-933-2013, 2013.

Goldstein, A. H., and Galbally, I. E.: Known and unexplored organic constituents in the Earth's atmosphere, Environ. Sci. Technol., 41, 1515–1521, 2007.

Harrison, R. M. and Yin, J.: Sources and processes affecting carbonaceous aerosol in central England, Atmos. Environ., 42, 1413–1423, 2008.

Harrison, R. M., Dall'Osto, M., Beddows, D. C. S., Thorpe, A. J., Bloss, W. J., Allan, J. D., Coe, H., Dorsey, J. R., Gallagher, M., Martin, C., Whitehead, J., Williams, P. I., Jones, R. L., Langridge, J. M., Benton, A. K., Ball, S. M., Langford, B., Hewitt, C. N., Davison, B., Martin, D., Petersson, K. F., Henshaw, S. J., White, I. R., Shallcross, D. E., Barlow, J. F., Dunbar, T., Davies, F., Nemitz, E., Phillips, G. J., Helfter, C., Di Marco, C. F., and Smith, S.: Atmospheric chemistry and physics in the atmosphere of a developed megacity (London): an overview of the REPARTEE experiment and its conclusions, Atmos. Chem. Phys., 12, 3065–3114, doi:10.5194/acp-12-3065-2012, 2012.

Heald, C. L., Kroll, J. H., Jimenez, J. L., Docherty, K. S., DeCarlo, P. F., Aiken, A. C., Chen, Q., Martin, S. T., Farmer, D. K., and Artaxo, P.: A simplified description of the evolution of organic aerosol composition in the atmosphere, Geophys. Res. Lett., 37, L08803, doi:10.1029/2010GL042737, 2010.

Holmes, R. E., Hopkins, J. R., Lidster, R. T., Lee, J. D., Evans, M. J., Lewis, A. C., and Hamilton, J. F.: Diesel-related hydrocarbons dominate reactive carbon in modern megacity atmospheres, in preparation, 2014.

Huffman, J. A., Ziemann, P. J., Jayne, J. T., Worsnop, D. R., and Jimenez, J. L.: Development and Characterization of a Fast-Stepping/Scanning Thermodenuder for Chemically-Resolved Aerosol Volatility Measurements, Aerosol Sci. Technol., 42, 395–407, 2008.

Jayne, J. T., Leard, D. C., Zhang, X. F., Davidovits, P., Smith, K. A., Kolb, C. E., and Worsnop, D. R.: Development of an aerosol mass spectrometer for size

and composition analysis of submicron particles, Aerosol Sci. Tech., 33, 49–70, doi:10.1080/027868200410840, 2000.

Jimenez, J. L., Canagaratna, M. R., Donahue, N. M., Prevot, A. S. H., Zhang, Q., Kroll, J. H., Decarlo, P. F., Allan, J. D., Coe, H., Ng, N. L., Aiken, A. C., Docherty, K. S., Ulbrich, I. M., Grieshop, A. P., Robinson, A. L., Duplissy, J., Smith, J. D., Wilson, K. R., Lanz, V. A., Hueglin, C., Sun, Y. L., Tian, J., Laaksonen, A., Raatikainen, T., Rautiainen, J., Vaattovaara, P., Ehn, M., Kulmala, M., Tomlinson, J. M., Collins, D. R., Cubison, M. J., E., Dunlea, E. J., Huffman, J. A., Onasch, T. B., Alfarra, M. R., Williams, P. I., Bower, K. N., Kondo, Y., Schneider, J., Drewnick, F., Borrmann, S., Weimer, S., Demerjian, K. L., Salcedo, D., Cottrell, L., Griffin, R., Takami, A., Miyoshi, T., Hatakeyama, S., Shimono, A., Sun, J. Y., Zhang, Y. M., Dzepina, K., Kimmel, J. R., Sueper, D., Jayne, J. T., Herndon, S. C., Trimborn, A. M.,Williams, L. R.,Wood, E. C., Middlebrook, A. M.,Kolb, C. E., Baltensperger, U., and Worsnop, D. R.: Evolution of organic aerosols in the atmosphere, Science, 326, 1525–1529, doi:10.1126/science.1180353, 2009.

Kroll, J. H., Donahue, N. M. Jimenez, J. L., Kessler, S. H., Canagaratna, M. R., Wilson, K. R., Altieri, K. E., Mazzoleni, L. R., Wozniak, A. S., Bluhm, H., Mysak, E. R., Smith, J. D., Kolb, C. E., and Worsnop, D. R.: Carbon oxidation state as a metric for describing the chemistry of atmospheric organic aerosol, Nat. Chem., 3, 133–139, doi:10.1038/NCHEM.948, 2011.

Lanz, V. A., Alfarra, M. R., Baltensperger, U., Buchmann, B., Hueglin, C., and Prévôt, A. S. H.: Source apportionment of submicron organic aerosols at an urban site by factor analytical modelling of aerosol mass spectra, Atmos. Chem. Phys., 7, 1503–1522, doi:10.5194/acp-7-1503-2007, 2007.

Lanz, V. A., Alfarra, M. R., Baltensperger, U., Buchmann, B., Hueglin, C., Szidat, S., Wehrli, M. N., Wacker, L., Weimer, S., Caseiro, A., Puxbaum, H., and Prévôt, A. S. H.: Source attribution of submicron organic aerosols during wintertime inversions by advanced factor analysis of aerosol mass spectra, Environ. Sci. Technol., 42, 214–220, doi:10.1021/es0707207, 2008.

Liu, D., Allan, J. D., Young, D. E., Coe, H. Beddows, D., Fleming, Z. L., Flynn, M. J., Gallagher, M. W., Harrison, R. M., Lee, J., Prévôt, A. S. H., Taylor, J. W., Yin, J., Williams, P. I., and Zotter, P.: Size distribution, mixing state and source apportionments of black carbon aerosols in London during winter time, Atmos. Chem. Phys. Discuss., 14, 16291–16349, doi:10.5194/acpd-14-16291-2014, 2014.

Martin, C. L., Allan, J. D., Crosier, J., Choularton, T. W., Coe, H., and Gallagher, M. W.: Seasonal variation of fine particulate composition in the centre of a UK city, Atmos. Environ., 45, 4379–4389, doi:10.1016/j.atmosenv.2011.05.050, 2011.

Megaritis, A. G., Fountoukis, C., Charalampidis, P. E., Pilinis, C., and Pandis, S. N.: Response of fine particulate matter concentrations to changes of emissions and temperature in Europe, Atmos. Chem. Phys., 13, 3423–3443, doi:10.5194/acp-13-3423-2013, 2013.

Middlebrook, A. M., Bahreini, R., Jimenez, J. L., and Canagaratna, M. R.: Evaluation of composition-dependent collection efficiencies for the Aerodyne aerosol mass spectrometer using field data, Aerosol Sci. Tech., 46, 258–271, doi:10.1080/02786826.2011.620041, 2012.

Mohr, C., Huffman, J. A., Cubison, M. J., Aiken, A. C., Docherty, K. S., Kimmel, J. R., Ulbrich, I. M., Hannigan, M., Garcia, J., and Jimenez, J. L.: Characterization of primary organic aerosol emissions from meat cooking, trash burning, and motor vehicles with high-resolution aerosol mass spectrometry and comparison with ambient and chamber observations, Environ. Sci. Technol., 43, 2443–2449, doi:10.1021/es8011518, 2009.

Mohr, C., DeCarlo, P. F., Heringa, M. F., Chirico, R., Slowik, J. G., Richter, R., Reche, C., Alastuey, A., Querol, X., Seco, R., Peñuelas, J., Jiménez, J. L., Crippa, M., Zimmermann, R., Baltensperger, U., and Prévôt, A. S. H.: Identification and quantification of organic aerosol from cooking and other sources in Barcelona using aerosol mass spectrometer data, Atmos. Chem. Phys., 12, 1649–1665, doi:10.5194/acp-12-1649-2012, 2012.

Monks, P. S., Granier, C., Fuzzi, S., Stohl, A., Williams, M. L., Akimoto, H., Amann, M., Baklanov, A., Baltensperger, U., Bey, I., Blake, N., Blake, R. S., Carslaw, K. S., Cooper, O. R., Dentener, F. J., Fowler, D., Fragkou, E., Frost, G. J., Generoso, S., Ginoux, P., Grewe, V., Guenther, A., Hansson, H. C., Henne, S., Hjorth, J., Hofzumahaus, A., Huntrieser, H., Isaksen, I. S. A., Jenkin, M. E., Kaiser, J., Kanakidou, M., Klimont, Z., Kulmala, M., Laj, P., Lawrence, M. G., Lee, J. D., Liousse, C., Maione, M., McFiggans, G. B., Metzger, A., Mieville, A., Moussiopoulos, N., Orlando, J. J., O'Dowd, C. D., Palmer, P. I., Parrish, D. D., Petzold, A., Platt, U., Pöschl, U., Prévôt, A. S. H., Reeves, C. E., Reimann, S., Rudich, Y., Sellegri, K., Steinbrecher, R., Simpson, D., ten Brink, H., Theloke, J., van Der Werf, G. R., Vautard, R., Vestreng, V., Vlachokostas, C., and von Glasow, R.: Atmospheric composition change – global and regional air quality, Atmos. Environ., 43, 5268–5350, doi:10.1016/j.atmosenv.2009.08.021, 2009.

Morgan, W. T., Allan, J. D., Bower, K. N., Capes, G., Crosier, J., Williams, P. I., and Coe, H.: Vertical distribution of sub-micron aerosol chemical composition from North-Western Europe and the North-East Atlantic, Atmos. Chem. Phys., 9, 5389–5401, doi:10.5194/acp-9-5389-2009, 2009.

Morgan, W. T., Allan, J. D., Bower, K. N., Highwood, E. J., Liu, D., McMeeking, G. R., Northway, M. J., Williams, P. I., Krejci, R., and Coe, H.: Airborne measurements of the spatial distribution of aerosol chemical composition across Europe and evolution of the organic fraction, Atmos. Chem. Phys., 10, 4065–4083, doi:10.5194/acp-10-4065-2010, 2010.

National atmospheric emissions inventory (NAEI): http://naei.defra.gov.uk/ (last access: 24 December 2013), 2013.

Ng, N. L., Canagaratna, M. R., Zhang, Q., Jimenez, J. L., Tian, J., Ulbrich, I. M., Kroll, J. H., Docherty, K. S., Chhabra, P. S., Bahreini, R., Murphy, S. M., Seinfeld, J. H., Hildebrandt, L., Donahue, N. M., DeCarlo, P. F., Lanz, V. A., Prévôt, A. S. H., Dinar, E., Rudich, Y., and Worsnop, D. R.: Organic aerosol components observed in Northern Hemispheric datasets from Aerosol Mass Spectrometry, Atmos. Chem. Phys., 10, 4625–4641, doi:10.5194/acp-10-4625-2010, 2010.

Ng, N. L., Herndon, S. C., Trimborn, A., Canagaratna, M. R., Croteau, P., Onasch, T. M., Sueper, D., and Worsnop, D. R.: An Aerosol Chemical Speciation Monitor (ACSM) for routine monitoring of atmospheric aerosol composition, Aerosol Sci. Tech., 45, 770–784, 2011a.

Ng, N. L., Canagaratna, M. R., Jimenez, J. L., Chhabra, P. S., Seinfeld, J. H., and Worsnop, D. R.: Changes in organic aerosol composition with aging inferred from aerosol mass spectra, Atmos. Chem. Phys., 11, 6465–6474, doi:10.5194/acp-11-6465-2011, 2011b.

Oberdörster, G., Oberdörster, E., and Oberdörster, J.: Nanotoxicology: an emerging discipline evolving from studies of ultrafine particles, Environ. Health Persp., 113, 823–839, 2005.

Paatero, P. and Tapper, U.: Positive matrix factorization – a nonnegative factor model with optimal utilization of error-estimates of data values, Environmetrics, 5, 111–126, 1994.

Pöschl, U.: Atmospheric aerosols: composition, transformation, climate and health effects, Angew. Chem. Int. Ed., 44, 7520–7540, 2005.

Pope III, C. A. and Dockery, D. W.: Health effects of fine particulate air pollution: lines that connect, J. Air Waste Manage., 56, 709–742, doi:10.1080/10473289.2006.10464485, 2006.

Schaap, M., van Loon, M., ten Brink, H. M., Dentener, F. J., and Builtjes, P. J. H.: Secondary inorganic aerosol simulations for Europe with special attention to nitrate, Atmos. Chem. Phys., 4, 857–874, doi:10.5194/acp-4-857-2004, 2004.

Seinfeld, J. H. and Pandis, S. N.: Atmospheric Chemistry and Physics: from Air Pollution to Climate Change, second edn., John Wiley & Sons, New York, 2006.

Stelson, A. and Seinfeld, J.: Relative humidity and temperature dependence of the ammonium nitrate dissociation constant, Atmos. Environ., 16, 983–992, doi:10.1016/j.atmosenv.2007.10.063, 1982.

Sueper, D.: ToF-AMS High Resolution Analysis Software – Pika, available at: http://cires.colorado.edu/jimenez-group/ToFAMSResources/ToFSoftware/index.html 2008.

Sun, Y.-L., Zhang, Q., Schwab, J. J., Demerjian, K. L., Chen, W.-N., Bae, M.-S., Hung, H.-M., Hogrefe, O., Frank, B., Rattigan, O. V., and Lin, Y.-C.: Characterization of the sources and processes of organic and inorganic aerosols in New York city with a high-resolution time-of-flight aerosol mass apectrometer, Atmos. Chem. Phys., 11, 1581–1602, doi:10.5194/acp-11-1581-2011, 2011.

Sun, Y. L., Wang, Z. F., Fu, P. Q., Yang, T., Jiang, Q., Dong, H. B., Li, J., and Jia, J. J.: Aerosol composition, sources and processes during wintertime in Beijing, China, Atmos. Chem. Phys., 13, 4577–4592, doi:10.5194/acp-13-4577-2013, 2013.

Sutton, M. A., Dragosits, U. Tang, Y. S., and Fowler, D.: Ammonia emissions from non-agricultural sources in the UK, Atmos. Environ., 34, 855–869, 2000.

Takegawa, N., Miyakawa, T., Kondo, Y., Jimenez, J. L., Zhang, Q., Worsnop, D. R., and Fukuda, M.: Seasonal and diurnal variations of submicron organic aerosol in Tokyo observed using the Aerodyne aerosol mass spectrometer, J. Geophys. Res., 111, D11206, doi:10.1029/2005JD006515, 2006.

Ulbrich, I. M., Canagaratna, M. R., Zhang, Q., Worsnop, D. R., and Jimenez, J. L.: Interpretation of organic components from Positive Matrix Factorization of aerosol mass spectrometric data, Atmos. Chem. Phys., 9, 2891–2918, doi:10.5194/acp-9-2891-2009, 2009.

Wagener, S., Langner, M., Hansen, U., Moriske, H. J. and Endlicher, W. R.: Spatial and seasonal variations of biogenic tracer compounds in ambient PM_{10} and PM_1 samples in Berlin, Germany, Atmos. Environ., 47, 33–42, 2012.

Watson, J. G.: Visibility: science and regulation, J. Air Waste Manage., 52, 628–713, doi:10.1080/10473289.2002.10470813, 2002.

WHO: Air Quality Guidelines, Global update 2005, Particulate matter, ozone, nitrogen dioxide and sulphur dioxide, World Health Organization European Office, Copenhagen, 2005.

Yin, J., Harrison, R. M., Chen, Q., Rutter, A. and Schauer, J. J.: Source apportionment of fine particles at urban background and rural sites in the UK atmosphere, Atmos. Environ., 44, 841–851, 2010.

Zhang, Q., Jimenez, J. L., Canagaratna, M. R., Allan, J. D., Coe, H., Ulbrich, I., Alfarra, M. R., Takami, A., Middlebrook, A. M., Sun, Y. L., Dzepina, K., Dunlea, E. J., Docherty, K. S., Decarlo, P. F., Salcedo, D., Onasch, T., Jayne, J. T., Miyoshi, T., Shimono, A., Hatakeyama, S., Takegawa, N., Kondo, Y., Schneider, J., Drewnick, F., Borrmann, S., Weimer, S., Demerjian, K. L., Williams, P., Bower, K. N., Bahreini, R., Cottrell, L., Griffin, R. J., Rautiainen, J., Sun, J. Y., Zhang, Y. M., and Worsnop, D. R.: Ubiquity and dominance of oxygenated species in organic aerosols in anthropogenically-influenced Northern Hemisphere midlatitudes, Geophys. Res. Lett., 34, L13801, doi:10.1029/2007GL029979, 2007.

Table 1. Average annual sulphate concentrations (in $\mu g\,m^{-3}$) from two UK locations measured between 2001 and 2012 as part of the AURN and Particulates networks. London North Kensington is an urban background monitoring site and Harwell is a rural background monitoring site.

Year	Location	
	London North Kensington	Harwell
2012	1.39[a], 1.21[b,d]	–
2011	2.2[b]	–
2010	2.3[c]	1.6[c]
2009	1.7[c]	1.3[c]
2008	2.6[c]	2.4[c]
2007	2.8[c]	2.4[c]
2006	3.5[c]	3[c]
2005	3[c]	2.4[c]
2004	3[c]	2.3[c]
2003	2.6[c]	2.4[c]
2002	3.1[c]	2.3[c]
2001	3.1[c]	2.1[c]

[a] AMS (PM_1), ClearfLo, this study.
[b] URG 9000B Ambient Ion Monitor (AIM) (PM_{10}), KCL (Courtesy of Dr. D. Green).
[c] Thermo Scientific Partisol 2025 ion chromatography (PM_{10}), KCL (Courtesy of Dr. D. Green).
[d] Calculated non-sea salt sulphate.

Table 2. Time series comparison of the PMF factors from the cToF-AMS and HR-ToF-AMS for the winter IOP.

cToF-PMF factor	HR-PMF factor	Slope	Pearson's *r*
HOA	HOA	0.95	0.90
COA	COA	0.58	0.89
$SFOA_{PMF}$	SFOA1	0.80	0.87
$SFOA_{PMF}$	SFOA2	0.85	0.72
$SFOA_{PMF}$	Combined SFOA	0.52	0.90
$OOA2_{PMF}$	OOA	0.12	0.16
OOA1	OOA	0.90	0.91
$OOA2_{PMF}$ + OOA1	OOA	1.02	0.69
$SFOA_{PMF}$ + $OOA2_{PMF}$	Combined SFOA	0.93	0.89

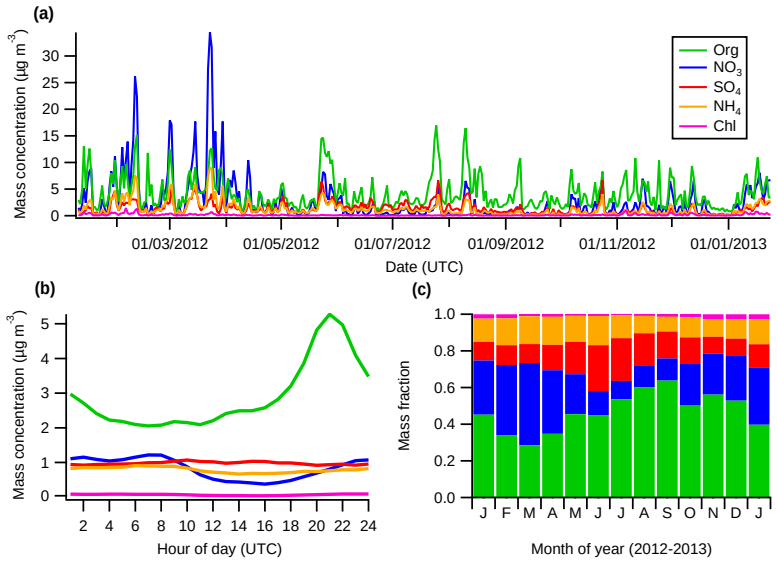

Figure 1. (a) Daily averaged time series of all NR-PM_1 species. **(b)** Median diurnal profiles of all NR-PM_1 species. **(c)** Average monthly fractional contribution of all species to total PM_1. The months are grouped as seasons: January 2012, February, December, and January 2013 are in winter; March, April, and May are in spring; June, July, and August are in summer; September, October, and November are in autumn.

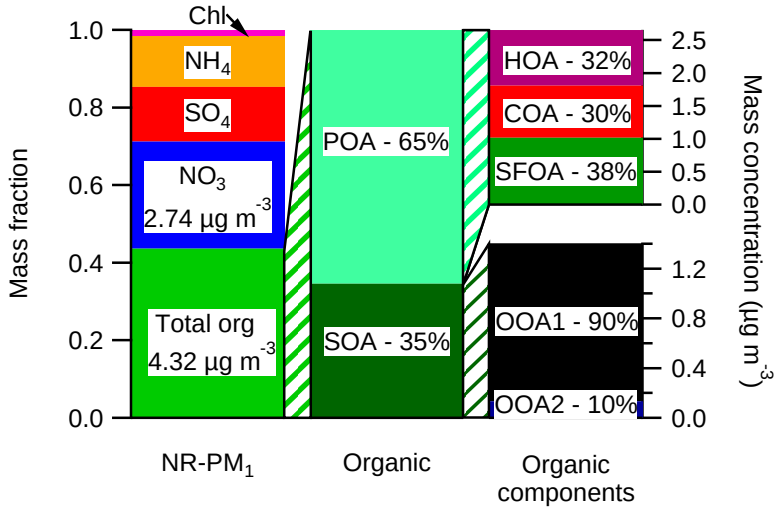

Figure 2. Left: average annual fractional contribution of all species to total PM_1. The average annual PM_1 concentrations of SO_4, NH_4, and Chl were 1.39, 1.30, and 0.15 µg m^{-3}, respectively. Middle: expansion of the organic fraction into its primary and secondary components following PMF analysis. Right top: expansion of the POA fraction into its three components. Right bottom: magnification of the SOA fraction showing its two subtypes. SFOA and OOA2 refer to $SFOA_{mod}$ and $OOA2_{mod}$, respectively. See text in Sect. 4.4 for more details.

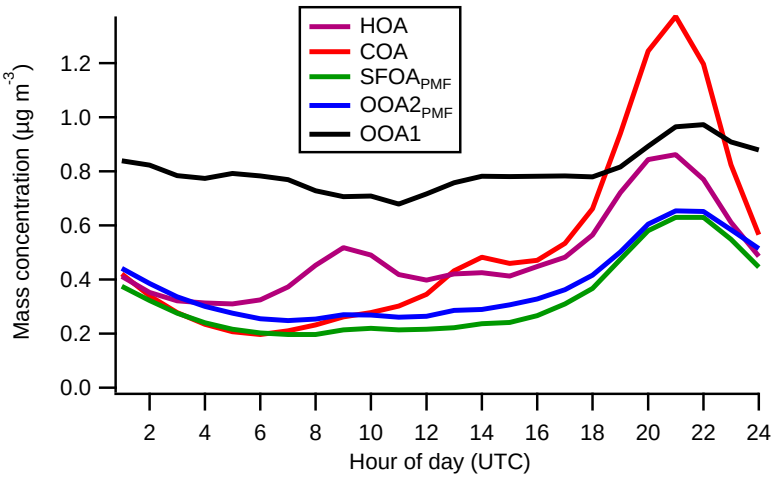

Figure 3. Median diurnal profiles for each of the five PMF factors.

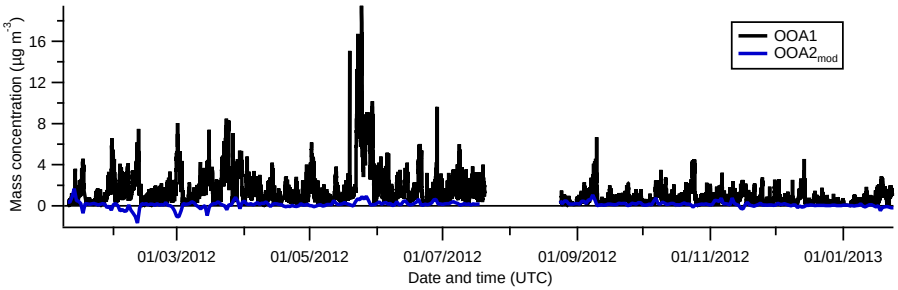

Figure 4. Time series of OOA1 and OOA2$_{mod}$, where OOA2$_{mod}$ is the daily average.

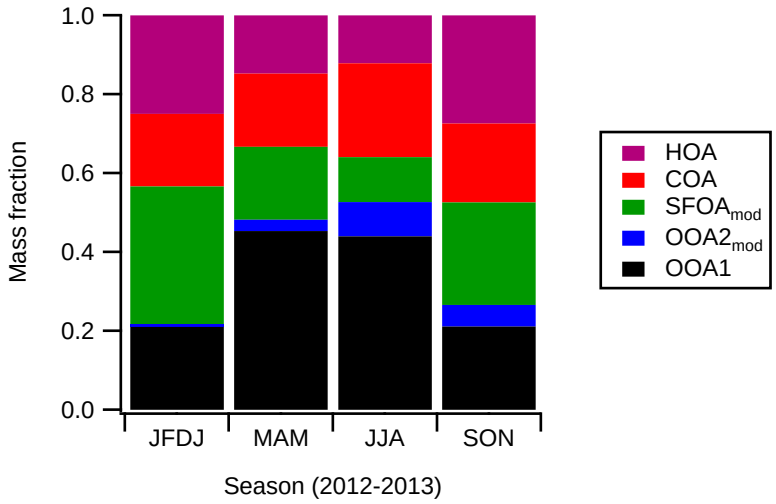

Figure 5. Seasonal fraction of total OA mass, with revised masses (see Sect. 4.4).

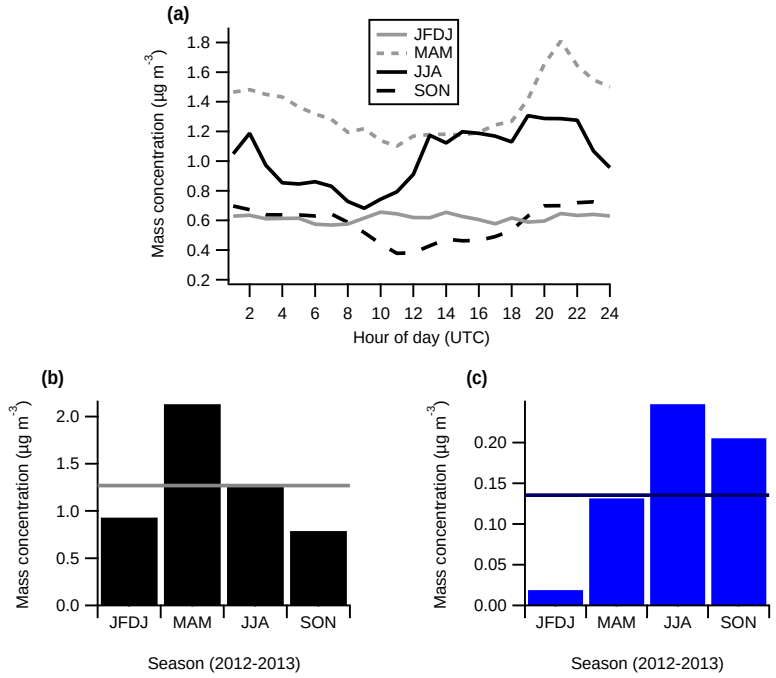

Figure 6. (a) OOA1 seasonal median diurnal profiles. **(b)** Average monthly concentration of OOA1, with the annual average denoted by the thick horizontal line. **(c)** Average monthly concentration of OOA2$_{mod}$, with the annual average denoted by the thick horizontal line, both estimated in Sect. 4.4.

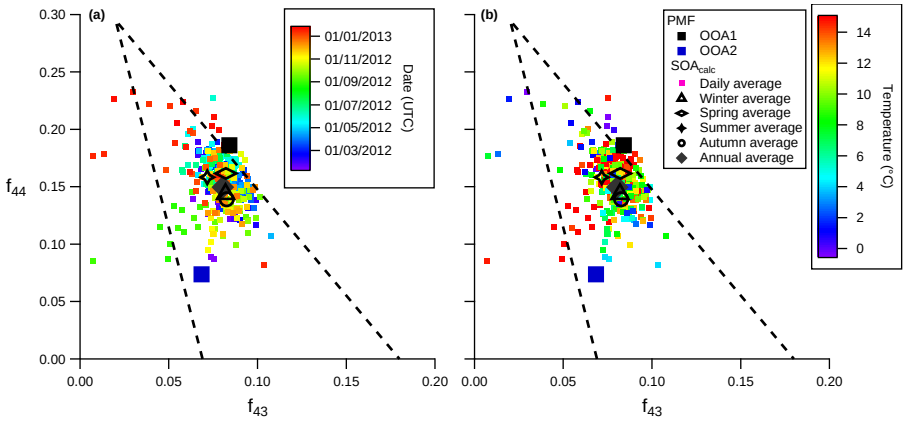

Figure 7. Daily averaged SOA within f_{44} vs. f_{43} space coloured by time **(a)** and temperature **(b)** where f_{44} and f_{43} refer to m/z 44 : SOA_{calc} and m/z 43 : SOA_{calc}, respectively. See text for more details. Daily averaged temperatures ranged from −0.5 to 26 °C although are only coloured up to a maximum of 15 °C here for clarity. Average annual and seasonal f_{44}/f_{43} values for SOA are denoted by the text. OOA1, OOA2 PMF factors are also plotted. The outline of the triangle as defined by Ng et al. (2010) is shown by the dashed black lines.

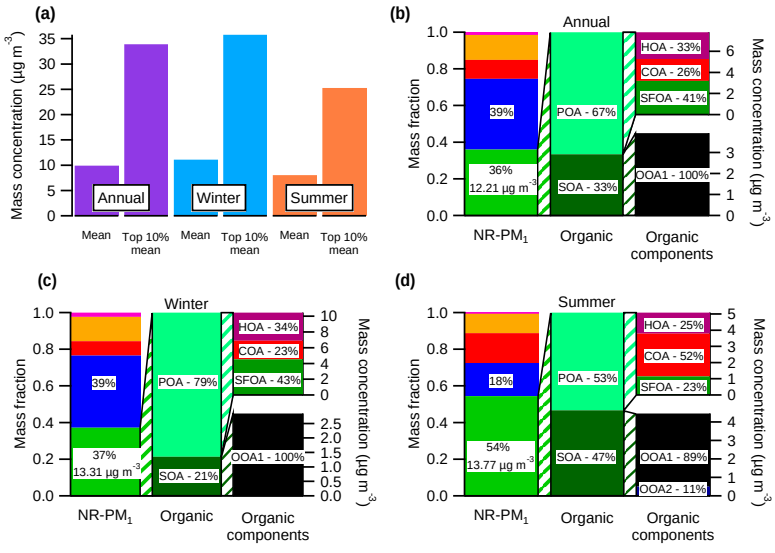

Figure 8. (a) Mean concentrations of the full calendar year (2012–2013), winter, and summer months. The average concentration of the top 10th percentile for the year as well as the top 10th percentile in the winter and summer are also shown. **(b)** Average fractional contributions of all species to the top 10th percentile for the year, with an expansion of the organic fraction into each of its primary and secondary components. **(c)** Average fraction contributions of all species to the top 10th percentile in the winter, with an expansion of the organic fraction into each of its primary and secondary components. **(d)** Average fraction contributions of all species to the top 10th percentile in the summer, with an expansion of the organic fraction into each of its primary and secondary components. In all figures, SFOA and OOA2 refer to $SFOA_{mod}$ and $OOA2_{mod}$ respectively.

4.3 Paper II: Investigating the two-component model of solid fuel organic aerosol in London: processes, PM_1 contributions, and seasonality

Dominique E. Young, James D. Allan, Paul I. Williams, David C. Green, Roy M. Harrison, Jianxin Yin, Michael J. Flynn, Martin W. Gallagher, and Hugh Coe.

The following manuscript has been published in the journal of Atmospheric Chemistry and Physics Discussions (www.atmos-chem-phys-discuss.net/14/20845/2014/, doi:10.5194/acpd-14-20845-2014) and is currently under review for Atmospheric Chemistry and Physics.

Overview

In this paper, the differences between two solid fuel organic aerosol (SFOA) factors derived from Positive Matrix Factorisation (PMF) analysis of the organic fraction of non-refractory submicron aerosol as measured by the High-Resolution Time-of-Flight Aerosol Mass Spectrometer (HR-ToF-AMS) in London during winter 2012 were investigated. Temporal variations in the concentrations of both SFOA factors were consistent with domestic space heating activities. Spatial differences were also observed, where high concentrations of SFOA1 occurred in the south whereas high concentrations of SFOA2 occurred in the east and west. Various methods were used to distinguish between the two SFOA factors on the process level and determine the importance of the variables known to influence the chemical profile of SFOA in governing the split between the two factors. Based on levoglucosan and potassium measurements, it was demonstrated that the split is likely governed predominantly by differences in burn conditions, where SFOA1 best represents more efficient burns and SFOA2 best represents less efficient burns. The two factors are also likely influenced by differences in fuel type and levels of atmospheric processing. As the mass spectral profile of SFOA is highly variable, the findings from this study could improve future source apportionment and factorisation analyses and subsequently influence the formation of pollution mitigation strategies and air quality policies.

Author contributions

Dominique Young performed aerosol measurements, analysed and interpreted the data,

and wrote the manuscript. James Allan helped to run instruments in the field and assisted with interpretation of results and preparation of the manuscript. Paul Williams and David Green assisted with the aerosol measurements. Michael Flynn helped prepare the instrumentation both before and during the field campaigns. Roy Harrison and Jianxin Yin provided levoglucosan and potassium ion data. Martin Gallagher assisted in the planning of the field campaigns. Hugh Coe assisted with the interpretation of the data and preparation of the manuscript.

Atmos. Chem. Phys. Discuss., 14, 20845–20882, 2014
www.atmos-chem-phys-discuss.net/14/20845/2014/
doi:10.5194/acpd-14-20845-2014

Atmospheric Chemistry and Physics Discussions

Investigating the two-component model of solid fuel organic aerosol in London: processes, PM_1 contributions, and seasonality

D. E. Young[1], J. D. Allan[1,2], P. I. Williams[1,2], D. C. Green[3], R. M. Harrison[4,5], J. Yin[4], M. J. Flynn[1], M. W. Gallagher[1], and H. Coe[1]

[1]School of Earth, Atmospheric and Environmental Sciences, University of Manchester, Oxford Road, Manchester, M13 9PL, UK
[2]National Centre for Atmospheric Science, University of Manchester, Oxford Road, Manchester, M13 9PL, UK
[3]School of Biomedical and Health Sciences, King's College London, London, UK
[4]School of Geography, Earth and Environmental Sciences, University of Birmingham, Edgbaston, Birmingham, B15 2TT, UK
[5]Department of Environmental Sciences/Center of Excellence in Environmental Studies, King Abdulaziz University, Jeddah, 21589, Saudi Arabia

Received: 30 July 2014 – Accepted: 1 August 2014 – Published: 13 August 2014

Correspondence to: H. Coe (hugh.coe@manchester.ac.uk)

Published by Copernicus Publications on behalf of the European Geosciences Union.

Abstract

Solid fuel emissions, including those from biomass burning, are increasing in urban areas across the European Union due to rising energy costs and government incentives to use renewable energy sources for heating. In order to help protect human health as well as to improve air quality and pollution abatement strategies, the sources of combustion aerosols, their contributions, and the processes they undergo need to be better understood. A high-resolution time-of-flight aerosol mass spectrometer (HR-ToF-AMS) was therefore deployed at an urban background site between January and February 2012 to investigate solid fuel organic aerosols (SFOA) in London. The variability of SFOA was examined and the factors governing the split between the two SFOA factors derived from positive matrix factorisation (PMF) were assessed. The concentrations of both factors were found to increase during the night and during cold periods, consistent with domestic space heating activities. The split between the two factors is likely governed predominantly by differences in burn conditions where SFOA1 best represents more efficient burns in the south and SFOA2 best represents less efficient burns in the east and west. The differences in efficiency may be due to burner types or burn phase, for example. Different fuel types and levels of atmospheric processing also likely contribute to the two factors. As the mass spectral profile of SFOA is highly variable, the findings from this study have implications for improving future source apportionment and factorisation analyses.

During the winter, SFOA was found to contribute 38 % to the total submicron organic aerosol (OA) mass, with SFOA2 contributing slightly more than SFOA1 (20 % compared to 18 %). A similar contribution of SFOA was derived for the same period from compact time-of-flight AMS (cToF-AMS), which measured for a full calendar year at the same site. The seasonality of SFOA was investigated using the year-long data set where concentrations were greatest in the autumn and winter. During the summer, SFOA contributed 11 % to the organic fraction, where emissions resulted from different anthropogenic activities such as barbecues and domestic garden wood burning. The significant contribution of SFOA to total organic mass throughout the year suggests that the negative effects on health and air quality, as well as climate, are not just confined to winter as exposure to these aerosols and the associated black carbon can also occur during the summer, which may have significant implications for air-quality policies and mitigation strategies.

1 Introduction

The association between adverse health effects and ambient particles has long been recognised (e.g. Pope and Dockery, 2006), where regulations on particulate pollution are based on PM_{10} and more recently, $PM_{2.5}$ (particulate matter (PM) with aerodynamic dynamic diameters less than 10 µm and 2.5 µm respectively, European Union, 2008). Along with $PM_{2.5}$, PM_1 is also receiving greater attention from the air quality community, including the medical sector, as these particles can penetrate more deeply in to the lungs. Particles less than 100 nm in diameter, termed nanoparticles, have the potential to enter the blood stream where they can be distributed throughout the body, causing further damage (Oberdörster et al., 2005). Furthermore, particle toxicity varies greatly with chemical composition, with smaller particles likely to be most detrimental to human health as they are typically composed of toxic constituents such as organics, secondary inorganics, and metals (Donaldson et al., 2003).

In addition to their effects on health, aerosol emissions from anthropogenic activities significantly contribute to poor air quality and visibility, frequently resulting in severe pollution events, particularly in urban areas (e.g. Dall'Osto et al., 2013; Zhang et al., 2014). Organic aerosols (OA) are of particular interest as they can often represent a substantial fraction, and up to 90 %, of total fine particulate mass depending on location (Kanakidou et al., 2005). In urban areas such as Paris and Cork during the winter, organic aerosols have been found to contribute 30–62 % to the total non-refractory PM_1 (NR-PM_1, Crippa et al., 2013; Dall'Osto et al., 2013; Young et al., 2014). Furthermore, meteorological conditions and boundary layer dynamics in the winter result in elevated

concentrations of the primary fraction of OA, resulting in pollution events (Zhang et al., 2007). When the sources of primary organic aerosols (POA) are explored, transport, cooking, and solid fuel burning aerosols are found to contribute significantly to the total POA mass in urban areas (Allan et al., 2010; Mohr et al., 2012; Crippa et al., 2013; Dall'Osto et al., 2013).

Sources of combustion aerosols are frequently categorised into solid fuel, biofuel, biomass burning, and fossil fuel where solid fuel includes various types of solid material such as wood, coal, and peat, whereas biofuel refers to a solid, liquid, or gaseous fuel converted from biomass (e.g. Bond et al., 2004) and biomass burning often refers to wildfires and agricultural burning. It is important to make the distinction between the types of burning when identifying anthropogenic and biogenic sources of combustion aerosols and assessing the importance of emissions from the different sources due to their effects on air quality, health, and climate (Szidat et al., 2006).

Particulate emissions from burning biomass, wood, and coal as well as other fossil fuel combustion related activities such as vehicular transport, industry, and residential space heating are particularly important in terms of contributing to poor air quality. In the UK various legislative measures have been implemented to reduce emissions from such activities; the Low Emission Zone (LEZ; TfL, 2008), introduced across most of Greater London in 2008, aims to encourage cleaner transportation by reducing exhaust emissions from heavy diesel vehicles. The burning of coal by industry and domestic heating resulted in significant pollution events such as the Great Smog of 1952 in London, with coal combustion still playing a key role in wintertime pollution in China, contributing 15–17 % to NR-PM_1 (Sun et al., 2013; Zhang et al., 2014). Although still important, emissions from coal burning in the UK have decreased owing to the Clean Air Acts, where Smoke Control Areas were also introduced across the country. Only the burning of smokeless fuels is permitted in such areas, although some fuels, including seasoned wood, may be burned if carried out in approved burners (Defra, 2014). Wood burning is widely used in domestic heating across Europe (e.g. Finland, Hellén et al., 2008; Austria, Caseiro et al., 2009; Portugal, Borrego et al., 2010) with additional fuel

types used in cooking stoves across the world (e.g. Washington, Maykut et al., 2003; China, Peabody et al., 2005) and is further suggested to be used within the UK as a source of secondary heating as well as for decoration (Fuller et al., 2014).

The LEZ and Smoke Control Areas have largely been successful, with reduced emissions in London from transport and smoke. However, a recent study (Fuller et al., 2013) suggested that such legislative measures may no longer be effective, with evidence of wood burning and solid fuel identified as a potential source of OA in many European cities (e.g. Oslo, Yttri et al., 2005; London, Allan et al., 2010; Barcelona, Mohr et al., 2012; Paris, Crippa et al., 2013; Cork, Dall'Osto et al., 2013). Burning in residential areas is difficult to control and with rising fossil fuel prices and government schemes encouraging the use of renewable energy sources such as biomass, emissions from solid fuel and wood burning are likely to increase over the coming years (Fuller et al., 2013). In Denmark, Glasius et al. (2006) found that increasing fossil fuel costs partly contributed to the doubling in wood-combustion stoves and boilers within a ten year period, a time when there were no regulations on the emissions from such activities.

Black carbon (BC) is strongly associated with combustion emissions, where the dominant source is from traffic emissions, although solid fuel and biomass burning sources have also been found to be important during the winter (Crilley et al., 2014; Liu et al., 2014). Wood burning emissions could be considered to be as important as traffic related emissions in terms of their contribution to POA (Ries et al., 2009; Fuller et al., 2014), where the latter are more stringently regulated. As exposure to aerosols is ubiquitous, it is important to understand aerosol sources, with better quantification of their concentrations to assess their role in pollution events and potential impacts to better inform abatement policies and strategies. Furthermore, as the contribution of solid fuel and other primary organic aerosols to the total aerosol loading is increasing, there are significant implications on human health (Bølling et al., 2009), air quality, and climate due to the strong association between these particulates and BC (Liu et al., 2014).

The sources and contributions of combustion aerosols in London have been investigated using various methods where Crilley et al. (2014) performed a multi-site BC

comparison using the Aethalometer as well as ^{14}C, levoglucosan, and potassium measurements. Liu et al. (2014) used the single particle soot photometer (SP2) to characterise BC in London during winter. Furthermore, Mohr et al. (2013) used a micro-orifice volatilization impactor high-resolution time-of-flight chemical ionization mass spectrometer (MOVI-HRToF-CIMS) to investigate wood burning. In comparison, in this paper, we focus on the solid fuel component from positive matrix factorisation of the organic fraction of aerosol mass spectrometer (AMS) data, where we investigate the sources of solid fuel aerosols and their contributions to total mass in a densely populated area. The high-resolution time-of-flight AMS (HR-ToF-AMS) was deployed for a 4-week intensive measurement campaign during winter 2012, a time when solid fuel aerosols would be prominent. Furthermore, a compact time-of-flight AMS (cToF-AMS) was deployed at the same urban background site in London for a full calendar year (Young et al., 2014), allowing the temporal trends of submicron aerosols to be evaluated.

2 Experimental

2.1 Sampling site

A suite of state-of-the-art instrumentation, measuring aerosols, gases, radicals and meteorological parameters was deployed for two major intensive observation periods (IOPs) during 2012 as part of the NERC funded Clean Air for London (ClearfLo) Project (http://www.clearflo.ac.uk). Measurements were conducted in a residential area 7 km to the west of Central London at the ClearfLo urban background supersite in the grounds of a school in North Kensington (51.521055° N, 0.213432° W). Long-term measurement campaigns also took place in various locations in and around London between 2011 and 2013 as part of this large, multi-institutional collaborative scientific project based in the UK. Details on the ClearfLo experimental campaigns and locations are described in Bohnenstengel et al. (2014) and Young et al. (2014).

2.2 Aerosol Mass Spectrometer measurements

Aerosol chemical composition was measured by the high-resolution time-of-flight AMS (HR-ToF-AMS, DeCarlo et al., 2006) during January and February 2012 and by the compact time-of-flight AMS (cToF-AMS, Drewnick et al., 2005) for a full calendar year (11 January 2012–23 January 2013). The HR-ToF-AMS was located in a shipping container containing several other aerosol instruments, where aerosols were sub-sampled from a sampling stack with a flow of 30 L min^{-1} via a 3.5 µm cut-off cyclone. The cToF-AMS sampled through a $PM_{2.5}$ inlet, with a bypass flow of 16 L min^{-1} and split using an asymmetric Y-piece. The time resolution of the HR-ToF-AMS used in this study was 5 min, obtained once every 30 min, as sampling occurred in an alternating sequence with other black carbon and aerosol volatility measurements using a thermodenuder (Huffman et al., 2008). The time resolution of the cToF-AMS was 5 min throughout the measurement period. An overview of the AMS can be found in Canagaratna et al. (2007), where details regarding the sampling protocol and data analysis procedures including the applied corrections, such as relative ionisation efficiencies and collection efficiency, can be found in Young et al. (2014). Details regarding the data pre-treatment and quality assurance for the data sets used in this study, including for positive matrix factorisation (PMF) analysis can also be found in Young et al. (2014) and the supporting information.

2.3 Gas measurements

CO was measured using an Aerolaser AL 5002 UV fluorescence instrument which was calibrated using an Air Products 200 ppb CO in air standard that was certified to NPL standards. NO and NO_2 were measured using an Air Quality Design custom built high sensitivity Chemiluminesence analyser with a Blue Light NO_2 converter. The NO instrument was calibrated using a 5 ppm NO in nitrogen cylinder from BOC, which was diluted to 20 ppb using scrubbed zero air (BOC BTCA 178). The NO_2 instrument was calibrated using gas phase titration of the NO standard with O_3.

2.4 Levoglucosan and potassium ion measurements

24 h $PM_{2.5}$ samples were collected on quartz fibre filters (Whatman QM-A) using a high volume Digitel DHA-80 sampler at a flow of 500 L min and were analysed for wood smoke marker levoglucosan as described in Young et al. (2014) using a slightly modified version of the method of Yin et al. (2010) and Wagener et al. (2012).

Potassium ion (K^+) data were obtained using a small portion of the Digitel filter samples which was extracted with distilled de-ionised water (10 mL) by undergoing 40 min mechanical agitation to ensure thorough removal of the water-soluble aerosol. The resulting solutions were filtered and analysed for K^+ using a DIONEX ICS-2000 ion chromatography system coupled with a gradient pump, which generates one eluent from two different solutions, de-ionised water and concentrated potassium hydroxide solution. The sample concentrations were calibrated with a series of mixed standards of known concentration (0.01–10 ppm).

3 Results

3.1 Identification of the components of the organic fraction

Four main components were identified from PMF analysis on the organic fraction of the HR-ToF-AMS data from the winter IOP: hydrocarbon-like OA (HOA), cooking OA (COA), solid fuel OA (SFOA), and oxygenated OA (OOA), where an additional SFOA factor was identified from the 5-factor solution set. Both the 4- and 5-factor solution sets produced data that satisfied the selection criteria for the appropriate number of factors and could be considered valid from various diagnostic tests, which assess the quality and suitability of the solution. The 6-factor solution was discarded due to its significant dependency on initialisation seed as well as the production of a factor that did not appear physically meaningful. The details of the PMF analysis are covered in a separate publication where we refer the reader to Sect. 5.1 of the Supplement of Young

et al. (2014) for a detailed discussion on the number of factors chosen from the high resolution data set and the criteria used to select the best solution. Here we describe the methods used to choose between the 4- and 5-factor solutions.

Increasing the number of factors derived from PMF analysis of AMS data often improves mathematical PMF diagnostics used to select the appropriate solution set. However, the introduction of a new factor can sometimes result in a phenomenon known as "splitting", whereby factors that bear similar temporal and/or mass spectral profiles are representative of the variations within a single factor. Factors with varying profiles can manifest within PMF as rotational ambiguity, divergence, or factor mixing. Therefore, the comparison of retrieved factors with reference mass spectra and time series from ancillary measurements can determine their physical meaningfulness. This method of factorisation validation enabled Lanz et al. (2007) to split OOA in to type 1 and type 2, which was the first time OOA2 had been reported in the literature. However, it is not always possible to separate OOA in to its two subtypes if ambient temperature and photochemistry are not sufficiently variable such as in the winter (e.g. Allan et al., 2010). OOA1 and OOA2 are now widely recognised as representing end members of OOA evolution where OOA1 is highly aged with low volatility and OOA2 is less processed and more volatile (e.g. Jimenez et al., 2009; Ng et al., 2010).

Therefore, in order to identify the most atmospherically reasonable solution set and further investigate the two SFOA factors from the 5-factor solution, comparisons were made with ancillary measurements. It has been shown that NO_x and CO are strongly related to HOA (Zhang et al., 2005) as they are emitted from fuel combustion in vehicle engines. However, traffic activity is not the only source of these gases, which are used as tracers for combustion. Space heating has been found to be another potential combustion source and therefore contributes to SFOA (Allan et al., 2010). The Pearson's *r* values derived between the gas tracers and the SFOA factor from the 4-factor solution (hereon in termed SFOA-4fac) are shown in Table 1. When the two SFOA factors from the 5-factor solution (SFOA-combined) are summed and compared to the gas tracers the Pearson's *r* values are better than those for SFOA-4fac. However, as both traffic

and domestic fuel burning from space heating contribute to CO and NO_x concentrations a multi-linear regression fit as detailed in Allan et al. (2010) was performed to assess the relative contributions of traffic (HOA) and wood burning (SFOA) to these trace gases.

Fitting was performed according to the function:

$$f(\text{HOA, SFOA}) = A[\text{HOA}] + B[\text{SFOA}] + C \quad (1)$$

where [HOA] and [SFOA] are the concentrations of the HOA and SFOA PMF factors and A, B, and C are arbitrary fitting parameters optimised to minimise the squared difference between f (HOA, SFOA) and NO_x or CO. This multi-linear regression fit was performed on the HOA and SFOA factors from the 4-factor solution and the HOA and combined SFOA factors from the 5-factor solution. The Pearson's r values derived between the PMF factors and combustion tracers are shown in Table 1. Including both sources in this way significantly improves the correlations with the gas tracers for both sets of solutions. However, there is little difference between the regression fit r values for the two solution sets with the 4-factor solution showing a very slightly greater correlation with NO_x than the 5-factor solution.

Overall there is little difference between the SFOA derived in the 4-factor solution to the combined factor from the 5-factor solution, so both could be valid solution sets. However, because the 5-factor solution with the two SFOA factors combined gave improvements to diagnostics such as Q/Q_{expected} (4.375 compared to 4.7764 for the 4-factor solution) and correlations with ancillary data (see Sect. 5.1.4 in the Supplement for Young et al. (2014) for details), it was deemed that the 5-factor solution with the split SFOA factors was the most appropriate so is used in further analyses.

3.2 Temporal variations and trends of the organic components

The time series, average contributions to total organic mass, and diurnal profiles of all 5 factors identified from PMF analysis of the HR-ToF-AMS are shown in Fig. 1. The

organic fraction is dominated by the POA components (78 %) with the remainder comprising OOA. The contributions of HOA, COA, SFOA1, and SFOA2 to the total organic mass are nearly equal (19 %, 21 %, 18 %, and 20 %, respectively). When combined, the SFOA factors represent the largest contribution to the organic fraction of NR-PM_1 in the winter in London.

The average (±standard deviation) HOA concentration during the winter was 0.83 (±1.37) $\mu g\,m^{-3}$, with a maximum concentration of 24.5 $\mu g\,m^{-3}$ measured on 16 January. This is the largest HOA event as well as the greatest concentration measured for all factors during the winter measurement period. As HOA is related to traffic emissions, this event is likely the result of a vehicle parked close to the site with its engine running. The diurnal profile of HOA only exhibits one main peak in concentration at 10:00 UTC, although there is possibly a broad peak between 16:00 and 23:00 where concentrations are approximately two-thirds that of the morning peak. These peaks are associated with rush hours in London.

COA has a mean concentration of 0.88 (±1.73) $\mu g\,m^{-3}$ and a peak in concentration of 18.3 $\mu g\,m^{-3}$ on 14 January. COA exhibits the most pronounced diurnal profile of all the factors, with a peak in concentrations between 20:00 and 22:00, and a smaller peak at 14:00, both associated with meal times. The timing of the evening peak is more likely associated with commercial activities than domestic meal times in the UK.

The average SFOA1 concentration was 0.75 (±0.98) $\mu g\,m^{-3}$ with a maximum concentration of 8.0 $\mu g\,m^{-3}$ measured on 17 January. SFOA1 exhibits a relatively smooth diurnal profile with greater concentrations during the night compared to the day. In contrast, the average concentration SFOA2 was 0.86 (±0.77) $\mu g\,m^{-3}$ and peaked on 14 January, with a concentration of 5.2 $\mu g\,m^{-3}$. The diurnal profile of SFOA2 is similar to SFOA1 with greater concentrations during the night, but SFOA2 also exhibits a small peak in concentrations between 10:00 and 11:00.

Finally, the mean concentration of OOA was 0.93 (±1.11) $\mu g\,m^{-3}$ and peaked on 31 January with a concentration of 5.4 $\mu g\,m^{-3}$. OOA does not exhibit a discernable diurnal pattern, which is consistent with it representing a regional, oxygenated aerosol.

4 Investigating the SFOA factors

In this paper, we investigate the behaviour of the solid fuel component of the organic fraction including the differences between the two SFOA factors from the HR-ToF-AMS for the winter IOP as well as the annual and seasonal trends of SFOA using the factors from the cToF-AMS. Details of the PMF analysis of both data sets are covered in a separate publication, where the annual behaviour of the secondary inorganic and organic aerosols is also investigated (Young et al., 2014).

Both SFOA1 and SFOA2 increase in concentration during the night (Fig. 1), as well as during the colder periods of the campaign (Fig. 2), which is consistent with them being associated with space heating activities. In addition to anthropogenic activities, there is reduced mixing in the boundary layer during the winter and therefore less dispersion, resulting in increased levels of aerosols. Other dynamical effects, such as episodic wintertime inversions, also play a role in driving changes in concentrations whereby local pollution is trapped resulting in a build-up of pollution (Martin et al., 2011). Such influences are evident during the winter of 2012 where the concentrations of all factors increase simultaneously in some events.

4.1 Role of air mass history

Imported pollution can also affect aerosol concentrations (e.g. Young et al., 2014). Liu et al. (2014) considered the influence of air mass history on black carbon concentrations in London during the winter including the influence of solid fuel burning sources in different air masses, as black carbon is produced from combustion processes. Increases in black carbon mass were primarily coincident with easterly air masses. Here, the concentrations of the two SFOA factors were investigated as a function of wind speed and direction to determine whether different sources in terms of spatial locations are governing the split between the two factors. Polar plots are used to explore spatial differences in the concentrations of SFOA1 and SFOA2 and are shown in Fig. 3. The wind data used in these plots are from the meteorological station at Heathrow airport

rather than local meteorological data as the latter are strongly influenced by surrounding buildings (e.g. Bigi and Harrison, 2010) thus do not provide representative insight in to spatial differences in the SFOA concentrations. The greatest SFOA1 concentrations are in the south, whereas the greatest SFOA2 concentrations are in the east and west and occur at slightly lower wind speeds compared to SFOA1.

4.2 Investigating the behaviour of SFOA

The mass spectra of biomass burning and solid fuel OA are not constant (DeCarlo et al., 2010); they vary due to different combustion types, fuel types, and levels of processing. Weimer et al. (2008) suggest that the mass spectral signature of wood burning is influenced more by the burning conditions than the fuel type. Crippa et al. (2014) also recommend that in factorisation analyses using the multilinear engine ME-2, mass spectra representative of typical burning conditions for a particular measurement site should be used if they are known. In this study, a combination of these variables may govern the split in to the two SFOA factors, where several different fuel types may also be contributing to the two SFOA factors identified in this study, so they are classed more generally as solid fuel OA as opposed to biomass burning OA (BBOA).

The high variability of the SFOA mass spectral profile has been identified in many studies (Weimer et al., 2008; Grieshop et al., 2009) including those where factor analysis and apportionment techniques have been applied (DeCarlo et al., 2010; Ng et al., 2011; Crippa et al., 2013, 2014). Some markers frequently used to identify biomass and solid fuel burning aerosols may not always be appropriate depending on the measurement conditions (DeCarlo et al., 2010; Hennigan et al. 2010) including ambient temperatures, duration of the measurements, and other sources of OA such as cooking (Mohr et al., 2009). Furthermore, BBOA evolves in the atmosphere through oxidation, whereby aged biomass burning aerosols have mass spectra similar to that of fulvic acid, used to represent highly oxidised OA with a large signal at m/z 44 (Capes et al., 2008; Grieshop et al., 2009; DeCarlo et al., 2010; Cubison et al, 2011; Lack et al., 2013). Consequently, it can sometimes be difficult to determine from the mass spectra

and time series derived from PMF alone whether a factor represents primary SFOA, processed primary SFOA, SOA formed from SFOA, or a mixture of SFOA and OOA which are co-emitted (e.g. Crippa et al., 2013). Therefore, various metrics and graphical representations of the data are used in order to better interpret and characterise combustion related aerosols, where additional measurements support and improve interpretations.

In this study, the two SFOA factors are correlated in time (Fig. 2) whereby, although differing in magnitude, most of the high concentration events for both factors occur during the same period, although not necessarily simultaneously such as on 17 January. The two factors are therefore linked but as the chemical profile changes with time the two factors represent the range of variability of SFOA composition. The two SFOA factors differ by way of diurnal variation (Fig. 1c inset) as well as chemical composition (Fig. 4). The mass spectra of SFOA1 and SFOA2 exhibit the typical peaks used as BBOA tracers at m/zs 60 and 73 (Alfarra et al., 2007) and compare very strongly with reference mass spectra (Pearson's r of 0.94 and 0.88, respectively; BBOA, Ng et al., 2011). Although both factors comprise several similar peaks, such as at m/z 43, 55, 57, 60, and 73, SFOA1 also has a greater signal at m/z 44. Furthermore, SFOA1 also comprises more oxygenated compounds than SFOA2.

The difference in the mass spectra (MS) of the two factors highlights the variation within SFOA, which likely led to the derivation of a split factor by the PMF algorithm. The main chemical differences between the two factors are shown in the difference MS in Fig. 4 where SFOA1 is represented above the zero line and SFOA2 below the line. However there are differences in structure of the peaks above and below the line, compared to the individual MS of SFOA1 and SFOA2. For example, the peaks above the line are primarily composed of oxidised hydrocarbons at m/z 43, 44, 57, and 60 and compared to the SFOA1 MS, peaks such as m/z 41 and 55 missing. The peaks below the line are primarily composed of reduced hydrocarbons where peaks at m/z 43 and 57 are missing compared to the SFOA2 MS. This suggests that the chemical groups are affected differently by what is driving the split between the factors. Therefore, to

better understand these differences the roles of atmospheric processing, fuel type, and burn conditions, including burn phase, in varying the MS of SFOA and their influences in governing the split into two factors are investigated in the following sections.

4.3 Role of atmospheric processing

Analogous to OOA, the two SFOA factors derived from PMF analysis in this study may also represent end members of a continuum, where conditions during the winter enable the separation of SFOA into the two factors. The O : C ratio can be used to indicate the degree of oxygenation and level of processing the aerosols have undergone. Here, the O : C ratio for SFOA1 is 0.41, whereas for SFOA2 it is 0.15 and 0.53 for OOA. This suggests that SFOA1 and SFOA2 differ by degree of oxygenation and therefore age, whereby SFOA1 is more processed than SFOA2. However, the type and phase of combustion can also affect the signal at m/z 44. Increases in f_{44} are typically found to coincide with decreases in f_{60} (e.g. Cubison et al., 2011) (the ratio of the organic signal at m/z 60 to the total organic signal in the component mass spectrum) from oxidative decay of species such as levoglucosan. The f_{60} vs. f_{44} space (Cubison et al., 2011) is therefore used to characterise the evolution of biomass burning aerosols, with data from many studies exhibiting a negative correlation between f_{44} and f_{60} (Cubison et al., 2011; Ortega et al., 2013; Jolleys et al., 2014a). If the two SFOA factors represented different levels of processing of the same fuel type under similar conditions then SFOA1 would be expected to have higher f_{44} and lower f_{60} compared SFOA2. Fig. 5 shows how the two SFOA factors map in the f_{44} vs. f_{60} space, with SFOA1 exhibiting higher f_{60} as well as f_{44} compared to SFOA1. From this, it can be inferred that the other factors such as differences in fuel types or burn conditions are also contributing to governing the split between the two factors rather than just differences in the degree of atmospheric processing.

4.3.1 Role of fuel type

In the latest National Atmospheric Emissions Inventory from 2011, wood was the largest contributor to PM_1 from domestic combustion activities (51 %, NAEI, 2014), followed by coal (31 %) with only small contributions from natural gas (9 %) and peat (2 %). In a recent study in Cork, Ireland (Dall'Osto et al., 2013) a peat and coal OA factor was identified from PMF analysis of ambient data, with mass spectra of wood, peat, and coal obtained from laboratory experiments. However, due to the high variability of AMS mass spectra of biomass burning and solid fuel aerosols as mentioned previously, comparisons with other ancillary measurements and apportionment techniques are required to determine the role of fuel type on governing the split between the two SFOA factors.

Along with anhydrous sugars such as levoglucosan and mannosan, chloride is used as a tracer for biomass burning (Dall'Osto et al., 2013) as well as for coal combustion (Sun et al., 2013); contributions of chloride from coal have been found to be greater than that from wood (Zhang et al., 2012). However, a comparison of the sum of the SFOA factors with potential sources from Chemical Mass Balance (CMB) modelling of filter samples revealed a greater correlation when the sum of wood smoke and coal was considered rather than wood smoke alone (Yin et al., 2014). Moreover, the stronger correlation was achieved when the two SFOA factors were also summed suggesting that although several fuel types are contributing to SFOA, the split between the two factors is not solely driven by a difference in fuel type.

4.3.2 Role of burn conditions

Burn conditions can result in variations in the emissions from solid fuel burning, where such conditions include different burners or technologies and burn phase. Weimer et al. (2008) suggested a low m/z 44 signal is indicative of the flaming phase whereas high signals occur during the smouldering phase. Contrastingly, Jolleys et al. (2014b) found increased f_{44} occurred more frequently during flaming combustion

than smouldering burns. These opposing conclusions highlight the dependency of emissions from fires on a variety of factors, including burn conditions and fuel type. Therefore additional information and various metrics have been used to better understand the influences from variations within each of these factors such as whether a burn is predominantly flaming or smouldering (Yokelson et al., 1996). Puxbaum et al. (2007) used the ratio of organic carbon to levoglucosan to determine the type of combustion, such as fires in small ovens and open wild fires. In this study, the ratio of SFOA1 to levoglucosan is 13.2, whereas for SFOA2 it is 10.1, which are similar to the value obtained by Sciare et al. (2011) in Paris (10.3) for $PM_{2.5}$ wood burning organic matter/levoglucosan. The similarity of the ratios of the two factors suggests different phases of combustion may be occurring under similar conditions. However, levoglucosan is not completely stable in the atmosphere (Hennigan et al., 2010) so may not be a suitable tracer when used on its own.

Due to the sensitivity of wood smoke tracers to combustion conditions, Harrison et al. (2012a) used the levoglucosan : potassium ratio to evaluate wood smoke in the UK. Two potential sources of wood smoke were suggested: wood stoves/fireplaces, with a high ratio, and modern appliances, with a low ratio. Low temperature flaming combustion results in a high organic content whereas a low ratio results from very high burn-out efficiency. In Fig. 6, the difference between the two SFOA factors is plotted against the levoglucosan : potassium ratio from 24 h filter samples from North Kensington. In general, higher SFOA1 concentrations are coincident with a lower levoglucosan : potassium ratio, whereas higher SFOA2 concentrations are coincident with a higher ratio. This could therefore suggest that SFOA1 represents a more efficient burn compared to SFOA2. Such conditions could be the result of efficient burner types, the use of well-seasoned wood, or represent the flaming phase of the burn. This is in keeping with the mass spectral profile of SFOA1 exhibiting a large signal at m/z 44 as well as low signals at m/zs 60 and 73, indicative of fast combustion which results in the conversion of organic matter to CO_2^+. The converse represents less efficient burn conditions, which is seen in the mass spectral profile of SFOA2. Furthermore, flaming

combustion involves high temperatures, evident in the MS of SFOA1, which appears to favour greater functionalization whereas SFOA2 is predominantly composed of alkanes (Fig. 4).

5 Contributions of SFOA to total NR-PM$_1$ and longer term temporal trends

SFOA1 contributes 18 % to the total organic fraction and SFOA2 contributes 20 % (Fig. 1b), where the sum of both factors is similar to the contribution of the SFOA factor in Young et al. (2014) derived from PMF analysis of the organic matrix from the cToF-AMS (33 %) for the same period. The contribution of cToF-AMS SFOA to total organics during the whole winter season (January, February, December 2012 and January 2013) was 35 %. Since no SFOA factor was derived from PMF analysis of the summer HR-ToF-AMS data set, the long-term cToF-AMS data set described in Young et al. (2014) is used to investigate the seasonal trends of SFOA.

Only one SFOA factor was derived from PMF analysis of the cToF-AMS data, due to the lower resolution of this version of the instrument compared to the HR-ToF-AMS where different ions at the same nominal m/z can be distinguished. The derivation of a single SFOA factor is also likely a result of the broad range of photochemical conditions and time that are covered by the year-long data set. If significantly aged, some SFOA may be apportioned to SOA by PMF due to the chemical similarity. Furthermore, if SFOA has been aged or advected, f_{60} may no longer be a reliable marker (Cubison et al., 2011). Heringa et al. (2011) also found that SOA significantly contributed to m/z 60 depending on the burning conditions. Nevertheless, SFOA contributes 18 % to the total organic mass in spring, 11 % in summer and 26 % in autumn. This is consistent with the findings of Allan et al. (2010) for autumn 2007 as part of the REPARTEE experiment (Harrison et al., 2012b), where SFOA was also found to represent 26 % of POA. This seasonality, where the contribution of SFOA to total organic mass as well as actual mass concentration increases during the autumn and winter, is consistent with domestic space heating activities.

As expected, temperatures were greater in the summer compared to the winter, which is why solid fuel aerosols were not discernable from the HR-ToF-AMS data set from the summer IOP. However, as SFOA is still a significant contributor to the total organic mass during this period it is likely that this factor represents a different activity to domestic space heating during the winter. Gardening waste and forest wood burning occurs in the summer, with wood and other fuel types burned for barbecues (Crippa et al., 2014; Lanz et al., 2007).

6 Conclusions

An investigation in to the differences between two SFOA factors derived from PMF analysis of the organic fraction of NR-PM$_1$ as measured by the HR-ToF-AMS in London during winter 2012 is presented. Spatial differences in the concentrations of both SFOA factors were found where SFOA1 had influences from the south whereas SFOA2 had influences from the east and west. However, the chemical profile of SFOA is known to vary due to differences in fuel type, the degree of atmospheric processing and burn conditions; various methods were therefore used to distinguish between the two factors on the process level and determine the importance of each of these variables in governing the split.

SFOA1 was found to be more oxygenated and contain more organic matter the SFOA2, however, correlations with ancillary data suggested that the split in SFOA was not likely to be primarily driven by differences in fuel type or degree of processing. The ratio of the biomass burning tracers, levoglucosan and potassium, was used to identify the importance of different burn conditions in controlling the split between the two SFOA factors. Higher SFOA1 than SFOA2 concentrations were coincident with a low ratio, indicating SFOA1 likely represents a high-efficiency burn whereas SFOA2 likely represents less efficient burn conditions such as the smouldering phase of a burn. Therefore, each of the SFOA factors represents different conditions where burn conditions can include the burner type/technology, whether fireplace or modern appliances,

burn phase, smouldering or flaming, and time since the fire was lit. When considering the spatial differences in concentrations of the two factors, SFOA1 could therefore represent more efficient burns in the south compared to those in the east and west, which are represented by SFOA2. As diagnostics in both PMF and CMB analyses improved by considering both SFOA factors and the differences between the two factors are identifiable on a chemical basis, there are implications for future source apportionment analyses and interpretation of other data. It is possible that the uncertainty surrounding SFOA in PMF and multi-linear engine ME-2 analyses (Canonaco et al., 2013) could be addressed by including two factors which better characterise the variability of solid fuel burning aerosols by improving the accuracy and reducing the rotational ambiguity in such analyses.

Increases in the concentrations of both SFOA factors are consistent with their association with space heating activities. During the winter, SFOA1 contributed 18 % to the total organic mass whereas SFOA2 contributed 20 %, where the sum of the two factors is comparable to the contribution of the single SFOA factor identified from the cToF-AMS data set. The seasonality of SFOA was investigated using the long-term data set where SFOA contributed 18 % to the total organic mass in spring, 11 % in summer and 26 % in autumn. The presence of SFOA during the summer could be due to activities such as barbecuing, as well as domestic garden and forest wood burning. This study highlights the importance of SFOA where it is evident that wood burning and other solid fuel burning activities are occurring in London despite the implementation of various legislative measures. Changes in the economy may lead to an increase in the contribution of SFOA to the total NR-PM_1 aerosol burden, which could have significant influences in forming future air quality policies and mitigation strategies due to the associations between fine combustion aerosols and adverse health, air quality, and climate effects. As the use of renewable energy sources is also set to increase across the EU, it may be expected that similar conclusions are reached in other countries with comparably significant implications for policies and pollution abatement.

Data availability

Processed data are available through the ClearfLo project archive at the British Atmospheric Data Centre (http://badc.nerc.ac.uk/browse/badc/clearflo). Raw data are archived at the University of Manchester and are available on request.

Acknowledgements. This work was supported in part by the UK Natural Environment Research Council (NERC) ClearfLo project (grant ref. NE/H008136/1) and is co-ordinated by the National Centre for Atmospheric Science (NCAS). Additional support for the aerosol measurements was provided by the Department of Environment, Food and Rural Affairs (DEFRA). D. E. Young was supported by a NERC PhD studentship (ref. NE/I528142/1). The authors would like to thank James Lee from NCAS at the University of York for the CO, NO, and NO_2 data as well as for logistical assistance at the North Kensington supersite during the IOPs. The authors would also like to thank Anja Tremper at King's College London for assisting with instrument maintenance. Additional thanks to the Sion Manning School in North Kensington and adjacent community centre.

References

Alfarra, M. R., Prevot, A. S. H., Szidat, S., Sandradewi, J., Weimer, S., Lanz, V. A., Schreiber, D., Mohr, M., and Baltensperger, U.: Identification of the mass spectral signature of organic aerosols from wood burning emissions, Environ. Sci. Technol., 41, 5770–5777, 2007.

Allan, J. D., Williams, P. I., Morgan, W. T., Martin, C. L., Flynn, M. J., Lee, J., Nemitz, E., Phillips, G. J., Gallagher, M. W., and Coe, H.: Contributions from transport, solid fuel burning and cooking to primary organic aerosols in two UK cities, Atmos. Chem. Phys., 10, 647–668, doi:10.5194/acp-10-647-2010, 2010.

Bigi, A. and Harrison, R. M.: Analysis of the air pollution climate at a central urban background site, Atmos. Environ., 44, 2004–2012, 2010.

Bohnenstengel, S. I., Belcher, S. E., Aiken, A. C., Allan, J. D., Allen, G., Bacak, A., Bannan, T. J., Barlow, J. F., Beddows, D. C. S., Bloss, W. J., Booth, A. M., Chemel, C., Coceal, O., Di Marco, C. F., Mavendra, D. K., Faloon, K. H., Fleming, Z., Furger, M., Geitl, J. K., Graves, R. R., Green, D. C., Grimmond, C. S. B., Halios, C., Hamilton, J. F., Harrison, R. M., Heal,

M. R., Heard, D. E., Helfter, C., Herndon, S. C., Holmes, R. E., Hopkins, J. R., Jones, A. M., Kelly, F. J., Kotthaus, S., Langford, B., Lee, J. D., Leigh, R. J., Lewis, A. C., Lidster, R. T., Lopez-Hilfiker, F. D., McQuaid, J. B., Mohr, C., Monks, P. S., Nemitz, E., Ng, N. L., Percival, C. J., Prévôt, A. S. H., Ricketts, H. M. A., Sokhi, R., Stone, D., Thornton, J. A., Tremper, A. H., Valach, A. C., Visser, S., Whalley, L. K., Williams, L. R., Xu, L., Young, D. E., and Zotter, P.: Meteorology, air quality and health in London: the ClearfLo project, B. Am. Meteorol. Soc., in press, 2014.

Bølling, A. K., Pagels, J., Yttri, K. E., Barregard, L., Sallsten, G., Schwarze, P. E., and Boman, C.: Health effects of residential wood smoke particles: the importance of combustion conditions and physicochemical particle properties, Part. Fibre Toxicol., 6, doi:10.1186/1743-8977-6-29, 2009.

Bond, T. C., Streets, D. G., Yarber, K. F., Nelson, S. M., Woo, J.-H., and Klimont, Z.: A technology-based global inventory of Black and Organic Carbon emissions from Combustion, J. Geophys. Res., 109, D14203, doi:10.1029/2003JD003697, 2004.

Borrego, C., Valente, J., Carvalho, A., Sá, E., Lopes, E., and Miranda, A. I.: Contribution of residential wood combustion to PM_{10} levels in Portugal, Atmos. Environ., 44, 642–651, 2010.

Canagaratna, M. R., Jayne, J. T., Jimenez, J. L., Allan, J. D., Alfarra, M. R., Zhang, Q., Onasch, T. B., Drewnick, F., Coe, H., Middlebrook, A., Delia, A. E., Williams, L. R., Trimborn, A. M., Northway, M. J., Decarlo, P. F., Kolb, C. E., Davidovits, P., and Worsnop, D. R.: Chemical and microphysical characterization of ambient aerosols with the aerodyne aerosol mass spectrometer, Mass Spectrom. Rev., 26, 185–222, doi:10.1002/mas.20115, 2007.

Canonaco, F., Crippa, M., Slowik, J. G., Baltensperger, U., and Prévôt, A. S. H.: SoFi, an IGOR-based interface for the efficient use of the generalized multilinear engine (ME-2) for the source apportionment: ME-2 application to aerosol mass spectrometer data, Atmos. Meas. Tech., 6, 3649–3661, doi:10.5194/amt-6-3649-2013, 2013.

Capes, G., Johnson, B., McFiggans, G., Williams, P. I., Haywood, J., and Coe, H.: Aging of biomass burning aerosols over West Africa: Aircraft measurements of chemical composition, micro-physical properties, and emission ratios, J. Geophys. Res., 113, D00C15, doi:10.1029/2008jd009845, 2008.

Carslaw, D. C.: The openair manual – open-source tools for analysing air pollution data, King's College London., 2013.

Carslaw, D. C. and Ropkins, K.: openair – an R package for air quality data analysis, Environ. Model. Softw., 27–28, 52–61, 2012.

Caseiro, A., Bauer, H., Schmidl, C., Pio, C. A., and Puxbaum, H.: Wood burning impact on PM_{10} in three Austrian regions, Atmos. Environ., 43, 2186–2195, 2009.

Crilley, L. R., Bloss, W. J., Yin, J., Beddows, D. C. S., Harrison, R. M., Allan, J. D., Young, D. E., Flynn, M., Williams, P. I., Zotter, P., Prévôt, A. S. H., Heal, M. R., Barlow, J. F., Halios, C. H., Lee, J. D., Szidat, S., and Mohr, C.: Sources and Contributions of Wood Smoke During Winter in London: Assessing Local and Regional Influences, in preparation, 2014.

Crippa, M., DeCarlo, P. F., Slowik, J. G., Mohr, C., Heringa, M. F., Chirico, R., Poulain, L., Freutel, F., Sciare, J., Cozic, J., Di Marco, C. F., Elsasser, M., Nicolas, J. B., Marchand, N., Abidi, E., Wiedensohler, A., Drewnick, F., Schneider, J., Borrmann, S., Nemitz, E., Zimmermann, R., Jaffrezo, J.-L., Prévôt, A. S. H., and Baltensperger, U.: Wintertime aerosol chemical composition and source apportionment of the organic fraction in the metropolitan area of Paris, Atmos. Chem. Phys., 13, 961–981, doi:10.5194/acp-13-961-2013, 2013.

Crippa, M., Canonaco, F., Lanz, V. A., Äijälä, M., Allan, J. D., Carbone, S., Capes, G., Ceburnis, D., Dall'Osto, M., Day, D. A., DeCarlo, P. F., Ehn, M., Eriksson, A., Freney, E., Hildebrandt Ruiz, L., Hillamo, R., Jimenez, J. L., Junninen, H., Kiendler-Scharr, A., Kortelainen, A.-M., Kulmala, M., Laaksonen, A., Mensah, A. A., Mohr, C., Nemitz, E., O'Dowd, C., Ovadnevaite, J., Pandis, S. N., Petäjä, T., Poulain, L., Saarikoski, S., Sellegri, K., Swietlicki, E., Tiitta, P., Worsnop, D. R., Baltensperger, U., and Prévôt, A. S. H.: Organic aerosol components derived from 25 AMS data sets across Europe using a consistent ME-2 based source apportionment approach, Atmos. Chem. Phys., 14, 6159–6176, doi:10.5194/acp-14-6159-2014, 2014.

Cubison, M. J., Ortega, A. M., Hayes, P. L., Farmer, D. K., Day, D., Lechner, M. J., Brune, W. H., Apel, E., Diskin, G. S., Fisher, J. A., Fuelberg, H. E., Hecobian, A., Knapp, D. J., Mikoviny, T., Riemer, D., Sachse, G. W., Sessions, W., Weber, R. J., Weinheimer, A. J., Wisthaler, A., and Jimenez, J. L.: Effects of aging on organic aerosol from open biomass burning smoke in aircraft and laboratory studies, Atmos. Chem. Phys., 11, 12049–12064, doi:10.5194/acp-11-12049-2011, 2011.

Dall'Osto, M., Ovadnevaite, J., Ceburnis, D., Martin, D., Healy, R. M., O'Connor, I. P., Kourtchev, I., Sodeau, J. R., Wenger, J. C., and O'Dowd, C.: Characterization of urban aerosol in Cork city (Ireland) using aerosol mass spectrometry, Atmos. Chem. Phys., 13, 4997–5015, doi:10.5194/acp-13-4997-2013, 2013.

DeCarlo, P. F., Kimmel, J. R., Trimborn, A., Northway, M. J., Jayne, J. T., Aiken, A. C., Gonin, M., Fuhrer, K., Horvath, T., Docherty, K. S., Worsnop, D. R., and Jimenez, J. L.:

Field-deployable, high-resolution, time-of-flight aerosol mass spectrometer, Anal. Chem., 78, 8281–8289, doi:10.1021/ac061249n, 2006.

DeCarlo, P. F., Ulbrich, I. M., Crounse, J., de Foy, B., Dunlea, E. J., Aiken, A. C., Knapp, D., Weinheimer, A. J., Campos, T., Wennberg, P. O., and Jimenez, J. L.: Investigation of the sources and processing of organic aerosol over the Central Mexican Plateau from aircraft measurements during MILAGRO, Atmos. Chem. Phys., 10, 5257–5280, doi:10.5194/acp-10-5257-2010, 2010.

Department for Environment, Food and Rural Affairs (Defra), UK Smoke Control Areas, http://smokecontrol.defra.gov.uk/, last access: 26 March 2014.

Donaldson, K., Stone, V., Borm, P. J., Jimenez, L. A., Gilmour, P. S., Schins, R. P., Knaapen, A. M., Rhaman, I., Faux, S. P., Brown, D. M., and MacNee, W.: Oxidative stress and calcium signaling in the adverse effects of environmental particles (PM_{10}), Free Radical Bio. Med., 34, 1369–1382, 2003.

Drewnick, F., Hings, S. S., Decarlo, P. F., Jayne, J. T., Gonin, M., Fuhrer, K.,Weimer, S., Jimenez, J. L., Demerjian, K. L., Borrmann, S., and Worsnop, D. R.: A new time-of-flight aerosol mass spectrometer (TOF-AMS) - Instrument description and first field deployment, Aerosol Sci. Tech., 39, 637–658, doi:10.1080/02786820500182040, 2005.

European Union: Directive 2008/50/EC of the European parliament and of the council of 21 May 2008 on ambient air quality and cleaner air for Europe, Official Journal of the European Union, L152, 2008.

Fuller, G. W., Sciare, J., Lutz, M., Moukhtar, S., and Wagener, S.: New Directions: Time to tackle urban wood burning?, Atmos. Environ., 68, 295–296, doi:10.1016/j.atmosenv.2012.11.045, 2013.

Fuller, G. W., Tremper, A. H., Baker, T. D., Yttri, K. E., and Butterfield, D.: Contribution of wood burning to PM_{10} in London, Atmos. Environ., 87, 87–94, doi:10.1016/j.atmosenv.2013.12.037, 2014.

Glasius, M., Ketzel, M., Wahlin, P., Jensen, B., Monster, J., Berkowicz, R., and Palmgren, F.: Impact of wood combustion on particle levels in a residential area in Denmark, Atmos. Environ., 40, 7115–7124, doi:10.1016/j.atmosenv.2006.06.047, 2006.

Grieshop, A. P., Donahue, N. M., and Robinson, A. L.: Laboratory investigation of photochemical oxidation of organic aerosol from wood fires 2: analysis of aerosol mass spectrometer data, Atmos. Chem. Phys., 9, 2227–2240, doi:10.5194/acp-9-2227-2009, 2009.

Harrison, R. M., Beddows, D. C. S., Hu, L., and Yin, J.: Comparison of methods for evaluation of wood smoke and estimation of UK ambient concentrations, Atmos. Chem. Phys., 12, 8271–8283, doi:10.5194/acp-12-8271-2012, 2012a.

Harrison, R. M., Dall'Osto, M., Beddows, D. C. S., Thorpe, A. J., Bloss, W. J., Allan, J. D., Coe, H., Dorsey, J. R., Gallagher, M., Martin, C., Whitehead, J., Williams, P. I., Jones, R. L., Langridge, J. M., Benton, A. K., Ball, S. M., Langford, B., Hewitt, C. N., Davison, B., Martin, D., Petersson, K. F., Henshaw, S. J., White, I. R., Shallcross, D. E., Barlow, J. F., Dunbar, T., Davies, F., Nemitz, E., Phillips, G. J., Helfter, C., Di Marco, C. F., and Smith, S.: Atmospheric chemistry and physics in the atmosphere of a developed megacity (London): an overview of the REPARTEE experiment and its conclusions, Atmos. Chem. Phys., 12, 3065–3114, doi:10.5194/acp-12-3065-2012, 2012b.

Hellén, H., Hakola, H., Haaparanta, S., Pietarila, H., and Kauhaniemi, M.: Influence of residential wood combustion on local air quality, Sci. Total Environ., 393, 283–290, 2008.

Hennigan, C. J., Sullivan, A. P., Collett, J. L., and Robinson, A. L.: Levoglucosan stability in biomass burning particles exposed to hydroxyl radicals, Geophys. Res. Lett., 37, L09806, doi:10.1029/2010GL043088, 2010.

Heringa, M. F., DeCarlo, P. F., Chirico, R., Tritscher, T., Dommen, J., Weingartner, E., Richter, R., Wehrle, G., Prévôt, A. S. H., and Baltensperger, U.: Investigations of primary and secondary particulate matter of different wood combustion appliances with a high-resolution time-of-flight aerosol mass spectrometer, Atmos. Chem. Phys., 11, 5945–5957, doi:10.5194/acp-11-5945-2011, 2011.

Huffman, J. A., Ziemann, P. J., Jayne, J. T., Worsnop, D. R., and Jimenez, J. L.: Development and Characterization of a Fast-Stepping/Scanning Thermodenuder for Chemically-Resolved Aerosol Volatility Measurements, Aerosol Sci. Tech., 42, 395–407, 2008.

Jimenez, J. L., Canagaratna, M. R., Donahue, N. M., Prevot, A. S. H., Zhang, Q., Kroll, J. H., Decarlo, P. F., Allan, J. D., Coe, H., Ng, N. L., Aiken, A. C., Docherty, K. S., Ulbrich, I. M., Grieshop, A. P., Robinson, A. L., Duplissy, J., Smith, J. D., Wilson, K. R., Lanz, V. A., Hueglin, C., Sun, Y. L., Tian, J., Laaksonen, A., Raatikainen, T., Rautiainen, J., Vaattovaara, P., Ehn, M., Kulmala, M., Tomlinson, J. M., Collins, D. R., Cubison, M. J., E., Dunlea, E. J., Huffman, J. A., Onasch, T. B., Alfarra, M. R., Williams, P. I., Bower, K. N., Kondo, Y., Schneider, J., Drewnick, F., Borrmann, S., Weimer, S., Demerjian, K. L., Salcedo, D., Cottrell, L., Griffin, R., Takami, A., Miyoshi, T., Hatakeyama, S., Shimono, A., Sun, J. Y., Zhang, Y. M., Dzepina, K., Kimmel, J. R., Sueper, D., Jayne, J. T., Herndon, S. C., Trimborn, A. M.,Williams, L. R., Wood,

E. C., Middlebrook, A. M.,Kolb, C. E., Baltensperger, U., and Worsnop, D. R.: Evolution of Organic Aerosols in the Atmosphere, Science, 326, 1525–1529, doi:10.1126/science.1180353, 2009.

Jolleys, M. D., Coe, H., McFiggans, G., Taylor, J., O'Shea, S. J., Le Breton, M., Bauguitte., S. J.-B., Moller, S., Di Carlo, P., Aruffo, E., Palmer, P. I., and Lee, J. D.: Properties and evolution of biomass burning organic aerosol from Canadian boreal forest fires, submitted, 2014a.

Jolleys, M. D., Coe, H., McFiggans, G., McMeeking, G. R., Lee, T., Sullivan, A. P., Kreidnweis, S. M., and Collett, J. L.: Organic aerosol emission ratios from the laboratory combustion of biomass fuels, submitted, 2014b.

Kanakidou, M., Seinfeld, J. H., Pandis, S. N., Barnes, I., Dentener, F. J., Facchini, M. C., Van Dingenen, R., Ervens, B., Nenes, A., Nielsen, C. J., Swietlicki, E., Putaud, J. P., Balkanski, Y., Fuzzi, S., Horth, J., Moortgat, G. K., Winterhalter, R., Myhre, C. E. L., Tsigaridis, K., Vignati, E., Stephanou, E. G., and Wilson, J.: Organic aerosol and global climate modelling: a review, Atmos. Chem. Phys., 5, 1053–1123, doi:10.5194/acp-5-1053-2005, 2005.

Lack, D. A., Bahreini, R., Langridge, J. M., Gilman, J. B., and Middlebrook, A. M.: Brown carbon absorption linked to organic mass tracers in biomass burning particles, Atmos. Chem. Phys., 13, 2415–2422, doi:10.5194/acp-13-2415-2013, 2013.

Lanz, V. A., Alfarra, M. R., Baltensperger, U., Buchmann, B., Hueglin, C., and Prévôt, A. S. H.: Source apportionment of submicron organic aerosols at an urban site by factor analytical modelling of aerosol mass spectra, Atmos. Chem. Phys., 7, 1503–1522, doi:10.5194/acp-7-1503-2007, 2007.

Liu, D., Allan, J. D., Young, D. E., Coe, H., Beddows, D., Fleming, Z. L., Flynn, M. J., Gallagher, M. W., Harrison, R. M., Lee, J., Prevot, A. S. H., Taylor, J. W., Yin, J., Williams, P. I., and Zotter, P.: Size distribution, mixing state and source apportionments of black carbon aerosols in London during winter time, Atmos. Chem. Phys. Discuss., 14, 16291–16349, doi:10.5194/acpd-14-16291-2014, 2014.

Martin, C. L., Allan, J. D., Crosier, J., Choularton, T. W., Coe, H., and Gallagher, M. W.: Seasonal variation of fine particulate composition in the centre of a UK city, Atmos. Environ., 45, 4379–4389, 10.1016/j.atmosenv.2011.05.050, 2011.

Maykut, N. N., Lewtas, J., Kim, E., and Larson, T. V.: Source apportionment of $PM_{2.5}$ at an urban IMPROVE site in Seattle, Washington, Environ. Sci. Technol., 37, 5135–5142, doi:10.1021/es030370y, 2003.

Mohr, C., Huffman, J. A., Cubison, M. J., Aiken, A. C., Docherty, K. S., Kimmel, J. R., Ulbrich, I. M., Hannigan, M., Garcia, J., and Jimenez, J. L.: Characterization of Primary Organic Aerosol Emissions from Meat Cooking, Trash Burning, and Motor Vehicles with High-Resolution Aerosol Mass Spectrometry and Comparison with Ambient and Chamber Observations, Environ. Sci. Technol., 43, 2443–2449, doi:10.1021/es8011518, 2009.

Mohr, C., DeCarlo, P. F., Heringa, M. F., Chirico, R., Slowik, J. G., Richter, R., Reche, C., Alastuey, A., Querol, X., Seco, R., Peñuelas, J., Jiménez, J. L., Crippa, M., Zimmermann, R., Baltensperger, U., and Prévôt, A. S. H.: Identification and quantification of organic aerosol from cooking and other sources in Barcelona using aerosol mass spectrometer data, Atmos. Chem. Phys., 12, 1649–1665, doi:10.5194/acp-12-1649-2012, 2012.

Mohr, C., Lopez-Hilfiker, F. D., Zotter, P., Prevot, A. S. H., Xu, L., Ng, N. L., Herndon, S. C., Williams, L. R., Franklin, J. P., Zahniser, M. S., Worsnop, D. R., Knighton, W. B., Aiken, A. C., Gorkowski, K. J., Dubey, M. K., Allan, J. D., and Thornton, J. A.: Contribution of nitrated phenols to wood burning brown carbon light absorption in Delting, United Kingdom during winter time, Environ. Sci. Technol., 47, 6316–6324, doi:10.1021/es400683v, 2013.

National atmospheric emissions inventory (NAEI): http://naei.defra.gov.uk/ (last access: 1 April 2014), 2014.

Ng, N. L., Canagaratna, M. R., Zhang, Q., Jimenez, J. L., Tian, J., Ulbrich, I. M., Kroll, J. H., Docherty, K. S., Chhabra, P. S., Bahreini, R., Murphy, S. M., Seinfeld, J. H., Hildebrandt, L., Donahue, N. M., DeCarlo, P. F., Lanz, V. A., Prévôt, A. S. H., Dinar, E., Rudich, Y., and Worsnop, D. R.: Organic aerosol components observed in Northern Hemispheric datasets from Aerosol Mass Spectrometry, Atmos. Chem. Phys., 10, 4625–4641, doi:10.5194/acp-10-4625-2010, 2010.

Ng, N., Canagaratna, M., Jimenez, J., Zhang, Q., Ulbricht, I., and Worsnop, D.: Real-time methods for estimating organics component mass concentrations from Aerosol Mass Spectrometry data, Environ. Sci. Technol., 45, 910–916, 2011.

Oberdörster, G., Oberdörster, E., and Oberdörster, J.: Nanotoxicology: An emerging discipline evolving from studies of ultrafine particles, Environ. Health Persp., 113, 823–839, 2005.

Ortega, A. M., Day, D. A., Cubison, M. J., Brune, W. H., Bon, D., de Gouw, J. A., and Jimenez, J. L.: Secondary organic aerosol formation and primary organic aerosol oxidation from biomass-burning smoke in a flow reactor during FLAME-3, Atmos. Chem. Phys., 13, 11551–11571, doi:10.5194/acp-13-11551-2013, 2013.

Peabody, J. W., Riddell, T. J., Smith, K. R., Liu, Y., Zhao, Y., Gong, J., Milet, M., and Sinton, J. E.: Indoor Air Pollution in Rural China: Cooking Fuels, Stoves, and Health Status, Arch. Environ. Occup. H., 60, 86–95, 2005.

Pope III, C. A. and Dockery, D. W.: Health effects of fine particulate air pollution: lines that connect, J. Air Waste Manage., 56, 709–742, doi:10.1080/10473289.2006.10464485, 2006.

Puxbaum, H., Caseiro, A., Sánchez-Ochos, A., Kasper-Giebl, A., Claeys, M., Gelencser, A., Legrand, M., Preunkert, S., and Pio, C.: Levoglucosan levels at background sites in Europe for assessing the impact of biomass combustion on the European aerosol background, J. Geophys. Res., 112, D23S05, doi:10.1029/2006JD008114, 2007.

Ries, F., Marshall, J. D., and Brauer, M.: Intake fraction of urban wood smoke, Environ. Sci. Technol., 43, 4701–4706, doi:10.1021/es803127d, 2009.

Sciare, J., D'Argouges, O., Esteve, R. S., Gaimoz, C., Dolgorouky, C., Bonnaire, N., Favez, O., Bonsang, B., and Gros, V.: Large contribution of water insoluble secondary organic aerosols in the region of Paris (France) during wintertime, J. Geophys. Res., 116, D22203, doi:10.1029/2011JD015756, 2011.

Sun, Y. L., Wang, Z. F., Fu, P. Q., Yang, T., Jiang, Q., Dong, H. B., Li, J., and Jia, J. J.: Aerosol composition, sources and processes during wintertime in Beijing, China, Atmos. Chem. Phys., 13, 4577–4592, doi:10.5194/acp-13-4577-2013, 2013.

Szidat, S., Jenk, T. M., Synal, H.-A., Kalberer, M., Wacker, L., Hajdas, I., Kasper-Giebl, A., and Baltensperger, U.: Contributions of fossil fuel, biomass burning, and biogenic emissions to carbonaceous aerosols in Zurich as traced by 14C, J. Geophys. Res., 111, D07206, doi:10.1029/2005JD006590, 2006.

Transport for London (TfL): London Low Emission Zone Impacts Monitoring Baseline Report, July 2008, Transport for London, London, UK, 2008.

Wagener, S., Langner, M., Hansen, U., Moriske, H. J., and Endlicher, W. R.: Spatial and seasonal variations of biogenic tracer compounds in ambient PM_{10} and PM_1 samples in Berlin, Germany, Atmos. Environ., 47, 33–42, 2012.

Weimer, S., Alfarra, M. R., Schreiber, D., Mohr, M., Prévôt, A. S. H., and Baltensperger, U.: Organic aerosol mass spectral signatures from wood burning emissions: Influence of burning conditions and wood type, J. Geophys. Res., 113, D10304, doi:10.1029/2007JD009309, 2008.

Yin, J., Harrison, R. M., Chen, Q., Rutter, A., and Schauer, J. J.: Source apportionment of fine particles at urban background and rural sites in the UK atmosphere, Atmos. Environ., 44, 841–851, 2010.

Yin, J., Cumberland, S., Harrison, R. M., Allan, J., Young, D. E., Williams, P. I., and Coe, H.: Receptor modelling of fine particles in southern England using CMB including comparison with AMS-PMF factors, in preparation, 2014.

Yttri, K. E., Dye, C., Siørdal, L. H., and Braathen O.-A.: Quantification of monosaccharide anhydrides by liquid chromatography combined with mass spectrometry: application to aerosol samples from an urban and a suburban site influenced by small-scale wood burning, J. Air Waste Manage., 55, 1169–1177, doi:10.1080/10473289.2005.10464720, 2005.

Yokelson, R. J., Griffith, D. W. T., and Ward, D. E.: Open-path Fourier transform infrared studies of large-scale laboratory biomass fires, J. Geophys. Res., 101, 21067–21080, doi:10.1029/96jd01800, 1996.

Young, D. E., Allan, J. D., Williams, P. I., Green, D. C., Flynn, M. J., Harrison, R. M., Yin, J., Gallagher, M. W., and Coe, H.: Investigating the annual behaviour of submicron secondary inorganic and organic aerosols in London, Atmos. Chem. Phys. Discuss., 14, 18739–18784, doi:10.5194/acpd-14-18739-2014, 2014.

Zhang, H., Wang, S., Hao, J., Wan, L., Jiang, J., Zhang, M., Mestl, H. E. S., Alnes, L. W. H., Aunan, K., and Mellouki, A. W.: Chemical and size characterization of particles emitted from the burning of coal and wood in rural households in Guizhou, China, Atmos. Environ., 51, 94–99, doi:10.1016/j.atmosenv.2012.01.042, 2012.

Zhang, J. K., Sun, Y., Liu, Z. R., Ji, D. S., Hu, B., Liu, Q., and Wang, Y. S.: Characterization of submicron aerosols during a month of serious pollution in Beijing, 2013, Atmos. Chem. Phys., 14, 2887–2903, doi:10.5194/acp-14-2887-2014, 2014.

Zhang, Q., Worsnop, D. R., Canagaratna, M. R., and Jimenez, J. L.: Hydrocarbon-like and oxygenated organic aerosols in Pittsburgh: insights into sources and processes of organic aerosols, Atmos. Chem. Phys., 5, 3289–3311, doi:10.5194/acp-5-3289-2005, 2005.

Zhang, Q., Jimenez, J. L., Canagaratna, M. R., Allan, J. D., Coe, H., Ulbrich, I., Alfarra, M. R., Takami, A., Middlebrook, A. M., Sun, Y. L., Dzepina, K., Dunlea, E. J., Docherty, K. S., Decarlo, P. F., Salcedo, D., Onasch, T., Jayne, J. T., Miyoshi, T., Shimono, A., Hatakeyama, S., Takegawa, N., Kondo, Y., Schneider, J., Drewnick, F., Borrmann, S., Weimer, S., Demerjian, K. L., Williams, P., Bower, K. N., Bahreini, R., Cottrell, L., Griffin, R. J., Rautiainen, J., Sun, J. Y., Zhang, Y. M., and Worsnop, D. R.: Ubiquity and dominance of oxygenated species in or-

ganic aerosols in anthropogenically-influenced Northern Hemisphere midlatitudes, Geophys. Res. Lett., 34, L13801, doi:10.1029/2007GL029979, 2007.

Table 1. Pearson's *r* correlation coefficients for linear and multi-linear regressions between PMF factors from the 4 and 5-factor solutions and combustion tracers.

	CO	NO_x
SFOA-4fac	0.56	0.43
SFOA-combined	0.65	0.51
f(HOA,SFOA)-4fac	0.77	0.74
f(HOA,SFOA)-combined	0.77	0.71

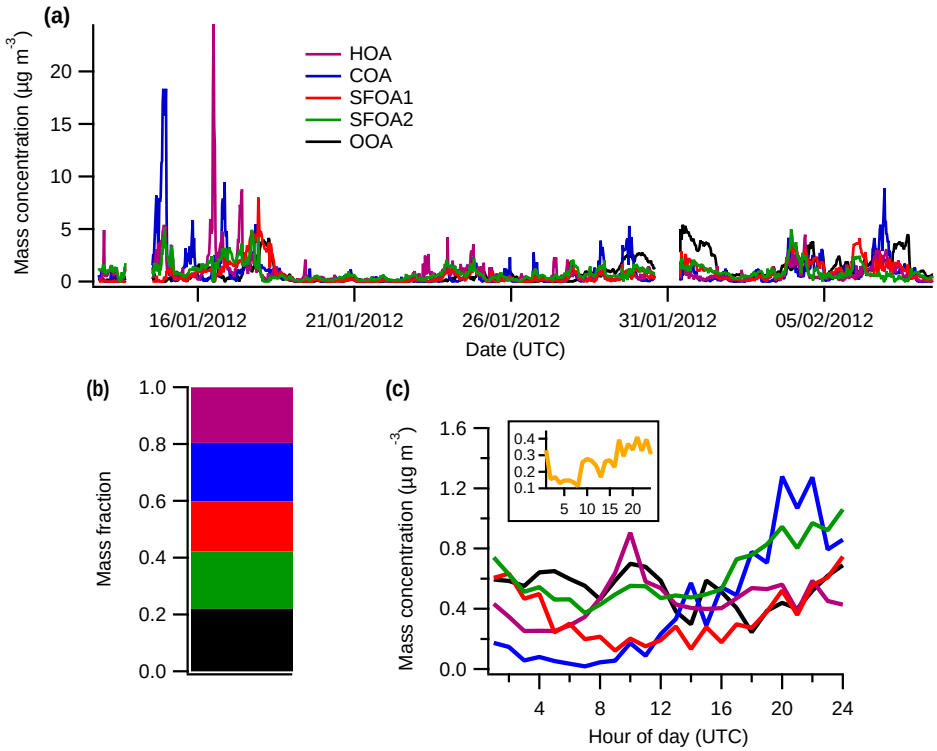

Figure 1. **(a)** Time series of the 5-factor-PMF solution from the HR-ToF-AMS PMF. **(b)** Average fractional contribution to the total submicron organic aerosol mass. **(c)** Median diurnal profiles for each of the 5 factors and the diurnal profile of the difference between the two SFOA factors (SFOA2-SFOA1, inset).

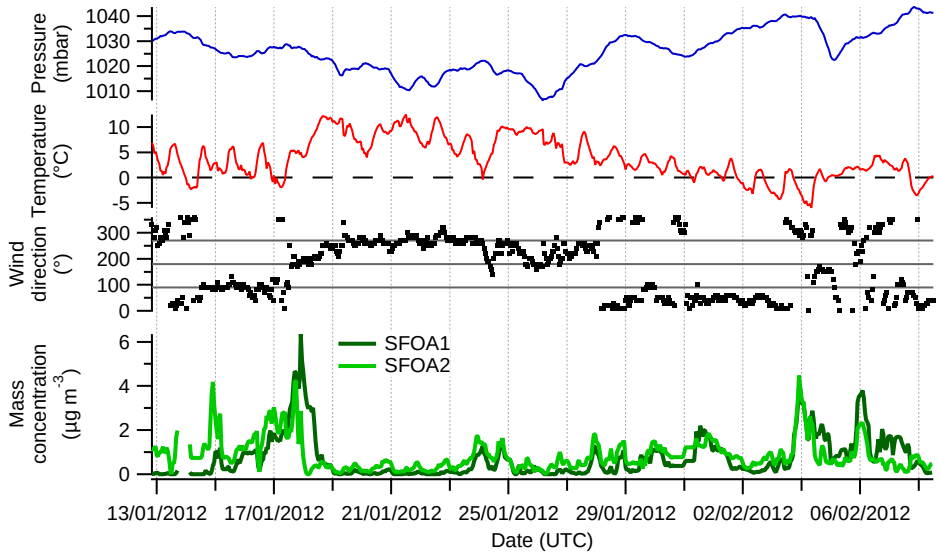

Figure 2. Time series of SFOA1 and SFOA2 concentration and meteorological data from Heathrow.

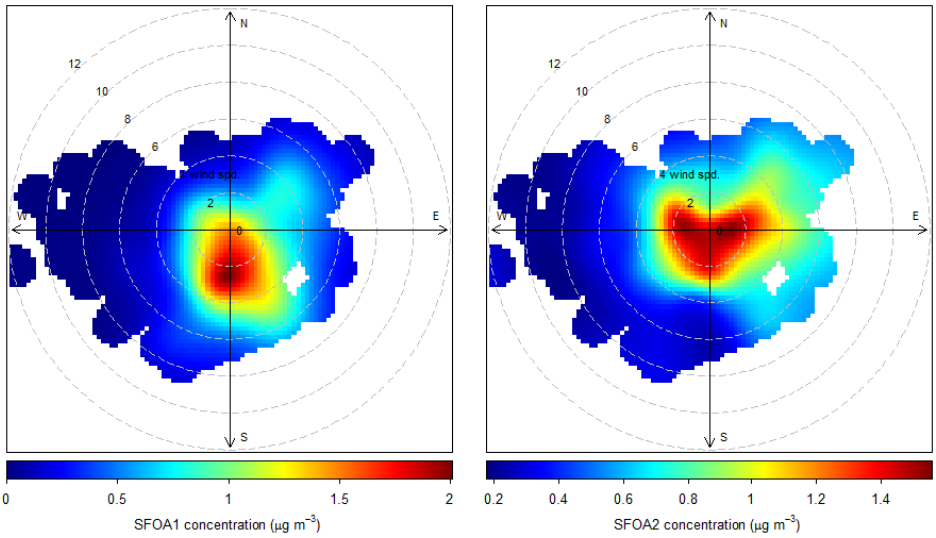

Figure 3. Polar plots of hourly averaged SFOA1 (left) and SFOA2 (right) concentrations as a function of wind speed and direction, where the wind data are from the Heathrow airport meteorological station, which are unaffected by large buildings. These polar plots were plotted in R using the opeanair package (Carslaw and Ropkins, 2012; Carslaw, 2013), which is a data analysis tool used to investigate air pollution.

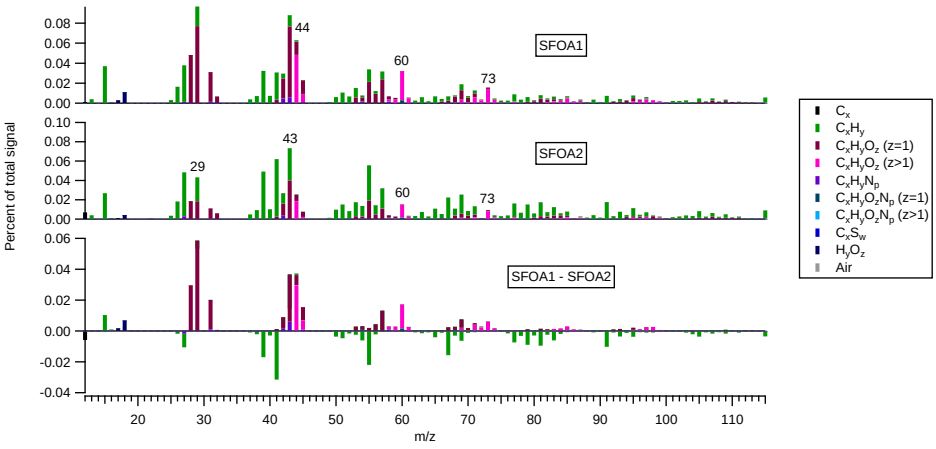

Figure 4. Mass spectra of SFOA1 (top) and SFOA2 (middle) as derived from PMF analysis on the HR-ToF-AMS organic data. Bottom: the difference between the mass spectral profiles of SFOA1 and SFOA2.

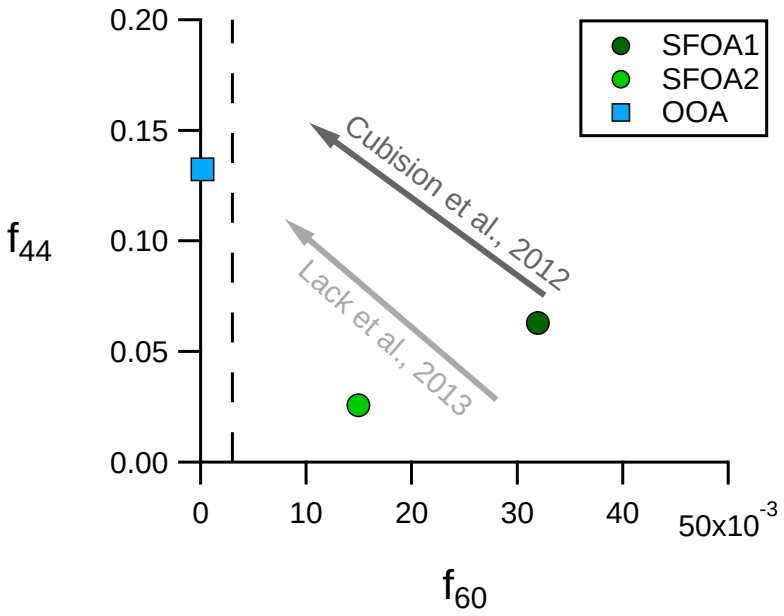

Figure 5. f_{44} vs. f_{60} for the SFOA1 and SFOA2 factors derived from PMF analysis of the HR-ToF-AMS organic data. OOA is also plotted for reference. The dashed line indicates the background f_{60} level of 0.3 % as defined by Cubison et al. (2011). The arrows indicate direction of aging observed in various plumes measured in Cubison et al. (2011, dark grey arrow) and Lack et al. (2013, light grey arrow).

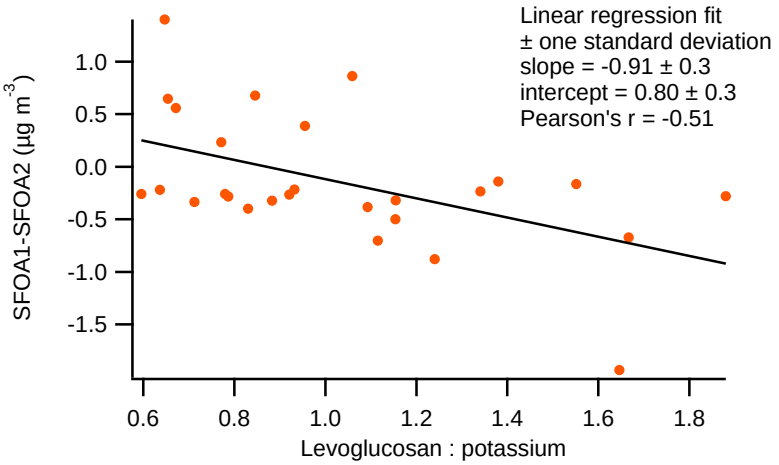

Figure 6. Variation of the difference between SFOA1 and SFOA2 concentrations with the levoglucosan : potassium ratio as derived from 24 h filter samples.

4.4 Paper III: Evidence for the presence of primary organic nitrates associated with anthropogenic emissions in London

Dominique E. Young, James D. Allan, Paul I. Williams, David C. Green, Rachel E. Holmes, James R. Hopkins, Jacqueline F. Hamilton, Alastair C. Lewis, James D. Lee, Zoe L. Fleming, Thomas J. Bannan, Asan Bacak, Carl J. Percival, Janet F. Barlow, Michael J. Flynn, Martin W. Gallagher, and Hugh Coe.

This paper will be submitted to the journal of Atmospheric Chemistry and Physics.

Overview

In this paper, the chemical composition and variations in concentration of a component of organic aerosol (OA) derived from Positive Matrix Factorisation (PMF) analysis of the OA data measured by the High-Resolution Time-of-Flight Aerosol Mass Spectrometer (HR-ToF-AMS) during summer 2012 was examined to investigate its behaviour. The factor is shown to be a significant fraction of the total submicron organic aerosol mass observed in London during summertime. Correlations with excess NO^+ ion signals at m/z 30 indicated the factor was strongly associated with organic nitrates thus potential origins and formation pathways of the organic nitrate factor were explored. The highest concentrations of the organic nitrate factor were observed over night and the analysis in the paper shows that the factor does not appear to be influenced by nitrate radical chemistry. Furthermore, the analysis shows that regional transport is not an important factor in the variability of the organic nitrate factor. Comparisons with the primary organic aerosol factors derived from PMF as well as with volatile organic compounds (VOCs) indicated the organic nitrate factor is directly emitted into the atmosphere with strong associations with anthropogenic emissions. Whilst the analyses presented in the paper did not lead to particular sources being identified it is likely that the observed organic nitrate arises from a range of evaporative sources. The observations presented in this paper therefore indicate a potentially important yet unidentified primary source of OA in the urban environment which requires further investigation and characterisation through detailed laboratory and field measurements in order to better inform pollution abatement strategies and air quality policies.

Author contributions

Dominique Young performed aerosol measurements, analysed and interpreted the data, and wrote the manuscript. James Allan helped to run instruments in the field and assisted with interpretation of results and preparation of the manuscript. Paul Williams and David Green assisted with the aerosol measurements. Rachel Holmes and James Hopkins provided the VOC data. Jacqueline Hamilton, Alistair Lewis, and Rachel Holmes assisted in the interpretation of the results and manuscript preparation. James Lee provided the ozone (O_3), nitrogen dioxide (NO_2), and nitrogen monoxide (NO) data. Zoe Fleming provided the NAME footprints and Janet Barlow provided the boundary layer data. Thomas Bannan, Asan Bacak, and Carl Percival provided the Chemical Ionisation Mass Spectrometer (CIMS) data. Michael Flynn helped prepare the instrumentation both before and during the field campaigns. Martin Gallagher assisted in the planning of the field campaigns. Hugh Coe assisted with the interpretation of the data and preparation of the manuscript.

Evidence for the presence of primary organic nitrates associated with anthropogenic emissions in London

D. E. Young[1], J. D. Allan[1,2], P. I. Williams[1,2], D. C. Green[3], R. E. Holmes[4], J. R. Hopkins[4], J. F. Hamilton[4], A. C. Lewis[4,5], J. D. Lee[4], Z. L. Fleming[6,7], T. J. Bannan[1], A. Bacak[1], C. J. Percival[1], J. F. Barlow[8], M. J. Flynn[1], M. W. Gallagher[1], and H. Coe[1]

[1]{School of Earth, Atmospheric and Environmental Sciences, University of Manchester, Oxford Road, Manchester, M13 9PL, UK}

[2]{National Centre for Atmospheric Science, University of Manchester, Oxford Road, Manchester, M13 9PL, UK}

[3]{School of Biomedical and Health Sciences, King's College London, London, UK}

[4]{Wolfson Atmospheric Chemistry Laboratories, Department of Chemistry, University of York, York, YO10 5DD, UK}

[5]{National Centre for Atmospheric Science, University of York, York UK}

[6]{Department of Chemistry, University of Leicester, Leicester, LE1 7RH, UK}

[7]{National Centre for Atmospheric Science, University of Leicester, Leicester, UK}

[8]{Department of Meteorology, University of Reading, Reading RG6 6BB, UK}

Correspondence to: Hugh Coe (hugh.coe@manchester.ac.uk)

Abstract

The largest component of the total submicron aerosol loading in urban areas is often organic aerosols (OA) yet their sources and behaviour are poorly characterised. A High-Resolution Time-of-Flight Aerosol Mass Spectrometer (HR-ToF-AMS) was used to investigate OA at an urban background site in London during summer 2012 as part of the Clean Air for London (ClearfLo) project. The components of the

organic aerosol fraction were derived using positive matrix factorisation (PMF) where five factors were identified: hydrocarbon-like OA (HOA), cooking OA (COA), semi-volatile oxygenated OA (SV-OOA), low-volatility oxygenated OA (LV-OOA), and a fifth component whose chemical composition and concentrations are examined to investigate its behaviour. This factor has an average concentration of 1.01 μg m^{-3} and contributes 17% to the total OA mass on average. Through comparisons with excess NO^+ ion signals at m/z 30, we propose that the factor is composed of organic nitrates, which are directly emitted into the atmosphere. This method presents an independent diagnostic for estimating the organic nitrate contribution. Furthermore, strong correlations with various volatile organic compounds (VOCs) suggest the factor has a strong association with anthropogenic emissions. These observations therefore indicate a potentially important yet unidentified primary source of OA, thus we suggest efforts should focus on determining what could be a significant contribution to particulate matter in the urban environment.

1 Introduction

The properties of ambient aerosols are important in determining their impacts once emitted into the atmosphere where particle size and chemical composition likely play substantial roles in the processes leading to adverse effects on human health (Donaldson et al., 2003; Oberdörster et al., 2005; Pope and Dockery, 2006). Furthermore, such properties have significant implications for the influence of aerosols on air quality (AGEQ, 2012) and climate (Boucher et al., 2013). The chemical composition of atmospheric aerosols varies considerably owing to their numerous natural and anthropogenic sources (Seinfeld and Pandis, 2006) resulting in aerosols that are composed of many different compounds. Of particular interest are organic aerosols (OA) as they often represent a large fraction of the total mass loading in a range of environments across the world (Kanakidou et al., 2005; Zhang et al., 2007). However, the evolution and fate of organic species are uncertain.

Additionally, the sources of OA are not well understood, with models often under predicting observed mass concentrations (de Gouw et al., 2005; Heald et al., 2005; Volkamer et al., 2006). Several measurement studies have highlighted the importance of biogenic secondary OA (SOA) precursors, particularly in summer (Szidat et al., 2006; Gelencsér et al., 2007), with strong associations between anthropogenic sources

and SOA also identified (Weber et al., 2007). Water soluble ON (WSON) were successfully identified in both the gas and particle phase by González Benítez et al. (2010), however, a range of sources of WSON were suggested including anthropogenic and non-anthropogenic as well as sources which varied spatially. Particulate organic nitrates (ON) have been shown to be present in or associated with SOA (Ng et al., 2008; Fry et al., 2009) yet they are a poorly explored aspect of the atmosphere as they are challenging to characterise in the laboratory and there is a lack of instrumentation to measure them. Part of the uncertainty surrounding OA therefore arises from the difficulties in speciation and quantification of ON.

ON can either be primary or secondary, where direct emissions include those from some industrial processes and oceans (e.g. Atlas et al., 1993; Cape et al., 2011) and formation in the atmosphere is via reactions of volatile organic compounds (VOCs) (Perring et al., 2013 and references therein). Secondary formation of ON can occur during the night as well as the day from oxidation and photochemical reactions, respectively, where hydroxy radicals (OH) play a key role during the day, nitrate radicals (NO_3) are the main oxidant at night, and ozone (O_3) can be important during the day and night (e.g. Lim and Ziemann, 2005; Ng et al., 2008; Fry et al., 2009; Hallquist et al., 2009; Lim and Ziemann, 2009). Day et al. (2010) suggest that during polluted urban conditions, ON concentrations may be significant, contributing up to 10% of the organic matter. Furthermore, anthropogenic pollution is proposed to enhance SOA formation from biogenic VOCs (Weber et al., 2007; Goldstein et al., 2009; Hoyle et al., 2011; Spracklen et al., 2011; Worton et al., 2011), with a potential mechanism suggested to be through emissions of nitrogen oxides (NO_x) (Ng et al., 2007, 2008; Chan et al., 2010; Rollins et al., 2012*)* which produce NO_3 that subsequently react with VOCs. Consequently, higher yields of ON can be found at night compared to the day (Rollins et al., 2012).

Despite their importance in atmospheric chemistry, contribution to OA mass, and potential adverse effects on health, air quality, and climate, the formation, properties, and evolution of ON are not well characterised. Few ambient studies have quantified particulate organic nitrates, owing in part to the sampling and analytical methodologies deployed where there are trade-offs between chemical specificity and time resolution (Farmer et al., 2010). However, the Aerosol Mass Spectrometer (AMS) can quantitatively measure chemical composition of aerosols with high time

resolution. Various factorisation models have been applied to measurements from different instruments to probe the components of the organic fraction such as Positive Matrix Factorisation (PMF), a receptor-based factorisation model often applied to AMS measurements. The most common sources of OA identified from PMF analysis of AMS data are traffic, cooking, and solid fuel burning (including biomass and wood), with regional and transboundary OA also being important (Zhang et al., 2005; Lanz et al., 2007; Jimenez et al., 2009; Allan et al., 2010; Crippa et al., 2014). It is not always possible to attribute OA factors derived from PMF analysis to specific sources, although the chemical composition and temporal variation of the factor as well as comparisons with other measurements can enable unknown factors to be classified as local or regional and primary or secondary (Aiken et al., 2009; Docherty et al., 2011; Sun et al., 2011; Hayes et al., 2013). Several studies have termed such factors local OA (LOA) (Aiken et al., 2009; Huffman et al., 2009; Docherty et al., 2011) where OA factors containing contributions from many nitrogen-containing fragments have been reported and termed local-OA-amine containing (LOA-AC Aiken et al., 2009, Huffman et al., 2009) or nitrogen-containing OA (NOA, Sun et al., 2011). ON has also been successfully identified from AMS measurements (Bae et al., 2007; Farmer et al., 2010) and micro-orifice volatilization impactor (MOVI) high-resolution chemical ionization mass spectrometer measurements (Mohr et al., 2013) where contributions from organic nitrogen species to the AMS nitrate signal have been previously reported in forested environments (Allan et al., 2006; Allan et al., 2014) and rural locations (Bae et al., 2007). Here we present the results of PMF analysis applied to the organic aerosol data from the High-Resolution Time-of-Flight AMS (HR-ToF-AMS) which was deployed at an urban background site in London to characterise aerosol chemical composition and sources. Furthermore, we present evidence for the presence of primary organic nitrates in London during summer.

2 Experimental

2.1 Sampling site

A suite of state-of-the-art instrumentation, measuring aerosols, gases, radicals and meteorological parameters was deployed for a major summer intensive observation period (IOP) between July and August 2012 as part of the NERC funded Clean Air

for London (ClearfLo) Project (www.clearflo.ac.uk). Measurements were conducted in a residential area 7 km to the west of Central London at the ClearfLo urban background supersite in the grounds of Sion Manning School in North Kensington (51.521055 N, 0.213432 W). Further details on the experimental campaigns and locations of this large, multi-institutional collaborative scientific project based in the UK can be found in Bohnenstengel et al. (2014) and Young et al. (2014).

2.2 Aerosol Mass Spectrometer measurements

Aerosol chemical composition was measured by the high-resolution time-of-flight AMS (HR-ToF-AMS, DeCarlo et al., 2006) between 20 July and 19 August 2012. The HR-ToF-AMS was located in a shipping container containing several other aerosol instruments, where aerosols were sub-sampled from a sampling stack with a flow of 30 l min^{-1} via a 3.5 µm cut-off cyclone. The time resolution of the HR-ToF-AMS used in this study was 5 minutes, obtained every 12 minutes. An overview of the AMS can be found in Canagaratna et al. (2007) and a detailed description of the HR-ToF-AMS can be found in DeCarlo et al. (2006). Details regarding the sampling protocol and data analysis procedures including the applied corrections, such as relative ionisation efficiencies and collection efficiency, and use of the Peak Integration by Key Analysis (PIKA) software can be found in Young et al. (2014). Data pre-treatment and quality assurance details, including for PMF analysis can also be found in Young et al. (2014) and the supporting information.

2.3 Additional measurements

Several different co-located gas phase measurements are used in conjunction with those from the AMS and an overview of each of these is given in Bohnenstengel et al. (2014). In brief, the volatile organic compounds (VOCs) were measured using two gas chromatographs (GC): a comprehensive two-dimensional GC (GC×GC) for C_5 to C_{13} and a dual channel GC (DC-GC) for C_2 to C_8. The DC-GC instrument set up is described in detail in Hopkins et al. (2003). The GC×GC instrument set up is described in Lidster et al. (2011) with specifics provided in Holmes et al. (2014). In brief, an Agilent 7890 GC, equipped with splitless injector and FID operating at 200 Hz (Agilent Technologies, Wilmington, DE, USA), was coupled to a Markes TT24-7 thermal desorption unit with an air server attachment (Markes International,

Llantrisant, UK). GC×GC modulation was perfromed using a total transfer flow modulator (6-port, 2-way diaphragm valve modulator, Valco Instruments, Houston, TX, USA) actuated using a solenoid valve and controlled by 'in house' software.

Ozone (O_3) was measured using a TEI 49C UV absorption analyser and calibrated to NPL standards using a TEI 49PS. CO was measured using an Aerolaser AL 5002 UV fluorescence instrument and calibrated using an Air Products 200 ppb CO in air standard certified to NPL standards. NO and NO_2 were measured using an Air Quality Design custom built high sensitivity Chemiluminesence analyser with a Blue Light NO_2 converter. The NO instrument was calibrated using a 5ppm NO in nitrogen cylinder from BOC diluted to 20 ppb using scrubbed zero air (BOC BTCA 178). The NO_2 instrument was calibrated using gas phase titration of the NO standard with O_3.

The Manchester ground based chemical ionisation mass spectrometer (CIMS) was used to make measurements N_2O_5, at a frequency of 1 Hz. The N_2O_5 measurements used in this study have been reported by Bannan et al. (2014a) which includes detailed descriptions of calibrations and instrument operation. Previous measurements of N_2O_5 using this method have also been reported by Le Breton et al. (2014) and Bannan et al. (2014b).

Boundary layer mixing heights were measured using a HALO Photonic Doppler LiDAR and was calculated with the vertical velocity variance threshold as described in Barlow et al. (2013) with additional details regarding the mixing height methods described in Dunbar (2011), Hogan et al. (2009), and Barlow et al. (2010).

The UK Met Office Numerical Atmospheric-dispersion Modelling Environment (NAME) model (Jones et al., 2007) was run using the Unified Model (UM) reanalysis meteorological data at 25 km resolution to generate surface source footprints (0-100m) for each 3 hourly period of the campaign. 10,000 theoretical air particles are released from the measurement site and their backward movement are followed as they spread according to atmospheric conditions and turbulence. 1 day backwards footprints were used for this analysis. The technique has been described in detail in Fleming et al. (2012). The footprints are used to determine the origin and pathways of air masses arriving at the site.

3 Results

Five components were identified from PMF analysis of the organic fraction of the HR-ToF-AMS data from the summer IOP: hydrocarbon-like OA (HOA), cooking OA (COA), an unknown factor, semi-volatile oxygenated OA (SV-OOA), and low volatility OA (LV-OOA). The time series, median diurnal profiles, and average fractional contributions to the total submicron organic aerosol mass are shown in Figure 1. The details of the PMF analysis are covered in a separate publication where we refer the reader to Section 5.2 of the Supplementary Information of Young et al. (2014) for a detailed discussion on the number of factors chosen from the high-resolution dataset and the criteria used to select the best solution. Briefly, the 5-factor solution was deemed the most suitable solution set, with strong correlations of the factor mass spectra and time series with reference mass spectra and ancillary data. There was clear separation between the factors, with distinctive mass spectra, time series, and diurnal profiles. Other criteria used to test the stability of the solution set such as seed dependence were improved for the 5-factor solution set compared to the 4- and 6-factor solutions. Although one of the diagnostics used to assess the quality of the fit, Q, was not as low as the value obtained for high order solution sets (see Section 5.2 of the Supplementary Information of Young et al., 2014), all other criteria were satisfied so the 5-factor solution was considered valid. The 4-factor solution was discarded as there was some dependency on the initialisation seed and the 6-factor solution was discarded due to similarities in the time series of some factors, which were indicative of factor splitting.

During the summer, HOA had an average concentration of 0.63 μg m^{-3} and a peak in concentration of 184 μg m^{-3} measured on 31 July. However, this is a relatively short-lived event, represented by a single measurement point. Several similar events also occur throughout the measurement period although of much lower concentrations in comparison, such as one on 31 July (32.5 μg m^{-3}). As HOA is associated with traffic in London these short-lived events are likely to be local sources and could be due to a stationary vehicle with its engine running when close to the site. The diurnal pattern of HOA exhibits a broad morning peak, with a maximum at 8:00 and a larger peak at 21:00 that correspond to the morning and evening rush hours, respectively. Note that all times are in Coordinated Universal Time (UTC), where British Summer Time (BST) is an hour later. HOA contributes 10 % on average to the total organic mass.

The average concentration of COA was 1.30 µg m^{-3}, with a maximum concentration of 25.4 µg m^{-3} measured on 17 August. COA exhibits the most distinctive diurnal profile of all the derived factors, with a very large evening peak at 21:00. There is also a small increase in mass at midday. These peaks are associated with main meal times. On average, COA contributes 22 % to the total organic mass.

SV-OOA had a mean concentration of 2.3 µg m^{-3} during the measurement period. The maximum concentration of 13.5 µg m^{-3} was measured on 25 July. The diurnal pattern of SV-OOA exhibits two peaks and two minima, where the larger peak in concentration occurs at 17:00, with a broader peak during the morning with a maximum peak at 05:00. SV-OOA dominates the total organic mass, contributing 38 % on average.

The mean concentration of LV-OOA was 0.78 µg m^{-3}, with a maximum concentration of 5.2 µg m^{-3} measured on 27 July. LV-OOA does not exhibit a discernable diurnal pattern, which is consistent with it representing a regional, oxygenated aerosol. LV-OOA contributes 13 % to the total organic mass on average.

Finally, the unknown factor had an average concentration of 1.01 µg m^{-3} and peaked on 28 July with a maximum concentration of 8.8 µg m^{-3}. However, this was a relatively short-lived event, lasting approximately 12-36 minutes (due to the time resolution of the measurements). The maximum concentration not including this event was 5.6 µg m^{-3} measured on 9 August. The diurnal pattern of this factor exhibits a minimum at 20:00 with a subsequent increase in concentration, peaking at midnight with a gradual decrease throughout the day. This factor contributes 17 % on average to the total organic mass.

4 Characterisation of the unknown organic factor

In the following sections we will present observations of the unknown factor including variations in concentration and chemical composition. We will then use these observations and correlations to investigate the behaviour of this factor and subsequently form hypotheses regarding its formation and sources.

4.1 Temporal variations in concentration

The median diurnal pattern of the unknown PMF factor from the measurement period exhibits an increase in concentration during the night, with a gradual decrease during

the day. One of the highest concentrations of the campaign of the unknown PMF factor was measured on the night of the 8 August, going into the 9 August. Isoprene concentrations also remain high on this night. Isoprene is mainly produced from biogenic sources during the day, evident in the diurnal profile (not shown), and has a short lifetime owing to its high reactivity with the oxidants OH, O_3, and NO_3 (Ng et al., 2008). However, the OH oxidant is unlikely to be present as this event occurs overnight and the O_3 mixing ratio is observed to be close to zero during this time. Furthermore, high concentrations of NO and NO_2 suggest NO_3 concentrations are likely to be very low on this night. Therefore, for isoprene concentrations to remain high overnight there must be a near absence of oxidants, which is inferred from these observations.

In order to explore the correlations with known tracer species, the concentrations of the unknown PMF factor were systematically compared with those of several volatile organic compounds (VOCs) also measured at the North Kensington (NK) site using the GC×GC and DC-GC. Relatively strong correlations were found with various VOCs (Pearson's r up to 0.79, Table 1), where the strongest correlations are with anthropogenic VOCs, which are typically associated with traffic emissions. Conversely, weak correlations were found between the PMF factor and biogenic VOCs such as limonene and isoprene as well as with solvents used by the instruments operating at the North Kensington site such as butanol.

4.2 Chemical characteristics

The unknown factor exhibits a large peak at m/z 43 in its mass spectrum, of which the oxidised compound $C_2H_3O^+$ is a predominant component (Fig. 2). The O:C ratio of this factor is 0.20 (Table 2), which is higher than the primary OA (POA) factors, HOA and COA, but less than for the secondary OA (SOA) factors. In addition, several peaks contain nitrogen in the form of $C_xH_yN_p^+$ fragments, where no $C_xH_yO_zN_p^+$ peaks were successfully retrieved using PIKA. The N:C ratio for this factor is relatively low at 0.009 and is nearly a factor of 2 smaller than that of LV-OOA, which has an N:C ratio of 0.02 (Table 2). Nevertheless, the unknown factor contains more nitrogen than the other OA components where the N:C ratios range between 0.0001 and 0.005.

Nitrogen-containing factors have previously been associated with reduced nitrogen species such as amines (Aiken et al., 2009; Huffman et al., 2009; Sun et al., 2011). However, organic nitrates (ON) could also potentially contribute to OA. Comparison of measured AMS ammonium concentrations with predicted ammonium concentrations can indicate the acidity of the particles in the population (Zhang et al., 2007) as well as the presence of ON and/or organosulphates (OS, Huffman et al., 2009; Farmer et al., 2010). However, inaccuracies in the AMS ammonium calibrations can also be reflected by a low measured to predicted ratio. Nevertheless, in this study the slope of the fit of the measured and predicted ammonium concentrations is 0.94. Ratios close to unity are often considered to represent pH neutral aerosols (Zhang et al., 2007) and are common in north-west Europe due to the abundance of ammonia (e.g. Morgan et al., 2010). Therefore, the presence of N-containing fragments in the PMF factor indicates further analyses are required to assess the presence of nitrogen species and/or ON.

4.3 Organic nitrate factor

The presence of organic nitrogen species can be indicated through the signals at m/z 30 and 46, where in ambient spectra these peaks are typically dominated by the NO^+ and NO_2^+ ions, respectively. However, the nitrate component of both inorganic and organic nitrates fragment to these ions. It would be expected that if inorganic nitrate, in the form of ammonium nitrate, was the only compound contributing to the signals at m/z 30 and 46 then they would follow a similar trend resulting in a ratio that varied little through time. However, in the ClearfLo dataset we find that the time series of the ratio of m/z 30 to 46 has structure (Fig. 3), indicating that there is an additional contribution to the signal at one of the m/z's. In ambient data the signal at m/z 46 can be interpreted as being predominantly of inorganic composition whereas signals at m/z 30 could also contain contributions from other compounds such as organic nitrate or amines. Organic nitrates contribute to m/z 30 and 46 from NO^+ and NO_2^+ ions, with stronger signals at m/z 30 compared to ammonium nitrate and the amine fragment, CH_4N^+ (e.g. Huffman et al., 2009, Allan et al. 2014).

Differences in the ratio of m/z 30 to 46 between ambient measurements and that from ammonium nitrate calibrations can indicate that the reported nitrate was not all ammonium nitrate. The presence of organic nitrogen is implied when measured ratios

are higher than calibrations. In this study, the ratio of m/z 30 to 46 is the slope of the linear regression with the intercept fixed at zero and is 0.91 for the ambient measurements and 0.80 from the calibration. Further indication for the presence of a species in addition to ammonium nitrate is demonstrated by the histogram of the 30/46 ratio (Fig. 3 inset), which is not normally distributed and has a peak value higher than the calibration value. Excess m/z 30 has been suggested as being attributable to organic-linked m/z 30 and/or organic-linked nitrate (Bae et al., 2007). Following the method of Bae et al. (2007), the excess m/z 30 is estimated using Equation 1 to investigate the the presence of organic nitrate in this study.

$$\Delta\, m/z\ 30\ =\ m/z\ 30_{measured} - R_{cal} \times m/z\ 46_{measured} \qquad (1)$$

where R_{cal} is the ratio of m/z 30 to m/z 46 in ammonium nitrate from AMS calibrations. This method allows a minimum contribution from organic nitrate to be estimated. A strong correlation exists between the excess m/z 30 and the PMF factor, with a Pearson's r correlation coefficient of 0.76 and a linear regression slope of 0.08 (Fig. 4). In comparison, when m/z 46 is correlated with the PMF factor there is much more scatter, indicated by the weaker Pearson's r of 0.52 (Fig. 4). Therefore, this suggests that the PMF factor is associated with organic nitrates. Note that inorganic ions are not included in the PMF data matrix input and the peaks at m/z 30 and 46 were removed from the organic matrix as they were not deemed to have been successfully retrieved using PIKA. The PMF fitting should therefore not be affected by an inorganic nitrate contribution. Although not a quantitative measure, this method presents an independent diagnostic to assess the presence of organic nitrates.

In the AMS, other inorganic nitrate salts and nitrite are also potential sources of NO^+ and NO_2^+ ions, where the ratio of m/z 30 to 46 of $NaNO_3$, for example, tends to be much larger and variable compared to that of organic nitrate (e.g. Alfarra, 2004). Using data from the co-located URG-9000B Ambient Ion Monitor (AIM, AURN and Particle Numbers and Concentrations Network, http://uk-air.defra.gov.uk/networks/network-info?view=particle), the contribution from $NaNO_3$ to the total nitrate signal was estimated. Figure 5 presents a time series of the excess m/z 30 and the mass of nitrate that would be needed to produce $NaNO_3$. The inorganic nitrate from Na^+ mass is greater than that of the excess m/z 30 during some of the measurement period, thus when the site experiences significant sea salt input

no enhancement is observed in the unknown factor. Due to these differences in temporal variability a significant contribution of $NaNO_3$ can be excluded. The differences in mass are also likely due to the differences in measured size fraction between the two instruments where the AIM measures PM_{10} and the AMS measures PM_1. Furthermore, sea salt is typically found in the coarse mode (Seinfeld and Pandis, 2006) so it is likely that the AMS would only measure the tail end of the size distribution.

We use the following observations to investigate the behaviour of the unknown factor and form hypotheses regarding its formation: concentrations of the unknown factor increase overnight; the highest concentration occurs on a night where there are likely to be no oxidants present; there are strong correlations of the factor with anthropogenic species; there is a strong association of the factor with excess m/z 30. Thus we infer the unknown factor is organic nitrate which either forms at night or the observed increase in concentrations is due to reductions in the boundary layer height.

4.4 Factors affecting formation and source attribution of the organic nitrate factor

4.4.1 Night-time formation through nitrate radical chemistry

The main pathway for night-time formation of organic nitrates is via nitrate radical initiated reactions of VOCs. The nitrate radical is formed through the reaction of between nitrogen dioxide and ozone (e.g. Johnston and Yost, 1949), thus can be considered as being of anthropogenic origin. In order to test whether the organic nitrate (ON) factor is formed at night, the presence of NO_3 is assessed by estimating the NO_3 radical mixing ratio using the following steady state approximation (Platt and Perner, 1980)

$$[NO_3] = \frac{k_2[NO_2][O_3]+k_8[N_2O_5]}{k_3[NO_2]+k_7[NO]} \qquad (2)$$

where $[NO_2]$, $[O_3]$, $[N_2O_5]$, and [NO] are the concentrations of nitrogen dioxide, ozone, dinitrogen pentoxide, and nitrogen monoxide, respectively. Rate coefficients, k, are all of second order and were derived at 298K from the NIST Chemical Kinetics Database (http://kinetics.nist.gov/kinetics/index.jsp). The reactions and rate coefficients used in Equation 2 can be found in Table 3. Although this calculation

does not take account of photolysis and the conditions in London are unlikely to be steady state, it offers insight into the possibility of nighttime formation of the ON factor.

Although on average an anti-correlation exists between the PMF factor and the NO_3 radical (not shown), the highest concentrations of the ON factor do not occur after the highest predicted NO_3 radical concentrations and is the case on the night of the 8 August. The lack of oxidants on this night suggests that the ON factor is not forming at night through in situ chemistry.

4.4.2 Gas-to-particle partitioning

Another hypothesis for the increase in the concentrations of the ON factor overnight involves its volatility. The vapour pressures of organic nitrates span many orders of magnitudes (Perring et al., 2013 and references therein) where ON with high vapour pressures are generally short-chained whereas multifunctional ON have low vapour pressures so partition to the particle phase (Farmer et al., 2010). However, the volatility of organic nitrates is not fully understood (Cape et al., 2011; Docherty et al., 2011), thus posing a further complication in determining the source and formation mechanisms of these species.

Although no volatility measurements were available during the measurement period, the behaviour of the ON factor in response to changes in temperature and relative humidity (RH) could offer insight into the volatility of the species. For example, semi-volatile species preferentially partition to the particle phase when temperatures are low and RH is high. Consequently, if the ON factor is semi-volatile it would be expected that the greatest concentrations would be observed during periods of low temperatures. However, the highest ON factor concentrations are measured during the warmest periods at the beginning and end of the measurement period (Fig. 6). Furthermore, the weak correlation with m/z 46, which is assumed to be primarly of inorganic nitrate, which is semi-volatile, suggests that the ON factor is of different volatility. Therefore, it is unlikely that the concentrations of the ON factor are driven by equilibrium gas-to-particle partitioning.

4.4.3 Role of air mass trajectory and boundary layer dynamics

As it is unlikely that the ON factor is forming through in situ chemistry or as a result of gas-to-particle partitioning, an alternative hypothesis could therefore be that the factor is formed outside of London and transported in. Synoptic charts and NAME footprints were therefore examined with a focus on nights where the concentrations were highest. For the night of the 24 July, going into the 25 July, the 1 day backwards NAME footprint shows that the air mass was local, situated predominantly over London and the south-west UK. Similarly, on the night of 8th August, low wind speeds accompanied a local and stagnant air mass, which had previously been a predominantly westerly trajectory. These footprints and low wind speeds suggest stagnant conditions during these periods thus allowing concentrations to build up. However, there are several other high concentration events such as the 27 July, 9th and 15th August where the NAME footprints indicate different air mass trajectories and synoptic conditions prevailed. For example, on the night of the 9th August the air mass was located further south compared to the 8 August so there could be some small influence from France. The other two events are particularly interesting as the concentrations of the ON factor continue to increase late into the morning, with peaks occurring around midday. The air mass begins as an easterly at the start of the 27 July, then is spread widely over the UK, and becomes a westerly. Synoptic charts show a front passed through at this time, indicating that the air mass was likely influenced by a mix of sources. Therefore an influence from north-west Europe cannot be discounted. Consistent with westerly masses being cleaner compared to easterlies (e.g. Martin et al., 2011), the concentration of the ON factor decreases with this change in air mass trajectory. Similar conditions occur on the 15 August although the NAME footprint suggests there may be a greater influence from north-west Europe. However, the wind speeds are greater during this time, seen by both a greater distance covered by a 1 day footprint and higher local measured wind speeds.

To further assess the meteorological conditions, measurements of the boundary layer height were analysed and indicate that deep inversions occurred during the measurement period with the boundary layer reaching (median) heights of approximately 2600 m during the day and reducing to less than 100 m at night (Fig. 6). This further suggests the air was extremely stagnant at night on many occasions during the measurement period, which resulted in increased aerosol concentrations.

On the night of the 8 August, measurements of ozone at the North Kensington site were close to zero, with similar concentrations also measured at the rural site in Chilbolton. However, at the elevated BT Tower site in London, the concentrations were comparatively high suggesting that the ground sites were decoupled from the elevated site due to a reduced boundary layer. As this was a night when the ON factor concentrations were high it is implied that the sources are local, particularly as the air mass had previously advected from the west suggesting that little pollution had been transported in prior to any reductions in the mixing layer height. Therefore, although the influence and contribution from transported pollution cannot be explicity determined, there is evidence that the ON factor is predominantly from local sources.

4.4.4 Primary or secondary origin

To assess the likely origin of the ON factor various tracer species were examined. As mentioned in Section 4.1 the strongest correlations between the ON factor and several VOCs were with the anthropogenic species, which are associated with traffic emissions. Interestingly, on the night of 8 August, HOA concentrations increase simultaneously with those of the ON factor as well as COA. In contrast, the concentrations of the two OOA factors increase more gradually through the night and over the following days. Bae et al. (2007) suggest that correlations observed between HOA and excess m/z 30 are related to the environment type; aerosols at rural or remote locations tend to be well mixed and aged. However, this study is performed in an urban envrionment where the ON factor is less oxygenated than the two secondary factors, SV-OOA and LV-OOA, suggesting that this component has not been subject to significant levels of atmospheric processing and thus represents fresher emissions (Jimenez et al., 2009; Docherty et al., 2011). Furthermore, the association of the ON factor with anthropogenic VOC species, COA, and HOA implies that the factor is likely of primary anthropogenic origin rather than secondary.

4.4.5 Presence of a reactive species

Finally, the absence of oxidants on several occassions during the measurement period suggests there is a lack of in situ chemistry but does not mean that atmospheric oxidants do not have any role in governing the ON factor concentrations. Particularly low ozone concentrations were measured on the night of the 8 August, where any subsequent increase in ozone was coincident with a decrease in the PMF factor

concentration. This could therefore suggest that the factor is usually relatively reactive but in the absence of significant levels of ozone and other possible oxidants, the concentration of the factor builds up. Further support for this hypothesis arises from the night of the 9 August, where the concentration of ozone decreases to a minimum at 21:45 with a relatively rapid increase in concentrations to a similar level as those measured during the day, with a peak at 23:15. The opposite trend is observed in the ON factor, implying that concentrations are strongly governed by the presence of oxidants in the atmosphere. Interestingly, this small event is not evident in the excess m/z 30 concentrations.

5 Conclusions

Presented here are in situ AMS observations of organic aerosols measured in an urban environment during summer in the UK, taken as part of the ClearfLo project. The components of the organic fraction were investigated through PMF analysis, where 5 main factors were derived. It was possible to identify four of the components as HOA, COA, SV-OOA, and LV-OOA. Through investigation of the chemical composition and behaviour of the remaining component, which has an average concentration of 1.01 μg m^{-3} and contributes 17% to the total OA mass, we present evidence for the occurrence of organic nitrates in London, where we propose that the unidentified component is directly emitted and is of anthropogenic origin.

The concentration of the unknown PMF factor increases over night, with the highest concentration occurring on the night of the 8 August. The strong association of the factor with organic nitrates identified from correlations with excess m/z 30 implies the two organic species may be of similar origin. Therefore potential origins and formation pathways of the organic nitrate PMF factor are explored, where the night of the 8 August provides a particularly interesting case study. Although an anti-correlation generally exists between the factor and estimated nitrate radical mixing ratios, on the night of the 8 August NO_3 radicals are not predicted to be present, suggesting that it is unlikely the factor forms in situ via nocturnal oxidation reactions. Gas-to-particle partitioning is also unlikely to have a role in governing the high overnight concentrations as the highest concentrations of the factor occur during the warmest periods, with weak correlations observed between the factor and inorganic nitrates. Deep inversions and stagnant air masses lead to increased concentrations of

the factor, suggesting the factor is not formed predominantly outside of London and transported in. Moreover, simultaneous increases in COA and HOA concentrations during the case study imply the factor is directly emitted from a local source, where the strong correlations between the factor and various VOCs suggest an anthropogenic origin rather than biogenic. The highest concentrations of the factor are observed when oxidants are absent, thus the factor may be highly reactive where concentrations build up in the absence of oxidants in the atmosphere.

The findings from this work suggest that organic nitrates have a non-negligible contribution to total organic mass in the urban environment in the summer. However, few direct sources of organic nitrates are known, particularly in urban environments. Furthermore, a limited number of ambient observations and laboratory measurements of these species currently exist thus little is known about their properties. The hypotheses formed regarding the formation and behaviour of the unidentified organic factor in this study therefore require further investigation in order to better inform pollution abatement strategies and air quality policies. Moreover, detailed laboratory and field measurements are necessary in order to better characterise organic nitrates, particularly as they have the potential to adversely affect human health and climate.

Data availability

Processed data are available through the ClearfLo project archive at the British Atmospheric Data Centre (http://badc.nerc.ac.uk/browse/badc/clearflo). Raw data are archived at the University of Manchester and are available on request.

Acknowledgements

This work was supported in part by the UK Natural Environment Research Council (NERC) ClearfLo project [grant ref. NE/H008136/1] and is co-ordinated by the National Centre for Atmospheric Science (NCAS). D. E. Young was supported by a NERC PhD studentship [ref. NE/I528142/1]. The authors would like to thank Dr. James Lee from NCAS at the University of York for logistical assistance at the North Kensington supersite during the IOPs. Thanks to the Met Office for use of the NAME model. Additional thanks to the Sion Manning School in North Kensington and adjacent community centre.

References

Aiken, A. C., Salcedo, D., Cubison, M. J., Huffman, J. A., DeCarlo, P. F., Ulbrich, I. M., Docherty, K. S., Sueper, D., Kimmel, J. R., Worsnop, D. R., Trimborn, A., Northway, M., Stone, E. A., Schauer, J. J., Volkamer, R. M., Fortner, E., de Foy, B., Wang, J., Laskin, A., Shutthanandan, V., Zheng, J., Zhang, R., Gaffney, J., Marley, N. A., Paredes-Miranda, G., Arnott, W. P., Molina, L. T., Sosa, G., and Jimenez, J. L.: Mexico City aerosol analysis during MILAGRO using high resolution aerosol mass spectrometry at the urban supersite (T0) – Part 1: Fine particle composition and organic source apportionment, Atmos. Chem. Phys., 9, 6633-6653, doi:10.5194/acp-9-6633-2009, 2009.

Alfarra, M. R.: Insights into atmospheric organic aerosols using an aerosol mass spectrometer., Ph.D. thesis, University of Manchester, UK, 2004.

Allan, J. D., Alfarra, M. R., Bower, K. N., Coe, H., Jayne, J. T., Worsnop, D. R., Aalto, P. P., Kulmala, M., Hyötyläinen, T., Cavalli, F., and Laaksonen, A.: Size and composition measurements of background aerosol and new particle growth in a Finnish forest during QUEST 2 using an Aerodyne Aerosol Mass Spectrometer, Atmos. Chem. Phys., 6, 315-327, doi:10.5194/acp-6-315-2006, 2006.

Allan, J. D., Williams, P. I., Morgan, W. T., Martin, C. L., Flynn, M. J., Lee, J., Nemitz, E., Phillips, G. J., Gallagher, M. W., and Coe, H.: Contributions from transport, solid fuel burning and cooking to primary organic aerosols in two UK cities, Atmos. Chem. Phys., 10, 647–668, doi:10.5194/acp-10-647-2010, 2010.

Allan, J. D., Morgan, W. T., Darbyshire, E., Flynn, M. J., Williams, P. I., Oram, D. E., Artaxo, P., Brito, J., Lee, J. D., and Coe, H.: Airborne observations of IEPOX-derived isoprene SOA in the Amazon during SAMBBA, Atmos. Chem. Phys. Discuss., 14, 12635-12671, doi:10.5194/acpd-14-12635-2014, 2014.

AQEG: Fine Particulate Matter ($PM_{2.5}$) in the United Kingdom. Defra, London.

Atlas, E., Pollock, W., Greenberg, J., Heidt, L., and Thompson, A. M.: Alkyl nitrates, nonmethane hydrocarbons, and halocarbon gases over the equatorial Pacific-ocean during SAGA-3, J. Geophys. Res., 98, 16 933–16 947, 1993.

Bae, M. S., Schwab, J. J., Zhang, Q., Hogrefe, O., Demerjian, K. L., Weimer, S., Rhoads, K., Orsini, D., Venkatachari, P., and Hopke, P. K.: Interference of organic signals in highly time resolved nitrate measurements by low mass resolution aerosol mass spectrometry, J. Geophys. Res.-Atmos., 112, D22305, doi:22310.21029/22007JD008614, 2007.

Bannan, T. J., Booth, A. M., Bacak, A., Muller, J. B. A., Leather, K. E., Le Breton, M., Jones, B., Young, D. E., Coe, H., Allan, J., Visser, S., Lee, J., Holmes, R., Hopkins, J. R., Hamilton, J. F., Lewis, A. C., Whalley, L. K., Sharp, T., Stone, D., Heard, D. E., Fleming, Z., Shallcross, D. E., and Percival, C. J.: The first UK measurements of nitryl chloride using a chemical ionisation mass spectrometer in central London in the summer of 2012, and an investigation of the role of Cl atom oxidation, in preparation, 2014a.

Bannan, T. J., Bacak, A., Le Breton, M., Ouyang, B, McLeod, M. W., Jones, R., Shallcross, D. E., and Percival, C. J.: Ground and Airborne U.K. Measurements of Nitryl Chloride and implications of this species to the total U.K. oxidising capacity, in preparation, 2014b.

Barlow, J. F., Dunbar, T. M., Nemitz, E. G., Wood, C. R., Gallagher, M. W., Davies, F., O'Connor, E., Harrison, R. M.: Boundary layer dynamics over London, UK, as observed using Doppler lidar during REPARTEE-II. Atmos. Chem. Phys., 11, 2111–2125, 2011.

Barlow, J. F., Halios, C. H., Lane, S., Wood, C. R.: Observations of urban boundary layer structure during a strong urban heat island event, Environ. Fluid Mech., 1-26 pp, 2014.

Bohnenstengel, S. I., Belcher, S. E., Aiken, A. C., Allan, J. D., Allen, G., Bacak, A., Bannan, T. J., Barlow, J. F., Beddows, D. C. S., Bloss, W. J., Booth, A. M., Chemel, C., Coceal, O., Di Marco, C. F., Mavendra, D. K., Faloon, K. H., Fleming, Z., Furger, M., Geitl, J. K., Graves, R. R., Green, D. C., Grimmond, C. S. B., Halios, C., Hamilton, J. F., Harrison, R. M., Heal, M. R., Heard, D. E., Helfter, C., Herndon, S. C., Holmes, R. E., Hopkins, J. R., Jones, A. M., Kelly, F. J., Kotthaus, S., Langford, B., Lee, J. D., Leigh, R. J., Lewis, A. C., Lidster, R. T., Lopez-Hilfiker, F. D., McQuaid, J. B., Mohr, C., Monks, P. S., Nemitz, E., Ng, N. L., Percival, C. J., Prévôt,

A. S. H., Ricketts, H. M. A., Sokhi, R., Stone, D., Thornton, J. A., Tremper, A. H., Valach, A. C., Visser, S., Whalley, L. K., Williams, L. R., Xu, L., Young, D. E., and Zotter, P.: Meteorology, air quality and health in London: the ClearfLo project, B. Am. Meteorol. Soc., in press, 2014.

Boucher, O., Randall, D., Artaxo, P., Bretherton, C., Feingold, G., Forster, P., Kerminen, V.-M., Kondo, Y., Liao, H., Lohmann, U., Rasch, P., Satheesh, S. K., Sherwood, S., Stevens, B. and Zhang, X. Y.: Clouds and aerosols, in: Climate Change 2013: The Physical Science Basis. Contribution of Working Group I to the Fifth Assessment Report of the Intergovernmental Panel on Climate Change, edited by: Stocker, T. F., Qin, D., Plattner, G.-K., Tignor, M., Allen, S. K., Boschung, J., Nauels, A., Xia, Y., Bex, V., and Midgley, P. M., Cambridge University Press, Cambridge, UK and New York, NY, USA, 2013.

Canagaratna, M. R., Jayne, J. T., Jimenez, J. L., Allan, J. D., Alfarra, M. R., Zhang, Q., Onasch, T. B., Drewnick, F., Coe, H., Middlebrook, A., Delia, A. E., Williams, L. R., Trimborn, A. M., Northway, M. J., Decarlo, P. F., Kolb, C. E., Davidovits, P., and Worsnop, D. R.: Chemical and microphysical characterization of ambient aerosols with the aerodyne aerosol mass spectrometer, Mass Spectrom. Rev., 26, 185–222, doi:10.1002/mas.20115, 2007.

Cape, J. N., Cornell, S. E., Jickells, T. D., and Nemitz, E.: Organic nitrogen in the atmosphere — Where does it come from? A review of sources and methods, Atmos. Res., 102, 30–48, 2011.

Chan, A. W. H., Chan, M. N., Surratt, J. D., Chhabra, P. S., Loza, C. L., Crounse, J. D., Yee, L. D., Flagan, R. C., Wennberg, P. O., and Seinfeld, J. H.: Role of aldehyde chemistry and NO_x concentrations in secondary organic aerosol formation, Atmos. Chem. Phys., 10, 7169-7188, doi:10.5194/acp-10-7169-2010, 2010.

Crippa, M., Canonaco, F., Lanz, V. A., Äijälä, M., Allan, J. D., Carbone, S., Capes, G., Ceburnis, D., Dall'Osto, M., Day, D. A., DeCarlo, P. F., Ehn, M., Eriksson, A., Freney, E., Hildebrandt Ruiz, L., Hillamo, R., Jimenez, J. L., Junninen, H., Kiendler-Scharr, A., Kortelainen, A.-M., Kulmala, M., Laaksonen, A., Mensah, A. A., Mohr, C., Nemitz, E., O'Dowd, C., Ovadnevaite, J., Pandis, S. N.,

Petäjä, T., Poulain, L., Saarikoski, S., Sellegri, K., Swietlicki, E., Tiitta, P., Worsnop, D. R., Baltensperger, U., and Prévôt, A. S. H.: Organic aerosol components derived from 25 AMS data sets across Europe using a consistent ME-2 based source apportionment approach, Atmos. Chem. Phys., 14, 6159-6176, doi:10.5194/acp-14-6159-2014, 2014.

Day, D. A., Liu, S., Russell, L. M., Ziemann, P. J.: Organonitrate group concentrations in submicron particles with high nitrate and organic fractions in coastal southern California, Atmos. Envrion., 44, 1970-1979, doi:10.1016/j.atmosenv.2010.02.045, 2010.

DeCarlo, P. F., Kimmel, J. R., Trimborn, A., Northway, M. J., Jayne, J. T., Aiken, A. C., Gonin, M., Fuhrer, K., Horvath, T., Docherty, K. S., Worsnop, D. R., and Jimenez, J. L.: Field-deployable, high-resolution, time-of-flight aerosol mass spectrometer, Anal. Chem., 78, 8281–8289, doi:10.1021/ac061249n, 2006.

de Gouw, J. A., Middlebrook, A. M., Warneke, C., Goldan, P. D., Kuster, W. C., Roberts, J. M., Fehsenfeld, F. C., Worsnop, D. R., Canagaratna, M. R., Pszenny, A. A. P., Keene, W. C., Marchewka, M., Bertman, S. B., Bates, T. S.: Budget of organic carbon in a polluted atmosphere: Results from the New England Air Quality Study in 2002, Journal of Geophysical Research: Atmospheres, 110, doi:10.1029/2004JD005623, 2005.

Docherty, K. S., Aiken, A. C., Huffman, J. A., Ulbrich, I. M., DeCarlo, P. F., Sueper, D., Worsnop, D. R., Snyder, D. C., Peltier, R. E., Weber, R. J., Grover, B. D., Eatough, D. J., Williams, B. J., Goldstein, A. H., Ziemann, P. J., and Jimenez, J. L.: The 2005 Study of Organic Aerosols at Riverside (SOAR-1): instrumental intercomparisons and fine particle composition, Atmos. Chem. Phys., 11, 12387-12420, doi:10.5194/acp-11-12387-2011, 2011.

Donaldson, K., Stone, V., Borm, P. J., Jimenez, L. A., Gilmour, P. S., Schins, R. P., Knaapen, A. M., Rhaman, I., Faux, S. P., Brown, D. M., MacNee, W.: Oxidative stress and calcium signaling in the adverse effects of environmental particles (PM_{10}), Free Radical Bio. Med., 34, 1369–1382, 2003.

Dunbar, T.: An Optimal Inverse method using Doppler Lidar measurements to estimate the surface heat flux, PhD Thesis, University of Reading, Department of Meteorology, 2011.

Farmer, D., Matsunaga, A., Docherty, K., Surratt, J., Seinfeld, J., Ziemann, P., and Jimenez, J.: Response of an aerosol mass spectrometer to organonitrates and organosulfates and implications for atmospheric chemistry, P. Natl. Acad. Sci. USA, 107, 6670–6675, doi:10.1073/pnas.0912340107, 2010.

Fleming, Z. L., Monks, P. S., and Manning, A. J.: Review: untangling the influence of air-mass history in interpreting observed atmospheric composition, Atmos. Res., 104–105, 1–39, 2012.

Fry, J. L., Kiendler-Scharr, A., Rollins, A. W., Wooldridge, P. J., Brown, S. S., Fuchs, H., Dubé, W., Mensah, A., dal Maso, M., Tillmann, R., Dorn, H.-P., Brauers, T., and Cohen, R. C.: Organic nitrate and secondary organic aerosol yield from NO_3 oxidation of β-pinene evaluated using a gas-phase kinetics/aerosol partitioning model, Atmos. Chem. Phys., 9, 1431-1449, doi:10.5194/acp-9-1431-2009, 2009.

Gelencsér, A., May, B., Simpson, D., Sanchez-Ochoa, A., Kasper-Giebl, A., Puxbaum, H., Caseiro, A., Pio, C., and Legrand, M.: Source apportionment of PM2.5 organic aerosol over Europe: primary/secondary, natural/anthropogenic, fossil/biogenic origin, J. Geophys. Res., 112, D23S04, doi:10.1029/2006JD008094, 2007.

Goldstein, A. H., Koven, C. D., Heald, C. L., and Fung, I. Y.: Bio- genic carbon and anthropogenic pollutants combine to form a cooling haze over the southeastern United States, P. Natl. Acad. Sci. USA, sure106, 8835–8840, 2009.

González Benítez, J. M., Cape, J. N., and Heal, M. R.: Gaseous and particulate water-soluble organic and inorganic nitrogen in rural air in southern Scotland, Atmos. Environ., 44, 1506–1514, 2010.

Hallquist, M., Wenger, J. C., Baltensperger, U., Rudich, Y., Simpson, D., Claeys, M., Dommen, J., Donahue, N. M., George, C., Goldstein, A. H., Hamilton, J. F., Herrmann, H., Hoffmann, T., Iinuma, Y., Jang, M., Jenkin, M. E., Jimenez, J. L., Kiendler-Scharr, A., Maenhaut, W., McFiggans, G., Mentel, Th. F., Monod, A.,

Prévôt, A. S. H., Seinfeld, J. H., Surratt, J. D., Szmigielski, R., and Wildt, J.: The formation, properties and impact of secondary organic aerosol: current and emerging issues, Atmos. Chem. Phys., 9, 5155-5236, doi:10.5194/acp-9-5155-2009, 2009.

Hayes, P. L., Ortega, A. M., Cubison, M. J., Froyd, K. D., Zhao, Y., Cliff, S. S., Hu, W. W., Toohey, D. W., Flynn, J. H., Lefer, B. L., Grossberg, N., Alvarez, S., Rappenglück, B., Taylor, J.W., Allan, J. D., Holloway, J. S., Gilman, J. B., Kuster, W. C., de Gouw, J. A., Massoli, P., Zhang, X., Liu, J.,Weber, R. J., Corrigan, A. L., Russell, L. M., Isaacman, G., Worton, D. R., Kreis- berg, N. M., Goldstein, A. H., Thalman, R., Waxman, E. M., Volkamer, R., Lin, Y. H., Surratt, J. D., Kleindienst, T. E., Offenberg, J. H., Dusanter, S., Griffith, S., Stevens, P. S., Brioude, J., Angevine, W. M., and Jimenez, J. L.: Organic aerosol composition and sources in Pasadena, California, during the 2010 CalNex campaign, J. Geophys. Res.-Atmos., 118, 9233–9257, doi:10.1002/jgrd.50530, 2013.

Heald, C. L., Jacob, D. J., Park, R. J., Russell, L. M., Huebert, B. J., Seinfeld, J. H., Liao, H., and Weber, R. J.: A large organic aerosol source in the free troposphere missing from current models, Geophys. Res. Lett., 32, L18809, doi:18810.11029/12005GL023831, 2005.

Hogan, R. J., Grant, A. L. M., Illingworth, A. J., Pearson, G. N., O'Connor, E. J.: Vertical velocity variance and skewness in clear and cloud-topped boundary layers as revealed by Doppler lidar, Q. J. Roy. Meteorol. Soc., 135, 635-643, 2009.

Holmes, R. E., Hopkins, J. R., Lidster, R. T., Lee, J. D., Evans, M. J., Lewis, A. C., and Hamilton, J. F.: Diesel-related hydrocarbons dominate reactive carbon in modern megacity atmospheres, in preparation, 2014.

Hopkins, J. R., Lewis, A. C., and Read, K. A.: A two-column method for long-term monitoring of non-methane hydrocarbons (NMHCs) and oxygenated volatile organic compounds (o-VOCs), Journal of Environmental Monitoring, 5, 8-13, doi:10.1039/b202798d, 2003.

Hoyle, C. R., Boy, M., Donahue, N. M., Fry, J. L., Glasius, M., Guenther, A., Hallar, A. G., Huff Hartz, K., Petters, M. D., Petäjä, T., Rosenoern, T., and Sullivan, A. P.: A review of the anthropogenic influence on biogenic secondary

organic aerosol, Atmos. Chem. Phys., 11, 321-343, doi:10.5194/acp-11-321-2011, 2011.

Huffman, J. A., Docherty, K. S., Aiken, A. C., Cubison, M. J., Ulbrich, I. M., DeCarlo, P. F., Sueper, D., Jayne, J. T., Worsnop, D. R., Ziemann, P. J., and Jimenez, J. L.: Chemically-resolved aerosol volatility measurements from two megacity field studies, Atmos. Chem. Phys., 9, 7161-7182, doi:10.5194/acp-9-7161-2009, 2009.

Jimenez, J. L., Canagaratna, M. R., Donahue, N. M., Prevot, A. S. H., Zhang, Q., Kroll, J. H., DeCarlo, P. F., Allan, J. D., Coe, H., Ng, N. L., Aiken, A. C., Docherty, K. S., Ulbrich, I. M., Grieshop, A. P., 5 Robinson, A. L., Duplissy, J., Smith, J. D., Wilson, K. R., Lanz, V. A., Hueglin, C., Sun, Y. L., Tian, J., Laaksonen, A., Raatikainen, T., Rautiainen, J., Vaattovaara, P., Ehn, M., Kulmala, M., Tomlinson, J. M., Collins, D. R., Cubison, M. J., E., Dunlea, E. J., Huffman, J. A., Onasch, T. B., Alfarra, M. R., Williams, P. I., Bower, K. N., Kondo, Y., Schneider, J., Drewnick, F., Borrmann, S., Weimer, S., Demerjian, K. L., Salcedo, D., Cottrell, L., Griffin, R., Takami, A., Miyoshi, T., Hatakeyama, S., Shimono, A., Sun, J. Y., Zhang, Y. M., Dzepina, K., Kimmel, J. R., Sueper, D., Jayne, J. T., Herndon, S. C., Trimborn, A. M., Williams, L. R.,Wood, E. C., Middlebrook, A. M.,Kolb, C. E., Baltensperger, U., and Worsnop, D. R.: Evolution of organic aerosols in the atmosphere, Science, 326, 1525–1529, doi:10.1126/science.1180353, 2009.

Johnston, H. S. and Yost, D. M.: The Kinetics of the Rapid Gas Reaction between Ozone and Nitrogen Dioxide, J. Chem. Phys., 17, 1949.

Jones, A. R., Thomson, D. J., Hort, M., and Devenish, B.: The UK Met Office's Next-Generation Atmospheric Dispersion Model, NAME III. Air Pollution Modeling and Its Application XVII, edited by: Borrego, C. and Norman, A.-L., Springer, 580–589, 2007.

Kanakidou, M., Seinfeld, J. H., Pandis, S. N., Barnes, I., Dentener, F. J., Facchini, M. C., Van Dingenen, R., Ervens, B., Nenes, A., Nielsen, C. J., Swietlicki, E., Putaud, J. P., Balkanski, Y., Fuzzi, S., Horth, J., Moortgat, G. K., Winterhalter, R., Myhre, C. E. L., Tsigaridis, K., Vignati, E., Stephanou, E. G., and

Wilson, J.: Organic aerosol and global climate modelling: a review, Atmos. Chem. Phys., 5, 1053-1123, doi:10.5194/acp-5-1053-2005, 2005.

Lanz, V. A., Alfarra, M. R., Baltensperger, U., Buchmann, B., Hueglin, C., and Prévôt, A. S. H.: Source apportionment of submicron organic aerosols at an urban site by factor analytical modelling of aerosol mass spectra, Atmos. Chem. Phys., 7, 1503–1522, doi:10.5194/acp-7-1503-2007, 2007.

Le Breton, M., Bacak, A., Muller, J. B. A., Bannan, T. J., Kennedy, O., Ouyang, B., Xiao, P., Bauguitte, S. J.-B., Shallcross, D. E., Jones, R. L., and Percival, C. J.: The first airborne comparison of N_2O_5 measurements over the UK using a Chemical Ionisation Mass Spectrometer (CIMS) and Broadband Cavity Enhanced Absorption Spectrometer (BBCEAS) during the RONOCO 2010/2011 campaign, in preparation, 2014.

Lidster, R. T., Hamilton, J. F., and Lewis, A. C.: The application of two total transfer valve modulators for comprehensive two-dimensional gas chromatography of volatile organic compounds, Journal of Separation Science, 34, 812-821, doi:10.1002/jssc.201000710, 2011.

Lim, Y. B. and Ziemann, P. J.: Products and mechanism of secondary organic aerosol formation from reactions of n-alkanes with OH radicals in the presence of NO_x, Environ. Sci. Technol., 39, 9229–9236, doi:10.1021/es051447g, 2005.

Lim, Y. B. and Ziemann, P. J.: Chemistry of secondary organic aerosol formation from OH radical-initiated reactions of linear, branched, and cyclic alkanes in the presence of NO_x, Aerosol Sci. Technol., 43, 604–619, 2009.

Martin, C. L., Allan, J. D., Crosier, J., Choularton, T. W., Coe, H., and Gallagher, M. W.: Seasonal variation of fine particulate composition in the centre of a UK city, Atmos. Environ., 45, 4379-4389, 10.1016/j.atmosenv.2011.05.050, 2011.

Mohr, C., Lopez-Hilfiker, F. D., Zotter, P., Prevot, A. S. H., Xu, L., Ng, N. L., Herndon, S. C., Williams, L. R., Franklin, J. P., Zahniser, M. S.,Worsnop, D. R., Knighton,W. B., Aiken, A. C., Gorkowski, K. J., Dubey, M. K., Allan, J. D., and Thornton, J. A.: Contribution of nitrated phenols to wood burning brown carbon light

absorption in Delting, United Kingdom during winter time, Environ. Sci. Technol., 47, 6316–6324, 2013.

Morgan, W. T., Allan, J. D., Bower, K. N., Highwood, E. J., Liu, D., McMeeking, G. R., Northway, M. J., Williams, P. I., Krejci, R., and Coe, H.: Airborne measurements of the spatial distribution of aerosol chemical composition across Europe and evolution of the organic fraction, Atmos. Chem. Phys., 10, 4065-4083, doi:10.5194/acp-10-4065-2010, 2010.

Ng, N. L., Chhabra, P. S., Chan, A. W. H., Surratt, J. D., Kroll, J. H., Kwan, A. J., McCabe, D. C., Wennberg, P. O., Sorooshian, A., Murphy, S. M., Dalleska, N. F., Flagan, R. C., and Seinfeld, J. H.: Effect of NO_x level on secondary organic aerosol (SOA) formation from the photooxidation of terpenes, Atmos. Chem. Phys., 7, 5159-5174, doi:10.5194/acp-7-5159-2007, 2007.

Ng, N. L., Kwan, A. J., Surratt, J. D., Chan, A. W. H., Chhabra, P. S., Sorooshian, A., Pye, H. O. T., Crounse, J. D., Wennberg, P. O., Flagan, R. C., and Seinfeld, J. H.: Secondary organic aerosol (SOA) formation from reaction of isoprene with nitrate radicals (NO_3), Atmos. Chem. Phys., 8, 4117-4140, doi:10.5194/acp-8-4117-2008, 2008.

Oberdörster, G., Oberdörster, E., and Oberdörster, J.: Nanotoxicology: An emerging discipline evolving from studies of ultrafine particles, Environ. Health Persp., 113, 823–839, 2005.

Perring, A. E., Pusede, S. E., and Cohen, R. C.: An Observational Perspective on the Atmospheric Impacts of Alkyl and Multifunctional Nitrates on Ozone and Secondary Organic Aerosol, Chem. Rev., 113, 5848-5870, 2013.

Platt, U., Perner, D., Winer, A., Harris, G., Pitts Jr., J., 1980. Detection of NO_3 in the polluted troposphere by differential optical-absorption. Geophysical Research Letters 7, 89–92.

Pope III, C. A. and Dockery, D. W.: Health effects of fine particulate air pollution: lines that connect, J. Air Waste Manage., 56, 709–742, doi:10.1080/10473289.2006.10464485, 2006.

Rollins, A. W., Browne, E. C., Min, K.-E., Pusede, S. E., Wooldridge, P. J., Gentner, D. R., Goldstein, A. H., Liu, S., Day, D. A., Russell, L. M., and Cohen, R. C.: Evidence for NO_x control over nighttime SOA formation, Science, 337, 1210–1212, doi:10.1126/science.1221520, 2012.

Seinfeld, J. H. and Pandis, S. N.: Atmospheric Chemistry and Physics: from Air Pollution to Climate Change, second edn., John Wiley & Sons, New York, 2006.

Sun, Y.-L., Zhang, Q., Schwab, J. J., Demerjian, K. L., Chen, W.-N., Bae, M.-S., Hung, H.-M., Hogrefe, O., Frank, B., Rattigan, O. V., and Lin, Y.-C.: Characterization of the sources and processes of organic and inorganic aerosols in New York city with a high-resolution time-of-flight aerosol mass spectrometer, Atmos. Chem. Phys., 11, 1581–1602, doi:10.5194/acp-11- 1581-2011, 2011.

Spracklen, D. V., Jimenez, J. L., Carslaw, K. S., Worsnop, D. R., Evans, M. J., Mann, G. W., Zhang, Q., Canagaratna, M. R., Allan, J., Coe, H., McFiggans, G., Rap, A., and Forster, P.: Aerosol mass spectrometer constraint on the global secondary organic aerosol budget, Atmos. Chem. Phys., 11, 12109-12136, doi:10.5194/acp-11-12109-2011, 2011.

Szidat, S., Jenk, T. M., Synal, H.-A., Kalberer, M., Wacker, L., Hajdas, I., Kasper-Giebl, A., and Baltensberger, U.: Contributions of fossil fuel, biomass-burning, and biogenic emissions to car- bonaceous aerosols in Zurich as traced by 14C, J. Geophys. Res., 111, D07206, doi:10.1029/2005JD006590, 2006.

Volkamer, R., Jimenez, J. L., San Martini, F., Dzepina, K., Zhang, Q., Salcedo, D., Molina, L. T., Worsnop, D. R., and Molina, M. J.: Secondary organic aerosol formation from anthropogenic air pollution: Rapid and higher than expected, Geophys. Res. Lett., 33, L17811, doi:10.1029/2006gl026899, 2006.

Weber, R. J., Sullivan, A. P., Peltier, R. E., Russell, A., Yan, B., Zheng, M., de Gouw, J., Warneke, C., Brock, C., Holloway, J. S., Atlas, E. L., and Edgerton, E.: A study of secondary organic aerosol formation in the anthropogenic-influenced southeastern United States, J. Geophys. Res., 112, D13302, doi:10.1029/2007JD008408, 2007.

Worton, D. R., Goldstein, A. H., Farmer, D. K., Docherty, K. S., Jimenez, J. L., Gilman, J. B., Kuster, W. C., de Gouw, J., Williams, B. J., Kreisberg, N. M., Hering, S. V., Bench, G., McKay, M., Kristensen, K., Glasius, M., Surratt, J. D., and Seinfeld, J. H.: Origins and composition of fine atmospheric carbonaceous aerosol in the Sierra Nevada Mountains, California, Atmos. Chem. Phys., 11, 10219-10241, doi:10.5194/acp-11-10219-2011, 2011.

Young, D. E., Allan, J. D., Williams, P. I., Green, D. C., Flynn, M. J., Harrison, R. M., Yin, J., Gallagher, M. W., and Coe, H.: Investigating the annual behaviour of submicron secondary inorganic and organic aerosols in London, Atmos. Chem. Phys. Discuss., 14, 18739-18784, doi:10.5194/acpd-14-18739-2014, 2014.

Zhang, Q., Worsnop, D. R., Canagaratna, M. R., and Jimenez, J. L.: Hydrocarbon-like and oxygenated organic aerosols in Pittsburgh: insights into sources and processes of organic aerosols, Atmos. Chem. Phys., 5, 3289-3311, doi:10.5194/acp-5-3289-2005, 2005.

Zhang, Q., Jimenez, J. L., Canagaratna, M. R., Allan, J. D., Coe, H., Ulbrich, I., Alfarra, M. R., Takami, A., Middlebrook, 5 A. M., Sun, Y. L., Dzepina, K., Dunlea, E. J., Docherty, K. S., Decarlo, P. F., Salcedo, D., Onasch, T., Jayne, J. T., Miyoshi, T., Shimono, A., Hatakeyama, S., Takegawa, N., Kondo, Y., Schneider, J., Drewnick, F., Borrmann, S., Weimer, S., Demerjian, K. L., Williams, P., Bower, K. N., Bahreini, R., Cottrell, L., Griffin, R. J., Rautiainen, J., Sun, J. Y., Zhang, Y. M., and Worsnop, D. R.: Ubiquity and dominance of oxygenated species in organic aerosols in anthropogenically-influenced Northern Hemisphere midlatitudes, Geophys. Res. Lett., 34, L13801, doi:10.1029/2007GL029979, 2007.

Table 1. Pearson's r correlation coefficients for linear regression fit between the unknown PMF factor and various VOCs. The aliphatic compounds are grouped by carbon number and include all the isomers except when identified individually. The groups include alkanes, alkenes, and cycloalkanes.

VOC	Pearson's r
methyl-vinyl-ketone (MVK)	-0.0508
isoprene	-0.0710
2-methyl-propanal	-0.0497
C_{10} monoterpenes	-0.0382
pentanal	-0.0376
methacrolein (MACR)	-0.0364
limonene	-0.0303
butanal	-0.0255
cyclohexanone	-0.0243
2-pentanone	-0.0234
3-methyl-butanal	-0.0196
2-hexanone	-0.0190
hexanal	-0.0173
2-methyl-butanal	-0.0166
ethyl-acetate	-0.0139
4-methyl-2-pentanone	-0.0137
butanone	-0.0025
α-pinene	0.0079
1,2-butadiene	0.0085
4-*iso*-propyl-toluene	0.0195
tert-butyl-benzene	0.1256
styrene	0.2027
butanol	0.2353
napthalene	0.3733
1,2,4-trimethyl-benzene	0.3796
C_{13} aliphatics	0.3881
1,3-diethyl-benzene	0.3930
1,3-butadiene	0.3967
2-ethyl-toluene	0.4245
4-ethyl-toluene	0.4268
2-methyl-nonane	0.4489
3-ethyl-toluene	0.4519
n-decane	0.4635
n-propyl-benzene	0.4651
C_6 aliphatics	0.4659
cyclopentane	0.4681
C_4 substituted mono aromatics	0.4831
C_{12} aliphatics	0.4854
acetone	0.4982
indan	0.5150
1,2,3-trimethyl-benzene	0.5170

C_{11} aliphatics	0.5241
benzaldehyde	0.5332
iso-propyl-benzene	0.5363
C_{10} aliphatics	0.5397
C_8 aliphatics	0.5512
methanol	0.5528
C_9 aliphatics	0.5583
trans-2-butene	0.5655
1,3,5-trimethyl-benzene	0.5680
cis-2-butene	0.5690
propyne	0.5705
propadiene	0.6028
C_7 aliphatics	0.6105
1-butene	0.6121
trans-2 pentene	0.6161
n-nonane	0.6300
dichloromethane	0.6354
2,2,4-trimethyl-pentane	0.6478
n-butane	0.6547
n-hexane	0.6550
iso-butene	0.6564
propene	0.6566
iso-butane	0.6640
acetylene	0.6662
propanol	0.6784
2,2,3-trimethyl-butane	0.6808
1-pentene	0.6900
n-octane	0.7025
1,4-diethyl-benzene	0.7042
iso-pentane	0.7072
methane	0.7142
ethene	0.7164
n-dodecane	0.7042
n-undecane	0.7166
trichloroethylene	0.7235
n-heptane	0.7254
n-ethane	0.7353
o-xylene	0.7433
n-pentane	0.7448
2,3-methylpentane	0.7448
m+*p*-xylene	0.7523
benzene	0.7630
ethyl benzene	0.7642
acetaldehyde	0.7682
ethanol	0.7703
toluene	0.7773
propane	0.7887

Table 2. Elemental ratios of each of the derived PMF factors.

	O:C	OM:OC	H:C	N:C
HOA	0.01	1.17	1.97	0.0001
COA	0.13	1.32	1.73	0.002
SVOOA	0.44	1.72	1.46	0.005
LVOOA	0.52	1.85	1.61	0.02
Unknown	0.20	1.41	1.58	0.009

Table 3. Details of the reactions and rate coefficients used to estimate nitrate radical (NO_3) concentrations.

Reaction	Rate coefficient (cm^3 $molecule^{-1}$ s^{-1})	
$NO_2 + O_3 \rightarrow NO_3 + O_2$	k2	3.52×10^{-17}
$NO_3 + NO_2 \rightarrow N_2O_5$	k3	1.90×10^{-12}
$NO_3 + NO \rightarrow 2NO_2$	k7	2.60×10^{-11}
$N_2O_5 \rightarrow NO_2 + NO_3$	k8	9.32×10^{-20}

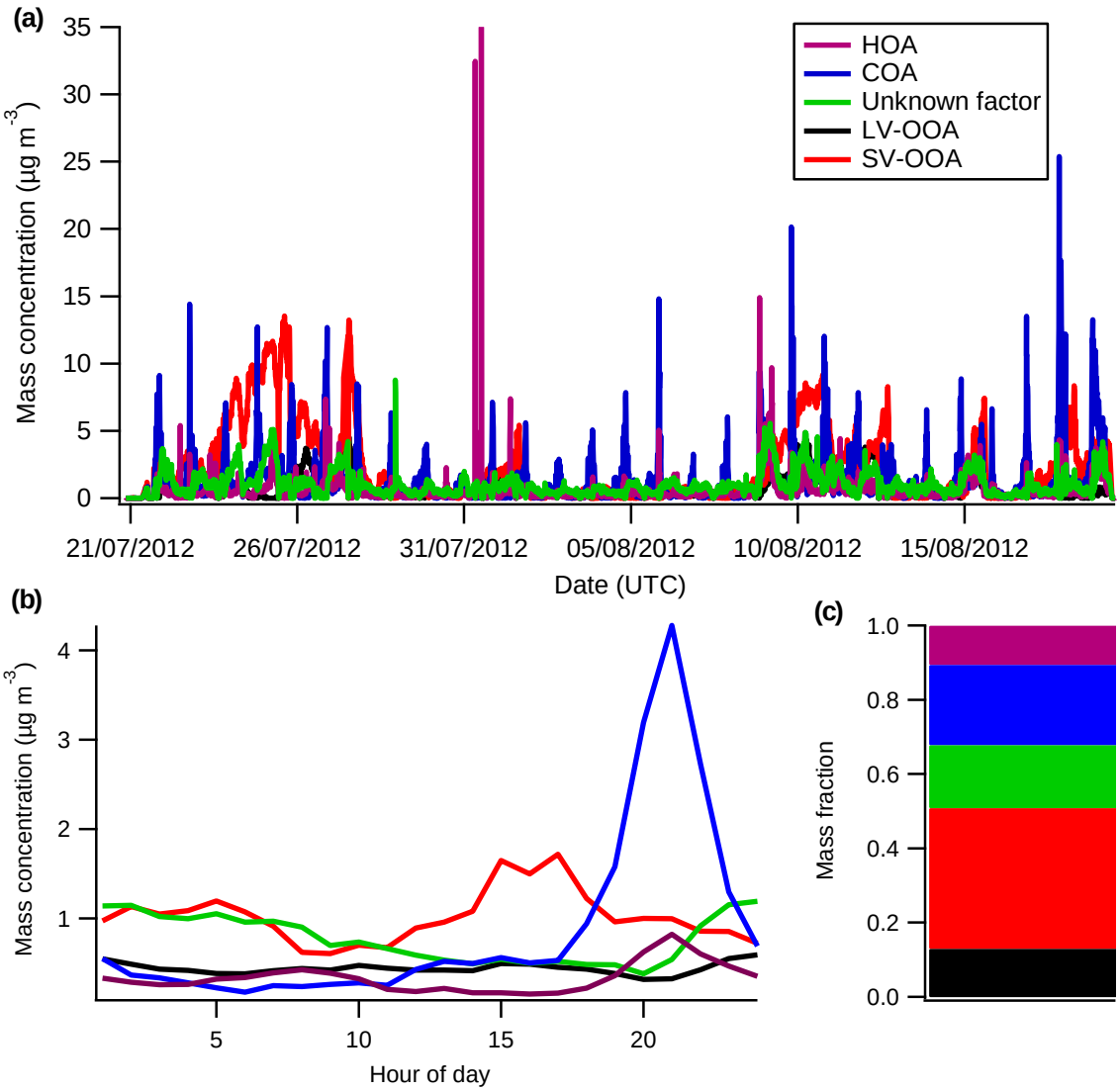

Figure 1. **(a)** Time series of the five factors derived from PMF analysis of the organic aerosol fraction. All times are in UTC. **(b)** Median diurnal profiles for each of the 5 factors. **(c)** Average fractional contributions of the five factors to the total submicron organic aerosol mass.

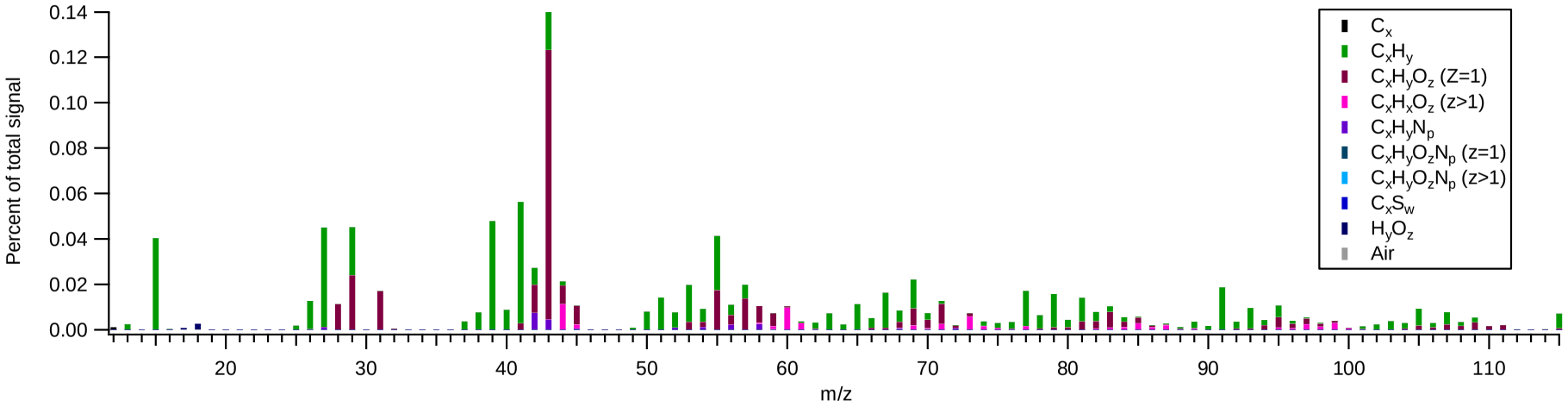

Figure 2. Mass spectrum of the unknown factor derived from PMF analysis on the HR-ToF-AMS organic data.

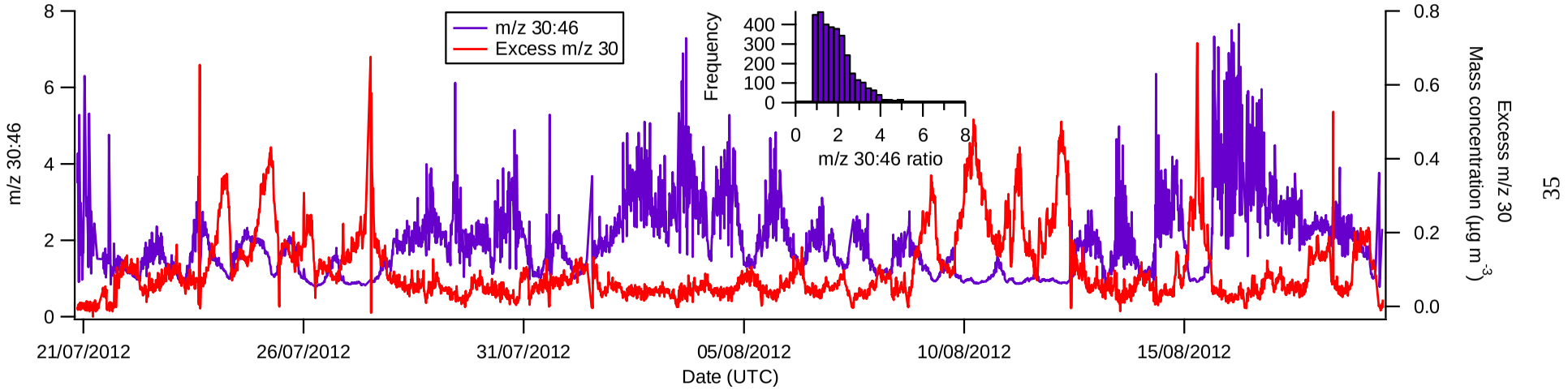

Figure 3. Time series of the m/z 30 to 46 ratio and excess m/z 30 (see text for details). Inset: histogram of the m/z 30 to 46 ratio.

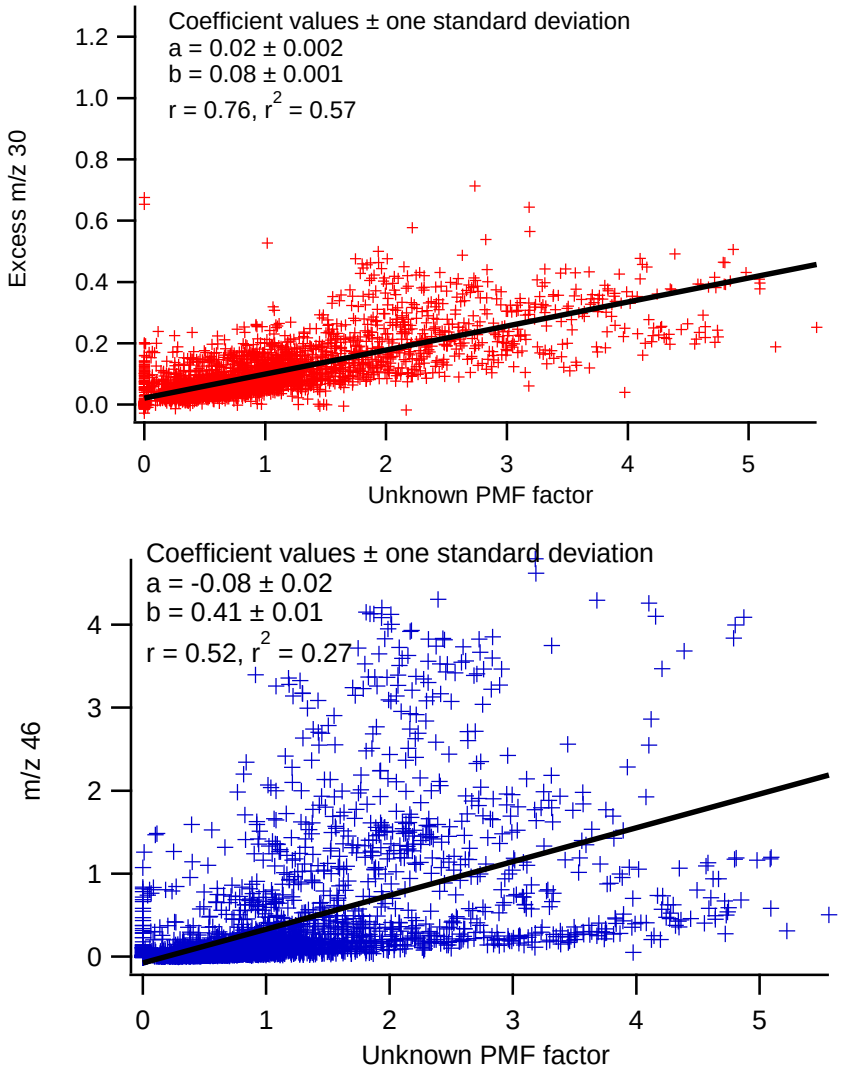

Figure 4. Scatter plots of the excess m/z 30 (top) and m/z 46 (bottom) against the unknown PMF factor.

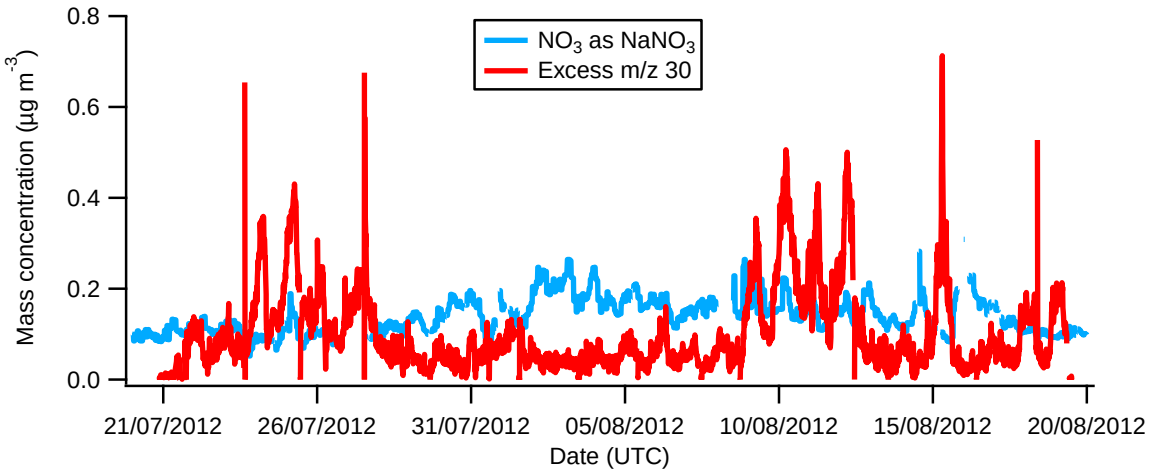

Figure 5. Time series of the nitrate that can be explained as being in $NaNO_3$, estimated using Na^+ measurements from the URG AIM from North Kensington (PM_{10}).

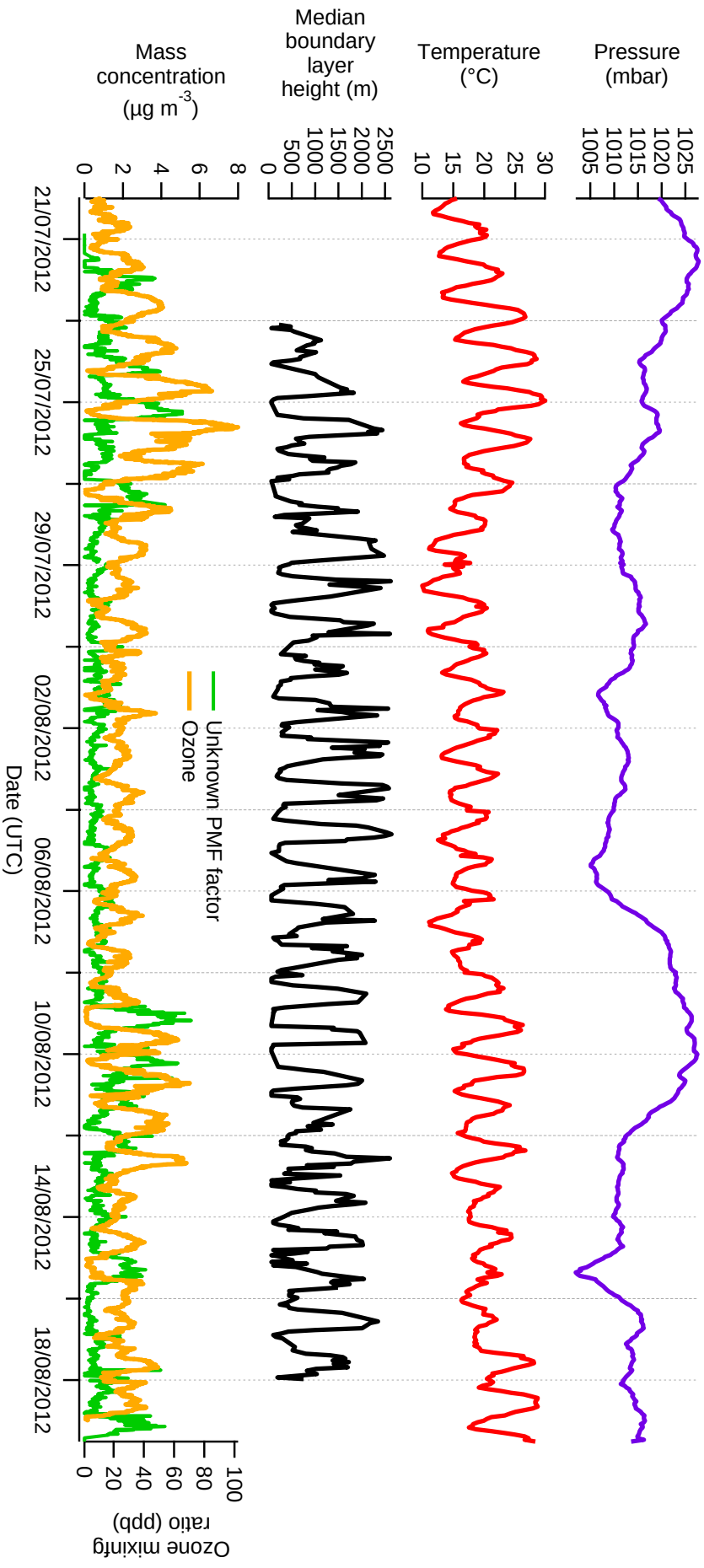

Figure 6. Time series of the unknown PMF factor, ozone mixing ratio, boundary layer height, temperature and pressure.

4.5 Contributions to other papers from the ClearfLo project

Meteorology, air quality and health in London: the ClearfLo project, Bohnenstengel et al. (2014). *This manuscript has been accepted to the journal Bulletin of the American Meteorological Society (2014) and is currently in press.*

In this paper, the ClearfLo project is introduced and includes details of the measurement campaigns, sites, and instrumentation used in both the short-term and long-term measurement periods. Initial results are also presented and discussed, demonstrating the type of information that can be gleaned from this project with analyses that are currently being performed. As part of the project, Aerosol Mass Spectrometer (AMS) measurements were made at four sites during the winter (North Kensington, Marylebone Road, Harwell, Detling) and at the two inner city London sites during the summer enabling spatial and temporal trends in the aerosol species to be identified and interpreted. Dominique Young performed the AMS measurements at the North Kensington site, provided the data from both intensive observation periods (IOPs), and assisted in the discussions to interpret the data.

Receptor Modelling of Fine Particles in southern England using CMB including Comparison with AMS-PMF Factors, Yin et al. (2014). *This manuscript is published in Atmospheric Chemistry and Physics Discussions (doi:10.5194/acpd-14-24523-2014) and is currently under review for Atmospheric Chemistry and Physics.*

In this paper, fine particles ($PM_{2.5}$) in London measured during winter 2012 are apportioned into their sources using the chemical mass balance (CMB) model. The results from the CMB model are discussed and compared with those derived from Positive Matrix Factorisation (PMF) analysis of High-Resolution Time-of-Flight Aerosol Mass Spectrometer (HR-ToF-AMS) data. Dominique Young performed the AMS measurements, applied PMF to the organic aerosol data, interpreted the results from PMF analysis, and provided the results for this study.

Size distribution, mixing state and source apportionments of black carbon aerosols in London during winter time, Liu et al. (2014). *This manuscript is published in Atmospheric Chemistry and Physics (doi:10.5194/acp-14-10061-2014).*

In this paper, black carbon aerosols in London during wintertime are characterised, including their attribution to traffic and solid fuel burning activities. Three approaches to apportion BC into the two sources are presented where each approach uses a different instrument, namely the single particle soot photometer (SP2), AMS, and Aethalometer. Dominique Young performed the AMS measurements and assisted with other aerosols measurements. Dominique Young also applied PMF to the organic aerosol data from the AMS, interpreted the results, and provided the outputs for this study.

Chapter 5

Conclusions

5.1 Summary of research findings

Presented in this thesis is a comprehensive review of the chemical composition and behaviour of submicron non-refractory aerosols in London. The sources and components of London's aerosols were assessed in terms of their contributions to total mass and pollution events as well as the temporal variations in behaviour. Consistent with other urban studies in Europe, organic aerosols (OA) were found to represent the largest component (44%) of the total mass in London between 11 January 2012 and 23 January 2013, with nitrate aerosols contributing 28%, on average. Furthermore, a significant fraction of the total submicron aerosol burden was accounted for by secondary inorganic and organic aerosols. The application of Positive Matrix Factorisation (PMF) enabled the components of the organic fraction to be further investigated; five factors were identified, of which many have been identified in other urban source apportionment studies. These factors were attributed as hydrocarbon-like OA (HOA), cooking OA (COA), solid fuel OA (SFOA), type 1 oxygenated OA (OOA1) and type 2 oxygenated OA (OOA2) and contributed, on average, 21%, 19%, 25%, 31%, and 4% to the total OA mass, respectively. The main factors governing the diurnal, monthly, and seasonal trends observed in all organic and inorganic species were found to be meteorological conditions, specific nature of the aerosols, and availability of precursors. In addition, regional and transboundary pollution influenced the total aerosol concentrations in London. As expected, the mass of the secondary organic aerosols (SOA) increased during the summer, however, the extent of oxidation of SOA, as defined by the oxygen content, did not vary across the year suggesting that in the urban background of London the range of precursors and chemical processing are insufficiently

variable to yield SOA that has been exposed to significantly different levels of chemical processing.

In order to understand the composition, and therefore the sources, of the aerosols contributing to exceedences of air quality limits, high pollution events during 2012 in London were assessed. In winter, high concentration events were governed by nitrate formation and primary organic particulate emissions, which contributed 39% and 29% to the total non-refractory submicron mass, respectively. In comparison, during the summer high concentrations were driven by SOA formation, where SOA contributed 25% to the total submicron mass. Factor analysis of higher resolution chemical composition measurements from the ClearfLo winter measurement campaign further highlighted the importance of primary organic aerosol (POA) emissions, particularly SFOA as two factors were identified along with HOA, COA, and a single OOA factor. The concentrations of both SFOA factors were found to increase during the night and during cold periods, consistent with domestic space heating activities. The SFOA profile is known to be influenced by the fuel type, atmospheric processing, and the burn conditions including open fireplaces compared to modern burners in residential dwellings as well as phase of the burn such as smouldering or flaming. Different fuel types and levels of atmospheric processing likely contribute to the differences between the two SFOA factors with influences from air masses of different trajectories, but the split is likely governed predominantly by differences in burn conditions identified from correlations with the combustion tracers levoglucosan and potassium ion. The two SFOA factors also exhibited some spatial differences whereby the highest concentrations of SFOA1 were in the south of the city, which best represents more efficient burns compared to SFOA2, which had high concentrations in the east and west of the city. Differences in burn efficiencies could be due to the type of burner used, where it could be suggested that modern appliances are predominantly used in the south and fireplaces are used in the east and west. Different burn conditions could also be due to differences in burn phase where the flaming phase is a more efficient burn.

In contrast, the photochemical conditions and dynamic range in ambient temperatures in the summer resulted in the identification of two OOA components as well as HOA and COA from factor analysis of the high-resolution summer data, where the two OOA components were attributed as semi-volatile oxygenated OA (SV-OOA) and low volatility oxygenated OA (LV-OOA). An additional factor was identified, which contributed 17% to the total OA mass and increased in concentration over night. The origin and behaviour of this OA factor were investigated through examination of its

chemical composition and concentrations as well as comparisons with ancillary measurements. A strong correlation was observed between the factor and excess NO^+ ion signals at m/z 30, indicating the factor is likely composed of organic nitrates. Variations in the concentration of the factor were coincident with known primary OA sources and anthropogenic trace gases thus was suggested to be of primary anthropogenic origin. However, few direct sources of organic nitrates are currently known (Mohr et al., 2013).

5.2 Technical implications and recommendations

5.2.1 Source apportionment and factorisation techniques

As discussed in Chapter 3, the characterisation of organic aerosols has been the focus of many studies, where significant advances in understanding OA have been made over the last two decades. However, some uncertainties remain along with large gaps in scientific knowledge surrounding the sources and fate of OA in the atmosphere. Some of these uncertainties arise from the approaches to apportion OA into its different components.

The work presented in Section 4.2 was the first time PMF had been applied to a year of organic aerosol data from the AMS in an urban environment. As the annual trends of the components of the organic fraction were to be investigated, PMF was applied to the full dataset rather than applying to data split into seasons as this is subjective and would have likely resulted in a bias of the retrieved factors. Furthermore, information on annual trends of the OA components may also have been lost. However, the application of PMF to a long-term dataset yielded mixed factors whereby the covariance of two factors (termed $SFOA_{PMF}$ and $OOA2_{PMF}$) resulted in the assignment of some $SFOA_{PMF}$ mass to $OOA2_{PMF}$. Separating organic components measured by the AMS using the multilinear engine (Canonaco et al., 2013), ME-2, has in some circumstances, produced more representative results (e.g. Lanz et al., 2008), particularly when temporal co-variation of factors arises. However, in order to utilise ME-2 a priori knowledge by way of factor profiles and/or time series is required. Consequently, performing factor analysis without a priori assumption, such as by unconstrained PMF analysis, is preferred as a first stage in any further analysis in order to identify the likely components of OA and is recommended here. It is therefore important to understand the outputs from PMF analysis before applying ME-2, and as shown in Section

4.2, the limitation of PMF can be overcome by careful scrutiny of the data as well as from the use and support of associated measurements such as from the HR-ToF-AMS. Similarly, Crippa et al. (2013a) applied PMF analysis to a combination of AMS and Proton Transfer Reaction Mass Spectrometry (PTR-MS) data with an aim of improving the separation of factors. In addition, it is likely that separation of mixed sources identified from ME-2 analysis would not be achieved without additional information as several of the factorisation problems that ME-2 overcomes when applied to data from the Aerosol Chemical Speciation Monitor (ACSM, Ng et al., 2011b) compared to the AMS are related to the fact that the ACSM has much lower signal-to-noise ratio.

Several source apportionment techniques have been used in ClearfLo to separate London's aerosols into the different components, with very encouraging results. For example, Yin et al. (2014) present the first study to compare results from different source apportionment methods in the UK, where the chemical mass balance (CMB) model was employed to investigate the sources of $PM_{2.5}$ in the winter. The main sources were identified as traffic, inorganic salts, food cooking, coal combustion, woodsmoke, natural gas, dust/soil, and vegetative detritus. Secondary organic aerosols also contributed to the total organic carbon mass. The factors identified from CMB analysis were compared to those from PMF analysis of the high-resolution AMS data, where relatively strong correlations were found between most components. A particularly strong correlation was observed between the primary organic components identified from both methods where the two SFOA factors derived from PMF analysis in Section 4.3 were summed ($r^2 = 0.91$). However, differences were found between the concentrations of each of the factors estimated by the two methods, including solid fuel and cooking aerosols. Consequently, the split between primary and secondary organic aerosols varied significantly between CMB and PMF. Some of these discrepancies can be explained by the differences in the techniques and methodologies employed including the size fraction observed and model inputs. Substantial discrepancies remain, however, indicating the need for further work to constrain the issues of each of the methods although the strong correlations between the two methods is encouraging.

In addition, the BC fraction was apportioned in Liu et al. (2014), where three methods involving measurements from the single particle soot photometer (SP2), AMS, and a 7-wavelength Aethalometer (MAGEE Scientific, model AE31), were used to apportion BC mass concentrations from solid fuel and traffic sources. The results from the approach using SP2 data and the approach using the two-component SFOA model from PMF analysis of AMS data described in Section 4.3 were observed to be strongly

correlated for the whole measurement period. Such a high level of agreement between the two methods therefore increases confidence in the applicability and accuracy of the source attribution techniques in this study and in future studies. In addition, these results are also very encouraging for improving the understanding of the sources and physical properties of black carbon aerosols in the urban environment.

5.2.2 Long-term Aerosol Mass Spectrometer measurements

With the introduction of the ACSM, an instrument designed for long-term monitoring of aerosol chemical composition, it may be that the study in this thesis study will be unique in the acquisition and analysis of a year of cToF-AMS data. Nevertheless, these measurements were possible and successful for a number of reasons including the instrument set up, maintenance, and quality assurance of the data, which are stated here as recommendations for any future studies. In order to prolong the life of the multichannel plate (MCP, Section 2.1), the filament was run at a lower value than usual and the heater bias was tuned to minimise the signal from surface ionised potassium. This configuration, however, results in a reduced signal, which in turn reduces the signal-to-noise ratio (Allan et al., 2003b). The cToF-AMS was calibrated using ammonium nitrate particles approximately once a month and ammonium sulphate calibrations were performed where possible. It is recommended that both ammonium nitrate and sulphate calibrations are performed at least once a month for long-term measurements, and even more frequently if possible. However, this would depend on the availability of the additional instruments required to perform these calibrations, such as a differential mobility particle sizer (DMPS) or scanning mobility particle sizer (SMPS) and condensation particle counter (CPC), where the data from these instruments are also used to validate corrections applied to AMS data when processed (e.g. the AMS collection efficiency, Section 2.3.2). Furthermore, it is recommended for personnel close to the measurement site to be available for regular checks and calibrations, where remote access to the AMS computer is also highly recommended for checking the instrument on a daily basis. Finally, although not essential, additional chemical composition measurements are useful for data analyses and interpretation, as was proven in this study where data from the URG Ambient Ion Monitor were used.

5.3 Air quality implications and recommendations

The contributions and behaviour of the major secondary inorganic aerosols (SIA) identified in this work are consistent with the findings from previous studies in the urban environment both in the UK (Abdalmogith and Harrison, 2005; Harrison and Yin, 2008; Martin et al., 2011; Harrison et al., 2012) and within Europe (Putaud et al., 2004; Bressi et al., 2013; Dall'Osto et al., 2013; Freutel et al., 2013). AMS measurements are used in the studies by Martin et al. (2011), Harrison et al. (2012), Dall'Osto et al. (2013), and Freutel et al. (2013) whereas the other studies predominantly use filter-based measurements. Ammonium nitrate is often the dominant component of the inorganic aerosol fraction, particularly in the winter when meteorological conditions lead to preferential partitioning to the particle phase, where the highest concentrations occur in spring due to the availability of precursors. As highlighted in many studies, ammonium nitrate concentrations in urban environments are significantly influenced by regional and transboundary air masses indicating the importance of transboundary pollution; increased concentrations are associated with air masses that have advected from Europe whereas lower concentrations are associated with the cleaner air masses from the west (Abdalmogith and Harrison, 2006; Morgan et al., 2010b; Martin et al., 2011). The findings presented in this thesis therefore reinforce the influence of the various factors that govern nitrate concentrations, namely a combination of meteorological conditions, availability of precursors, and air mass trajectory. However, there are serious implications for future concentrations of nitrate and thus the impacts on pollution events as well as climate owing to the greater availability of ammonia to form ammonium nitrate as sulphate concentrations are decreasing in line with decreasing sulphur dioxide (SO_2) precursor emissions (e.g. Bauer et al., 2007; Monks et al., 2009; Morgan et al., 2010a). An additional complicating matter regarding the outlook of SIA relates to the non-linear response of their concentrations to changes in precursor emissions. Therefore, in order to accurately predict nitrate concentrations there is a need to combine detailed measurements and modelling, particularly of aerosol chemistry and thermodynamics, as this study has demonstrated that no single factor dominates in governing ammonium nitrate concentrations.

The results presented in Section 4.2 illustrate the importance of particulate emissions during the winter in urban areas, where nitrate and POA play significant roles at a time when air quality limits are likely to be exceeded. Although most primary organic sources are known, as discussed in Section 3.4, the temporal and spatial variations of several sources are not fully understood. Furthermore, it is likely there are

numerous sources of OA that are unidentified or uncharacterised. Previously identified components of OA that were attributed to local sources for which more specific sources could not be determined, contributed between approximately 3% and 9% of the total OA mass (Aiken et al., 2009; Huffman et al., 2009; Docherty et al., 2011; Sun et al., 2011; Hayes et al., 2013). The results presented in Section 4.4 suggest that currently unidentified sources of OA could be as important, if not more so, than known sources in terms of contributing to urban particle matter where during the summer in London, 17% of the total OA mass was attributed to an unknown local source. The identification of an unexpected organic factor in the urban environment highlights the need for more source apportionment studies to identify the importance of other components. Emissions of some primary organic aerosols have already been reduced, such as HOA due to their association with traffic where emissions of nitrogen oxides (NO_x) have been addressed in pollution abatement schemes. Consequently, the importance of other known sources such as cooking may increase. Furthermore, the signals of other OA components may become large enough to be detected and therefore these sources could become significant contributors to aerosol mass.

One of the largest uncertainties surrounding typical primary sources arises from solid fuel burning as the mass spectral profile varies due to fuel type, atmospheric processing, and burn phase. The application of the PMF model to high-resolution organic aerosol measurements, however, provided insight into the importance of each of the influencing factors during the winter, when solid fuel burning activities are prominent, as shown in Section 4.3. The results presented in this thesis further the understanding regarding the formation and processing of aerosols from solid fuel combustion. Including more than one SFOA profile in factorisation studies may improve the accuracy of the derived results as the variability of solid fuel organic aerosols is better characterised. The two SFOA factors derived in this study have been used in Liu et al. (2014) and Yin et al. (2014), with positive results. Consequently, parametrisation of solid fuel aerosols in air quality models may be improved if their emissions are better characterised in source apportionment studies and consequently improve predictions of high concentration events. However when looking to the future, government incentives to use renewable energy sources for heating in order to reduce the carbon footprint and comply with regulations to reduce carbon dioxide (CO_2) emissions and mitigate climate change will likely result in an increase in solid fuel burning emissions. Consequently, air quality will be adversely affected with increased exposure to the public.

SOA concentrations in London presented in Section 4.2 were consistent with other studies as they were observed to increase in summer due to the availability of precursors and increased photochemistry. SOA formation was also observed to significantly influence pollution events in London. However, the properties and evolution of SOA present the largest uncertainties when assessing the impacts of aerosols and parametrising aerosols in air pollution and climate models. Many studies have explored the transformation of SOA with ageing in the atmosphere (Jimenez et al., 2009; Heald et al., 2010; Morgan et al., 2010b; Ng et al., 2010; Kroll et al., 2011; Donahue et al., 2012), however these have predominantly employed laboratory and short-term ambient measurements at a number of different locations. Nevertheless, the evolution of SOA from freshly emitted, semi-volatile oxygenated organic aerosol to aged oxygenated organic aerosol of low volatility is observed in all cases. Although two oxygenated organic aerosol components were identified in London from long-term measurements, the results presented in Section 4.2 illustrate that at a single location, namely the urban background site at North Kensington, over the course of a full calendar year there is little variability in SOA oxidation despite significant differences in precursor emissions and photochemistry with season. More long-term chemical composition studies at urban background sites are required to determine if the findings from this work are representative of SOA in similar urban locations. In addition, it would be beneficial for such studies to employ a suite of gas and particle phase instruments in order to investigate the reason for the minimal variation in SOA oxidation. Nevertheless, characterisation of SOA in future studies may be more straightforward thus improving the parametrisation of SOA in models and subsequently improve the predictive capability for air quality, including pollution events.

5.4 Policy implications and recommendations

5.4.1 Secondary inorganic aerosols

Due to the importance of nitrate in contributing to pollution events, the focus of pollution abatement strategies should be directed towards reducing particulates in the winter including through the moderation of sources of nitrate. In addition, reducing emissions of ammonia should be considered to mitigate the effects on air quality as this will likely reduce concentrations of ammonium nitrate as well as other SIA (Deutsch et al., 2008). However, there are several uncertainties surrounding the emissions inventory

for ammonia in the UK (Sutton et al., 2000; Misselbrook et al., 2011) and Europe (e.g. Reis et al., 2009), thus improved knowledge of the sources, strengths, and trends of ammonia emissions should be a major aim of future studies investigating atmospheric aerosols and their impacts. The influence of imported pollution could, however, reduce the efficiency of any abatement strategies in the UK thus indicating the need to collaborate with neighbouring countries to reduce emissions in order to achieve compliance with EU air quality limits.

5.4.2 Organic aerosols

Accurate identification of the different organic aerosol components is important for understanding their importance in contributing to the effects on air quality and health. Furthermore, gaining a comprehensive understanding of aerosol sources is fundamental to predicting concentrations, where emission factors are required inputs for chemical transport models in order to budget for the production of OA, particularly POA, from each of the sources. The results obtained as part of ClearfLo are therefore very encouraging, where similar components are identified from the different factorisation methods used (Section 5.2.1). Thus a consistent picture of the sources of aerosols in London is obtained, which can be used to inform policy makers and help focus the direction of pollution abatement strategies. However, the implications on air quality and health associated with each of the PM components require different measures to enable them to be addressed in future policies. These implications are discussed in the following sections.

5.4.2.1 Solid fuel organic aerosol

The results presented in Sections 4.2 and 4.3 illustrate the importance of particulate emissions from solid fuel burning in urban areas, particularly during the winter. The substantial emissions from solid fuel burning detected in London suggest that current legislation to improve air quality and reduce exposure to pollutants, such as the Smoke Control Areas, may not be effective (Fuller et al., 2014). As shown in Section 4.2, particulate emissions from solid fuel burning are as important as traffic emissions in terms of contributions to total submicron mass, thus may become more important in the future as emissions from traffic are more stringently regulated compared to those from solid fuel burning. Consequently, the effects on air quality and health are only going to get worse. Therefore, as a first step to achieve compliance with current air quality

limits sources of solid fuel burning emissions should be moderated and be the focus of strategies to mitigate pollution with the enforcement of more stringent regulations, which are regularly checked for compliance. In addition, as it is highly likely solid fuel burning emissions will increase in the future due to rising energy costs and government incentives for renewable sources to be used for energy, it is recommended that the implications on air quality and human health are taken into serious consideration when schemes to mitigate climate change are proposed and developed.

Emission factors for bulk POA as well as HOA and SFOA have been estimated through various techniques in different locations over several years (e.g. Allan et al., 2003a, 2010; Zhang et al., 2005b; Chirico et al., 2011; Mohr et al., 2013). However, improvement of quantification techniques, through improvements to instrument measurements and source profiles used in, and derived from, factorisation models provides the opportunity to quantify emission factors much more reliably. The results presented in this thesis could improve existing emission factors for HOA and SFOA in London as long-term measurements of their concentrations and co-located trace gases are available, which can be used to derive such estimates. Furthermore, as some of the variability of solid fuel burning has been captured in the identification of two SFOA factors in Section 4.3 from the high-resolution measurements, such results could further improve the emissions estimates. More reliable and accurate emission factors could have significant influences in forming future air quality policies and mitigation strategies and consequently moderating sources of POA is more likely to be achieved.

5.4.2.2 Cooking organic aerosol

Cooking activities have been predominantly recognised as an indoor air pollution problem to date yet a significant proportion of outdoor aerosol concentrations have been attributed to emissions from cooking (Abdullahi et al., 2013 and references therein). Therefore the potential for cooking emissions to have adverse effects on human health are significant in both the indoor and outdoor environments. Zhang et al. (2010) suggest several relatively simple methods to reduce indoor exposure to emissions from cooking, particularly from ultrafine particles, including using efficient ventilation devices and using extractor fume hoods whilst cooking. Such methods may help to improve air quality within the home by efficiently reducing levels of volatile organic compounds (VOCs) and particulates. However, the subsequent ramifications for outdoor pollution and human exposure are currently unclear as previous studies have tended to only assess the influence of outdoor pollution on indoor pollution (e.g. Abt et al., 2000;

Buonanno et al., 2009). As shown in this work, particulate emissions from cooking are as important as, and may become even more important than, those from traffic in the outdoor urban environment. Therefore, improvements could be made to both indoor and outdoor air quality through the use of extractor fume hoods and filters, which efficiently capture the emissions from cooking and consequently reduce exposure to the public (Abdullahi et al., 2013).

In comparison to solid fuel burning and traffic, emissions from cooking activities are severely lacking in national inventories in the US (e.g. Simon et al., 2008) and are not included in the UK National Atmospheric Emissions Inventory. However, several studies have estimated the emissions from cooking in the US where Rogge et al. (1991) investigated meat cooking using charbroilers in the Los Angeles area and Roe et al. (2002) estimated the emissions from commercial cooking processes with an aim of developing a national emission inventory. In order to design effective pollution abatement strategies, emissions from cooking activities need to be quantified and included in national emissions inventories, where the results presented in this thesis could be used to build an emissions estimate for cooking processes in London as concentrations of cooking organic aerosol (COA) are available. Although tracers such as cholesterol and oleic acid are used to estimate emissions from cooking activities, Simon et al. (2008) suggest there are few tracer species which are unique to these emissions thus using a combination of tracers will help distinguish cooking from other types of emissions. Consequently, emissions from cooking in London may be more accurately estimated if both the particulate and gas phase measurements, including VOCs, from the ClearfLo intensive observation periods (IOPs) are used.

5.4.2.3 Organic nitrates

The organic nitrate OA factor in London was proposed to be of anthropogenic origin and unlikely to be secondary in nature. However, few direct sources of organic nitrates in urban environments are known. Furthermore, little is known about the properties of particulate organic nitrates thus the effects of these aerosols on air quality, human health, and climate are unquantified. However, it is suggested that nitrogen-containing organic compounds are very toxic and are therefore of great concern for human health (e.g. Huang et al., 1995; Enya et al., 1997). Detailed laboratory and field measurements are therefore necessary to improve the characterisation of such aerosols. In order to better inform pollution abatement strategies and air quality policies, efforts should be made as a matter of urgency to determine the sources and properties of organic

nitrates, which have a non-negligible contribution to total organic mass in London and could be an important contribution to urban particulate matter in other locations. As highlighted in Cape et al. (2011), the potentially adverse effects of organic nitrates and other nitrogen-containing organic compounds on human health can only be addressed and mitigated once their sources are identified.

5.5 Remaining questions and further work

The work presented in this thesis will contribute to and further the understanding of the chemical components of urban aerosols and their behaviour. However, COA has been identified as an important component of ambient urban aerosol yet its variability has not been fully characterised such as how the properties and mass spectral profile change with atmospheric processing, for example. Consequently, estimated mass fractions of COA vary between studies, part of which is attributable to the different factorisation techniques used such as CMB and PMF. Detailed laboratory measurements of a range of cooking techniques using a combination of on-line and off-line instrumentation and receptor-based apportionment techniques should be performed to investigate the effect of atmospheric processing on cooking emissions. Ambient measurements should also be performed to assess the understanding of processes learnt from laboratory studies. Furthermore, in order to assess the contribution of COA to total mass over the whole of London, chemical composition measurements should be obtained at a variety of site types both in and around London, particularly as cooking activities are prevalent in both residential areas and city centres where restaurants and other commercial spaces are abundant. As part of the ClearfLo project, AMS measurements are available from four locations during the winter: Harwell, Detling, Marylebone Road, and North Kensington. A multi-site comparison of the cooking profiles determined from PMF analysis of the organic fraction may offer insight into the evolution of cooking aerosols particularly if the air mass has advected across London towards the two rural sites. In addition, laboratory and field measurements will enable SOA formation from VOC emissions from cooking to be observed. Similarly to SFOA, improved representation in air quality models could be achieved through accurate quantification of the contribution from cooking emissions to total OA mass.

To understand the extent to which findings from the long-term AMS measurements in 2012 are characteristic of the behaviour of aerosols in London from other years, the results from the AMS should be compared with those from the ACSM, which has been

measuring at the North Kensington site in London since April 2013. Moreover, once substantial data have been obtained, the AMS dataset should be assessed against such long-term ACSM measurements in order to determine how representative the trends identified from one year of measurements are compared to trends on even longer time scales. Finally, the profiles derived from PMF analysis in Sections 4.2 and 4.3 could be used to improve ME-2 studies, especially when applied to ACSM measurements and when the two-component SFOA model is used.

In general, future measurement campaigns should employ a number of instruments to enable a comprehensive characterisation of the chemical properties and behaviour of ambient particulate matter. Furthermore, the use of both gas and particle phase measurements in future source apportionment studies should be encouraged if accurate identification and mass contribution estimations of the different components of OA are to be achieved.

5.6 Closing remarks

Several studies have investigated the chemical composition of particulate matter in urban environments to separate into the different components to identify sources as well as to examine the chemical and temporal behaviour of ambient pollution. However, there are still substantial uncertainties in the sources, formation, and evolution of PM components, which is in part owing to the techniques employed. The work in this thesis presents the first long-term chemical composition measurements from an urban environment using an AMS, with the first application of PMF to a year of organic aerosol data from this instrument in this type of environment. The findings make a considerable contribution to further the understanding of the sources and components of urban aerosols, their behaviour, and contributions to total mass and pollution events. Although more measurements of a similar nature are needed to further constrain source profiles and thus accurately apportion the chemical components, the implications from this research highlight the need to target emissions, particularly from anthropogenic sources and during wintertime. Furthermore, the need to collaborate with countries in relatively close proximity to the UK in order to reduce the levels of pollution as well as the frequency and severity of pollution events in cities is illustrated. This work therefore provides a significant contribution towards bridging the gap between identifying and understanding the chemical components of particulate matter in the urban environment.

Appendix A

Appendix

A.1 Supplementary material for Paper I

The following supplementary material supports the analyses conducted as part of Paper I in Section 4.2 where details regarding quality assurance of the Aerosol Mass Spectrometer (AMS) data are provided. Additional information is presented including comparisons of the data from both versions of the AMS used in this thesis (compact Time-of-Flight AMS (cToF-AMS) and High Resolution Time-of-Flight AMS (HR-ToF-AMS)) and seasonal variations in the mass and diurnal profiles of each of the species measured by the cToF-AMS. Further details regarding the factor analysis methods and results are also included.

Supplement of Atmos. Chem. Phys. Discuss., 14, 18739–18784, 2014
http://www.atmos-chem-phys-discuss.net/14/18739/2014/
doi:10.5194/acpd-14-18739-2014-supplement

Atmospheric Chemistry and Physics Discussions

Supplement of

Investigating the annual behaviour of submicron secondary inorganic and organic aerosols in London

D. E. Young et al.

Correspondence to: H. Coe (hugh.coe@manchester.ac.uk)

Supplementary information for manuscript

Investigating the Annual Behaviour of Submicron Secondary Inorganic and Organic Aerosols in London

D. E. Young[1], J. D. Allan[1,2], P. I. Williams[1,2], D. C. Green[3], M. J. Flynn[1], R. M. Harrison[4,5], J. Yin[4], M. W. Gallagher[1], and H. Coe[1]

[1]{School of Earth, Atmospheric and Environmental Sciences, University of Manchester, Oxford Road, Manchester, M13 9PL, UK}

[2]{National Centre for Atmospheric Science, University of Manchester, Oxford Road, Manchester, M13 9PL, UK}

[3]{School of Biomedical and Health Sciences, King's College London, London, UK}

[4]{School of Geography, Earth and Environmental Sciences, University of Birmingham, Edgbaston, Birmingham, B15 2TT, United Kingdom}

[5]{Department of Environmental Sciences / Center of Excellence in Environmental Studies, King Abdulaziz University, Jeddah, 21589, Saudi Arabia}

Correspondence to: Dominique Young (dominique.young@postgrad.manchester.ac.uk)

1 NR-PM_1 data quality assurance

1.1 Relative Ionisation Efficiencies (RIEs)

	NH_4	SO_4
cToF-AMS long-term	3.8455	1.1379
HR-ToF-AMS winter IOP	2.9875	1.2
HR-ToF-AMS summer IOP	3.272	1.4809

Table S1. RIE values for ammonium and sulphate calculated from ammonium nitrate and ammonium sulphate calibrations of the cToF-AMS and HR-ToF-AMS. Ammonium sulphate calibrations of the HR-ToF-AMS were only performed during the summer IOP and so the default RIE for sulphate (1.2) is applied in the winter IOP. The RIEs calculated are the average values from all available calibrations for each of the IOPs for the HR-ToF-AMS and from the whole measurement period for the cToF-AMS.

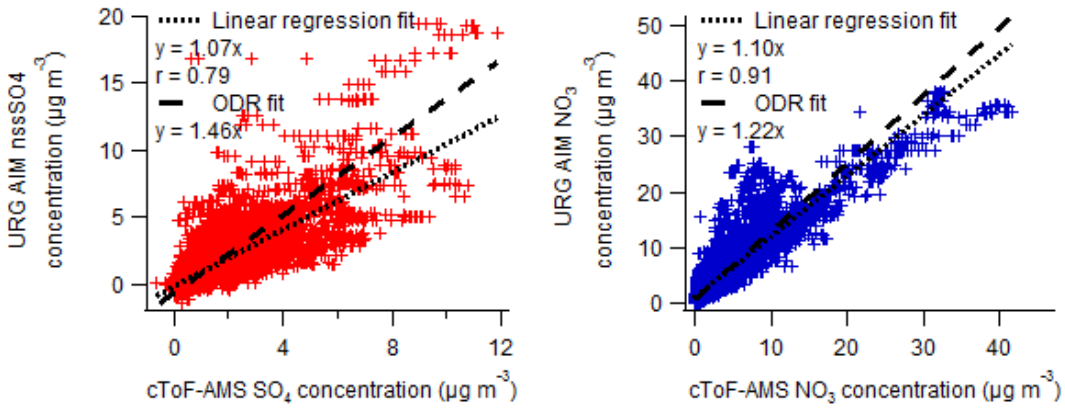

Figure S1. Left: Comparison of the sulphate concentration from the cToF-AMS (corrected using the RIEs in Table S1) with the calculated concentration of non-sea salt sulphate from the URG-9000B Ambient Ion Monitor (AIM) at North Kensington (PM_{10}) for the full calendar year. Right: Comparison of the nitrate concentrations between the cToF-AMS and URG AIM for the full calendar year. The data are fitted using both linear and orthogonal distance regressions (ODR).

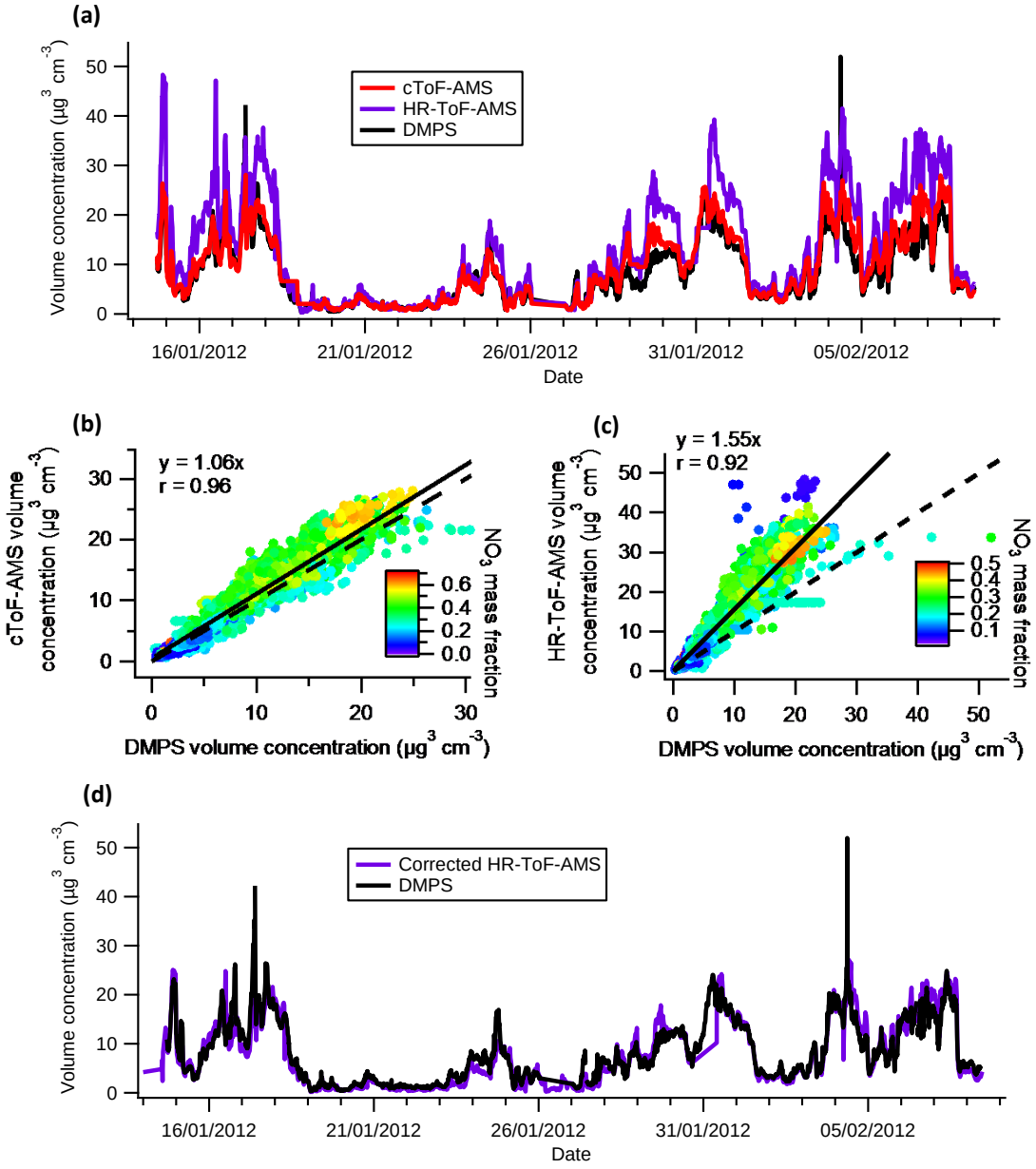

Figure S2. (a) Volume concentration comparison between the DMPS and the two AMS instruments for the winter IOP. Densities of 1.27 and 1.77 g cm^{-3} (reported by Cross et al., 2007) for organic and inorganic contributions, respectively, were assumed for estimating the AMS volume concentrations. (b) Correlation of the volume concentrations for the cToF-AMS and DMPS, coloured as a function of nitrate mass fraction. (c) Correlation of the volume concentrations of the HR-ToF-AMS and DMPS coloured as a function of nitrate mass fraction. (d) Time series of the volume concentrations of the DMPS and HR-ToF-AMS data where the HR-ToF-AMS concentrations of all species but nitrate have been scaled by 0.5 for the winter IOP following the previous volume concentration comparisons.

1.2 Changes in flow rate

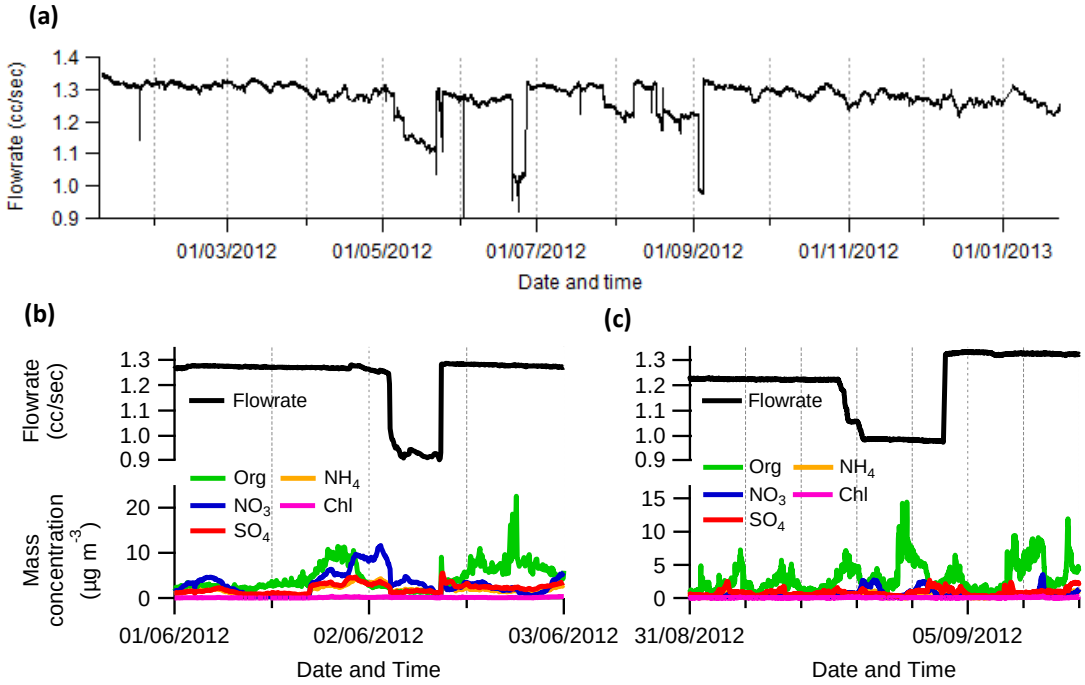

Figure S3. (a) Time series of the flow rate. (b) Step change in mass concentration concurrent with a step change in the flow rate. These data were removed from further analyses. (c) No obvious change in the mass concentration associated with a step change in the flow rate.

2 cToF-AMS vs. HR-ToF-AMS concentrations

2.1 Winter IOP

The HR-ToF-AMS sulphate RIE during the winter IOP was ambiguous as a sulphate calibration was not performed during this measurement period. The HR-ToF-AMS concentrations were compared to those of the cToF-AMS, which was calibrated later during the campaign. The slopes from the linear and ODR fits indicated that the HR-ToF-AMS concentrations were approximately double that of the cToF-AMS. The concentrations of all the HR-ToF-AMS species except nitrate were scaled by 0.5.

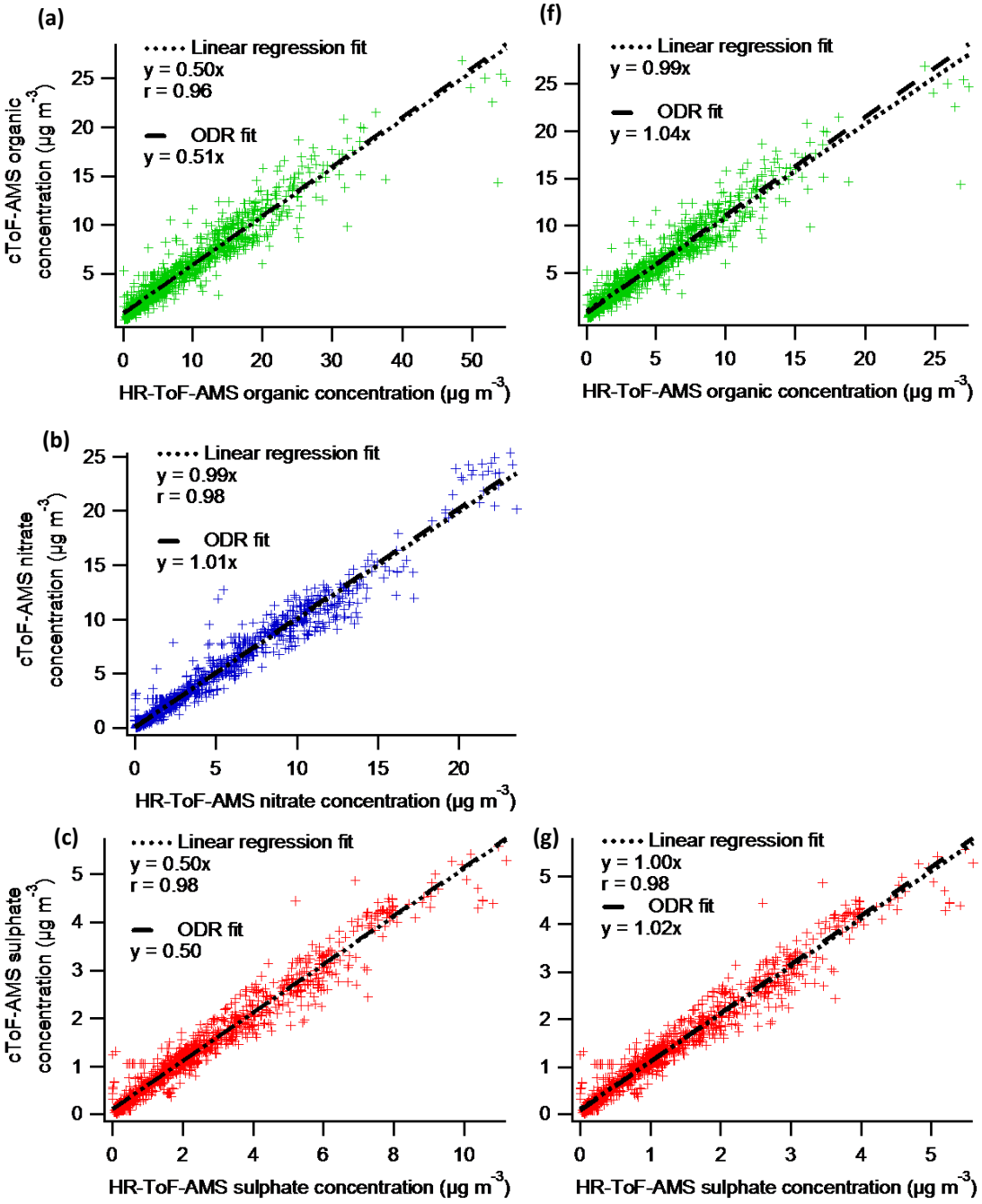
(a)
Linear regression fit
y = 0.50x
r = 0.96
ODR fit
y = 0.51x
cToF-AMS organic concentration (µg m-3)
HR-ToF-AMS organic concentration (µg m-3)
(f)
Linear regression fit
y = 0.99x
ODR fit
y = 1.04x
HR-ToF-AMS organic concentration (µg m-3)
(b)
Linear regression fit
y = 0.99x
r = 0.98
ODR fit
y = 1.01x
cToF-AMS nitrate concentration (µg m-3)
HR-ToF-AMS nitrate concentration (µg m-3)
(c)
Linear regression fit
y = 0.50x
r = 0.98
ODR fit
y = 0.50
cToF-AMS sulphate concentration (µg m-3)
HR-ToF-AMS sulphate concentration (µg m-3)
(g)
Linear regression fit
y = 1.00x
r = 0.98
ODR fit
y = 1.02x
HR-ToF-AMS sulphate concentration (µg m-3)

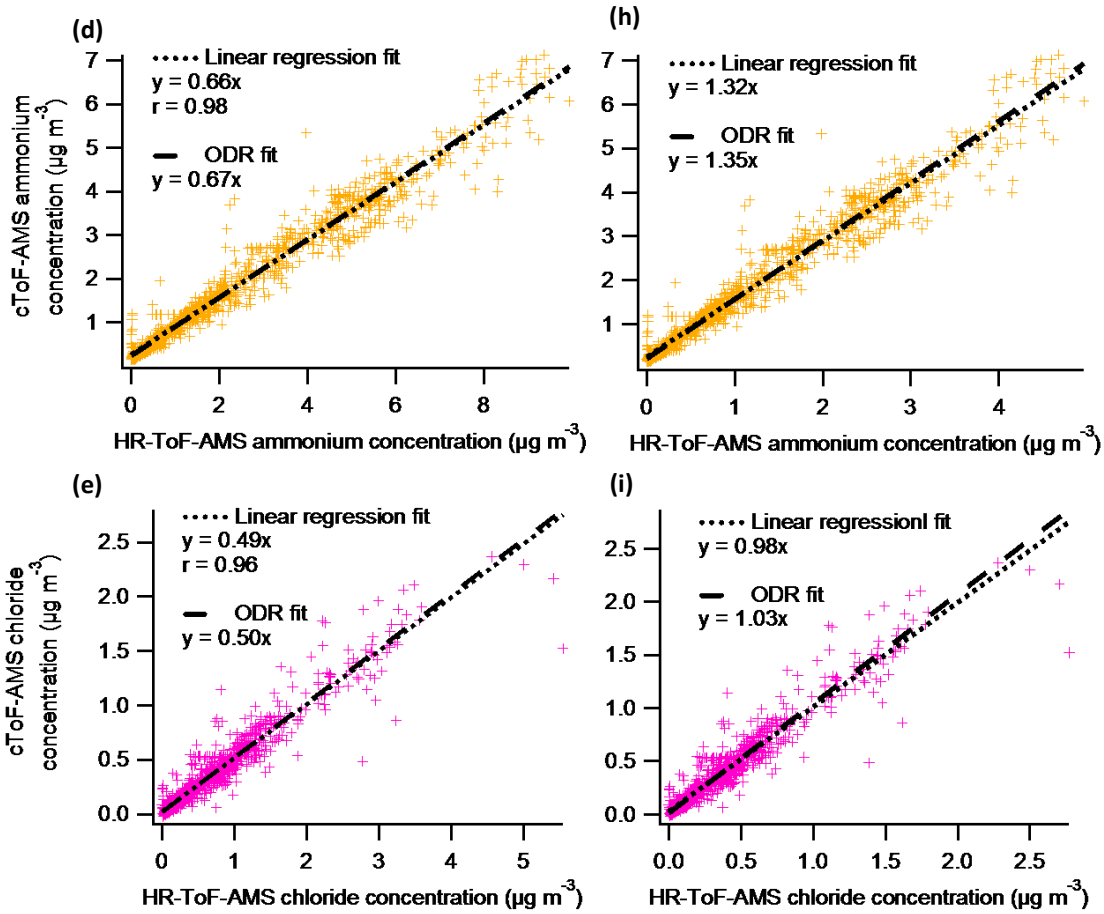

Figure S4. Correlation of the time series of NR-PM_1 species between the cToF-AMS and HR-ToF-AMS for the winter IOP: (a-e) uncorrected concentrations, (f-i) corrected concentrations whereby the concentrations of all HR-ToF-AMS species except nitrate are scaled by 0.5.

2.2 Summer IOP

Sulphate calibrations were performed on the HR-ToF-AMS during the summer IOP, where the resulting concentrations were very similar and compared strongly with those of the cToF-AMS for the same period.

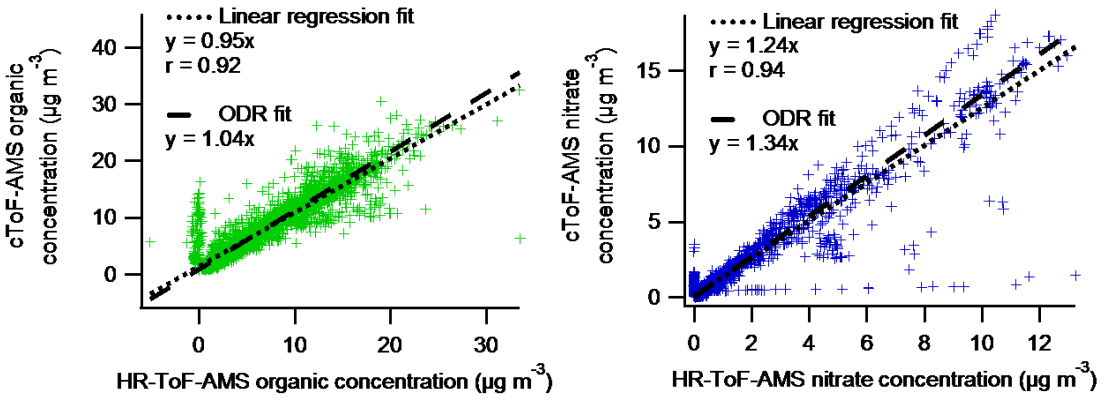

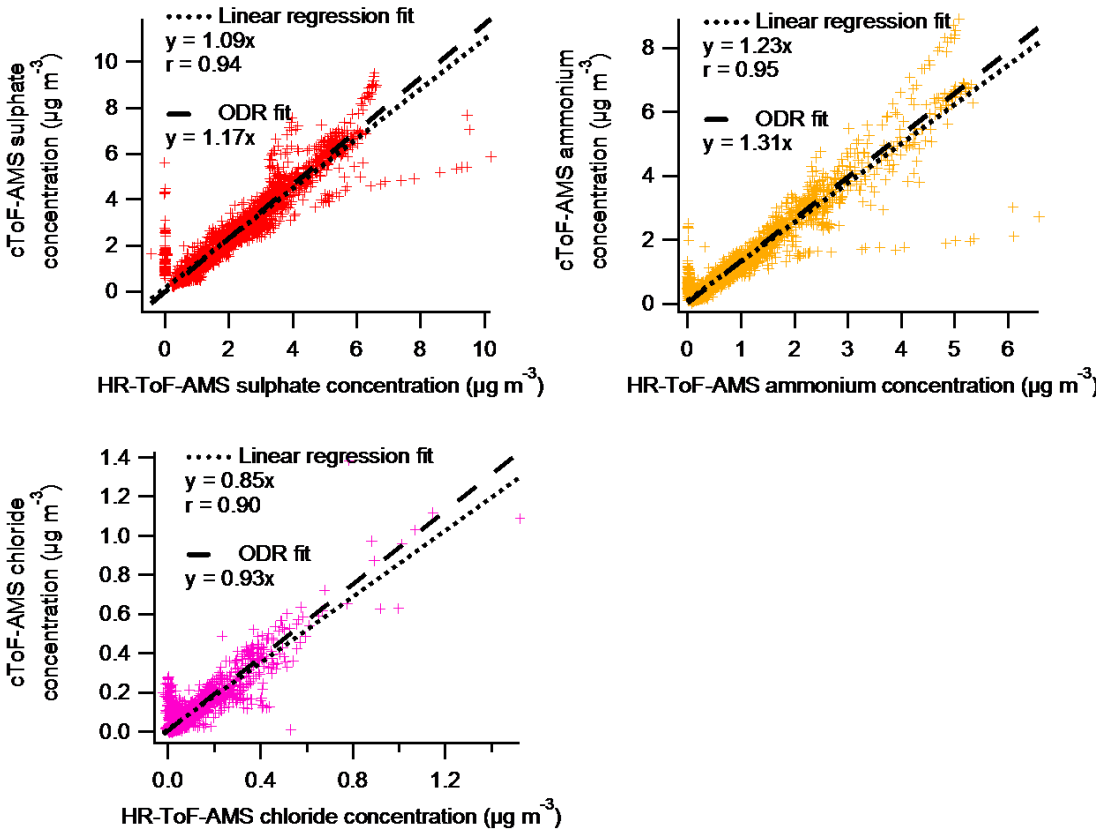

Figure S5. Correlation of the time series of NR-PM_1 species between the cToF-AMS and HR-ToF-AMS for the summer IOP.

3 cToF-AMS NR-PM_1 supplementary

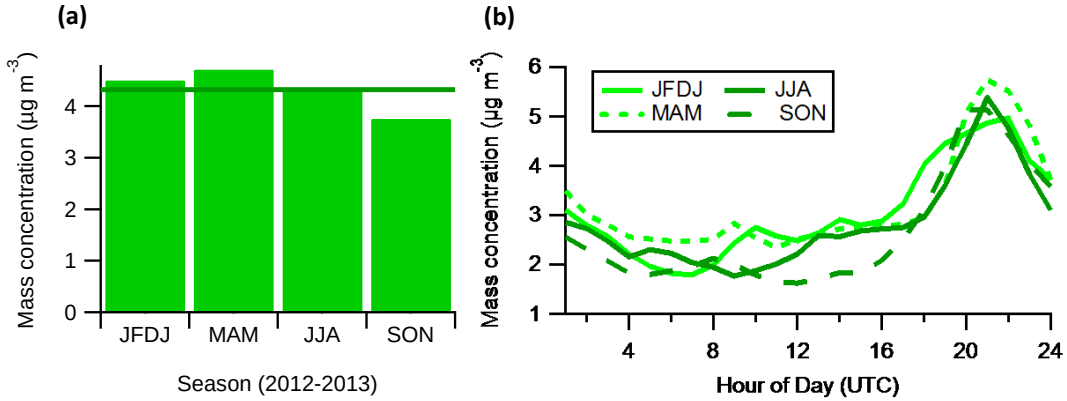

Figure S6. (a) Avearge organic seasonal mass bar chart. Thick line denotes annual average organic mass (b) Median organic diurnal profiles for each of the seasons.

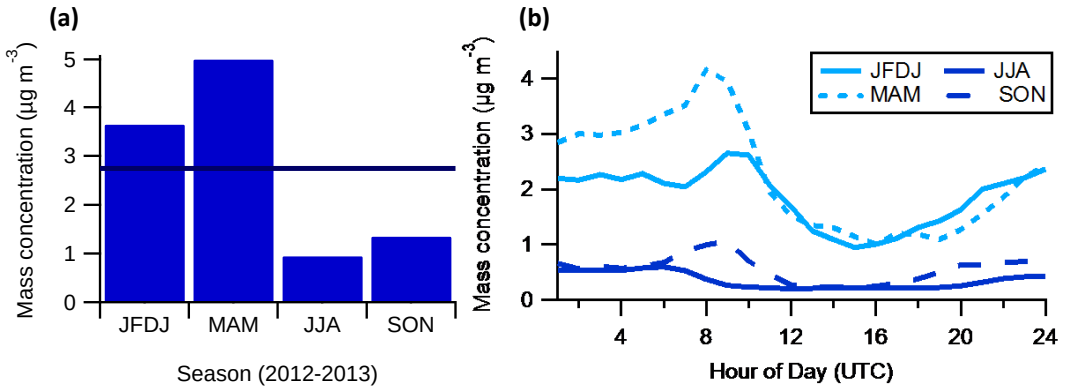

Figure S7. (a) Avearge nitrate seasonal mass bar chart. Thick line denotes annual average nitrate mass. (b) Median nitrate diurnal profiles for each of the seasons.

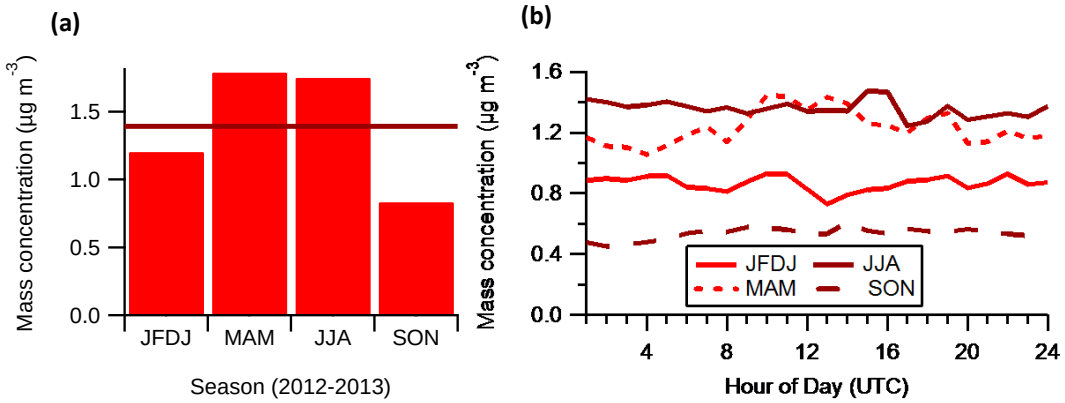

Figure S8. (a) Avearge sulphate seasonal mass bar chart. Thick line denotes annual average sulphate mass. (b) Median sulphate diurnal profiles for each of the seasons.

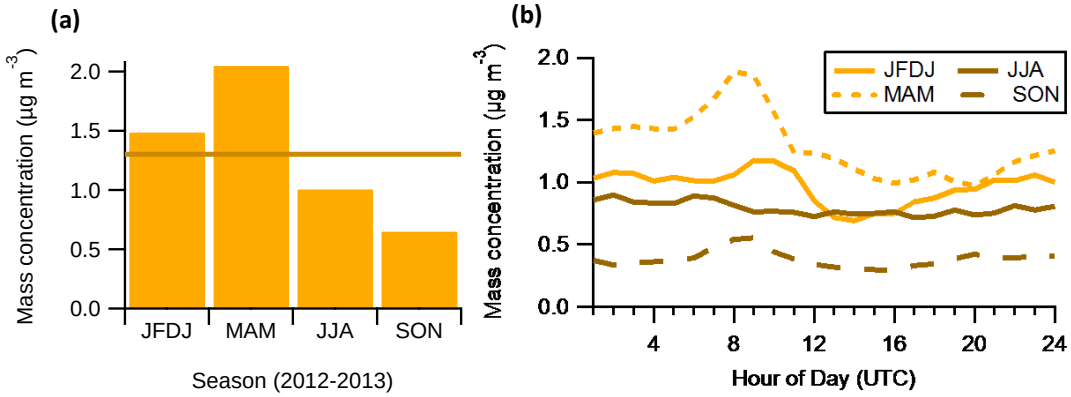

Figure S9. (a) Avearge ammonium seasonal mass bar chart. Thick line denotes annual average ammonium mass. (b) Median ammonium diurnal profiles for each of the seasons.

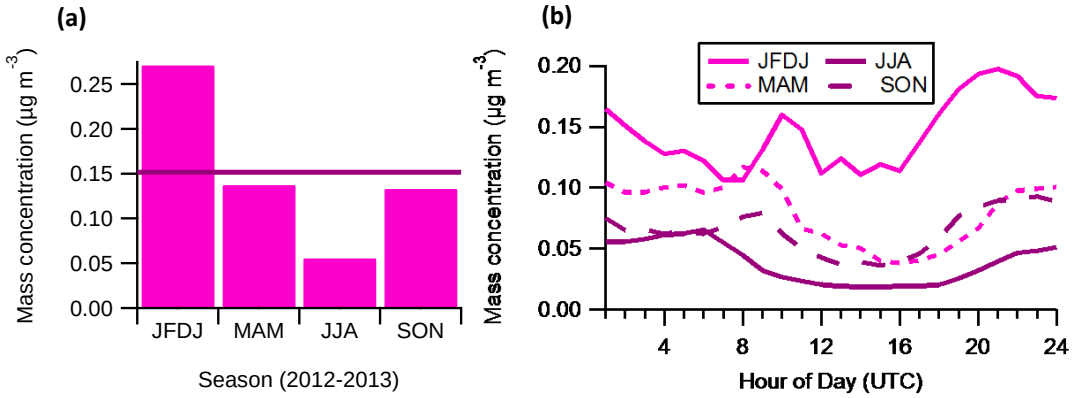

Figure S10. (a) Avearge chloride seasonal mass bar chart. Thick line denotes annual average chloride mass. (b) Median chloride diurnal profiles for each of the seasons.

4 cToF-AMS PMF supplementary

4.1 Data preparation methods

Positive matrix factorisation (PMF) was applied to the organic aerosol data from the cToF-AMS. The data were prepared in the recommended method of practice as described by Ulbrich et al. (2009) and the resulting matrix consisted of m/zs 12-150. Any "bad" ions with a signal to noise ratio less than 0.2 were removed from the data and error matrices before PMF analysis (Ulbrich et al., 2009; Paatero and Hopke, 2003). Ions with a signal to noise ratio of less than 2 were deemed 'weak' and downweighted by a factor of 2. Those peaks related to the CO_2^+ ion (m/z 44) were also downweighted to reduce the signal from duplicated ions.

Several criteria are used to select the appropriate number of factors, as this is the most subjective part of PMF analysis. Firstly, there are diagnostics within the PMF analysis toolkit, which can be used to assess the quality and suitability of a solution set. For example, the mathematical criterion Q determines the quality of fit of the data that is minimised through an iterative least squares fit of the PMF solution for the chosen number of factors. Q is defined as the sum of the weighted residuals divided by the standard deviations of the points in the data matrix. If the value of $Q/Q_{expected}$ is 1 then the model is appropriate and the estimation of the data uncertainties are accurate thus the solution set accounts for the variance associated with random errors. An underestimation of the errors in the data i.e. variance unaccounted for by the solution set, is indicated by values of $Q/Q_{expected}$ greater than 1. However, the solution set that is atmospherically realistic and the solution set with the number of factors resulting in a value of $Q/Q_{expected}$ closest to unity may not be the same. Therefore, the solution is validated with external parameters, both reference mass spectra and other measurement parameters. Furthermore, the fPeak parameter is used to explore ambiguity in the solution due to rotational freedom, a known problem with factor analyses (Paatero et el., 2002). Random initial values, or seeds, can also be used to explore the stability of a solution.

The reference mass spectra used in this discussion are from the AMS spectral database. The individual spectra used are referenced appropriately. Unit mass resolution (UMR) database: Ulbrich, I.M., Lechner, M., and Jimenez, J.L. AMS Spectral Database. URL: http://cires.colorado.edu/jimenez-group/AMSsd/. Details of the databases are described in Ulbrich et al. (2009). Ancillary data used for correlations between PMF factors are from other measurements made during the relevant

measuring campaign from the Manchester group such as the NO_3, SO_4, NH_4 masses. CO and NO_x have been provided by James Lee from the University of York and David Green from Kings College London, respectively. Note that the CO data only covers the period January-August inclusive.

In Section 4.2, the methods used to identify and remove a period of problematic data around the summer IOP are outlined. In Section 4.3, the different cToF-AMS PMF solution sets are explored and the criteria used for choosing the final solution set are discussed. In Section 5, the HR-ToF-AMS PMF analysis is outlined where the different solution sets and criteria for choosing the final solution for the winter IOP and summer IOP are explored in Sections 5.1 and 5.2, respectively. Finally, in Section 6, the mass spectra and time series of the final solutions from the cToF-AMS and the HR-ToF-AMS PMF are compared where possible.

For the year-long cToF-AMS data set, a 5-factor solution was chosen, where the five factors were identified as HOA, COA, SFOA, OOA1, and OOA2.

4.2 Exclusion of data during summer period

PMF was run on the organic matrix from the entire year of data (PMF_{full}). When the time series of the chosen five-factor solution were looked at in detail, a step change in the data was apparent between 20 July and 24 August 2012. This sudden (20-60 minutes including down time) increase in concentration resulted in the masses being approximately an order of magnitude greater than those of the period preceding the step change. This was most evident in the time series of factors 3 (OOA1), 5 (HOA), and possibly factor 4 (SFOA). Diagnostics in the main Squirrel analysis toolkit highlighted a simultaneous step change in the heater bias.

A change in the instrument's tuning was identified as being the cause for these changes. When the AMS was set up in January 2012, it was known that it would continue to be run at least until the end of the summer IOP. The instrument was therefore essentially 'detuned' in order to prolong the life of several components such as the MCP. At the start of the summer IOP the instrument was tuned and these settings were not returned to their original 'detuned' state until a month later (19 August). Furthermore, there were some variations in the concentrations and heater bias between 19 and 24 August, so this period was also questionable. However, these step changes in the data are only evident after PMF is applied whereby the total organic concentrations in this summer period are comparable to if not less than that of other events such as the one in May. This is also the case for org44 and other AMS species.

In order to evaluate the extent to which the data were affected and determine the most suitable PMF run for further analyses, PMF was run on the data set three more times: once with the summer period removed prior to running PMF (PMF_{noSum}), once on the dataset before the summer period (PMF_{before}) and finally once with the data after the summer (PMF_{after}). The same number of factors and the same factor types were identified in all three runs.

4.2.1 Comparison of mass spectral profiles

PMF appears to be sensitive to the data matrix on which it is applied, whereby, for example, there are missing peaks in the mass spectral profiles and very small peaks in places other than the main peaks used to identify the factors (Fig. S11). Factor 2 also contained unusually large peaks at m/z 58 and 94 in the after summer run, where m/z can be associated with amines. However, the time series

of both these peaks are noisy. Factor 2 for this particular PMF run may not actually be the same factor as identified in the other PMF runs (OOA2).

Correlations between the mass spectral profiles from PMF_{full} and the three other runs were performed (Table S2), as were correlations between PMF_{noSum} with PMF_{before} and PMF_{after} (Table S3), and between the factors from PMF_{before} and PMF_{after} (Table S4).

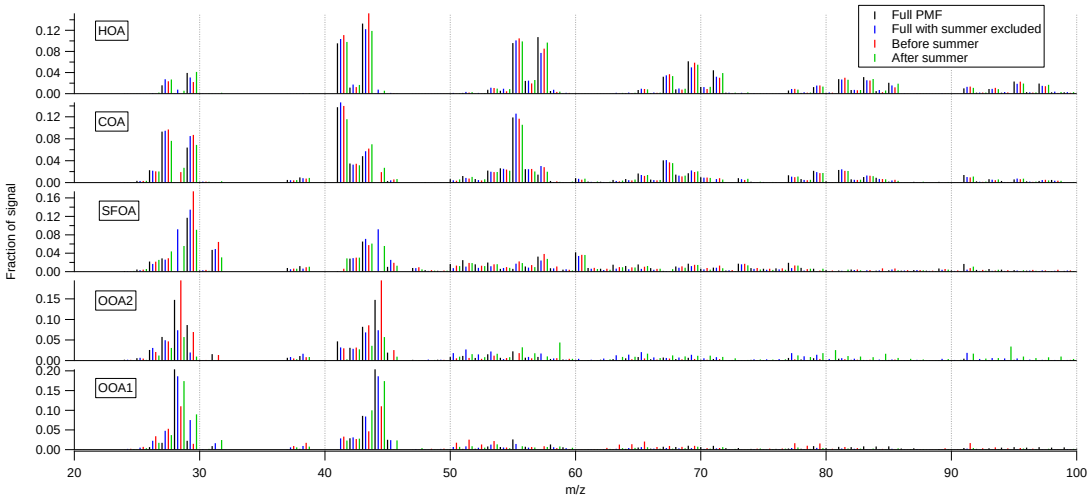

Figure S11. Mass spectra of the different factors for the different PMF runs.

Strong correlations between the mass spectra for the factors from PMF_{full} and PMF_{noSum} were found for most factors (0.72-0.99), with the highest Pearson's r values for comparisons of the COA and HOA factors and the lowest for SFOA. When the factors from PMF_{before} and PMF_{after} were compared, the weakest correlation was for SFOA (0.79). There is possibly some mixing/alternation between the two OOA subcomponents, where stronger correlations are found between OOA2 from one PMF run and OOA1 from another.

		PMF_{noSum}					PMF_{before}					PMF_{after}				
	Factor	**OOA2**	**COA**	**OOA1**	**SFOA**	**HOA**	**OOA2**	**COA**	**OOA1**	**SFOA**	**HOA**	**OOA2**	**COA**	**OOA1**	**SFOA**	**HOA**
PMF_{full}	**OOA2**	0.87	0.39	0.98	0.86	0.36	0.98	0.50	0.91	0.40	0.31	0.71	0.57	0.98	0.84	0.34
	COA	0.38	0.99	0.23	0.29	0.77	0.23	0.98	0.28	0.41	0.72	0.33	0.97	0.22	0.51	0.74
	OOA1	0.73	0.10	0.96	0.72	0.21	0.96	0.22	0.83	0.10	0.17	0.75	0.30	0.95	0.59	0.19
	SFOA	0.42	0.42	0.29	0.72	0.35	0.26	0.43	0.23	0.96	0.34	0.21	0.45	0.35	0.81	0.39
	HOA	0.33	0.73	0.19	0.30	0.98	0.19	0.73	0.16	0.37	0.98	0.30	0.74	0.24	0.43	0.99

Table S2. Comparison of the mass spectra from PMF_{full} with PMF_{noSum}, PMF_{before}, and PMF_{after}. All correlations are with PMF_{full} on the x-axis.

		PMF_{before}					PMF_{after}				
	Factor	**OOA2**	**COA**	**OOA1**	**SFOA**	**HOA**	**OOA2**	**COA**	**OOA1**	**SFOA**	**HOA**
PMF_{noSum}	**OOA2**	0.82	0.45	0.95	0.31	0.37	0.72	0.54	0.81	0.79	0.37
	COA	0.24	0.99	0.26	0.47	0.76	0.31	0.97	0.25	0.54	0.79
	OOA1	1.00	0.37	0.90	0.30	0.21	0.72	0.44	0.99	0.76	0.24
	SFOA	0.81	0.43	0.65	0.75	0.27	0.56	0.48	0.87	0.92	0.33
	HOA	0.25	0.81	0.23	0.35	0.99	0.37	0.83	0.29	0.46	0.99

Table S3. Comparison of the mass spectra from PMF_{noSum} with PMF_{before} and PMF_{after}. All correlations are with PMF_{noSum} on the x-axis.

		PMF_{after}				
	Factor	**OOA2**	**COA**	**OOA1**	**SFOA**	**HOA**
PMF_{before}	**OOA2**	0.73	0.43	0.99	0.74	0.23
	COA	0.39	0.99	0.37	0.61	0.79
	OOA1	0.73	0.44	0.87	0.71	0.21
	SFOA	0.17	0.48	0.36	0.79	0.39
	HOA	0.25	0.78	0.32	0.42	0.98

Table S4. Comparison of the mass spectra from PMF_{before} and PMF_{after}.

4.2.2 Comparison of time series

It was only possible to compare the time series from PMF_{full} with the other three runs (Table S5) and PMF_{noSum} with PMF_{before} and PMF_{after} (Table S6). As for the mass spectral profiles, the strong COA and HOA correlations and possible mixing of the OOA subtypes also holds true when comparing PMF_{full} with the three additional PMF runs and when PMF_{noSum} is compared to PMF_{before} and PMF_{after}. The correlations of the OOA1 and OOA2 time series are the weakest in all comparisons of the PMF runs. In all comparisons, the correlations of HOA, COA, and SFOA are very strong (0.95-1.00). Reducing the number of factors derived from PMF to 4, so that there is only a single OOA factor, does not resolve this issue as HOA and SFOA are still affected by the changes in instrument tuning.

A high-resolution ToF AMS was running during the summer IOP between 19 July and 19 August at the same site as the cToF-AMS although they were approximately 30m apart. As expected for the summer, an SFOA factor was not derived from the PMF run on this data set (see Section 5.2), so a correction factor could not be calculated using these outputs. The HR-ToF-AMS also operated within the period of changes in tuning of the cToF-AMS so there was no crossover period of HR-ToF-AMS measurements and unaffected cToF-AMS measurements. Furthermore, comparison of the time series of the two OOA subtypes from the cToF-AMS and the HR-ToF-AMS highlighted the rotation occurring within the SOA, especially at the beginning of the summer IOP (23-26 July). The mass is distributed between the two subtypes differently depending on the instrument. A correction factor would have to be time dependent and for particular events, which is unlikely to be reliable.

In summary, although the factor types did not change when PMF was applied to the different time periods from the cToF-AMS there is no obvious way to quantify the change in masses identified during the summer in order to apply a correction factor. If the data were used in further analyses, it would create an artefact in the way of an instrument factor rather than an ambient factor. PMF_{noSum} was therefore chosen to be the most suitable solution for further analyses where the OOA subtypes would be explored.

		PMF_{noSum}					PMF_{before}					PMF_{after}				
	Factor	**OOA2**	**COA**	**OOA1**	**SFOA**	**HOA**	**OOA2**	**COA**	**OOA1**	**SFOA**	**HOA**	**OOA2**	**COA**	**OOA1**	**SFOA**	**HOA**
PMF_{full}	**OOA2**	0.60		0.94			0.96		0.69			0.51		0.92		
	COA		0.96					0.96					0.99			
	OOA1	0.51		0.74			0.92		0.47			0.83		0.76		
	SFOA				0.97					0.95					0.99	
	HOA					0.99					1.00					1.00

Table S5. Comparison of the relevant time periods between PMF_{full} with those from PMF_{noSum}, PMF_{before}, and PMF_{after}. All correlations are with PMF_{full} on the x-axis.

		PMF_{before}					PMF_{after}				
	Factor	**OOA2**	**COA**	**OOA1**	**SFOA**	**HOA**	**OOA2**	**COA**	**OOA1**	**SFOA**	**HOA**
PMF_{noSum}	**OOA2**	0.45		0.98			0.82		0.60		
	COA		0.99					0.99			
	OOA1	0.99		0.52			0.34		0.94		
	SFOA				0.99					0.97	
	HOA					1.00					1.00

Table S6. Comparison of the relevant time periods between PMF_{noSum} with those from PMF_{before} and PMF_{after}. All correlations are with PMF_{noSum} on the x-axis.

4.3 Choosing the cToF-PMF solution set

PMF was run in the typical exploration mode, running from 4 to 7 factors and fPeaks -1 to +1 in 0.5 increments. A run of initialisation seeds 0-20 for the different factor solutions was also performed.

4.3.1 4-factor solution

Although the 4-factor solution gives a reasonable solution with a Q/Q_{exp} of 1.44208, factor 3 exhibits peaks at m/z 55 and m/z 60 (Fig. S12), which are typical marker peaks for two different sources. fPeak values between -1 and 0.5 produced solutions that could be considered valid.

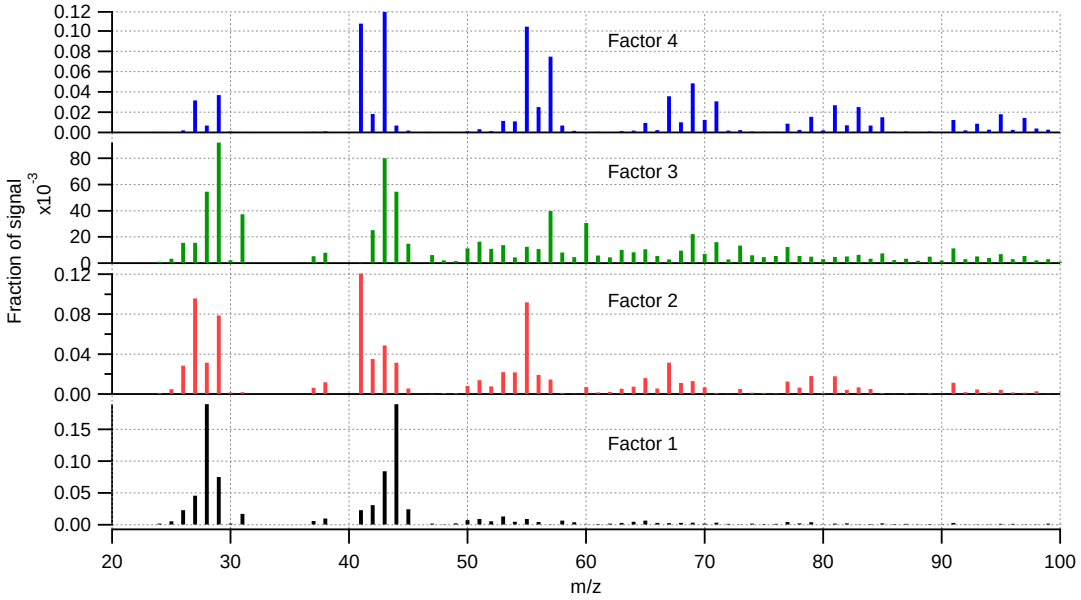

Figure S12. Mass spectra of the 4-factor solution.

4.3.2 5-factor solution

The mass spectra for the 5-factor solution (Fig. S13) are better separated compared to the 4-factor solution and the solution has a Q/Q_{exp} of 1.35003. Factor 3 from the 4-factor solution is separated in to the two different sources in the 5-factor solution. For an fPeak of 0, there is no dependence on the initialisation seed (Fig. S14).

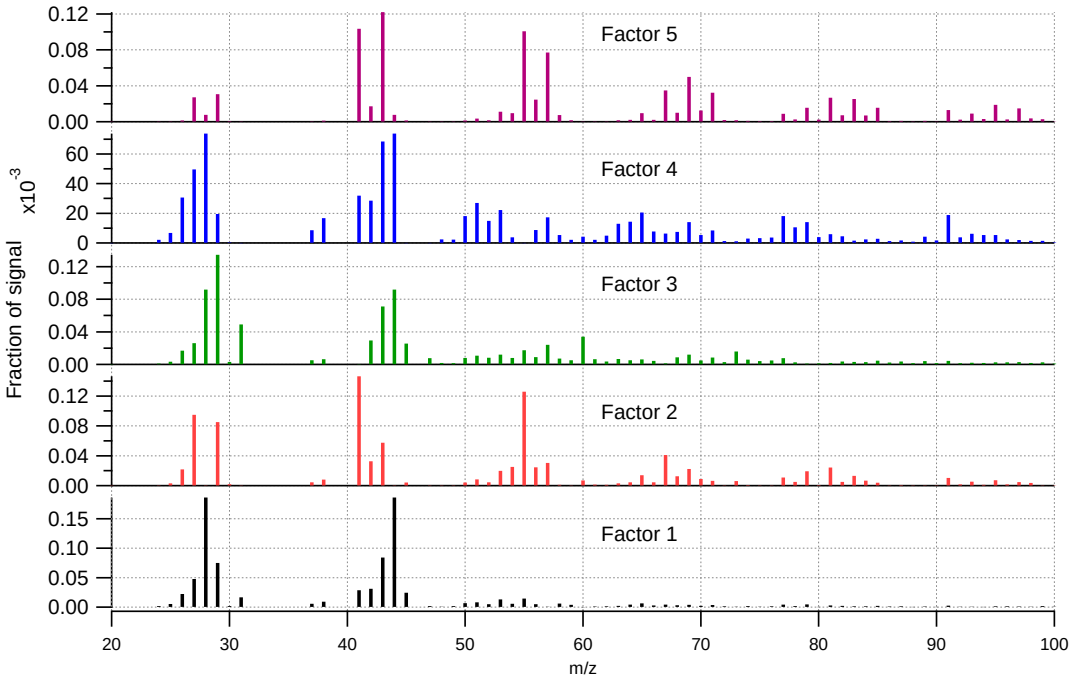

Figure S13. Mass spectra from the 5-factor solution.

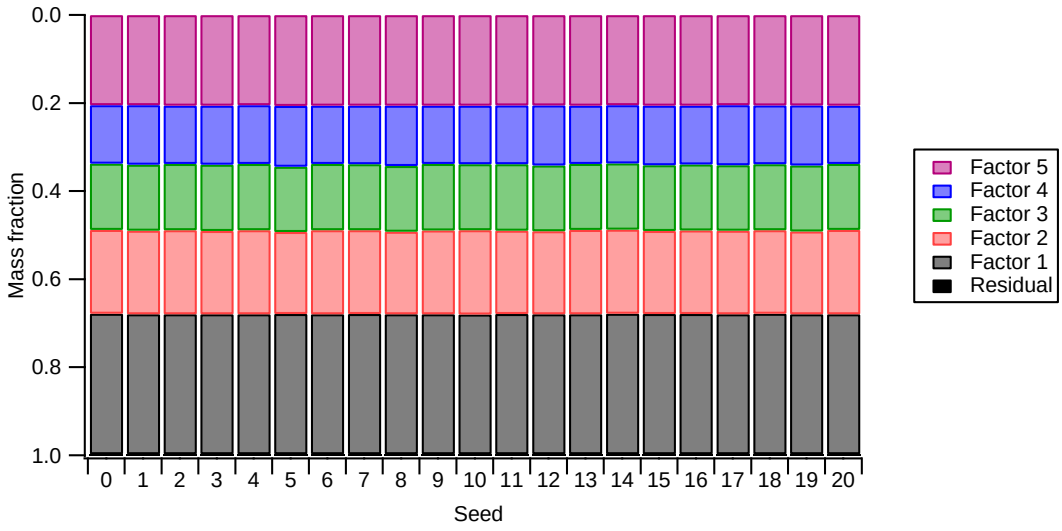

Figure S14. Variance of the factors as a function of seed from the 5-factor solution.

4.3.3 6-factor solution

Moving to the 6-factor solution, the Q/Q_{exp} decreased to 1.1433, however, the mass spectra for factors 2, 3, and 5 are similar (Fig. S15). Factors 3 and 5 exhibit alkane related peaks (e.g. at m/zs 41, 43, 55) but also additional peaks at m/zs 50, 51, 53 and 91. The time series of most of the factors co-vary in many places throughout the measurement period (sample time series shown in Fig. S16). The diurnal profiles of many of the factors are very similar, with a large peak at 21:00. This suggests that there is some mixing of the factors occurring. Furthermore, there is a little dependence on seed whereby one seed did not converge (Fig. S17). Only two fPeak values produced solutions that could be considered valid.

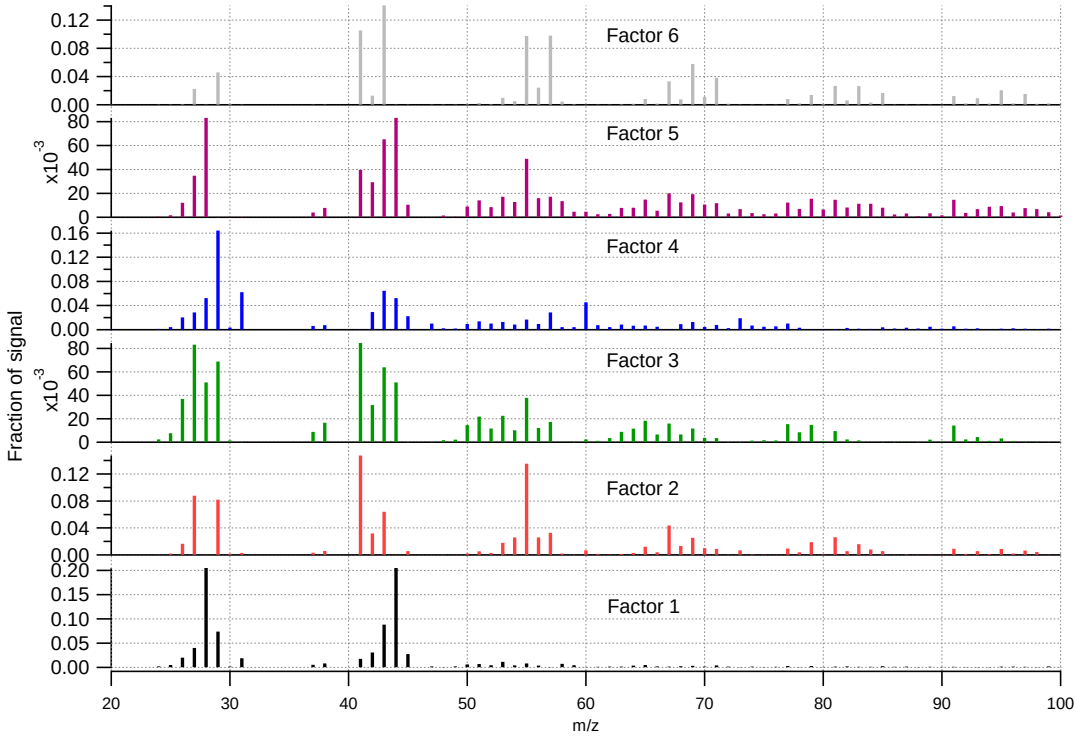

Figure S15. Mass spectra from the 6-factor solution.

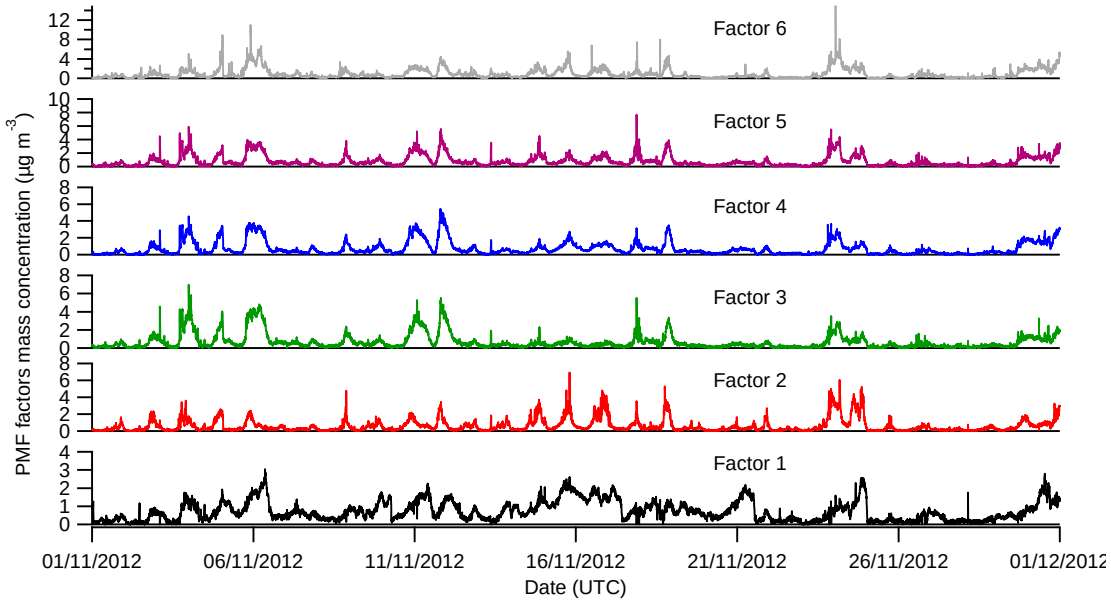

Figure S16. Sample of the time series of the 6-factor solution.

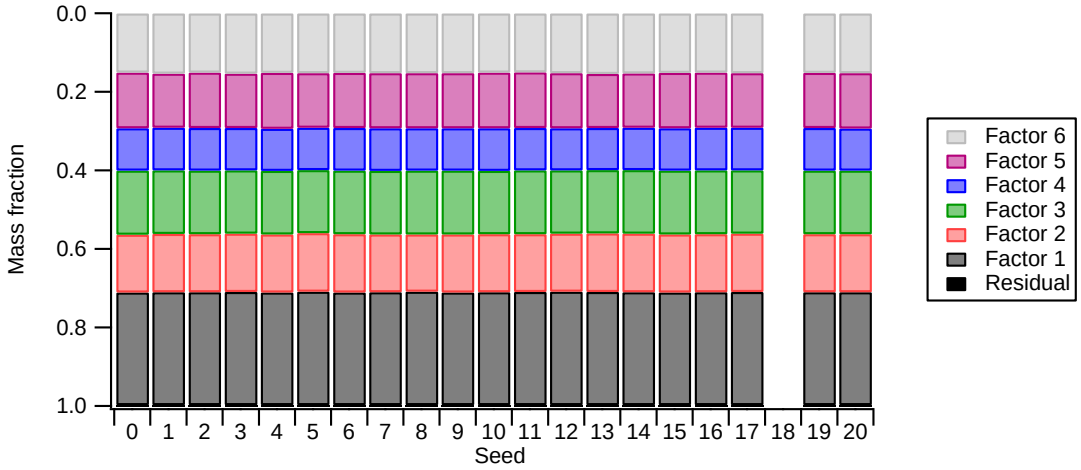

Figure S17. Variance of the factors as a function of seed from the 6-factor solution.

4.3.4 7-factor solution

The factors in this solution are even less clearly separated (Fig. S18), with factor 6 exhibiting a mass spectral profile similar to 3 and 4. Factor 1 mainly consists of peaks at m/z 28 and m/z 44 with little other signal, so is inconsistent with regular ion series. The time series of most of the factors show a similar evolution (Fig. S19), indicative of factor 'splitting'. There is also a great dependence on initialisation seed (Fig. S20) and only the solution from the most central fPeak value converged.

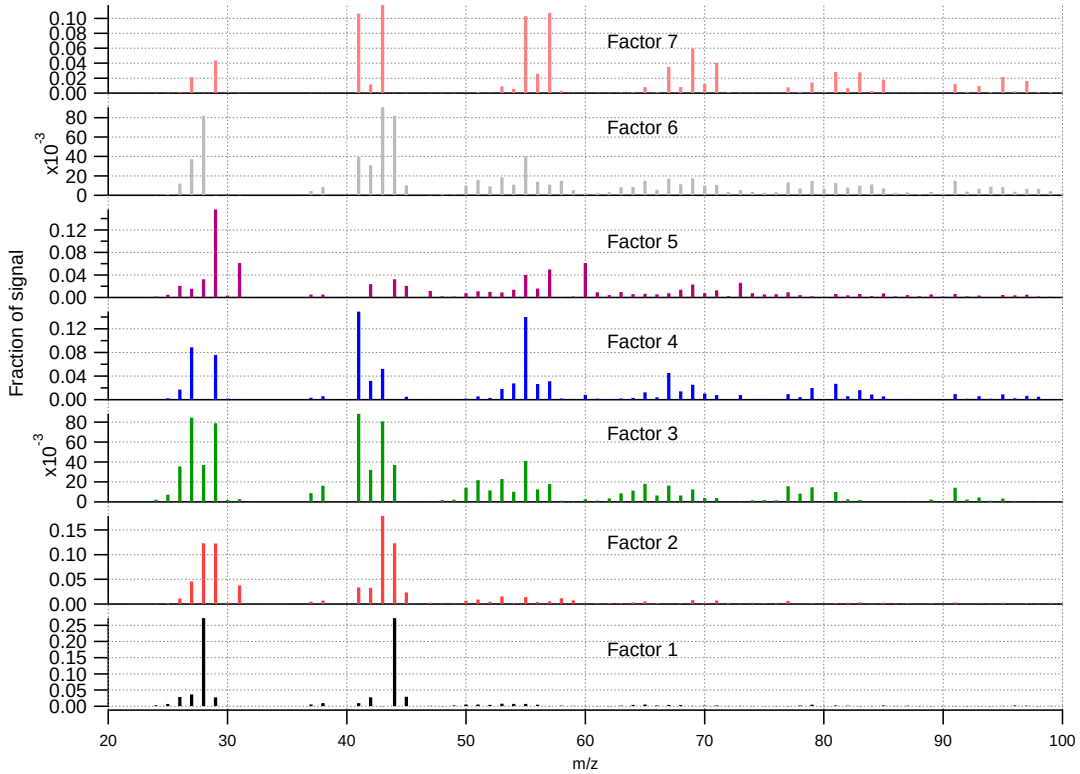

Figure S18. Mass spectra from the 7-factor solution.

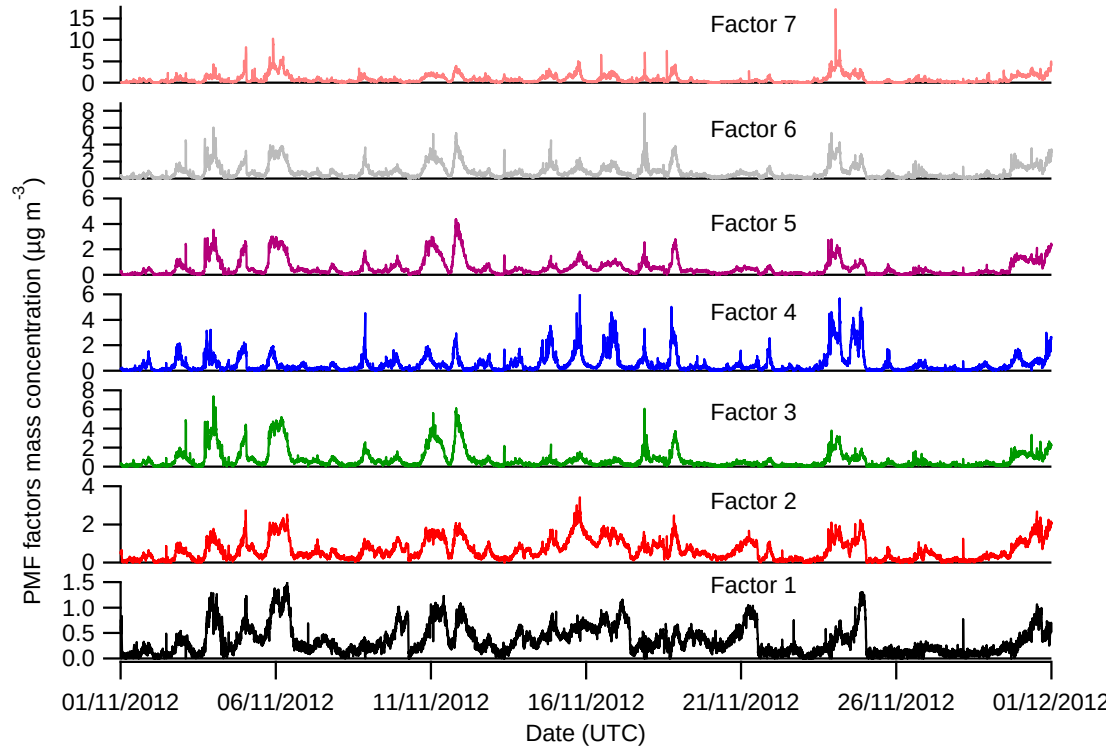

Figure S19. Sample of the time series of the 7-factor solution.

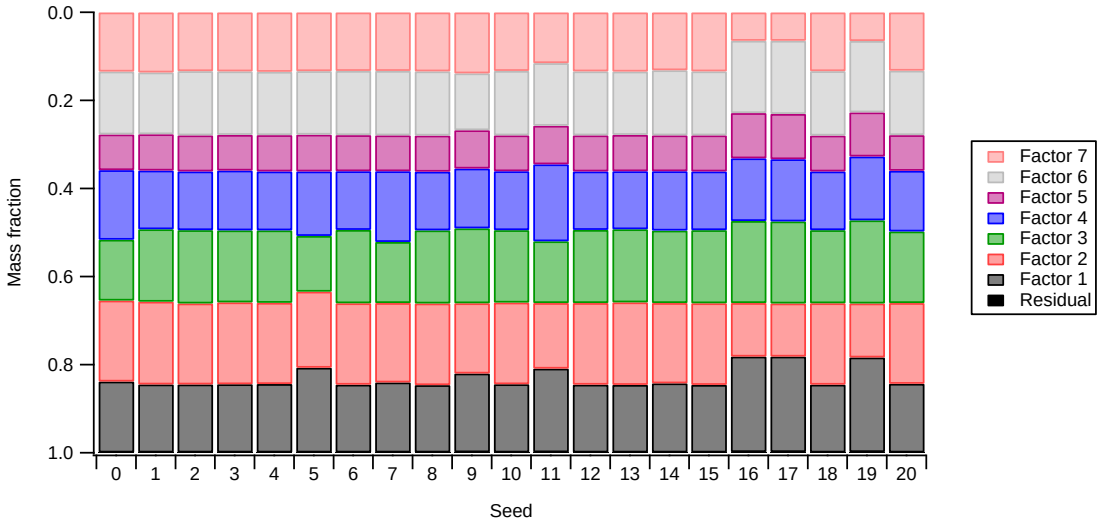

Figure S20. Variance of the factors as a function of seed from the 7-factor solution.

4.3.5 Exploring the chosen solution and identifying the factors

Table S7. Summary of the diagnostics from the different solution sets.

Number of factors (p)	Q/Qexp	fPeak values		Seed dependence?
		Convergent	Non-convergent	
4	1.44208	-1, -0.5, 0, +0.5	+1.0	No
5	1.35003	-0.6 -> +0.2 +0.6 -> +1.0	-3 -> -0.8 +0.4 +1.2 -> +3	No
6	1.26655	-0.5, 0	-1, +0.5, +1	Yes
7	1.20916	0	-1, -0.5, +0.5, +1	Yes

The 5-factor solution was chosen as it best satisfied the selection criteria (Table S7), so was further explored by running PMF with fPeak values ranging from -3 to 3 with increments of 0.2 (Fig. S21), with values between -0.6 and 0.2 as well as 0.6 and 1 producing valid solutions. Solutions from other fPeak values failed to converge.

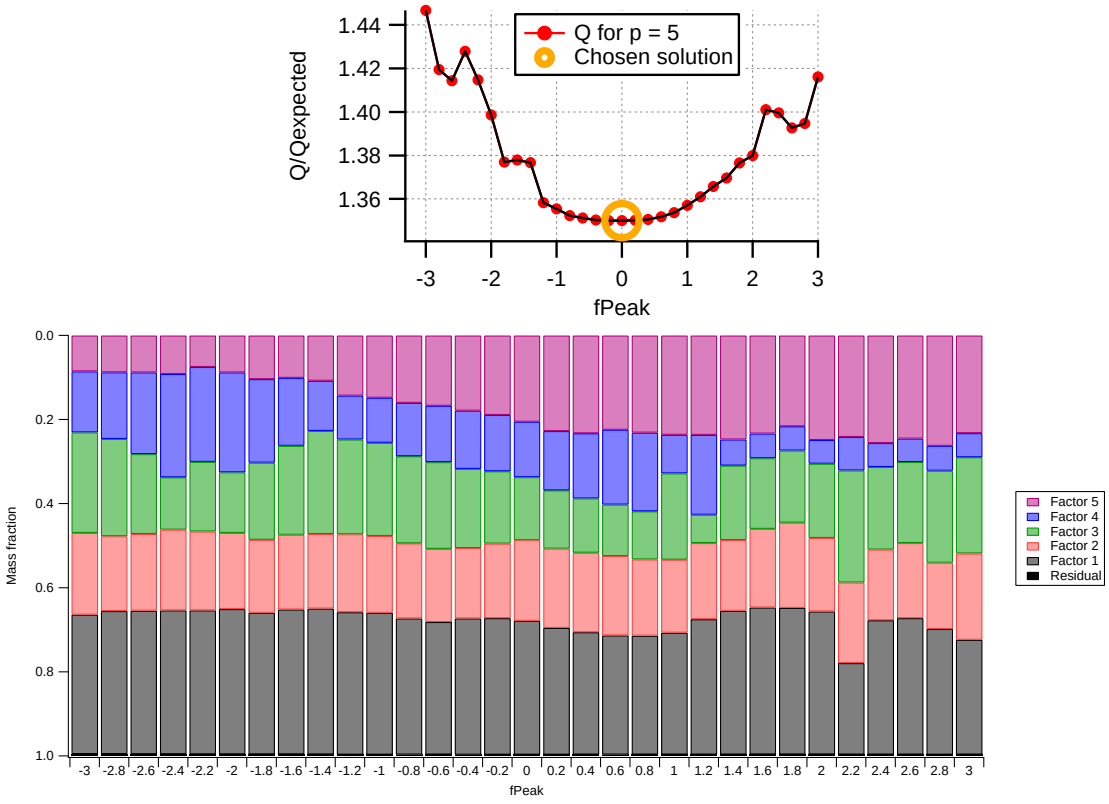

Figure S21. Top: $Q/Q_{expected}$ versus fPeak value. Bottom: Variance of the factors as a function of fPeak from the 5-factor solution.

The solutions from fPeak values -0.6 to 0.2 were investigated to further explore the rotational ambiguity of the 5-factor solution, where any changes in the concentrations of factors could be imply the amount of rotational ambiguity present in solutions (Allan et al., 2010). Here, the

concentrations of factors 3 and 5, in particular, showed some variation in concentration between the different fPeak values (Table S8). However, according to Paatero et al. (2002), the solution for fPeak=0 is most likely to be physically meaningful. Therefore, this solution set is used for further analysis.

Table S8. Average mass concentration of each of the 5 factors for different fPeak values.

	Factor				
fPeak value	Factor 1 mean mass ($\mu g\ m^{-3}$)	Factor 2 mean mass ($\mu g\ m^{-3}$)	Factor 3 mean mass ($\mu g\ m^{-3}$)	Factor 4 mean mass ($\mu g\ m^{-3}$)	Factor 5 mean mass ($\mu g\ m^{-3}$)
-0.6	1.25783	0.71989	0.841235	0.557374	0.691316
0	1.2721	0.792333	0.611022	0.547316	0.845594
+0.2	1.20389	0.778428	0.564659	0.583619	0.937554

Factor 1 and factor 4 are distinct by the ratio of the m/z 44 to m/z 43 peaks, with a greater ratio for factor 1. Factors 2 and 5 were identified and separated through ordering of the peaks at m/z 41, 43, 55 and 57. In particular, the m/z 55 to m/z 57 ratio is much greater for factor 2 than for factor 5. Factor 5 was also identifiable by the peaks at m/z 41 and m/z 43 repeating every 14 mass units. Factor 3 exhibits a large peak at m/z 60, and although smaller m/z60 peaks are present in factors 2 and 4, the largest peak is in factor 3. The factors identified were hydrocarbon-like OA (HOA, factor 5), solid fuel/biomass burning OA (SFOA, factor 3), cooking OA (COA, factor 2), and the type-1 and type-2 oxygenated organic aerosols (OOA1 - factor 1 and OOA2 - factor 4, respectively).

Although there are similarities in some of the time series, it is likely that meteorological conditions and seasonal differences will result in these similarities, especially across the primary factors in the winter. For validation and increased confidence in the factorisation, the mass spectra were compared with external mass spectral profiles (Table S9) as well as the HR-ToF-AMS profiles from the winter and summer IOPs (Section 5).

Table S9. Pearson's r correlation coefficients for comparison of the PMF factor mass spectra with reference spectra.

HOA	COA	SFOA	OOA2	OOA1
0.98	**0.86**	**0.81**	**0.83**	**0.87**
HOA	COA	BBOA	SV-OOA	LV-OOA
Reference MS	Barcelona	Reference MS	Reference MS	Reference MS
Ng et al., 2011	Mohr et al., 2012	Ng et al., 2011	Ng et al., 2011	Ng et al., 2011
0.98	**0.98**	**0.73**	**0.70**	**0.87**
HOA	COA	SFOA	OOA	OOA
Repartee 1	Repartee 1	Repartee 2	Reference MS	Reference MS
Allan et al., 2010	Allan et al., 2010	Allan et al., 2010	Ng et al., 2011	Ng et al., 2011
0.97	**0.96**	**0.94**	**0.75**	**0.98**
HOA	COA	OOA2-BBOA	OOA	OOA
Repartee 2	Repartee2	Paris	Repartee 1	Repartee 1
Allan et al., 2010	Allan et al., 2010	Crippa et al., 2013	Allan et al., 2010	Allan et al., 2010
			0.74	**0.97**
			OOA	OOA
			Repartee 2	Repartee 2
			Allan et al., 2010	Allan et al., 2010
			0.81	
			OOA2-BBOA	
			Paris	
			Crippa et al., 2013	

Furthermore, time series of additional measurements were used to validate the factors from the 5-factor solution (Fig. S22). As HOA has been found to bear a strong relationship with combustion tracers because they are emitted from car exhausts, this factor was correlated with CO and NO_x, yielding Pearson's r values of 0.66 and 0.79, respectively. The organic mass fragment at m/z 55 has been found to be an important mass fragment of COA (Lanz et al., 2007; Mohr et al., 2009; Allan et al., 2010) and is shown by the similarity of the time series of COA and org55 (0.82). SFOA correlates with org60 (0.95), a mass fragment associated with wood burning emissions (Alfarra et al 2007) and is frequently used as a tracer for SFOA/BBOA (Mohr et al., 2012; Dall'Osto et al., 2013; Crippa et al., 2013). Org60 is also associated with fatty acids from cooking POA (Mohr et al., 2009), so COA correlates relatively strongly with org60 (0.76). Relatively high correlations are shown between OOA1 and particulate sulphate and ammonium (0.71 and 0.70, respectively), similar to other urban locations (e.g. Lanz et al., 2007; Mohr et al., 2012). In contrast, OOA2 correlates only weekly with nitrate (0.28).

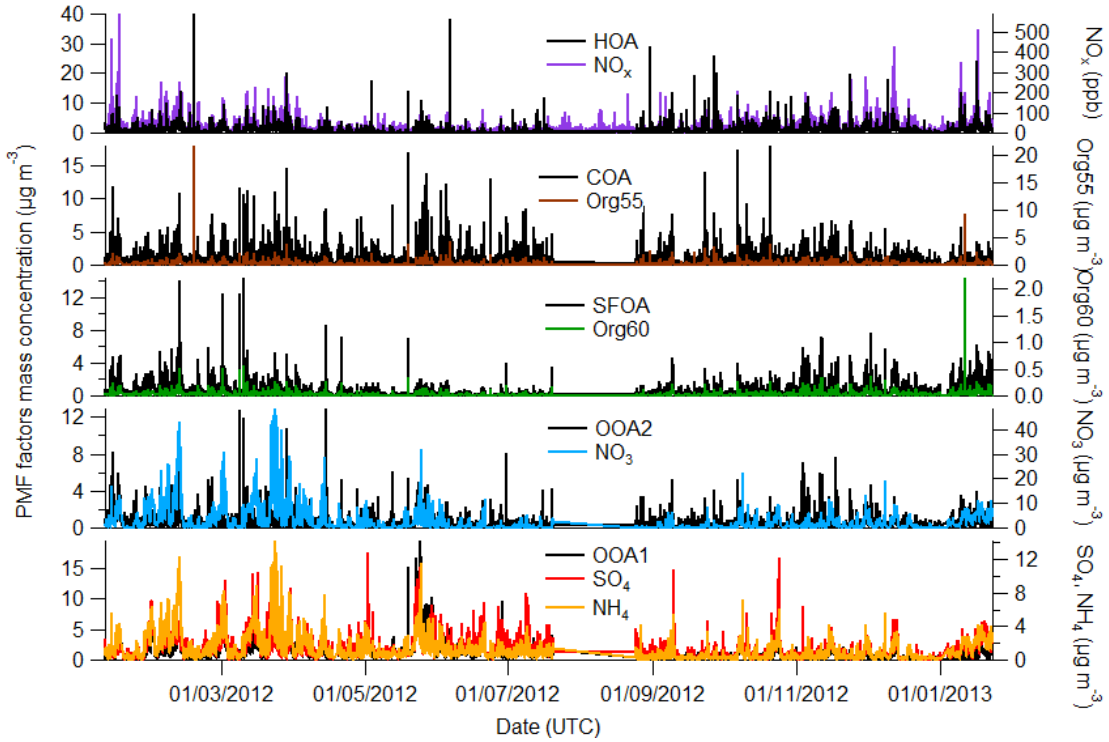

Figure S22. Time series of the 5-factor solution and ancillary data.

5 HR-ToF-AMS PMF supplementary

PMF analysis was performed on the organic data matrix from the HR-ToF-AMS from the winter and summer IOPs, where the data were pre-processed in the same way as outlined in Section 4.1.In addition, isotopes were not included in the organic matrices of the winter and summer data sets. Furthermore, the peaks at m/z 30 and 46 were removed from the organic matrices as they were not deemed to have been successfully retrieved using PIKA. The resulting matrix consisted of m/zs 12 – 115.12. APES light v1.05 (Sueper, 2008) was used for the elemental analysis of the HR-PMF factors.

The reference mass spectra used in this discussion are from the AMS spectral database. The individual spectra used are referenced appropriately. High-Resolution AMS Spectral Database. URL: http://cires.colorado.edu/jimenez-group/HRAMSsd/. Details of the databases are described in Ulbrich et al., ACP, 9, 2891-2918, 2009.

5.1 Winter IOP

5.1.1 4-factor solution

Each of the mass spectra show good separation with factor 1 being the only profile with a large peak at m/z 44 (Fig. S23). Factor 2 shows the largest peaks at m/z 60 and 73 compared to factors 1 and 2. Factors 3 and 4 can be differentiated by ordering the magnitudes of the peaks at m/z 41, 43, and 55. These factors can also be distinguished by comparing the m/z 55 to 57 ratio whereby factor 3 yields a ratio of 2.06 compared to 0.99 from factor 4. Although there are a few similarities between the

time series (Fig. S24), particularly of factors 2 and 3, real meteorological phenomena are likely influencing the mass concentrations of the aerosols emitted. The diurnal profiles (Fig. S25) exhibit unique features, such as factor 4, which has two main peaks in concentration: one at 10:00 and a broader peak in the evening with a maximum at 20:00. There was also no dependence on initialisation seed when the 4-factor solution was explored by running PMF with 50 initialisation seeds for an fPeak of 0.

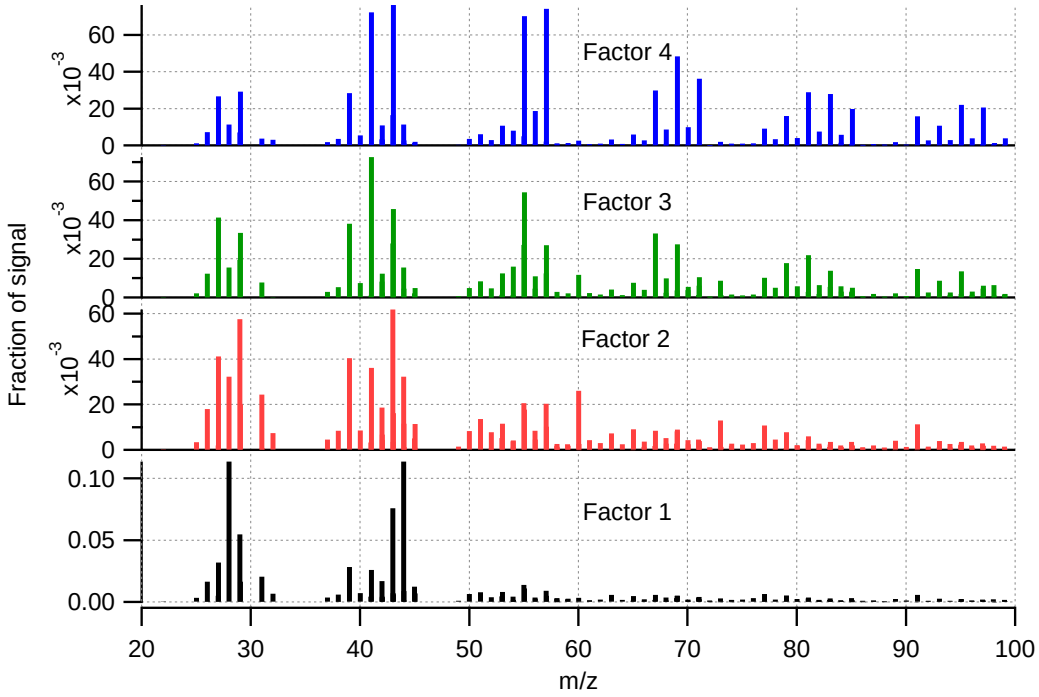

Figure S23. Mass spectra of the 4-factor solution. Note that the bars are not stacked.

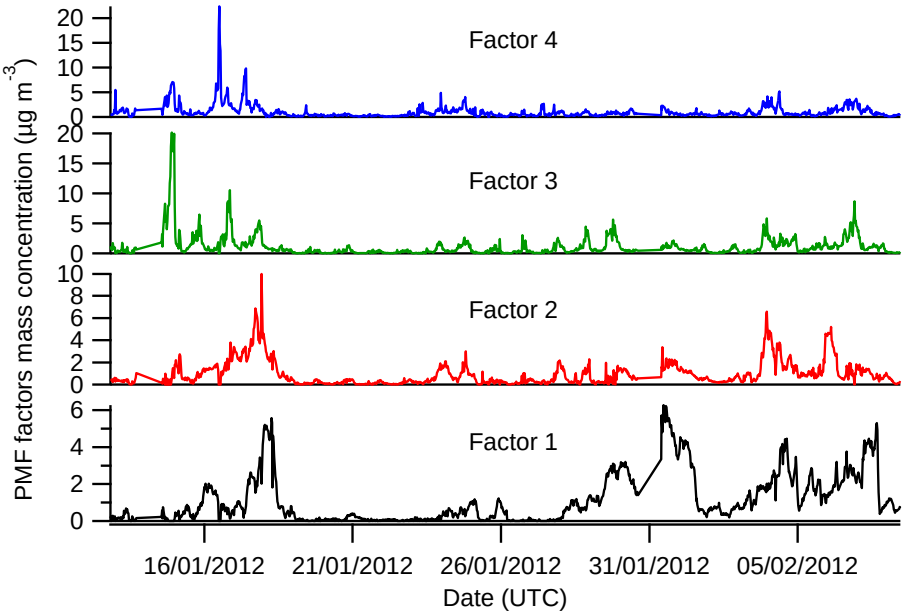

Figure S24. Time series of the factors from the 4-factor PMF solution.

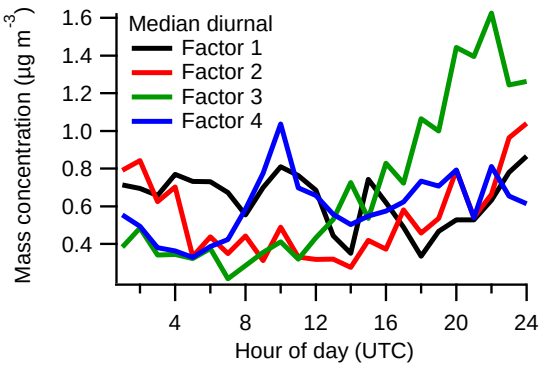

Figure S25. Median diurnal profiles of the four factors.

5.1.2 5-factor solution

Moving from the 4-factor solution to the 5-factor solution resulted in a decrease in Q/Q_{exp} to 4.375 from 4.7764. Factors 3 and 4 were found to have almost identical unit mass spectra with very similar ratios of marker m/zs such as 55/57 and 44/43, as well as similar composition (Fig. S26). However, there were some very subtle differences at m/zs 27, 29, and 41. There are also some similarities between the time series of several of the factors, particularly with factors 2 and 3 (Fig. S27). However, there are still a few differences in their time series, such as between the 4 and 6 February. It is therefore likely that factors 2 and 3 are actually a split factor, with particular events being split across the two factors.

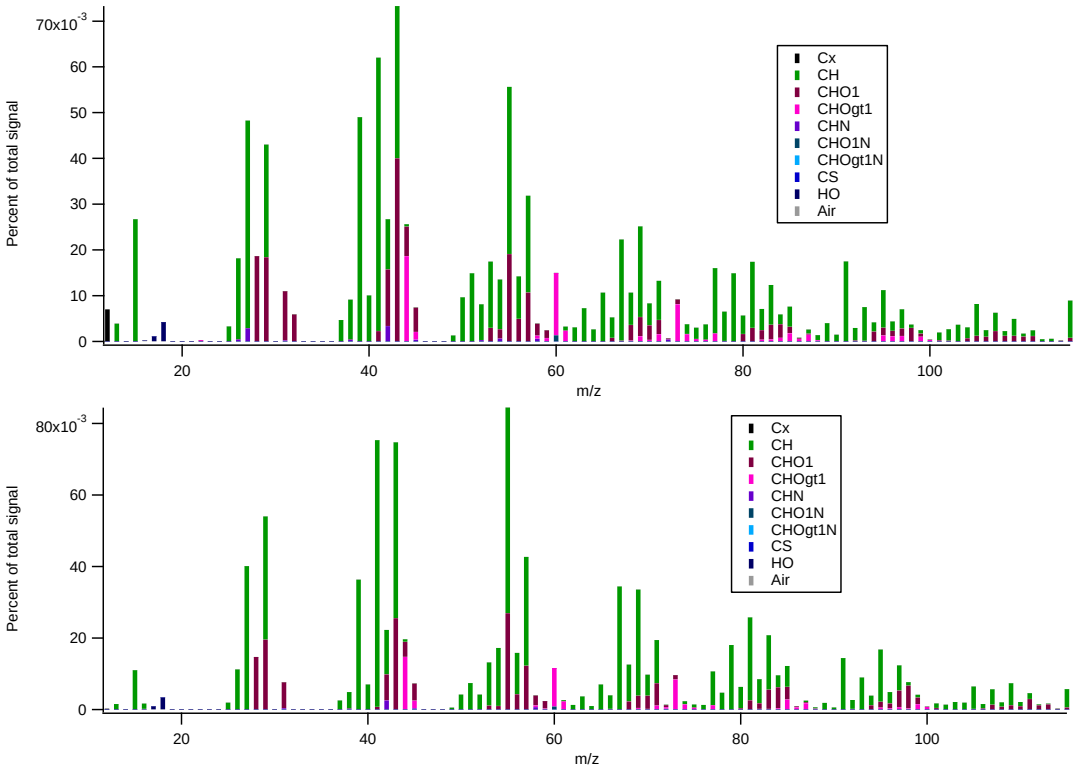

Figure S26. Mass spectra of factors 3 (top) and 4 (bottom) and their composition.

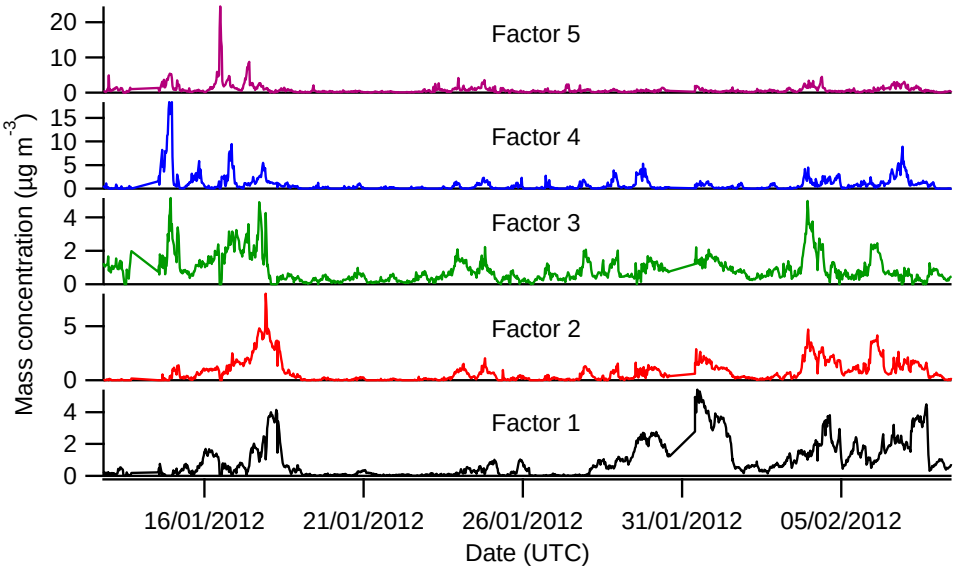

Figure S27. Time series of the factors from the 5-factor PMF solution.

This solution was explored further by running PMF with 50 seeds and it was found that there were some variations, where 2-3 different solutions were produced (Fig. S28). However, the fraction of each factor to the total does not vary significantly with seed whereby the standard deviation for each factor does not exceed 0.3% when seed 13 is excluded (Table S10).

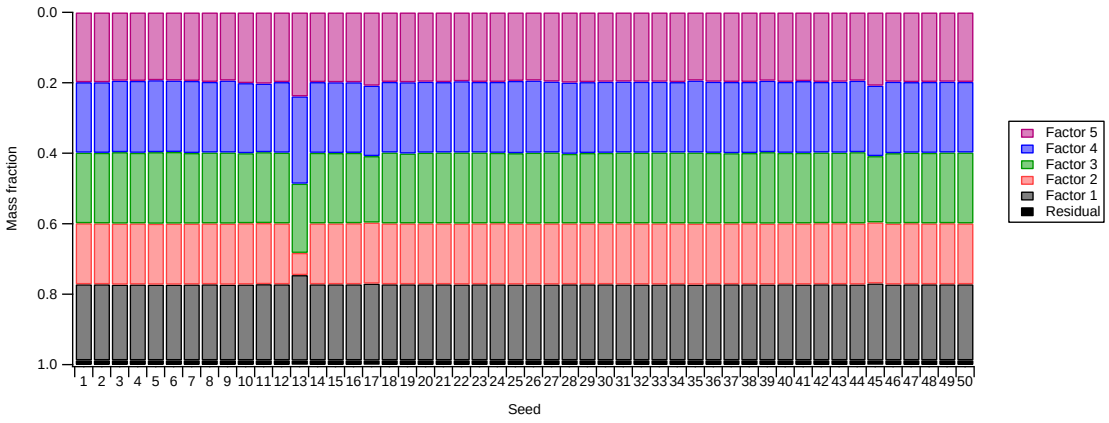

Figure. S28. Fraction of mass of each factor with change in initialisation value (seed).

Table S10. Standard deviation and percentage change of the fraction of each factor to the total mass.

	Standard deviation	%
Factor 1	0.00061147	0.061147
Factor 2	0.0001357	0.01357
Factor 3	0.00273873	0.273873
Factor 4	0.00185065	0.185065
Factor 5	0.00303816	0.303816

5.1.3 6-factor solution

The introduction of a new factor decreased Q/Q_{exp} to 4.1248 however, the solution set did not converge at fPeak=0. The lowest Q/Q_{exp} was obtained with an fPeak=-0.5, which resulted in the profiles in Fig. S29, where factor 1 consists mainly of a signal at m/z 32 and results in a noisy time series (Fig. S30) and the other mass spectra and times series appear very similar to the 5-factor solution.

There was also a significant dependence on the initialisation seed used, which produced two general types of solution, of which only one converged. Due to this considerable dependency on seed and unrealistic factor, this solution set was discarded.

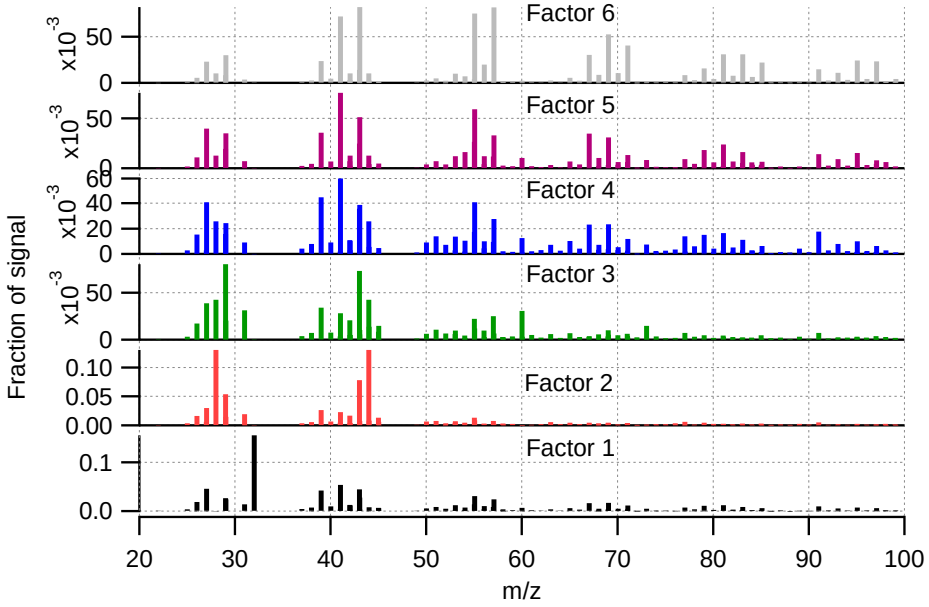

Figure S29. Mass spectra of the 6-factor solution. Note that the bars are not stacked.

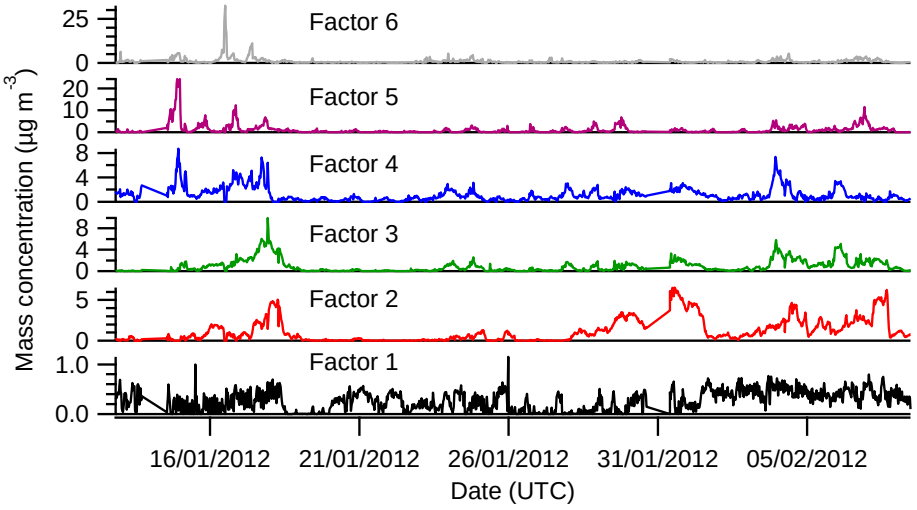

Figure S30. Time series of the 6-factor solution.

5.1.4 Exploring the 4 and 5-factor solutions

The factors for the 4-factor solution are identified as OOA, SFOA, COA, and HOA. The interpretation of each of the factor sources is supported by the comparison of both reference mass spectra and time series from other independent measurements taken at the North Kensington site.

For the mass spectra, factor 1 compares with the LV-OOA and SV-OOA reference spectra from Mohr et al. (2012) with Pearson's r values of 0.95 and 0.85, respectively, and also with the unit mass OOA from Ng et al. (2011) with an r of 0.82. The time series of this factor correlates with ambient HR-ToF-AMS data such as nitrate, sulphate, and ammonium with Pearson's r of 0.87, 0.85, and 0.91, respectively, which is consistent with other urban locations (Lanz et al., 2007; Crippa et al., 2013).

Comparison of factor 2 with the standard BBOA spectrum from Ng et al. (2011) yields a Pearson's r value of 0.96. The peaks at m/z 60 and 73 are smaller than those at m/z 29, 43, and 44 in factor 2. However, as peaks at m/z 29, 43, and 44 are found in most PMF mass spectra they cannot be used as a tracer for SFOA (Alfarra et al., 2007). Nevertheless, the correlation between the time series of SFOA and org60 yields a Pearson's r of 0.86. The mass increases from approximately 15:00 and peaks overnight, decreasing to the average daytime mass at 5:00. The greater mass at night compared to during the day is expected from evening activities in the house, where space heating is used during the winter months.

Factor 3 shows a strong correlation with the COA spectral profiles from Mohr et al (2012), with a Pearson's r of 0.88. Similarly when compared to ancillary data, factor 3 has a strong relationship with org55 (r=0.85). A large evening peak is observed in the diurnal cycle, which starts to increase from about 12:00, reaching a peak at 21:00 and rapidly decreasing. The large evening peak is likely associated with local residents cooking meals. In addition, this could be due to the cooking activities from the numerous restaurants on Portebello Road, which is approximately about 350 m from the site. The restaurants are likely to open for lunchtime, which could explain why the increase in mass occurs at this time.

A Pearson's r value of 0.99 is obtained when factor 4 is correlated with the HOA mass spectral profiles from Mohr et al. (2012) and Ng et al. (2011). OA has been found to show bear a strong relationship with combustion tracers because they are emitted from car exhausts, so factor 4 was correlated with the BC equivalent mass from the aethalometer (880 nm), CO, and NO_x and yielded Pearson's r values of 0.68, 0.64, and 0.69, respectively. However, the strongest correlation was found when the time series of factor 4 was correlated with org57 (r=0.87). This factor exhibits a diurnal pattern with a large peak at 9:00 and a smaller, broader peak in the evening, which correspond to rush-hour activity.

For the 5-factor solution, the factors were identified as OOA, SFOA1, SFOA2, COA, and HOA. Comparison of the factors with ancillary data (Fig. S31) supports the attribution of the factors, with Pearson's r values for ammonium, nitrate, and sulphate with respect to OOA of 0.90, 0.86, and 0.86, respectively. There is a strong correlation between the time series of COA and org55 (r=0.83). org57 has also been found to be a tracer for HOA (Zhang et al., 2005) and is found to strongly correlate with the time series of HOA (r=0.81). Factors 2 and 3 correlate with org60 (r=0.85 and 0.79 respectively). Furthermore, the time series of the factors correlated well with black carbon measurements (Liu et al., 2014) and CMB outputs (Yin et al., 2014).

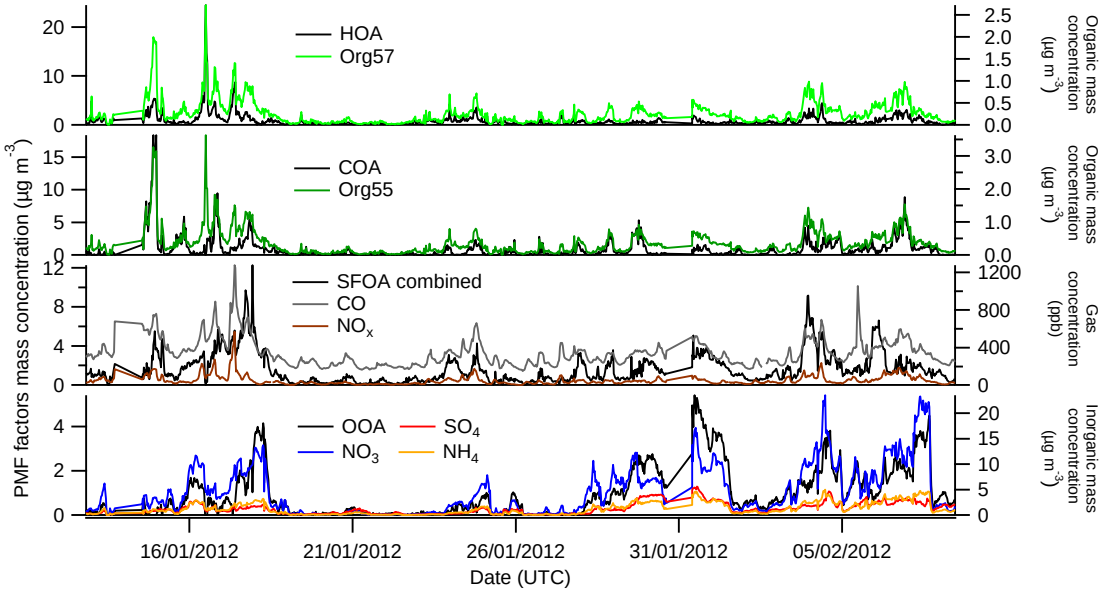

Figure S31. Time series of each PMF factor and time series of ancillary data. All data are measured by the AMS apart from CO and NO_x, which have been provided by James Lee.

Based on the similarities of the time series, diurnal cycles, and correlation with ancillary data factors 2 and 3 have been regrouped to one SFOA using the sum of their time series. Comparison of the time series from the combined SFOA factor and the remaining factors from the 5-factor solution with the corresponding factors from the 4-factors solution highlights some differences (Fig. S32). However, the factors from the two different solution spaces correlate very well (Table S11). With the exception of a few events where the mass of the 5-factor solution is less than that of the 4-factor solution, there is little difference between the HOA and COA factors between the two solution sets. For SFOA, the combined factor has a greater mass than that of the 4-factor solution, with the converse being true for the OOA factor.

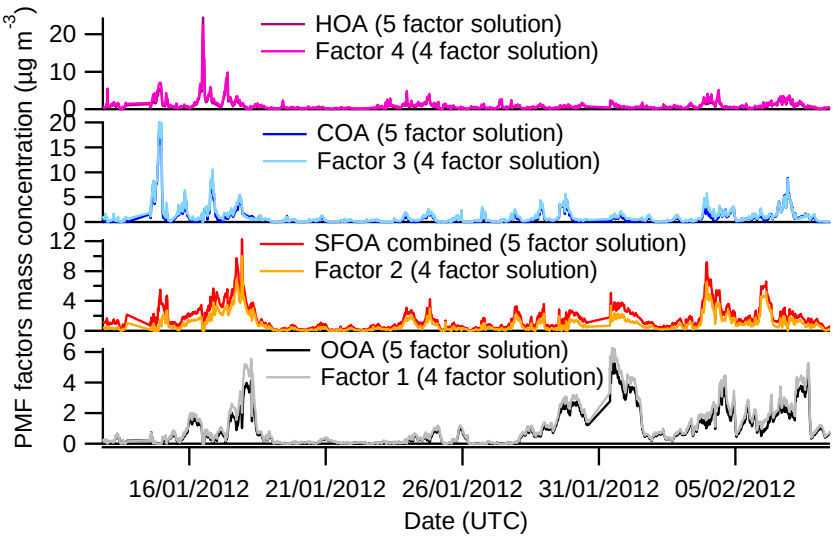

Figure S32. Comparison of the time series of the 4-factor solution and 5-factor solution with two factors combined.

Table S11. Pearson's r value (and slope) for each of the factor correlations.

	4-factor solution			
5-factor solution	HOA	COA	SFOA	OOA
HOA	0.99 (0.93)			
COA		0.99 (0.92)		
Combined SFOA			0.98 (1.34)	
OOA				1.00 (0.83)

The diurnal cycle of the combined factor clearly exhibits an increased concentration overnight (Fig. S33), which is consistent with the expected use of space heating in the evenings during winter.

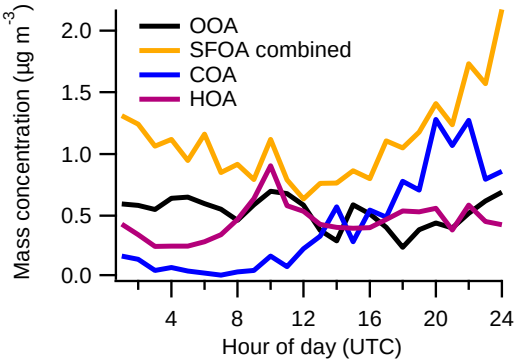

Figure S33. Diurnal cycle of the four factors from the 5-factor solution where the two SFOA factors have been combined.

It has been shown that NO_x and CO are strongly related to HOA (Zhang et al., 2005) as they are emitted from fuel combustion in vehicle engines. However, traffic activity is not the only source of these gases, which are used as tracers for combustion. Space heating has been found to be another

potential combustion source and therefore contributes to SFOA (Allan et al., 2010). The Pearson's r values derived between the gas tracers and the SFOA factor from the 4-factor solution (hereon in termed SFOA-4fac) are shown in Table S12. When the two SFOA factors from the 5-factor solution (SFOA-combined) are summed and compared to the gas tracers the Pearson's r values are better than those for SFOA-4fac. However, as both traffic and domestic fuel burning from space heating contribute to CO and NO_x concentrations a multi-linear regression fit as detailed in Allan et al. (2010) was performed to assess the relative contributions of traffic (HOA) and wood burning (SFOA) to these trace gases.

Fitting was performed according to the function:

$$f\,(\mathrm{HOA, SFOA}) = A[\mathrm{HOA}] + B[\mathrm{SFOA}] + C$$

where [HOA] and [SFOA] are the concentrations of the HOA and SFOA PMF factors and *A*, *B*, and *C* are arbitrary fitting parameters optimised to minimise the squared difference between *f* (HOA, SFOA) and NO_x or CO. This multi-linear regression fit was performed on the HOA and SFOA factors from the 4-factor solution and the HOA and combined SFOA factors from the 5-factor solution. The Pearson's r values derived are shown in Table S12. Including both sources in this way significantly improves the correlations with the gas tracers for both sets of solutions. However, there is little difference between the regression fit r values for the two solution sets with the 4-factor solution showing a very slightly greater correlation with NO_x than the 5-factor solution.

Table S12. Pearson's r correlation coefficients for linear and multi-linear regressions between PMF factors from the 4 and 5-factor solutions and combustion tracers.

	CO	NO_x
SFOA-4fac	0.56	0.43
SFOA-combined	0.65	0.51
f(HOA,SFOA)-4fac	0.77	0.74
f(HOA,SFOA)-combined	0.77	0.71

Ultimately, there is little difference between the SFOA derived in the 4-factor solution to the combined factor from the 5-factor solution and so both could be valid solution sets. However, because the 5-factor solution with the two SFOA factors combined has a lower Q/Q_{exp} than the 4-factor solution this is the solution set that is used in further analyses. In summary, four main components were identified: oxygenated OA (OOA), solid fuel OA (SFOA), cooking OA (COA), and hydrocarbon-like OA (HOA) where the two SFOA factors from the 5-factor solution were combined.

Finally, rotational ambiguity within the 5-factor solution was explored through the fPeak value where values between -0.6 and 1.0 produced solutions that could be considered valid and outside of this range, solutions produced nonphysical factors or failed to converge properly (Fig. S34). Between these values, however, the concentrations of HOA and COA showed some variation (Table S13) although the ambiguity was not a direct rotation between these two factors as the HOA profile was consistent between all fPeak values. Instead, the exchange of signals between profiles seemed to involve the COA and two SFOA factors. However, as the solution for fpeak=0 is most likely to be physically meaningful according to Paatero et al. (2002), this most central solution is used for further

analysis. Furthermore, this solution space was found to be relatively stable, produced good separation of the factors and the lowest $Q/Q_{expected}$.

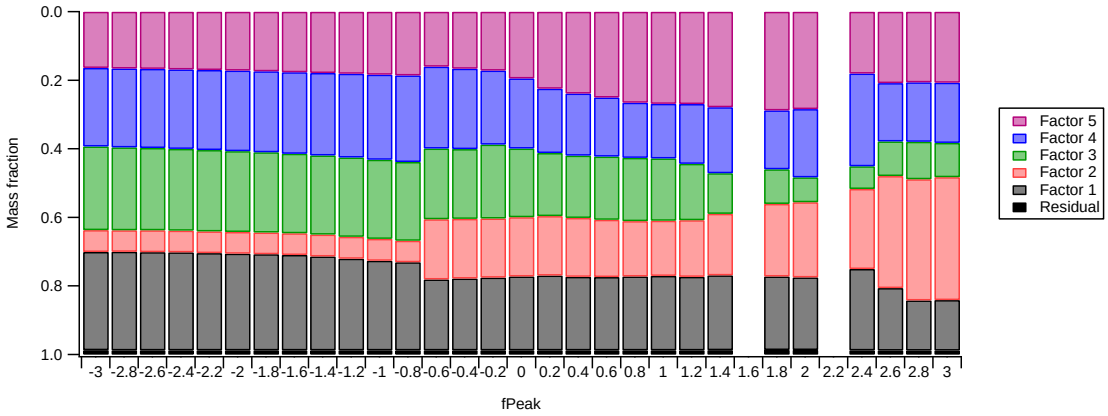

Figure S34. Variance of the factors as a function of fPeak from the 5-factor solution.

Table S13. Average mass concentration of each of the 5 factors for different fPeak values.

	Factor				
fPeak value	OOA	SFOA1	SFOA2	COA	HOA
-0.6	0.897374	0.757835	0.882626	1.02376	0.68164
0	0.933063	0.747544	0.857564	0.875335	0.829156
1	0.940803	0.696752	0.776001	0.682512	1.14724

5.2 Summer IOP – data in UTC (BST +1)

5.2.1 4-factor solution

There is a clear separation of the mass spectra for the 4-factor solution (Fig. S35) where the different factors are identified by their characteristics peaks. For example, although factors 1 and 2 exhibit very similar mass spectra they differ in m/z 44/43 ratio, with factor 1 having a larger m/z 44 peak indicative of a greater degree of oxidation, where this peak is associated with the CO_2^+ ion. Factors 3 and 4 differ in the ordering of the magnitudes of the peaks at m/z 41, 43, 55, 57. The time series of the factors are also distinct from each other (Fig. S36).

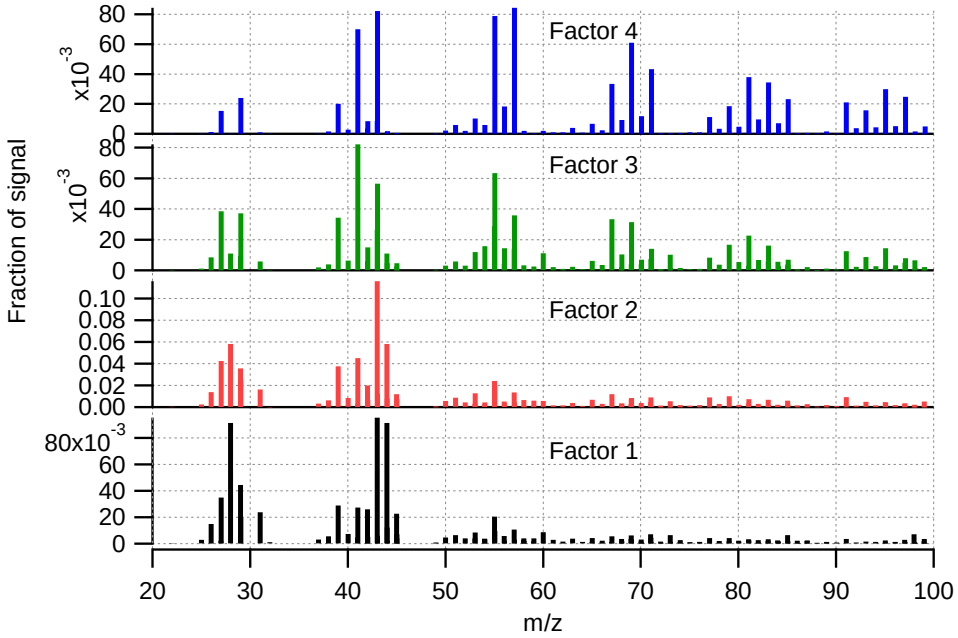

Figure S35. Mass spectra of the 4-factor solution. Note that the bars are not stacked.

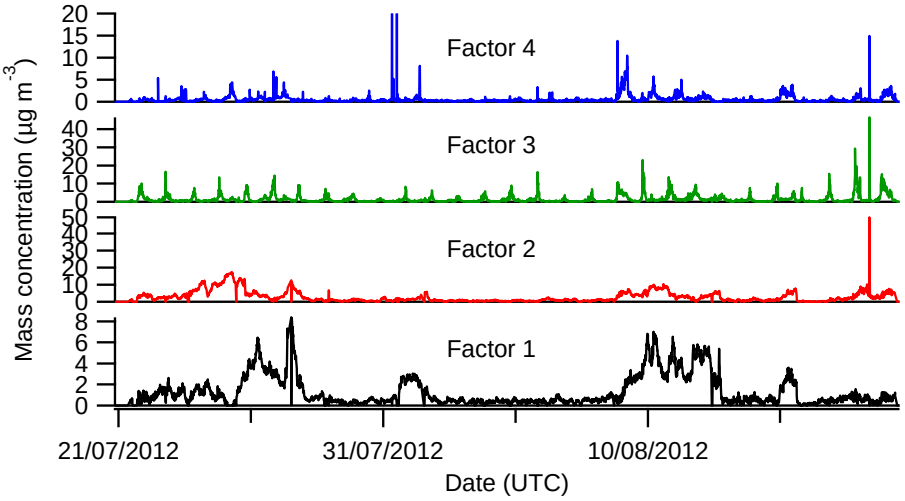

Figure S36. Time series of the 4-factor solution.

When this solution space was explored by running PMF with 50 seeds, some dependency was observed (Fig. S37). Although there was very little variation in the fraction of each factor with seed, there were some changes in fractional contribution between factor 1 and factor 2. This suggests some rotation between these two factors whereby both factors exhibit a larger m/z 43 peak than m/z 44. For these reasons, a 5-factor solution was explored.

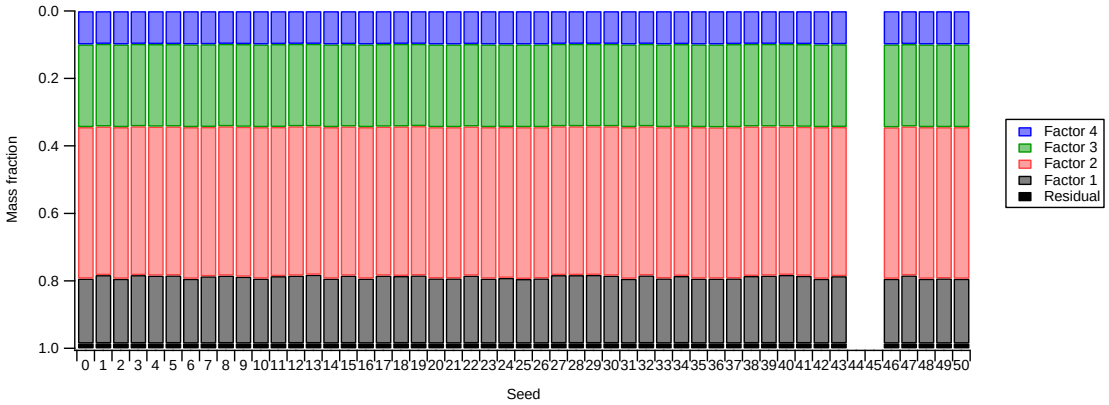

Figure S37. Fraction of mass of each factor with change in initialisation seed.

5.2.2 5-factor solution

Moving to a 5-factor solution the Q/Q_{exp} decreases to 2.4408 and there is still relatively good separation between the mass spectra (Fig. S38), each with a unique time series (Fig. S39) and diurnal profile (Fig. S40). Furthermore, there was no dependence on initialisation seed (Fig. S41). Factors 1 and 2 are better defined than in the 4-factor solution as factor 1 has a larger peak at m/z 44 than m/z 43, whereas the converse is true for factor 2. Factors 2, 4, and 5 are very similar to factors 2, 3, and 4 in the 4-factor solution. The new factor, factor 3, features similar peaks to factors 2 and 4, with a particularly large peak at m/z 43. The diurnal profile exhibits a unique increase in mass from around 21:00 and decreases late in the morning. No other profiles show this overnight peak.

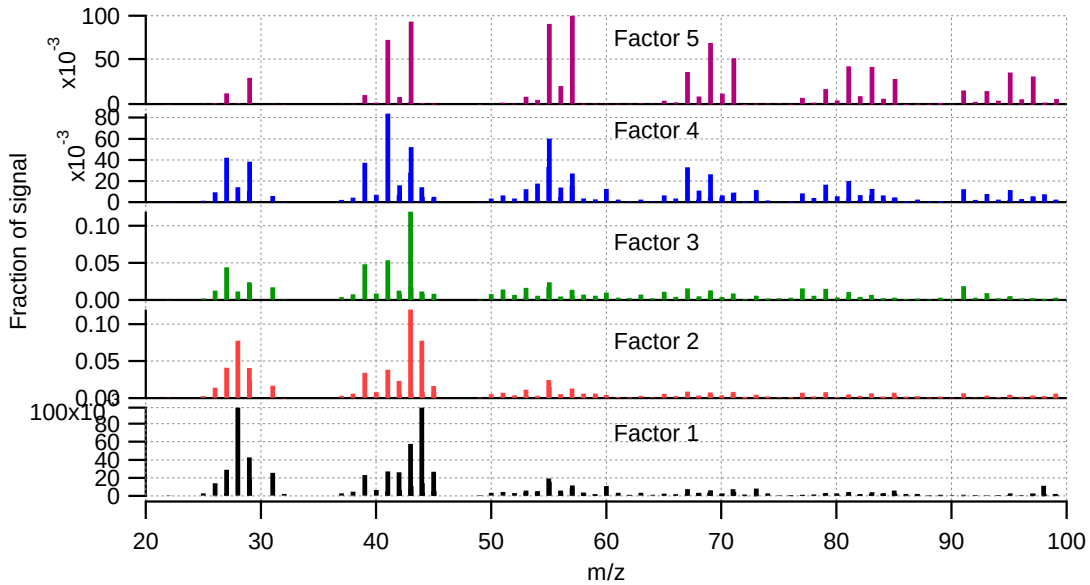

Figure S38. Mass spectra of the 5-factor solution. Note that the bars are not stacked.

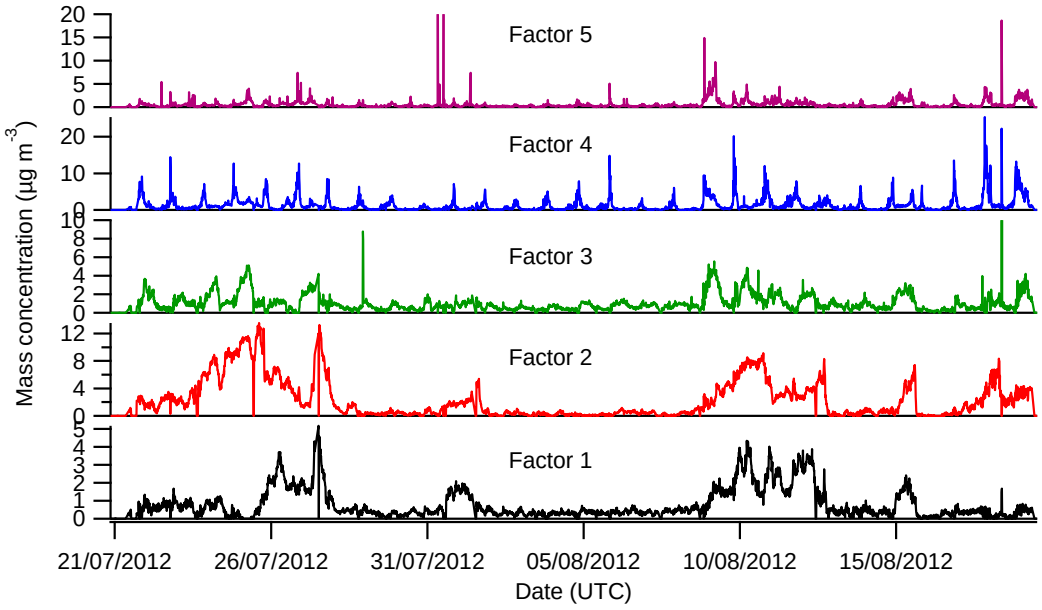

Figure S39. Time series of the 5-factor solution.

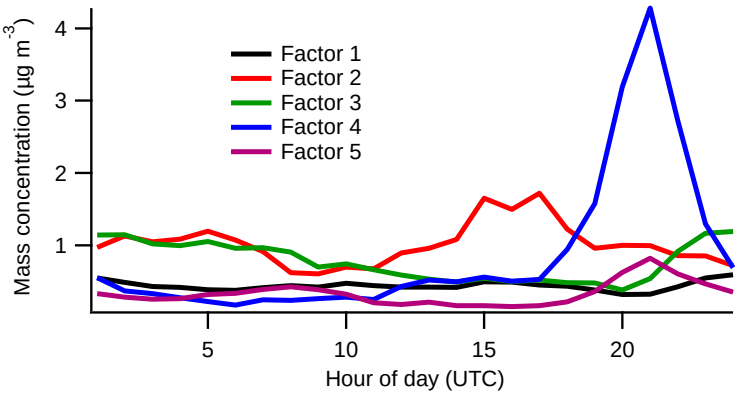

Figure S40. Median diurnal profiles of the 5 factors.

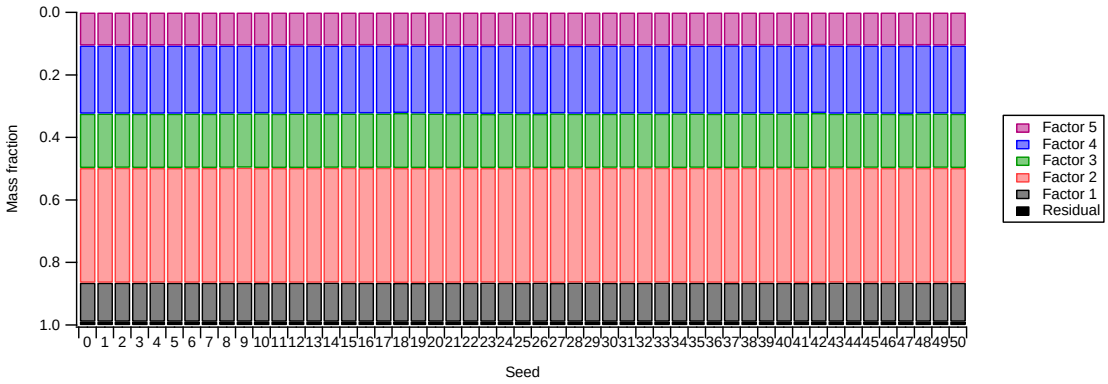

Figure S41. Fraction of mass of each factor with change in initialisation seed.

5.2.3 6-factor solution

Moving to a 6-factor solution the Q/Q_{exp} decreases to 2.272 from 2.4408, however the new factor, factor 4, consists mainly of a large peak at m/z 43 (Fig. S42). There are similarities in the time series between factors, with factor 4 showing similar trends to factors 1 and 3 (Fig. S43) as well as a very similar diurnal pattern to factor 1 (Fig. S44).

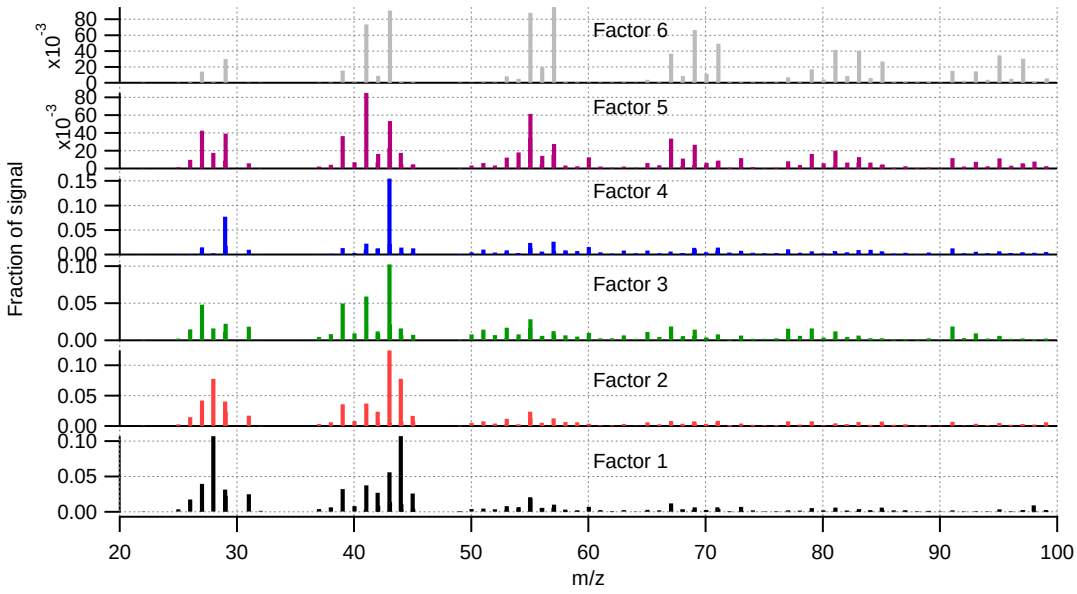

Figure S42. Mass spectra of the 6-factor solution. Note that the bars are not stacked.

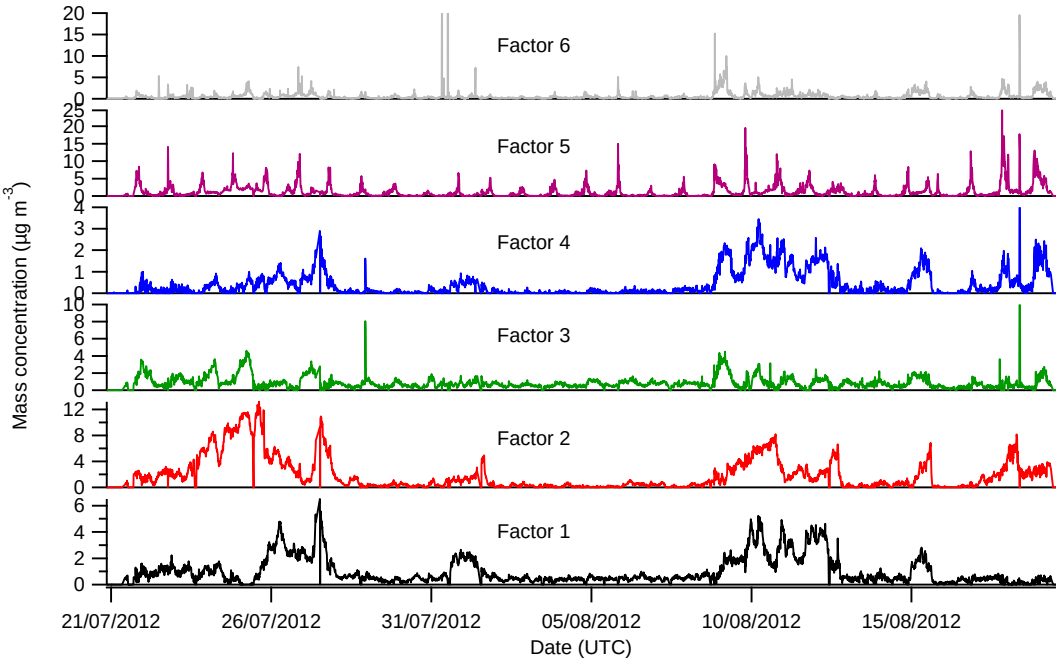

Figure S43. Time series of the 6-factor solution.

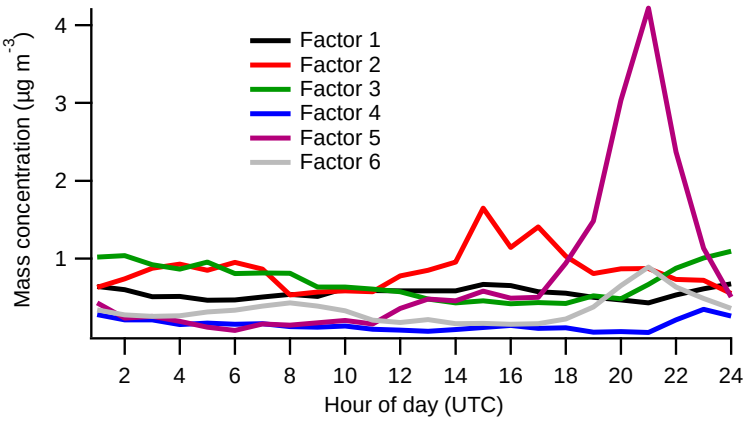

Figure S44. Median diurnal profiles of the 6 factors.

However, there are some subtle differences compared to the factors from the 5-factor solution including an increased m/z 57 to 55 ratio for factor 5 compared to factor 4 in the 5-factor solution. There are also several similarities in their time series as shown in Figure S45.

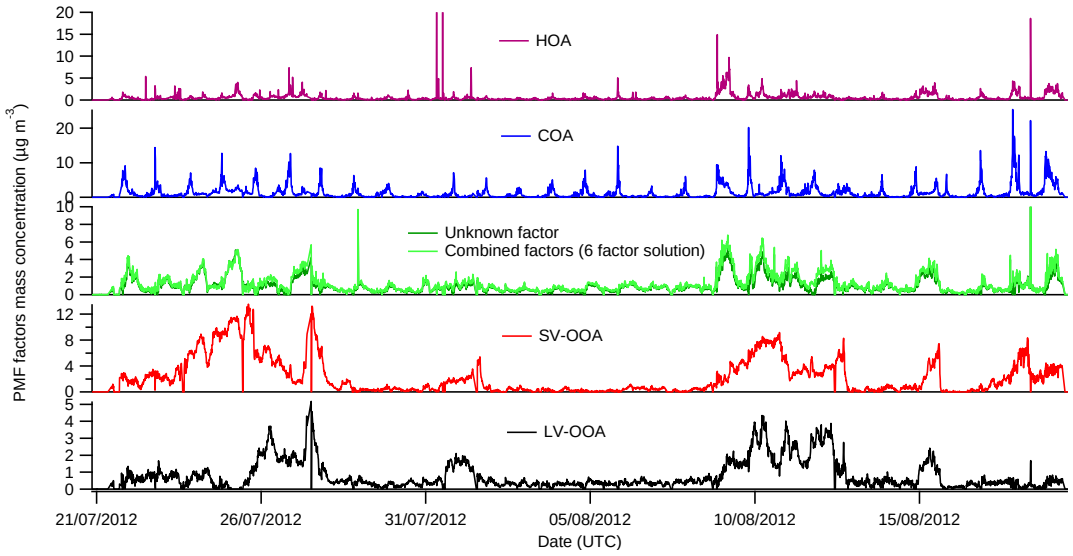

Figure S45. Time series of the 5-factor solution with factors 3 and 4 from the 6-factor solution combined, where factor 3 in the 5-factor solution is in dark green and the light green trace is factors 3 and 4 from the 6-factor solution summed.

There is negligible difference between the combined factor from the 6-factor solution and the unknown factor from the 5-factor solution, yielding an r of 0.97 when correlated. These similarities in time series and mass spectra are indicative of factor splitting. Furthermore, the 6-factor solution showed considerable dependency on initialisation seed used, whereby two main solutions result from the different seeds (Fig. S46). There is variance within each of these solution groups and one group of solutions does not converge. The 6-factor solution is therefore not stable and was discarded.

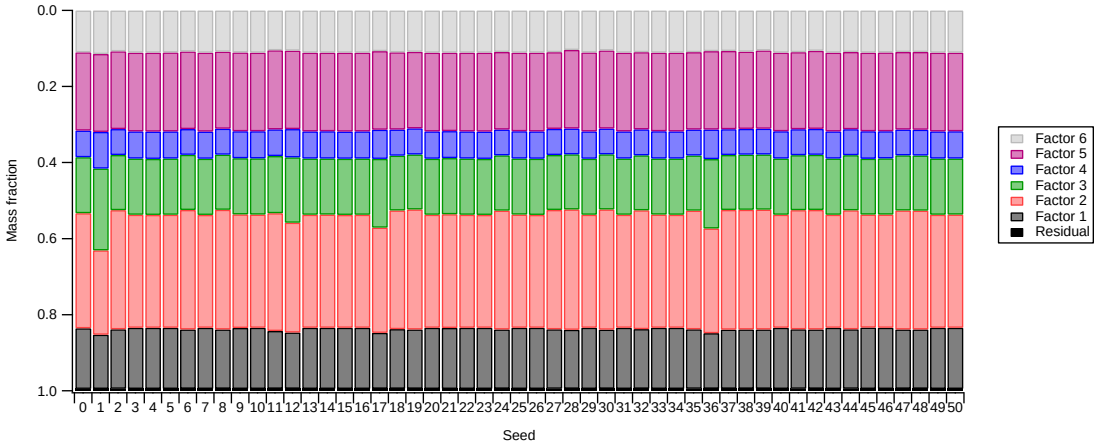

Figure S46. Fraction of mass of each factor with change in initialisation seed.

5.2.4 Factor identification and interpretation of the chosen solution set

In order to validate the solution set, the factors were correlated with reference spectra and ancillary data (Fig. S47), as discussed below. The five factors were therefore identified as LV-OOA, SV-OOA, COA, HOA, and an unknown factor.

Rotational ambiguity was explored through the fPeak value, where changes resulted in negligible difference in correlation between the mass spectra and time series with reference spectra and ancillary data, respectively. Although there was a change in mass fraction of each factor with different fPeaks (Table S14), this solution space was found to be relatively stable and produced good separation of the factors. Therefore, similarly to the winter IOP, the most central solution (fPeak=0) was chosen as this produced the lowest Q/Q_{exp} value and is most likely to be physically meaningful according to Paatero et al. (2002).

Table S14. Average mass concentration of each of the 5 factors for different fPeak values.

	Factor				
fPeak value	LV-OOA	SV-OOA	Unknown	COA	HOA
-0.8	1.17517	2.07502	1.16182	1.25825	0.368489
0	0.777415	2.27058	1.04627	1.30743	0.640502
1	0.616691	1.82052	1.56815	1.29725	0.738574

LV-OOA correlates strongly with reference spectra, yielding a Pearson's r value of 0.78 with the LV-OOA spectrum from Ng et al. (2011) and 0.94 with Mohr et al. (2012). The lack of a pronounced diurnal pattern and good correlation of the time series with SO_4 (r=0.84) supports the interpretation of this factor as being a well-aged, regional secondary organic aerosol (Jimenez et al., 2009; Lanz et al., 2007).

SV-OOA correlates with reference spectra, yielding a Pearson's r value of 0.79 (Mohr et al., 2012) and 0.92 (Ng et al., 2011). The time series correlates with particulate NO_3 (r=0.44), indicating its semi-volatile characteristics, however the correlation is weaker than for SO_4 (r=0.61). The difference between the time series of SV-OOA factor and NO_3 suggests that the gas-to-particle partitioning is

perhaps not the main driver for the temporal evolution of SV-OOA but rather local emissions and dynamics.

COA correlates with the mass spectral profile of COA from Mohr et al. (2012) with an r of 0.86, and the time series correlates with org55 (r=0.85). The diurnal pattern of COA exhibits a small increase in mass at midday with a very large increase in the evening, peaking at 21:00, corresponding to typical meal times.

The unknown factor, which will be discussed in a future publication, correlates very strongly with mass spectral profiles BBOA (r=0.91) and COA (r=0.87) from Mohr et al. (2012) and the time series correlates with org60 (r=0.60) and org55 (r=0.51). Interestingly, the increase in mass occurs as the COA mass starts to decrease after its peak at 21:00. This can be observed in the time series where the peaks in the COA profile occur in the evening and the peaks in the unknown factor occur shortly afterwards. Also, these peaks are greatest between the start of the measurement period and 28 July as well as from 9 August until the end of the campaign. This trend is similar to that of temperature, where the warmest temperatures are during these two periods.

HOA correlates extremely strongly with reference spectra (r=0.97 Mohr et al., 2012; r=0.95 Ng et al., 2011). A Pearson's r value of 0.85 is yielded when the time series of HOA is correlated with org57, with weaker correlations with combustion tracers CO (r=0.61) and NO_x (r=0.71). The diurnal pattern of HOA exhibits two peaks at 07:00 and 21:00, which correspond to the morning and evening rush hours.

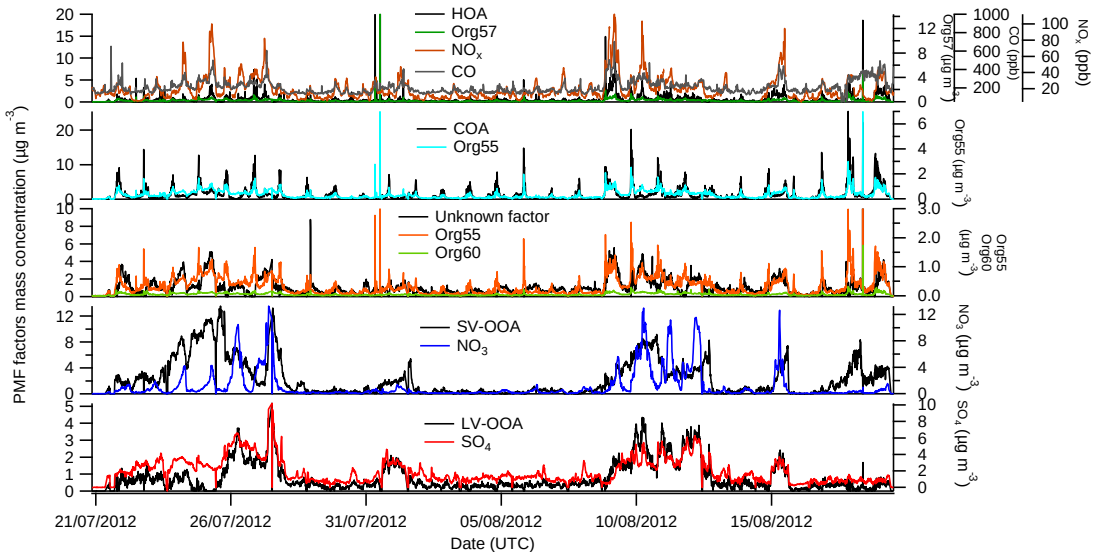

Figure S47. Time series of the 5-factor solution and ancillary data.

6 Comparison of chosen PMF solutions from cToF-AMS and HR-ToF-AMS

To increase confidence in the factorisation of the cToF-AMS, the mass spectra were compared to those from the HR-ToF-AMS PMF from both winter and summer IOPs (Fig. 48 a-g). As the summer period was omitted from the cToF-AMS PMF solution, only the time series from the winter IOP were compared between the solutions from the two instruments (Fig. 48 h-p).

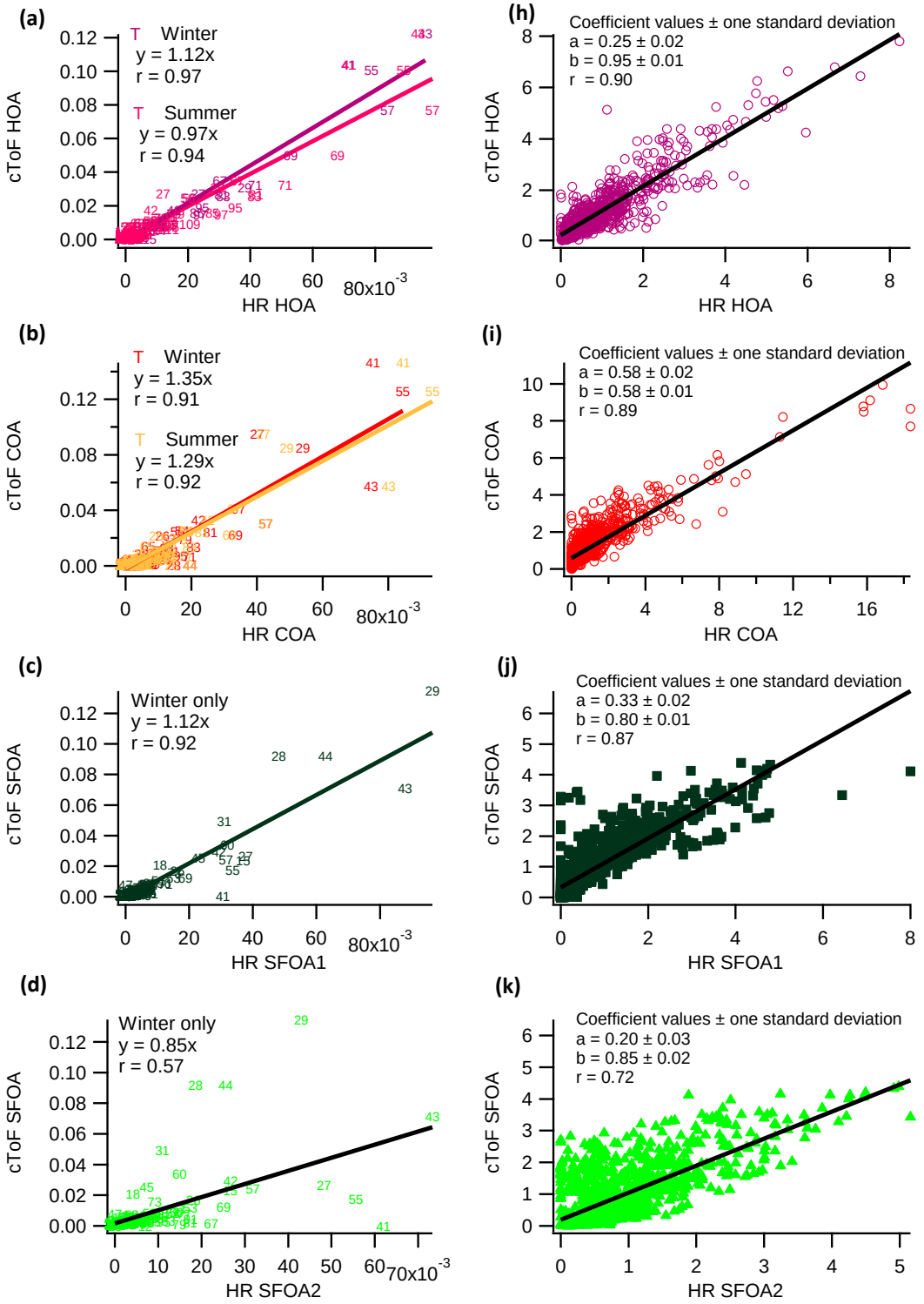
(a)
T Winter
y = 1.12x
r = 0.97
T Summer
y = 0.97x
r = 0.94
cToF HOA
HR HOA
80x10-3
(b)
T Winter
y = 1.35x
r = 0.91
T Summer
y = 1.29x
r = 0.92
cToF COA
HR COA
80x10-3
(c)
Winter only
y = 1.12x
r = 0.92
cToF SFOA
HR SFOA1
80x10-3
(d)
Winter only
y = 0.85x
r = 0.57
cToF SFOA
HR SFOA2
70x10-3
(h)
Coefficient values ± one standard deviation
a = 0.25 ± 0.02
b = 0.95 ± 0.01
r = 0.90
cToF HOA
HR HOA
(i)
Coefficient values ± one standard deviation
a = 0.58 ± 0.02
b = 0.58 ± 0.01
r = 0.89
cToF COA
HR COA
(j)
Coefficient values ± one standard deviation
a = 0.33 ± 0.02
b = 0.80 ± 0.01
r = 0.87
cToF SFOA
HR SFOA1
(k)
Coefficient values ± one standard deviation
a = 0.20 ± 0.03
b = 0.85 ± 0.02
r = 0.72
cToF SFOA
HR SFOA2

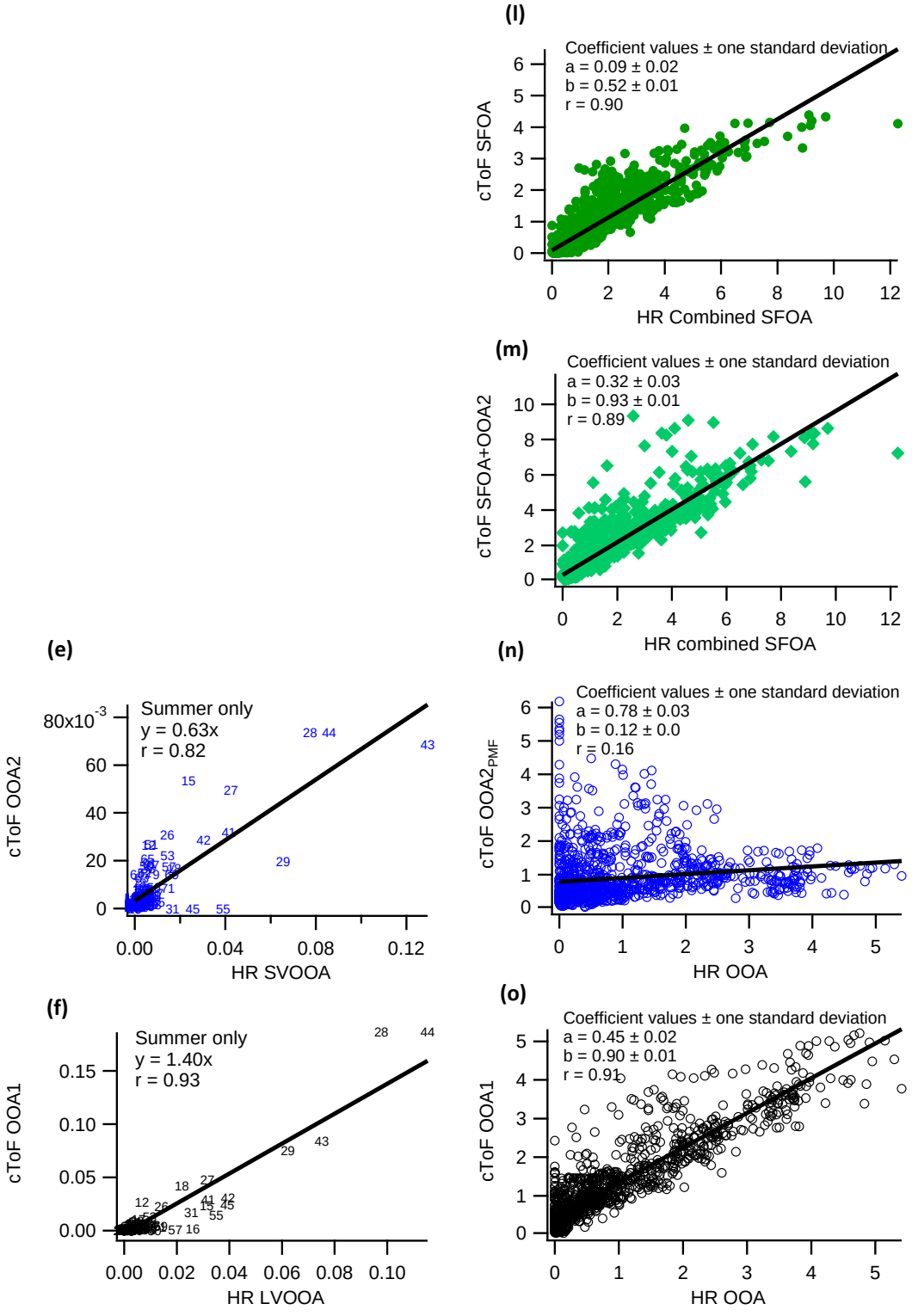
(l)
Coefficient values ± one standard deviation
a = 0.09 ± 0.02
b = 0.52 ± 0.01
r = 0.90
cToF SFOA
HR Combined SFOA
(m)
Coefficient values ± one standard deviation
a = 0.32 ± 0.03
b = 0.93 ± 0.01
r = 0.89
cToF SFOA+OOA2
HR combined SFOA
(e)
Summer only
y = 0.63x
r = 0.82
80x10-3
cToF OOA2
HR SVOOA
(f)
Summer only
y = 1.40x
r = 0.93
cToF OOA1
HR LVOOA
(n)
Coefficient values ± one standard deviation
a = 0.78 ± 0.03
b = 0.12 ± 0.0
r = 0.16
cToF OOA2PMF
HR OOA
(o)
Coefficient values ± one standard deviation
a = 0.45 ± 0.02
b = 0.90 ± 0.01
r = 0.91
cToF OOA1
HR OOA

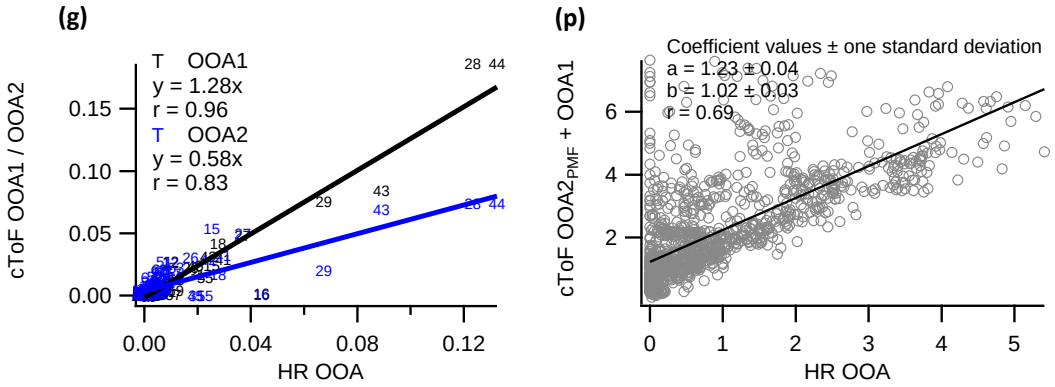

Figure S48. Comparison of the long-term cToF-PMF factors and IOP HR-PMF factors. Plots a-e are mass spectra and f-p are time series. Two SFOA factors were identified from the winter HR-PMF, with no SFOA factors in the summer HR-PMF. Also, it was not possible to separate the OOA factor in to the two subtypes from the winter HR-PMF. Finally, the summer period has been excluded from the long-term cToF-PMF and so there are no time series comparisons for the summer.

References

Alfarra, M. R., Prevot, A. S. H., Szidat, S., Sandradewi, J., Weimer, S., Lanz, V. A., Schreiber, D., Mohr, M., and Baltensperger, U.: Identification of the mass spectral signature of organic aerosols from wood burning emissions, Environ. Sci. Technol., 41, 5770–5777, 2007.

Allan, J. D., Williams, P. I., Morgan, W. T., Martin, C. L., Flynn, M. J., Lee, J., Nemitz, E., Phillips, G. J., Gallagher, M. W., and Coe, H.: Contributions from transport, solid fuel burning and cooking to primary organic aerosols in two UK cities, Atmos. Chem. Phys., 10, 647–668, doi:10.5194/acp-10-647-2010, 2010.

Crippa, M., DeCarlo, P. F., Slowik, J. G., Mohr, C., Heringa, M. F., Chirico, R., Poulain, L., Freutel, F., Sciare, J., Cozic, J., Di Marco, C. F., Elsasser, M., Nicolas, J. B., Marchand, N., Abidi, E., Wiedensohler, A., Drewnick, F., Schneider, J., Borrmann, S., Nemitz, E., Zimmermann, R., Jaffrezo, J.-L., Prévôt, A. S. H., and Baltensperger, U.: Wintertime aerosol chemical composition and source apportionment of the organic fraction in the metropolitan area of Paris, Atmos. Chem. Phys., 13, 961-981, doi:10.5194/acp-13-961-2013, 2013.

Cross, E. S., Slowik, J. G., Davidovits, P., Allan, J. D., Worsnop, D. R., Jayne, J. T., Lewis, D. K., Canagaratna, M., and Onasch, T. B.: Laboratory and ambient particle density determinations using light scattering in conjunction with aerosol mass spectrometry, Aerosol Sci. Tech., 41, 343–359, 2007.

Dall'Osto, M., Ovadnevaite, J., Ceburnis, D., Martin, D., Healy, R. M., O'Connor, I. P., Kourtchev, I., Sodeau, J. R., Wenger, J. C., and O'Dowd, C.: Characterization of urban aerosol in Cork city (Ireland) using aerosol mass spectrometry, Atmos. Chem. Phys., 13, 4997-5015, doi:10.5194/acp-13-4997-2013, 2013.

Jimenez, J. L., Canagaratna, M. R., Donahue, N. M., Prevot, A. S. H., Zhang, Q., Kroll, J. H., DeCarlo, P. F., Allan, J. D., Coe, H., Ng, N. L., Aiken, A. C., Docherty, K. S., Ulbrich, I. M., Grieshop, A. P., Robinson, A. L., Duplissy, J., Smith, J. D., Wilson, K. R., Lanz, V. A., Hueglin, C., Sun, Y. L., Tian, J., Laaksonen, A., Raatikainen, T., Rautiainen, J., Vaattovaara, P., Ehn, M., Kulmala, M., Tomlinson, J. M., Collins, D. R., Cubison, M. J., Dunlea, E. J., Huffman, J. A., Onasch, T. B., Alfarra, M. R., Williams, P. I., Bower, K., Kondo, Y., Schneider, J., Drewnick, F., Borrmann, S., Weimer, S., Demerjian, K., Salcedo, D., Cottrell, L., Griffin, R., Takami, A., Miyoshi, T., Hatakeyama, S., Shimono, A., Sun, J. Y., Zhang, Y. M., Dzepina, K., Kimmel, J. R., Sueper, D., Jayne, J. T., Herndon, S. C., Trimborn, A. M., Williams, L. R., Wood, E. C., Middlebrook, A. M., Kolb, C. E., Baltensperger, U., and Worsnop, D. R.: Evolution of organic aerosols in the atmosphere, Science, 326, 1525–1529, 2009.

Lanz, V. A., Alfarra, M. R., Baltensperger, U., Buchmann, B., Hueglin, C., and Prévôt, A. S. H.: Source apportionment of submicron organic aerosols at an urban site by factor analytical modelling of aerosol mass spectra, Atmos. Chem. Phys., 7, 1503–1522, doi:10.5194/acp-7-1503-2007, 2007.

Liu, D., Allan, J. D., Young, D. E., Coe, H. Beddows, D., Fleming, Z. L., Flynn, M. J., Gallagher, M. W., Harrison, R. M., Lee, J., Prévôt, A. S. H., Taylor, J. W., Yin, J., Williams, P. I., and Zotter, P.: Size

distribution, mixing state and source apportionments of black carbon aerosols in London during winter time, in preparation, 2014.

Mohr, C., Huffman, J. A., Cubison, M. J., Aiken, A. C., Docherty, K. S., Kimmel, J. R., Ulbrich, I. M., Hannigan, M., and Jimenez, J. L.: Characterization of primary organic aerosol emissions from meat cooking, trash burning, and motor vehicles with high resolution aerosol mass spectrometry and comparison with ambient and chamber observations, Environ. Sci. Technol., 43, 2443–2449, 2009.

Mohr, C., DeCarlo, P. F., Heringa, M. F., Chirico, R., Slowik, J. G., Richter, R., Reche, C., Alastuey, A., Querol, X., Seco, R., Peñuelas, J., Jiménez, J. L., Crippa, M., Zimmermann, R., Baltensperger, U., and Prévôt, A. S. H.: Identification and quantification of organic aerosol from cooking and other sources in Barcelona using aerosol mass spectrometer data, Atmos. Chem. Phys., 12, 1649-1665, doi:10.5194/acp-12-1649-2012, 2012.

Ng, N. L., Canagaratna, M. R., Jimenez, J. L., Zhang, Q., Ulbrich, I. M., and Worsnop, D. R.: Real-time methods for estimating organic component mass concentrations from aerosol mass spectrometer data. Environ. Sci. Technol., 45, 910-916, 2011.

Paatero, P., Hopke, P. K., Song, X. H., and Ramadan, Z.: Understanding and controlling rotations in factor analytic models, Chemometr. Intell. Lab, 60, 253-264, Doi 10.1016/S0169-7439(01)00200-3, 2002.

Paatero, P. and Hopke, P. K.: Discarding or downweighting high-noise variables in factor analytic models, Anal. Chim. Acta, 490, 277–289, doi:10.1016/s0003-2670(02)01643-4, 2003.

Sueper, D.: ToF-AMS High Resolution Analysis Software – Pika, online available at: http://cires.colorado.edu/jimenez-group/ToFAMSResources/ToFSoftware/PikaInfo/, 2008.

Ulbrich, I. M., Canagaratna, M. R., Zhang, Q., Worsnop, D. R., and Jimenez, J. L.: Interpretation of organic components from Positive Matrix Factorization of aerosol mass spectrometric data, Atmos. Chem. Phys., 9, 2891–2918, doi:10.5194/acp-9-2891-2918, 2009.

Yin, J., Cumberland, S. Harrison, R. M., Allan, J., Young, D., Williams, P., and Coe, H.: Receptor modelling of fine particles in Southern England including comparison of CMB model outputs with AMS-PMF factors, in preparation, 2014.

Zhang, Q., Worsnop, D. R., Canagaratna, M. R., and Jimenez, J. L.: Hydrocarbon-like and oxygenated organic aerosols in Pittsburgh: insights into sources and processes of organic aerosols, Atmos. Chem. Phys., 5, 3289–3311, doi:10.5194/acp-5-3289-2005, 2005.

Bibliography

Aas, W., Tsyro, S., Bieber, E., Bergström, R., Ceburnis, D., Ellermann, T., Fagerli, H., Frölich, M., Gehrig, R., Makkonen, U., Nemitz, E., Otjes, R., Perez, N., Perrino, C., Prévôt, A. S. H., Putaud, J.-P., Simpson, D., Spindler, G., Vana, M., and Yttri, K. E.: Lessons learnt from the first EMEP intensive measurement periods, Atmospheric Chemistry and Physics, 12, 8073–8094, doi:10.5194/acp-12-8073-2012, 2012.

Abdalmogith, S. S. and Harrison, R. M.: The use of trajectory cluster analysis to examine the long-range transport of secondary inorganic aerosol in the UK, Atmospheric Environment, 39, 6686–6695, doi:10.1016/j.atmosenv.2005.07.059, 2005.

Abdalmogith, S. S. and Harrison, R. M.: An analysis of spatial and temporal properties of daily sulfate, nitrate and chloride concentrations at UK urban and rural sites., Journal of Environmental Monitoring, 8, 691–9, doi:10.1039/b601562j, 2006.

Abdullahi, K. L., Delgado-Saborit, J. M., and Harrison, R. M.: Emissions and indoor concentrations of particulate matter and its specific chemical components from cooking: A review, Atmospheric Environment, 71, 260–294, doi:10.1016/j.atmosenv.2013.01.061, 2013.

Abt, E., Suh, H. H., Catalano, P., and Koutrakis, P.: Relative Contribution of Outdoor and Indoor Particle Sources to Indoor Concentrations, Environmental Science Technology, 34, 3579–3587, doi:10.1021/es990348y, 2000.

Aiken, A. C., Salcedo, D., Cubison, M. J., Huffman, J. A., DeCarlo, P. F., Ulbrich, I. M., Docherty, K. S., Sueper, D., Kimmel, J. R., Worsnop, D. R., Trimborn, A., Northway, M., Stone, E. A., Schauer, J. J., Volkamer, R. M., Fortner, E., de Foy, B., Wang, J., Laskin, A., Shutthanandan, V., Zheng, J., Zhang, R., Gaffney, J., Marley, N. A., Paredes-Miranda, G., Arnott, W. P., Molina, L. T., Sosa, G., and Jimenez, J. L.: Mexico City aerosol analysis during MILAGRO using high resolution aerosol mass spectrometry at the urban supersite (T0) Part 1: Fine particle composition and

organic source apportionment, Atmospheric Chemistry and Physics, 9, 6633–6653, doi:10.5194/acp-9-6633-2009, 2009.

Alfarra, M. R., Coe, H., Allan, J. D., Bower, K. N., Boudries, H., Canagaratna, M. R., Jimenez, J. L., Jayne, J. T., Garforth, A. A., Li, S.-M., and Worsnop, D. R.: Characterization of urban and rural organic particulate in the Lower Fraser Valley using two Aerodyne Aerosol Mass Spectrometers, Atmospheric Environment, 38, 5745 – 5758, doi:http://dx.doi.org/10.1016/j.atmosenv.2004.01.054, the Pacific 2001 Air Quality Study, 2004.

Alfarra, M. R., Prevot, A. S. H., Szidat, S., Sandradewi, J., Weimer, S., Lanz, V. A., Schreiber, D., Mohr, M., and Baltensperger, U.: Identification of the Mass Spectral Signature of Organic Aerosols from Wood Burning Emissions, Environmental Science Technology, 41, 5770–5777, doi:10.1021/es062289b, 2007.

Allan, J. D., Alfarra, M. R., Bower, K. N., Williams, P. I., Gallagher, M. W., Jimenez, J. L., McDonald, A. G., Nemitz, E., Canagaratna, M. R., Jayne, J. T., Coe, H., and Worsnop, D. R.: Quantitative sampling using an Aerodyne aerosol mass spectrometer 2. Measurements of fine particulate chemical composition in two U.K. cities, Journal of Geophysical Research: Atmospheres, 108, 4091, doi: 10.1029/2002JD002359, 2003a.

Allan, J. D., Jimenez, J. L., Williams, P. I., Alfarra, M. R., Bower, K. N., Jayne, J. T., Coe, H., and Worsnop, D. R.: Quantitative sampling using an Aerodyne aerosol mass spectrometer 1. Techniques of data interpretation and error analysis, Journal of Geophysical Research: Atmospheres, 108, 4090, doi:10.1029/2002JD002358, 2003b.

Allan, J. D., Bower, K. N., Coe, H., Boudries, H., Jayne, J. T., Canagaratna, M. R., Millet, D. B., Goldstein, A. H., Quinn, P. K., Weber, R. J., and Worsnop, D. R.: Submicron aerosol composition at Trinidad Head, California, during ITCT 2K2: Its relationship with gas phase volatile organic carbon and assessment of instrument performance, Journal of Geophysical Research: Atmospheres, 109, D23S24, doi: 10.1029/2003JD004208, 2004a.

Allan, J. D., Delia, A. E., Coe, H., Bower, K. N., Alfarra, M., Jimenez, J. L., Middlebrook, A. M., Drewnick, F., Onasch, T. B., Canagaratna, M. R., Jayne, J. T., and Worsnop, D. R.: A generalised method for the extraction of chemically resolved

mass spectra from Aerodyne aerosol mass spectrometer data, Journal of Aerosol Science, 35, 909 – 922, doi:http://dx.doi.org/10.1016/j.jaerosci.2004.02.007, 2004b.

Allan, J. D., Williams, P. I., Morgan, W. T., Martin, C. L., Flynn, M. J., Lee, J., Nemitz, E., Phillips, G. J., Gallagher, M. W., and Coe, H.: Contributions from transport, solid fuel burning and cooking to primary organic aerosols in two UK cities, Atmospheric Chemistry and Physics, 10, 647–668, doi:10.5194/acp-10-647-2010, 2010.

Amato, F., Pandolfi, M., Escrig, A., Querol, X., Alastuey, A., Pey, J., Perez, N., and Hopke, P.: Quantifying road dust resuspension in urban environment by Multilinear Engine: A comparison with PMF2, Atmospheric Environment, 43, 2770 – 2780, doi:http://dx.doi.org/10.1016/j.atmosenv.2009.02.039, 2009.

Andreae, M. O. and Gelencsér, A.: Black carbon or brown carbon? The nature of light-absorbing carbonaceous aerosols, Atmospheric Chemistry and Physics, 6, 3131–3148, doi:10.5194/acp-6-3131-2006, 2006.

Ansari, A. S. and Pandis, S. N.: Response of Inorganic PM to Precursor Concentrations, Environmental Science Technology, 32, 2706–2714, doi:10.1021/es971130j, 1998.

AQEG: Particulate Matter in the UK: Summary, Defra, London, URL `http://uk-air.defra.gov.uk/assets/documents/reports/aqeg/pm-summary.pdf`, 2005.

AQEG: Fine Particulate Matter ($PM_{2.5}$) in the United Kingdom, Defra, London, URL `http://uk-air.defra.gov.uk/assets/documents/reports/cat11/1212141150_AQEG_Fine_Particulate_Matter_in_the_UK.pdf`, 2012.

Bateman, A. P., Nizkorodov, S. A., Laskinb, J., and Laskinc, A.: Time-resolved molecular characterization of limonene/ozone aerosol using high-resolution electrospray ionization mass spectrometry, Physical Chemistry Chemical Physics, 11, 7931–7942, doi:10.1039/b905288g, 2009.

Bauer, S. E., Koch, D., Unger, N., Metzger, S. M., Shindell, D. T., and Streets, D. G.: Nitrate aerosols today and in 2030: a global simulation including aerosols and tropospheric ozone, Atmospheric Chemistry and Physics, 7, 5043–5059, doi:10.5194/acp-7-5043-2007, 2007.

Belis, C. A., Karagulian, F., Larsen, B. R., and Hopke, P. K.: Critical review and meta-analysis of ambient particulate matter source apportionment using receptor models in Europe, Atmospheric Environment, 69, 94–108, doi:http://dx.doi.org/10.1016/j.atmosenv.2012.11.009, 2013.

Bohnenstengel, S. I., Belcher, S. E., Aiken, A. C., Allan, J. D., Allen, G., Bacak, A., Bannan, T. J., Barlow, J. F., Beddows, D. C. S., Bloss, W. J., Booth, A. M., Chemel, C., Coceal, O., Di Marco, C. F., Mavendra, D. K., Faloon, K. H., Fleming, Z., Furger, M., Geitl, J. K., Graves, R. R., Green, D. C., Grimmond, C. S. B., Halios, C., Hamilton, J. F., Harrison, R. M., Heal, M. R., Heard, D. E., Helfter, C., Herndon, S. C., Holmes, R. E., Hopkins, J. R., Jones, A. M., Kelly, F. J., Kotthaus, S., Langford, B., Lee, J. D., Leigh, R. J., Lewis, A. C., Lidster, R. T., Lopez-Hilfiker, F. D., McQuaid, J. B., Mohr, C., Monks, P. S., Nemitz, E., Ng, N. L., Percival, C. J., Prévôt, A. S. H., Ricketts, H. M. A., Sokhi, R., Stone, D., Thornton, J. A., Tremper, A. H., Valach, A. C., Visser, S., Whalley, L. K., Williams, L. R., Xu, L., Young, D. E., and Zotter, P.: Meteorology, air quality and health in London: the ClearfLo project, in press, 2014.

Bressi, M., Sciare, J., Ghersi, V., Bonnaire, N., Nicolas, J. B., Petit, J.-E., Moukhtar, S., Rosso, A., Mihalopoulos, N., and Féron, A.: A one-year comprehensive chemical characterisation of fine aerosol ($PM_{2.5}$) at urban, suburban and rural background sites in the region of Paris (France), Atmospheric Chemistry and Physics, 13, 7825–7844, doi:10.5194/acp-13-7825-2013, 2013.

Brimblecombe, P.: Transformations in understanding the health impacts of air pollutants in the 20th century, EPJ Web of Conferences, 1, 47–53, doi:10.1140/epjconf/e2009-00909-8, 2009.

Brunekreef, B. and Holgate, S. T.: Air pollution and health, The Lancet, 360, 1233 – 1242, doi:http://dx.doi.org/10.1016/S0140-6736(02)11274-8, 2002.

Buonanno, G., Morawska, L., and Stabile, L.: Particle emission factors during cooking activities, Atmospheric Environment, 43, 3235–3242, 2009.

Cabada, J. C., Pandis, S. N., and Robinson, A. L.: Sources of Atmospheric Carbonaceous Particulate Matter in Pittsburgh, Pennsylvania, Journal of the Air & Waste Management Association, 52, 732–741, doi:10.1080/10473289.2002.10470811, 2002.

Canagaratna, M. R., Jayne, J. T., Jimenez, J. L., Allan, J. D., Alfarra, M. R., Zhang, Q., Onasch, T. B., Drewnick, F., Coe, H., Middlebrook, A., Delia, A., Williams, L. R., Trimborn, A. M., Northway, M. J., DeCarlo, P. F., Kolb, C. E., Davidovits, P., and Worsnop, D. R.: Chemical and microphysical characterization of ambient aerosols with the aerodyne aerosol mass spectrometer, Mass Spectrometry Reviews, 26, 185–222, doi:10.1002/mas.20115, 2007.

Canonaco, F., Crippa, M., Slowik, J. G., Baltensperger, U., and Prévôt, A. S. H.: SoFi, an IGOR-based interface for the efficient use of the generalized multilinear engine (ME-2) for the source apportionment: ME-2 application to aerosol mass spectrometer data, Atmospheric Measurement Techniques, 6, 3649–3661, doi:10.5194/amt-6-3649-2013, 2013.

Cape, J. N., Cornell, S. E., Jickells, T. D., and Nemitz, E.: Organic nitrogen in the atmosphere Where does it come from? A review of sources and methods, Atmospheric Research, 102, 30–48, doi:http://dx.doi.org/10.1016/j.atmosres.2011.07.009, 2011.

Capes, G., Murphy, J. G., Reeves, C. E., McQuaid, J. B., Hamilton, J. F., Hopkins, J. R., Crosier, J., Williams, P. I., and Coe, H.: Secondary organic aerosol from biogenic VOCs over West Africa during AMMA, Atmospheric Chemistry and Physics, 9, 3841–3850, doi:10.5194/acp-9-3841-2009, 2009.

Carslaw, D. C., Ropkins, K., and Bell, M. C.: Change-Point Detection of Gaseous and Particulate Traffic-Related Pollutants at a Roadside Location, Environmental Science Technology, 40, 6912–6918, doi:10.1021/es060543u, 2006.

Castro, L. M., Pio, C. A., Harrison, R. M., and Smith, D. J. T.: Carbonaceous aerosol in urban and rural European atmospheres: estimation of secondary organic carbon concentrations, Atmospheric Environment, 33, 2771–2781, doi:http://dx.doi.org/10.1016/S1352-2310(98)00331-8, 1999.

Chirico, R., Prévôt, A. S. H., DeCarlo, P. F., Heringa, M. F., Richter, R., Weingartner, E., and Baltensperger, U.: Aerosol and trace gas vehicle emission factors measured in a tunnel using an Aerosol Mass Spectrometer and other on-line instrumentation, Atmospheric Environment, 45, 2182 – 2192, doi:http://dx.doi.org/10.1016/j.atmosenv.2011.01.069, 2011.

Collaud Coen, M., Andrews, E., Asmi, A., Baltensperger, U., Bukowiecki, N., Day, D., Fiebig, M., Fjaeraa, A. M., Flentje, H., Hyvärinen, A., Jefferson, A., Jennings, S. G., Kouvarakis, G., Lihavainen, H., Lund Myhre, C., Malm, W. C., Mihapopoulos, N., Molenar, J. V., O'Dowd, C., Ogren, J. A., Schichtel, B. A., Sheridan, P., Virkkula, A., Weingartner, E., Weller, R., and Laj, P.: Aerosol decadal trends Part 1: In-situ optical measurements at GAW and IMPROVE stations, Atmospheric Chemistry and Physics, 13, 869–894, doi:10.5194/acp-13-869-2013, 2013.

COMEAP: The Mortality Effects of Long-Term Exposure to Particulate Air Pollution in the United Kingdom, A report by the Committee on the Medical Effects of Air Pollutants, 2010.

Crippa, M., Canonaco, F., Slowik, J. G., El Haddad, I., DeCarlo, P. F., Mohr, C., Heringa, M. F., Chirico, R., Marchand, N., Temime-Roussel, B., Abidi, E., Poulain, L., Wiedensohler, A., Baltensperger, U., and Prévôt, A. S. H.: Primary and secondary organic aerosol origin by combined gas-particle phase source apportionment, Atmospheric Chemistry and Physics, 13, 8411–8426, doi:10.5194/acp-13-8411-2013, 2013a.

Crippa, M., DeCarlo, P. F., Slowik, J. G., Mohr, C., Heringa, M. F., Chirico, R., Poulain, L., Freutel, F., Sciare, J., Cozic, J., Di Marco, C. F., Elsasser, M., Nicolas, J. B., Marchand, N., Abidi, E., Wiedensohler, A., Drewnick, F., Schneider, J., Borrmann, S., Nemitz, E., Zimmermann, R., Jaffrezo, J.-L., Prévôt, A. S. H., and Baltensperger, U.: Wintertime aerosol chemical composition and source apportionment of the organic fraction in the metropolitan area of Paris, Atmospheric Chemistry and Physics, 13, 961–981, doi:10.5194/acp-13-961-2013, 2013b.

Crippa, M., Canonaco, F., Lanz, V. A., Äijälä, M., Allan, J. D., Carbone, S., Capes, G., Ceburnis, D., Dall'Osto, M., Day, D. A., DeCarlo, P. F., Ehn, M., Eriksson, A., Freney, E., Hildebrandt Ruiz, L., Hillamo, R., Jimenez, J. L., Junninen, H., Kiendler-Scharr, A., Kortelainen, A.-M., Kulmala, M., Laaksonen, A., Mensah, A. A., Mohr, C., Nemitz, E., O'Dowd, C., Ovadnevaite, J., Pandis, S. N., Petäjä, T., Poulain, L., Saarikoski, S., Sellegri, K., Swietlicki, E., Tiitta, P., Worsnop, D. R., Baltensperger, U., and Prévôt, A. S. H.: Organic aerosol components derived from 25 AMS data sets across Europe using a consistent ME-2 based source apportionment approach, Atmospheric Chemistry and Physics, 14, 6159–6176, doi:10.5194/acp-14-6159-2014, 2014.

Crosier, J., Allan, J. D., Coe, H., Bower, K. N., Formenti, P., and Williams, P. I.: Chemical composition of summertime aerosol in the Po Valley (Italy), northern Adriatic and Black Sea, Quarterly Journal of the Royal Meteorological Society, 133, 61–75, doi:10.1002/qj.88, 2007.

Cross, E. S., Slowik, J. G., Davidovits, P., Allan, J. D., Worsnop, D. R., Jayne, J. T., Lewis, D. K., Canagaratna, M., and Onasch, T. B.: Laboratory and Ambient Particle Density Determinations using Light Scattering in Conjunction with Aerosol Mass Spectrometry, Aerosol Science and Technology, 41, 343–359, doi:10.1080/02786820701199736, 2007.

Crutzen, P.: Albedo Enhancement by Stratospheric Sulfur Injections: A Contribution to Resolve a Policy Dilemma?, Climatic Change, 77, 211–220, doi:10.1007/s10584-006-9101-y, 2006.

Cubison, M. J., Ortega, A. M., Hayes, P. L., Farmer, D. K., Day, D., Lechner, M. J., Brune, W. H., Apel, E., Diskin, G. S., Fisher, J. A., Fuelberg, H. E., Hecobian, A., Knapp, D. J., Mikoviny, T., Riemer, D., Sachse, G. W., Sessions, W., Weber, R. J., Weinheimer, A. J., Wisthaler, A., and Jimenez, J. L.: Effects of aging on organic aerosol from open biomass burning smoke in aircraft and laboratory studies, Atmospheric Chemistry and Physics, 11, 12 049–12 064, doi:10.5194/acp-11-12049-2011, 2011.

Dall'Osto, M., Ovadnevaite, J., Ceburnis, D., Martin, D., Healy, R. M., O'Connor, I. P., Kourtchev, I., Sodeau, J. R., Wenger, J. C., and O'Dowd, C.: Characterization of urban aerosol in Cork city (Ireland) using aerosol mass spectrometry, Atmospheric Chemistry and Physics, 13, 4997–5015, doi:10.5194/acp-13-4997-2013, 2013.

de Gouw, J. A., Middlebrook, A. M., Warneke, C., Goldan, P. D., Kuster, W. C., Roberts, J. M., Fehsenfeld, F. C., Worsnop, D. R., Canagaratna, M. R., Pszenny, A. A. P., Keene, W. C., Marchewka, M., Bertman, S. B., and Bates, T. S.: Budget of organic carbon in a polluted atmosphere: Results from the New England Air Quality Study in 2002, Journal of Geophysical Research: Atmospheres, 110, 1–22, doi:10.1029/2004JD005623, 2005.

DeCarlo, P. F., Kimmel, J. R., Trimborn, A., Northway, M. J., Jayne, J. T., Aiken, A. C., Gonin, M., Fuhrer, K., Horvath, T., Docherty, K. S., Worsnop, D. R., and Jimenez, J. L.: Field-Deployable, High-Resolution, Time-of-Flight Aerosol Mass Spectrometer, Analytical Chemistry, 78, 8281–8289, doi:10.1021/ac061249n, 2006.

Deutsch, F., Vankerkom, J., Janssen, L., Janssen, S., Bencs, L., Grieken, R. V., Fierens, F., Dumont, G., and Mensink, C.: Modelling concentrations of airborne primary and secondary PM_{10} and $PM_{2.5}$ with the BelEUROS-model in Belgium, Ecological Modelling, 217, 230 – 239, doi:http://dx.doi.org/10.1016/j.ecolmodel.2008.06.003, 2008.

Docherty, K. S., Aiken, A. C., Huffman, J. A., Ulbrich, I. M., DeCarlo, P. F., Sueper, D., Worsnop, D. R., Snyder, D. C., Peltier, R. E., Weber, R. J., Grover, B. D., Eatough, D. J., Williams, B. J., Goldstein, A. H., Ziemann, P. J., and Jimenez, J. L.: The 2005 Study of Organic Aerosols at Riverside (SOAR-1): instrumental intercomparisons and fine particle composition, Atmospheric Chemistry and Physics, 11, 12 387–12 420, doi:10.5194/acp-11-12387-2011, 2011.

Donahue, N. M., Kroll, J. H., Pandis, S. N., and Robinson, A. L.: A two-dimensional volatility basis set - Part 2: Diagnostics of organic-aerosol evolution, Atmospheric Chemistry and Physics, 12, 615–634, doi:10.5194/acp-12-615-2012, 2012.

Donaldson, K., Stone, V., Borm, P. J., Jimenez, L. A., Gilmour, P. S., Schins, R. P., Knaapen, A. M., Rahman, I., Faux, S. P., Brown, D. M., and MacNee, W.: Oxidative stress and calcium signaling in the adverse effects of environmental particles (PM_{10}), Free Radical Biology and Medicine, 34, 1369–1382, doi:http://dx.doi.org/10.1016/S0891-5849(03)00150-3, 2003.

Drewnick, F., Hings, S. S., DeCarlo, P., Jayne, J. T., Gonin, M., Fuhrer, K., Weimer, S., Jimenez, J. L., Demerjian, K. L., Borrmann, S., and Worsnop, D. R.: A New Time-of-Flight Aerosol Mass Spectrometer (TOF-AMS) - Instrument Description and First Field Deployment, Aerosol Science and Technology, 39, 637–658, doi:10.1080/02786820500182040, 2005.

Dzepina, K., Arey, J., Marr, L. C., Worsnop, D. R., Salcedo, D., Zhang, Q., Onasch, T. B., Molina, L. T., Molina, M. J., and Jimenez, J. L.: Detection of particle-phase polycyclic aromatic hydrocarbons in Mexico City using an aerosol mass spectrometer, International Journal of Mass Spectrometry, 263, 152–170, doi:http://dx.doi.org/10.1016/j.ijms.2007.01.010, 2007.

EEA: The European Environment - State and Outlook 2010: Synthesis, European Envrionment Agency, Copenhagen, 2010.

Enya, T., Suzuki, H., Watanabe, T., Hirayama, T., and Hisamatsu, Y.: 3-Nitrobenzanthrone, a Powerful Bacterial Mutagen and Suspected Human Carcinogen Found in Diesel Exhaust and Airborne Particulates, Environmental Science Technology, 31, 2772–2776, doi:10.1021/es961067i, 1997.

Fenger, J.: Urban air quality, Atmospheric Environment, 33, 4877–4900, doi:http://dx.doi.org/10.1016/S1352-2310(99)00290-3, 1999.

Fine, P. M., Chakrabarti, B., Krudysz, M., Schauer, J. J., and Sioutas, C.: Diurnal Variations of Individual Organic Compound Constituents of Ultrafine and Accumulation Mode Particulate Matter in the Los Angeles Basin, Environmental Science & Technology, 38, 1296–1304, doi:10.1021/es0348389, 2004.

Forster, P., Ramaswamy, V., Artaxo, P., Berntsen, T., Betts, R., Fahey, D. W., Haywood, J., Lean, J., Lowe, D. C., Myhre, G., Nganga, J., Prinn, R., Raga, G., M, S., and Van Dorland, R.: Changes in Atmospheric Constituents and in Radiative Forcing. In: Climate Change 2007: The Physical Science Basis. Contribution of Working Group I to the Fourth Assessment Report of the Intergovernmental Panel on Climate Change, Cambridge University Press, Cambridge, United Kingdom and New York, NY, USA, 881pp, 2007.

Fraser, M. P., Cass, G. R., and Simoneit, B. R. T.: Air Quality Model Evaluation Data for Organics. 6. C_3C_{24} Organic Acids, Environmental Science & Technology, 37, 446–453, doi:10.1021/es0209262, 2003.

Freutel, F., Schneider, J., Drewnick, F., von der Weiden-Reinmüller, S.-L., Crippa, M., Prévôt, A. S. H., Baltensperger, U., Poulain, L., Wiedensohler, A., Sciare, J., Sarda-Estève, R., Burkhart, J. F., Eckhardt, S., Stohl, A., Gros, V., Colomb, A., Michoud, V., Doussin, J. F., Borbon, A., Haeffelin, M., Morille, Y., Beekmann, M., and Borrmann, S.: Aerosol particle measurements at three stationary sites in the megacity of Paris during summer 2009: meteorology and air mass origin dominate aerosol particle composition and size distribution, Atmospheric Chemistry and Physics, 13, 933–959, doi:10.5194/acp-13-933-2013, 2013.

Friedlander, S. K.: Chemical element balances and identification of air pollution sources, Environmental Science & Technology, 7, 235–240, doi:10.1021/es60075a005, 1973.

Fuller, G. W., Tremper, A. H., Baker, T. D., Yttri, K. E., and Butterfield, D.: Contribution of wood burning to PM_{10} in London, Atmospheric Environment, 87, 87–94, doi:http://dx.doi.org/10.1016/j.atmosenv.2013.12.037, 2014.

Goldstein, A. H. and Galbally, I. E.: Known and unexplored organic constituents in the earth's atmosphere, Environmental Science & Technology, 41, 1514–1521, 2007.

Goldstein, A. H., Koven, C. D., Heald, C. L., and Fung, I. Y.: Biogenic carbon and anthropogenic pollutants combine to form a cooling haze over the southeastern United States, Proceedings of the National Academy of Sciences, 106, 8835–8840, doi: 10.1073/pnas.0904128106, 2009.

Grieshop, A. P., Donahue, N. M., and Robinson, A. L.: Laboratory investigation of photochemical oxidation of organic aerosol from wood fires 2: analysis of aerosol mass spectrometer data, Atmospheric Chemistry and Physics, 9, 2227–2240, doi: 10.5194/acp-9-2227-2009, 2009.

Guenther, A., Hewitt, C. N., Erickson, D., Fall, R., Geron, C., Graedel, T., Harley, P., Klinger, L., Lerdau, M., Mckay, W. A., Pierce, T., Scholes, B., Steinbrecher, R., Tallamraju, R., Taylor, J., and Zimmerman, P.: A global model of natural volatile organic compound emissions, Journal of Geophysical Research: Atmospheres, 100, 8873–8892, doi:10.1029/94JD02950, 1995.

Hallquist, M., Wenger, J. C., Baltensperger, U., Rudich, Y., Simpson, D., Claeys, M., Dommen, J., Donahue, N. M., George, C., Goldstein, A. H., Hamilton, J. F., Herrmann, H., Hoffmann, T., Iinuma, Y., Jang, M., Jenkin, M. E., Jimenez, J. L., Kiendler-Scharr, A., Maenhaut, W., McFiggans, G., Mentel, T. F., Monod, A., Prévôt, A. S. H., Seinfeld, J. H., Surratt, J. D., Szmigielski, R., and Wildt, J.: The formation, properties and impact of secondary organic aerosol: current and emerging issues, Atmospheric Chemistry and Physics, 9, 5155–5236, doi: 10.5194/acp-9-5155-2009, 2009.

Harrison, R. M. and Yin, J.: Particulate matter in the atmosphere: which particle properties are important for its effects on health?, Science of The Total Environment, 249, 85–101, doi:http://dx.doi.org/10.1016/S0048-9697(99)00513-6, 2000.

Harrison, R. M. and Yin, J.: Sources and processes affecting carbonaceous aerosol in central England, Atmospheric Environment, 42, 1413–1423, doi:http://dx.doi.org/10.1016/j.atmosenv.2007.11.004, 2008.

Harrison, R. M., Jones, A. M., and Lawrence, R. G.: Major component composition of PM_{10} and $PM_{2.5}$ from roadside and urban background sites, Atmospheric Environment, 38, 4531–4538, doi:http://dx.doi.org/10.1016/j.atmosenv.2004.05.022, 2004.

Harrison, R. M., Stedman, J., and Derwent, D.: New Directions: Why are PM_{10} concentrations in Europe not falling?, Atmospheric Environment, 42, 603–606, doi:http://dx.doi.org/10.1016/j.atmosenv.2007.11.023, 2008.

Harrison, R. M., Dall'Osto, M., Beddows, D. C. S., Thorpe, A. J., Bloss, W. J., Allan, J. D., Coe, H., Dorsey, J. R., Gallagher, M., Martin, C., Whitehead, J., Williams, P. I., Jones, R. L., Langridge, J. M., Benton, A. K., Ball, S. M., Langford, B., Hewitt, C. N., Davison, B., Martin, D., Petersson, K. F., Henshaw, S. J., White, I. R., Shallcross, D. E., Barlow, J. F., Dunbar, T., Davies, F., Nemitz, E., Phillips, G. J., Helfter, C., Di Marco, C. F., and Smith, S.: Atmospheric chemistry and physics in the atmosphere of a developed megacity (London): an overview of the REPARTEE experiment and its conclusions, Atmospheric Chemistry and Physics, 12, 3065–3114, doi:10.5194/acp-12-3065-2012, 2012.

Hayes, P. L., Ortega, A. M., Cubison, M. J., Froyd, K. D., Zhao, Y., Cliff, S. S., Hu, W. W., Toohey, D. W., Flynn, J. H., Lefer, B. L., Grossberg, N., Alvarez, S., Rappenglck, B., Taylor, J. W., Allan, J. D., Holloway, J. S., Gilman, J. B., Kuster, W. C., de Gouw, J. A., Massoli, P., Zhang, X., Liu, J., Weber, R. J., Corrigan, A. L., Russell, L. M., Isaacman, G., Worton, D. R., Kreisberg, N. M., Goldstein, A. H., Thalman, R., Waxman, E. M., Volkamer, R., Lin, Y. H., Surratt, J. D., Kleindienst, T. E., Offenberg, J. H., Dusanter, S., Griffith, S., Stevens, P. S., Brioude, J., Angevine, W. M., and Jimenez, J. L.: Organic aerosol composition and sources in Pasadena, California, during the 2010 CalNex campaign, Journal of Geophysical Research: Atmospheres, 118, 9233–9257, doi:10.1002/jgrd.50530, 2013.

He, L.-Y., Lin, Y., Huang, X.-F., Guo, S., Xue, L., Su, Q., Hu, M., Luan, S.-J., and Zhang, Y.-H.: Characterization of high-resolution aerosol mass spectra of primary organic aerosol emissions from Chinese cooking and biomass burning, Atmospheric Chemistry and Physics, 10, 11 535–11 543, doi:10.5194/acp-10-11535-2010, 2010.

Heal, M.: The application of carbon-14 analyses to the source apportionment of atmospheric carbonaceous particulate matter: a review, Analytical and Bioanalytical Chemistry, 406, 81–98, doi:10.1007/s00216-013-7404-1, 2014.

Heald, C. L., Jacob, D. J., Park, R. J., Russell, L. M., Huebert, B. J., Seinfeld, J. H., Liao, H., and Weber, R. J.: A large organic aerosol source in the free troposphere missing from current models, Geophysical Research Letters, 32, L18 809, doi:10.1029/2005GL023831, 2005.

Heald, C. L., Kroll, J. H., Jimenez, J. L., Docherty, K. S., DeCarlo, P. F., Aiken, A. C., Chen, Q., Martin, S. T., Farmer, D. K., and Artaxo, P.: A simplified description of the evolution of organic aerosol composition in the atmosphere, Geophysical Research Letters, 37, L08 803, doi:10.1029/2010GL042737, 2010.

Heintzenberg, J., Raes, F., and Schwartz, S. E.: Tropospheric aerosols, in: In Atmospheric Chemistry in a Changing World - An Integration and Synthesis of a Decade of Tropospheric Chemistry Research, Springer, 2003.

Hu, W. W., Hu, M., Yuan, B., Jimenez, J. L., Tang, Q., Peng, J. F., Hu, W., Shao, M., Wang, M., Zeng, L. M., Wu, Y. S., Gong, Z. H., Huang, X. F., and He, L. Y.: Insights on organic aerosol aging and the influence of coal combustion at a regional receptor site of central eastern China, Atmospheric Chemistry and Physics, 13, 10 095–10 112, doi:10.5194/acp-13-10095-2013, 2013.

Huang, Q., Wang, L., and Han, S.: The genotoxicity of substituted nitrobenzenes and the quantitative structure-activity relationship studies, Chemosphere, 30, 915 – 923, doi:http://dx.doi.org/10.1016/0045-6535(94)00450-9, 1995.

Huang, X.-F., He, L.-Y., Hu, M., Canagaratna, M. R., Sun, Y., Zhang, Q., Zhu, T., Xue, L., Zeng, L.-W., Liu, X.-G., Zhang, Y.-H., Jayne, J. T., Ng, N. L., and Worsnop, D. R.: Highly time-resolved chemical characterization of atmospheric submicron particles during 2008 Beijing Olympic Games using an Aerodyne High-Resolution Aerosol Mass Spectrometer, Atmospheric Chemistry and Physics, 10, 8933–8945, doi:10.5194/acp-10-8933-2010, 2010.

Huffman, J. A., Jayne, J. T., Drewnick, F., Aiken, A. C., Onasch, T., Worsnop, D. R., and Jimenez, J. L.: Design, Modeling, Optimization, and Experimental Tests of a Particle Beam Width Probe for the Aerodyne Aerosol Mass Spectrometer, Aerosol Science and Technology, 39, 1143–1163, doi:10.1080/02786820500423782, 2005.

Huffman, J. A., Docherty, K. S., Aiken, A. C., Cubison, M. J., Ulbrich, I. M., DeCarlo, P. F., Sueper, D., Jayne, J. T., Worsnop, D. R., Ziemann, P. J., and Jimenez, J. L.: Chemically-resolved aerosol volatility measurements from two

megacity field studies, Atmospheric Chemistry and Physics, 9, 7161–7182, doi: 10.5194/acp-9-7161-2009, 2009.

Ibald-Mulli, A., Wichmann, H.-E., Kreyling, W., and Peters, A.: Epidemiological evidence on health effects of ultrafine particles., Journal of Aerosol Medicine, 15, 189–201, doi:10.1089/089426802320282310, 2002.

Jacobson, M. Z.: Atmospheric Pollution: History, Science, and Regulation, Cambridge University Press, 2002.

Jathar, S. H., Farina, S. C., Robinson, A. L., and Adams, P. J.: The influence of semi-volatile and reactive primary emissions on the abundance and properties of global organic aerosol, Atmospheric Chemistry and Physics, 11, 7727–7746, doi:10.5194/acp-11-7727-2011, 2011.

Jayne, J. T., Leard, D. C., Zhang, X., Davidovits, P., Smith, K. A., Kolb, C. E., and Worsnop, D. R.: Development of an Aerosol Mass Spectrometer for Size and Composition Analysis of Submicron Particles, Aerosol Science and Technology, 33, 49–70, doi:10.1080/027868200410840, 2000.

Jimenez, J. L., Jayne, J. T., Shi, Q., Kolb, C. E., Worsnop, D. R., Yourshaw, I., Seinfeld, J. H., Flagan, R. C., Zhang, X., Smith, K. A., Morris, J. W., and Davidovits, P.: Ambient aerosol sampling using the Aerodyne Aerosol Mass Spectrometer, Journal of Geophysical Research: Atmospheres, 108, 1–13, doi:10.1029/2001JD001213, 2003.

Jimenez, J. L., Canagaratna, M. R., Donahue, N. M., Prevot, A. S. H., Zhang, Q., Kroll, J. H., DeCarlo, P. F., Allan, J. D., Coe, H., Ng, N. L., Aiken, A. C., Docherty, K. S., Ulbrich, I. M., Grieshop, A. P., Robinson, A. L., Duplissy, J., Smith, J. D., Wilson, K. R., Lanz, V. A., Hueglin, C., Sun, Y. L., Tian, J., Laaksonen, A., Raatikainen, T., Rautiainen, J., Vaattovaara, P., Ehn, M., Kulmala, M., Tomlinson, J. M., Collins, D. R., Cubison, M. J., E., Dunlea, J., Huffman, J. A., Onasch, T. B., Alfarra, M. R., Williams, P. I., Bower, K., Kondo, Y., Schneider, J., Drewnick, F., Borrmann, S., Weimer, S., Demerjian, K., Salcedo, D., Cottrell, L., Griffin, R., Takami, A., Miyoshi, T., Hatakeyama, S., Shimono, A., Sun, J. Y., Zhang, Y. M., Dzepina, K., Kimmel, J. R., Sueper, D., Jayne, J. T., Herndon, S. C., Trimborn, A. M., Williams, L. R., Wood, E. C., Middlebrook, A. M., Kolb, C. E., Baltensperger, U., and Worsnop, D. R.: Evolution of Organic Aerosols in the Atmosphere, Science, 326, 1525–1529, doi:10.1126/science.1180353, 2009.

Johnson, D., Utembe, S. R., Jenkin, M. E., Derwent, R. G., Hayman, G. D., Alfarra, M. R., Coe, H., and McFiggans, G.: Simulating regional scale secondary organic aerosol formation during the TORCH 2003 campaign in the southern UK, Atmospheric Chemistry and Physics, 6, 403–418, doi:10.5194/acp-6-403-2006, 2006.

Jolleys, M. D., Coe, H., McFiggans, G., Capes, G., Allan, J. D., Crosier, J., Williams, P. I., Allen, G., Bower, K. N., Jimenez, J. L., Russell, L. M., Grutter, M., and Baumgardner, D.: Characterizing the Aging of Biomass Burning Organic Aerosol by Use of Mixing Ratios: A Meta-analysis of Four Regions, Environmental Science Technology, 46, 13 093–13 102, doi:10.1021/es302386v, 2012.

Jolleys, M. D., Coe, H., McFiggans, G., Taylor, J., OShea, S. J., Le Breton, M., Bauguitte, S. J.-B., Moller, S., Di Carlo, P., Aruffo, E., Palmer, P. I., and Lee, J. D.: Properties and evolution of biomass burning organic aerosol from Canadian boreal forest fires, submitted, 2014.

Kanakidou, M., Seinfeld, J. H., Pandis, S. N., Barnes, I., Dentener, F. J., Facchini, M. C., Van Dingenen, R., Ervens, B., Nenes, A., Nielsen, C. J., Swietlicki, E., Putaud, J. P., Balkanski, Y., Fuzzi, S., Horth, J., Moortgat, G. K., Winterhalter, R., Myhre, C. E. L., Tsigaridis, K., Vignati, E., Stephanou, E. G., and Wilson, J.: Organic aerosol and global climate modelling: a review, Atmospheric Chemistry and Physics, 5, 1053–1123, doi:10.5194/acp-5-1053-2005, 2005.

Kim, S., Kramer, R. W., and Hatcher, P. G.: Graphical Method for Analysis of Ultrahigh-Resolution Broadband Mass Spectra of Natural Organic Matter, the Van Krevelen Diagram, Analytical Chemistry, 75, 5336–5344, doi:10.1021/ac034415p, 2003.

Koelemeijer, R., Homan, C., and Matthijsen, J.: Comparison of spatial and temporal variations of aerosol optical thickness and particulate matter over Europe, Atmospheric Environment, 40, 5304–5315, doi:http://dx.doi.org/10.1016/j.atmosenv.2006.04.044, 2006.

Kroll, J. H., Donahue, N. M., Jimenez, J. L., Kessler, S. H., Canagaratna, M. R., Wilson, K. R., Altieri, K. E., Mazzoleni, L. R., Wozniak, A. S., Bluhm, H., Mysak, E. R., Smith, J. D., Kolb, C. E., and Worsnop, D. R.: Carbon oxidation state as a metric for describing the chemistry of atmospheric organic aerosol, Nature Chemistry, 3, 133–139, doi:10.1038/nchem.948, 2011.

Laj, P., Klausen, J., Bilde, M., Pla-Duelmer, C., Pappalardo, G., Clerbaux, C., Baltensperger, U., Hjorth, J., Simpson, D., Reimann, S., Coheur, P.-F., Richter, A., Mazire, M. D., Rudich, Y., McFiggans, G., Torseth, K., Wiedensohler, A., Morin, S., Schulz, M., Allan, J., Atti, J.-L., Barnes, I., Birmili, W., Cammas, J., Dommen, J., Dorn, H.-P., Fowler, D., Fuzzi, S., Glasius, M., Granier, C., Hermann, M., Isaksen, I., Kinne, S., Koren, I., Madonna, F., Maione, M., Massling, A., Moehler, O., Mona, L., Monks, P., Mller, D., Mller, T., Orphal, J., Peuch, V.-H., Stratmann, F., Tanr, D., Tyndall, G., Riziq, A. A., Roozendael, M. V., Villani, P., Wehner, B., Wex, H., and Zardini, A.: Measuring atmospheric composition change, Atmospheric Environment, 43, 5351 – 5414, doi:http://dx.doi.org/10.1016/j.atmosenv.2009.08.020, 2009.

Lambe, A. T., Chacon-Madrid, H. J., Nguyen, N. T., Weitkamp, E. A., Kreisberg, N. M., Hering, S. V., Goldstein, A. H., Donahue, N. M., and Robinson, A. L.: Organic Aerosol Speciation: Intercomparison of Thermal Desorption Aerosol GC/MS (TAG) and Filter-Based Techniques, Aerosol Science and Technology, 44, 141–151, doi:10.1080/02786820903447206, 2010.

Lanz, V. A., Alfarra, M. R., Baltensperger, U., Buchmann, B., Hueglin, C., and Prévôt, A. S. H.: Source apportionment of submicron organic aerosols at an urban site by factor analytical modelling of aerosol mass spectra, Atmospheric Chemistry and Physics, 7, 1503–1522, doi:10.5194/acp-7-1503-2007, 2007.

Lanz, V. A., Alfarra, M. R., Baltensperger, U., Buchmann, B., Hueglin, C., Szidat, S., Wehrli, M. N., Wacker, L., Weimer, S., Caseiro, A., Puxbaum, H., and Prévôt, A. S. H.: Source Attribution of Submicron Organic Aerosols during Wintertime Inversions by Advanced Factor Analysis of Aerosol Mass Spectra, Environmental Science Technology, 42, 214–220, doi:10.1021/es0707207, 2008.

Liu, D., Allan, J. D., Young, D. E., Coe, H., Beddows, D., Fleming, Z. L., Flynn, M. J., Gallagher, M. W., Harrison, R. M., Lee, J., Prevot, A. S. H., Taylor, J. W., Yin, J., Williams, P. I., and Zotter, P.: Size distribution, mixing state and source apportionment of black carbon aerosol in London during wintertime, Atmospheric Chemistry and Physics, 14, 10 061–10 084, doi:10.5194/acp-14-10061-2014, 2014.

Liu, P., Ziemann, P. J., Kittelson, D. B., and McMurry, P. H.: Generating Particle Beams of Controlled Dimensions and Divergence: I. Theory of Particle Motion in

Aerodynamic Lenses and Nozzle Expansions, Aerosol Science and Technology, 22, 293–313, doi:10.1080/02786829408959748, 1995a.

Liu, P., Ziemann, P. J., Kittelson, D. B., and McMurry, P. H.: Generating Particle Beams of Controlled Dimensions and Divergence: II. Experimental Evaluation of Particle Motion in Aerodynamic Lenses and Nozzle Expansions, Aerosol Science and Technology, 22, 314–324, doi:10.1080/02786829408959749, 1995b.

Martin, C. L., Allan, J. D., Crosier, J., Choularton, T. W., Coe, H., and Gallagher, M. W.: Seasonal variation of fine particulate composition in the centre of a UK city, Atmospheric Environment, 45, 4379–4389, doi:http://dx.doi.org/10.1016/j.atmosenv.2011.05.050, 2011.

Matthew, B. M., Middlebrook, A. M., and Onasch, T. B.: Collection Efficiencies in an Aerodyne Aerosol Mass Spectrometer as a Function of Particle Phase for Laboratory Generated Aerosols, Aerosol Science and Technology, 42, 884–898, doi:10.1080/02786820802356797, 2008.

Mazzei, F., D'Alessandro, A., Lucarelli, F., Nava, S., Prati, P., Valli, G., and Vecchi, R.: Characterization of particulate matter sources in an urban environment, Science of The Total Environment, 401, 81–89, doi:http://dx.doi.org/10.1016/j.scitotenv.2008.03.008, 2008.

Megaritis, A. G., Fountoukis, C., Charalampidis, P. E., Pilinis, C., and Pandis, S. N.: Response of fine particulate matter concentrations to changes of emissions and temperature in Europe, Atmospheric Chemistry and Physics, 13, 3423–3443, doi:10.5194/acp-13-3423-2013, 2013.

Middlebrook, A. M., Bahreini, R., Jimenez, J. L., and Canagaratna, M. R.: Evaluation of Composition-Dependent Collection Efficiencies for the Aerodyne Aerosol Mass Spectrometer using Field Data, Aerosol Science and Technology, 46, 258–271, doi:10.1080/02786826.2011.620041, 2012.

Misra, A., Passant, N. R., Murrells, T. P., Thistlethwaite, G., Pang, Y., Norris, J., Walker, C., Stewart, R. A., MacCarthy, J., and Pierce, M.: UK Emission Projections of Air Quality Pollutants to 2030, National Atmospheric Emissions Inventory, 2012.

Misselbrook, T., Cape, J., Cardenas, L., Chadwick, D., Dragosits, U., Hobbs, P.,

Nemitz, E., Reis, S., Skiba, U., and Sutton, M.: Key unknowns in estimating atmospheric emissions from UK land management, Atmospheric Environment, 45, 1067–1074, doi:http://dx.doi.org/10.1016/j.atmosenv.2010.11.014, 2011.

Mohr, C., DeCarlo, P. F., Heringa, M. F., Chirico, R., Slowik, J. G., Richter, R., Reche, C., Alastuey, A., Querol, X., Seco, R., Peñuelas, J., Jiménez, J. L., Crippa, M., Zimmermann, R., Baltensperger, U., and Prévôt, A. S. H.: Identification and quantification of organic aerosol from cooking and other sources in Barcelona using aerosol mass spectrometer data, Atmospheric Chemistry and Physics, 12, 1649–1665, doi:10.5194/acp-12-1649-2012, 2012.

Mohr, C., Lopez-Hilfiker, F. D., Zotter, P., Prévôt, A. S. H., Xu, L., Ng, N. L., Herndon, S. C., Williams, L. R., Franklin, J. P., Zahniser, M. S., Worsnop, D. R., Knighton, W. B., Aiken, A. C., Gorkowski, K. J., Dubey, M. K., Allan, J. D., and Thornton, J. A.: Contribution of Nitrated Phenols to Wood Burning Brown Carbon Light Absorption in Detling, United Kingdom during Winter Time, Environmental Science Technology, 47, 6316–6324, doi:10.1021/es400683v, 2013.

Monks, P., Granier, C., Fuzzi, S., Stohl, A., Williams, M., Akimoto, H., Amann, M., Baklanov, A., Baltensperger, U., Bey, I., Blake, N., Blake, R., Carslaw, K., Cooper, O., Dentener, F., Fowler, D., Fragkou, E., Frost, G., Generoso, S., Ginoux, P., Grewe, V., Guenther, A., Hansson, H., Henne, S., Hjorth, J., Hofzumahaus, A., Huntrieser, H., Isaksen, I., Jenkin, M., Kaiser, J., Kanakidou, M., Klimont, Z., Kulmala, M., Laj, P., Lawrence, M., Lee, J., Liousse, C., Maione, M., McFiggans, G., Metzger, A., Mieville, A., Moussiopoulos, N., Orlando, J., O'Dowd, C., Palmer, P., Parrish, D., Petzold, A., Platt, U., Pöschl, U., Prévôt, A., Reeves, C., Reimann, S., Rudich, Y., Sellegri, K., Steinbrecher, R., Simpson, D., ten Brink, H., Theloke, J., van der Werf, G., Vautard, R., Vestreng, V., Vlachokostas, C., and von Glasow, R.: Atmospheric composition change global and regional air quality, Atmospheric Environment, 43, 5268–5350, doi:http://dx.doi.org/10.1016/j.atmosenv.2009.08.021, 2009.

Morgan, W. T., Allan, J. D., Bower, K. N., Esselborn, M., Harris, B., Henzing, J. S., Highwood, E. J., Kiendler-Scharr, A., McMeeking, G. R., Mensah, A. A., Northway, M. J., Osborne, S., Williams, P. I., Krejci, R., and Coe, H.: Enhancement of the aerosol direct radiative effect by semi-volatile aerosol components: airborne measurements in North-Western Europe, Atmospheric Chemistry and Physics, 10, 8151–8171, doi:10.5194/acp-10-8151-2010, 2010a.

Morgan, W. T., Allan, J. D., Bower, K. N., Highwood, E. J., Liu, D., McMeeking, G. R., Northway, M. J., Williams, P. I., Krejci, R., and Coe, H.: Airborne measurements of the spatial distribution of aerosol chemical composition across Europe and evolution of the organic fraction, Atmospheric Chemistry and Physics, 10, 4065–4083, doi:10.5194/acp-10-4065-2010, 2010b.

Murphy, D. M., Middlebrook, A. M., and Warshawsky, M.: Cluster Analysis of Data from the Particle Analysis by Laser Mass Spectrometry (PALMS) Instrument, Aerosol Science and Technology, 37, 382–391, doi:10.1080/02786820300971, 2003.

NAEI: National atmospheric emissions inventory, URL `http://naei.defra.gov.uk/`, 2014.

Nawrot, T. S., Torfs, R., Fierens, F., De Henauw, S., Hoet, P. H., Van Kersschaever, G., De Backer, G., and Nemery, B.: Stronger associations between daily mortality and fine particulate air pollution in summer than in winter: evidence from a heavily polluted region in western Europe, Journal of Epidemiology and Community Health, 61, 146–149, doi:10.1136/jech.2005.044263, 2007.

Ng, N. L., Canagaratna, M. R., Zhang, Q., Jimenez, J. L., Tian, J., Ulbrich, I. M., Kroll, J. H., Docherty, K. S., Chhabra, P. S., Bahreini, R., Murphy, S. M., Seinfeld, J. H., Hildebrandt, L., Donahue, N. M., DeCarlo, P. F., Lanz, V. A., Prévôt, A. S. H., Dinar, E., Rudich, Y., and Worsnop, D. R.: Organic aerosol components observed in Northern Hemispheric datasets from Aerosol Mass Spectrometry, Atmospheric Chemistry and Physics, 10, 4625–4641, doi:10.5194/acp-10-4625-2010, 2010.

Ng, N. L., Canagaratna, M. R., Jimenez, J. L., Chhabra, P. S., Seinfeld, J. H., and Worsnop, D. R.: Changes in organic aerosol composition with aging inferred from aerosol mass spectra, Atmospheric Chemistry and Physics, 11, 6465–6474, doi:10.5194/acp-11-6465-2011, 2011a.

Ng, N. L., Herndon, S. C., Trimborn, A., Canagaratna, M. R., Croteau, P. L., Onasch, T. B., Sueper, D., Worsnop, D. R., Zhang, Q., Sun, Y. L., and Jayne, J. T.: An Aerosol Chemical Speciation Monitor (ACSM) for Routine Monitoring of the Composition and Mass Concentrations of Ambient Aerosol, Aerosol Science and Technology, 45, 780–794, doi:10.1080/02786826.2011.560211, 2011b.

Oberdörster, G.: Pulmonary effects of inhaled ultrafine particles, International Archives of Occupational and Environmental Health, 74, 1–8, doi:10.1007/s004200000185, 2000.

Oberdörster, G., Sharp, Z., Atudorei, V., Elder, A., Gelein, R., Kreyling, W., and Cox, C.: Translocation of Inhaled Ultrafine Particles to the Brain, Inhalation Toxicology, 16, 437–445, doi:10.1080/08958370490439597, 2004.

Oberdörster, G., Oberdörster, E., and Oberdörster, J.: Nanotoxicology: An Emerging Discipline Evolving from Studies of Ultrafine Particles, Environmental Health Perspectives, 113, 823–839, 2005.

Onasch, T. B., Trimborn, A., Fortner, E. C., Jayne, J. T., Kok, G. L., Williams, L. R., Davidovits, P., and Worsnop, D. R.: Soot Particle Aerosol Mass Spectrometer: Development, Validation, and Initial Application, Aerosol Science and Technology, 46, 804–817, doi:10.1080/02786826.2012.663948, 2012.

ONS: Annual Mid-year Population Estimates, 2013, Office for National Statistics, Government Buildings, Cardiff Road, Newport NP10 8XG, URL `http://www.ons.gov.uk`, 2014.

Paatero, P.: Least squares formulation of robust non-negative factor analysis, Chemometrics and Intelligent Laboratory Systems, 37, 23–35, doi:http://dx.doi.org/10.1016/S0169-7439(96)00044-5, 1997.

Paatero, P. and Tapper, U.: Positive matrix factorization: A non-negative factor model with optimal utilization of error estimates of data values, Environmetrics, 5, 111–126, doi:10.1002/env.3170050203, 1994.

Paatero, P., Hopke, P. K., Song, X.-H., and Ramadan, Z.: Understanding and controlling rotations in factor analytic models, Chemometrics and Intelligent Laboratory Systems, 60, 253–264, doi:http://dx.doi.org/10.1016/S0169-7439(01)00200-3, 2002.

Paglione, M., Saarikoski, S., Carbone, S., Hillamo, R., Facchini, M. C., Finessi, E., Giulianelli, L., Carbone, C., Fuzzi, S., Moretti, F., Tagliavini, E., Swietlicki, E., Eriksson Stenström, K., Prévôt, A. S. H., Massoli, P., Canaragatna, M., Worsnop, D., and Decesari, S.: Primary and secondary biomass burning aerosols determined

by proton nuclear magnetic resonance (^{1}H-NMR) spectroscopy during the 2008 EUCAARI campaign in the Po Valley (Italy), Atmospheric Chemistry and Physics, 14, 5089–5110, doi:10.5194/acp-14-5089-2014, 2014.

Pandis, S. N., Harley, R. A., Cass, G. R., and Seinfeld, J. H.: Secondary organic aerosol formation and transport, Atmospheric Environment. Part A. General Topics, 26, 2269–2282, doi:http://dx.doi.org/10.1016/0960-1686(92)90358-R, 1992.

Passant, N., Wagner, A., Murrells, T., Li, Y., Okamura, S., Thistlethwaite, G., Walker, H., Walker, C., Whiting, R., Sneddon, S., Stewart, R., Broph, N., MacCarthy, J., Tsagatakis, I., and Bush, T.: UK Informative Inventory Report (1980 to 2009), URL http://uk-air.defra.gov.uk/reports/cat07/1103150849_UK_2011_CLRTAP_IIR.pdf, 2011.

Pope, C. A. and Dockery, D. W.: Health Effects of Fine Particulate Air Pollution: Lines that Connect, Journal of the Air amp; Waste Management Association, 56, 709–742, doi:10.1080/10473289.2006.10464485, 2006.

Pöschl, U.: Atmospheric Aerosols: Composition, Transformation, Climate and Health Effects, Angewandte Chemie International Edition, 44, 7520–7540, doi:10.1002/anie.200501122, 2005.

Putaud, J.-P., Raes, F., Dingenen, R. V., Brüggemann, E., Facchini, M.-C., Decesari, S., Fuzzi, S., Gehrig, R., Hüglin, C., Laj, P., Lorbeer, G., Maenhaut, W., Mihalopoulos, N., Müller, K., Querol, X., Rodriguez, S., Schneider, J., Spindler, G., ten Brink, H., Trseth, K., and Wiedensohler, A.: A European aerosol phenomenology2: chemical characteristics of particulate matter at kerbside, urban, rural and background sites in Europe, Atmospheric Environment, 38, 2579–2595, doi:http://dx.doi.org/10.1016/j.atmosenv.2004.01.041, 2004.

Pye, H. O. T. and Seinfeld, J. H.: A global perspective on aerosol from low-volatility organic compounds, Atmospheric Chemistry and Physics, 10, 4377–4401, doi:10.5194/acp-10-4377-2010, 2010.

Quincey, P., Butterfield, D., Green, D., Coyle, M., and Cape, J. N.: An evaluation of measurement methods for organic, elemental and black carbon in ambient air monitoring sites, Atmospheric Environment, 43, 5085–5091, doi:http://dx.doi.org/10.1016/j.atmosenv.2009.06.041, 2009.

Quinn, P. K., Bates, T. S., Coffman, D., Onasch, T. B., Worsnop, D., Baynard, T., de Gouw, J. A., Goldan, P. D., Kuster, W. C., Williams, E., Roberts, J. M., Lerner, B., Stohl, A., Pettersson, A., and Lovejoy, E. R.: Impacts of sources and aging on submicrometer aerosol properties in the marine boundary layer across the Gulf of Maine, Journal of Geophysical Research: Atmospheres, 111, 1–20, doi:10.1029/2006JD007582, 2006.

Ramgolam, K., Favez, O., Cachier, H., Gaudichet, A., Marano, F., Martinon, L., and Baeza-Squiban, A.: Size-partitioning of an urban aerosol to identify particle determinants involved in the proinflammatory response induced in airway epithelial cells, Particle and Fibre Toxicology, 6, 10, doi:10.1186/1743-8977-6-10, 2009.

Reis, S., Pinder, R. W., Zhang, M., Lijie, G., and Sutton, M. A.: Reactive nitrogen in atmospheric emission inventories, Atmospheric Chemistry and Physics, 9, 7657–7677, doi:10.5194/acp-9-7657-2009, 2009.

Roe, S. M., Spivey, M. D., Lindquist, H. C., Hemmer, P., and Huntley, R.: National Emissions Inventory for Commercial Cooking, The U.S. Environmental Protec- tion Agency (EPA) Emission Factor and Inventory Group (EFIG), 2002.

Rogge, W. F., Hildemann, L. M., Mazurek, M. A., Cass, G. R., and Simoneit, B. R. T.: Sources of fine organic aerosol. 1. Charbroilers and meat cooking operations, Environmental Science Technology, 25, 1112–1125, doi:10.1021/es00018a015, 1991.

Russell, A. and Dennis, R.: NARSTO critical review of photochemical models and modeling, Atmospheric Environment, 34, 2283–2324, doi:http://dx.doi.org/10.1016/S1352-2310(99)00468-9, 2000.

Saarikoski, S., Timonen, H., Saarnio, K., Aurela, M., Järvi, L., Keronen, P., Kerminen, V.-M., and Hillamo, R.: Sources of organic carbon in fine particulate matter in northern European urban air, Atmospheric Chemistry and Physics, 8, 6281–6295, doi:10.5194/acp-8-6281-2008, 2008.

Salcedo, D., Onasch, T. B., Canagaratna, M. R., Dzepina, K., Huffman, J. A., Jayne, J. T., Worsnop, D. R., Kolb, C. E., Weimer, S., Drewnick, F., Allan, J. D., Delia, A. E., and Jimenez, J. L.: Technical Note: Use of a beam width probe in an Aerosol Mass Spectrometer to monitor particle collection efficiency in the field, Atmospheric Chemistry and Physics, 7, 549–556, doi:10.5194/acp-7-549-2007, 2007.

Schaap, M., Mller, K., and ten Brink, H.: Constructing the European aerosol nitrate concentration field from quality analysed data, Atmospheric Environment, 36, 1323–1335, doi:http://dx.doi.org/10.1016/S1352-2310(01)00556-8, 2002.

Schaap, M., Otjes, R. P., and Weijers, E. P.: Illustrating the benefit of using hourly monitoring data on secondary inorganic aerosol and its precursors for model evaluation, Atmospheric Chemistry and Physics, 11, 11 041–11 053, doi:10.5194/acp-11-11041-2011, 2011.

Schauer, J. J., Rogge, W. F., Hildemann, L. M., Mazurek, M. A., Cass, G. R., and Simoneit, B. R.: Source apportionment of airborne particulate matter using organic compounds as tracers, Atmospheric Environment, 30, 3837–3855, doi:http://dx.doi.org/10.1016/1352-2310(96)00085-4, 1996.

Schauer, J. J., Fraser, M. P., Cass, G. R., and Simoneit, B. R. T.: Source Reconciliation of Atmospheric Gas-Phase and Particle-Phase Pollutants during a Severe Photochemical Smog Episode, Environmental Science Technology, 36, 3806–3814, doi:10.1021/es011458j, 2002.

Schwartz, J., Dockery, D. W., and Neas, L. M.: Is Daily Mortality Associated Specifically with Fine Particles?, Journal of the Air amp; Waste Management Association, 46, 927–939, doi:10.1080/10473289.1996.10467528, 1996.

Schwarz, J. P., Spackman, J. R., Fahey, D. W., Gao, R. S., Lohmann, U., Stier, P., Watts, L. A., Thomson, D. S., Lack, D. A., Pfister, L., Mahoney, M. J., Baumgardner, D., Wilson, J. C., and Reeves, J. M.: Coatings and their enhancement of black carbon light absorption in the tropical atmosphere, Journal of Geophysical Research: Atmospheres, 113, 1–10, doi:10.1029/2007JD009042, 2008.

Seinfeld, J. and Pandis, S.: Atmospheric chemistry and physics: from air pollution to climate change, John Wiley & Sons, New York, 1998, 2006.

Simon, H., Allen, D. T., and Wittig, A. E.: Fine Particulate Matter Emissions Inventories: Comparisons of Emissions Estimates with Observations from Recent Field Programs, Journal of the Air & Waste Management Association, 58, 320–343, doi:10.3155/1047-3289.58.2.320, 2008.

Skjøth, C. A., Geels, C., Berge, H., Gyldenkærne, S., Fagerli, H., Ellermann, T., Frohn, L. M., Christensen, J., Hansen, K. M., Hansen, K., and Hertel, O.: Spatial and temporal variations in ammonia emissions a freely accessible model code

for Europe, Atmospheric Chemistry and Physics, 11, 5221–5236, doi:10.5194/acp-11-5221-2011, 2011.

Spracklen, D. V., Jimenez, J. L., Carslaw, K. S., Worsnop, D. R., Evans, M. J., Mann, G. W., Zhang, Q., Canagaratna, M. R., Allan, J., Coe, H., McFiggans, G., Rap, A., and Forster, P.: Aerosol mass spectrometer constraint on the global secondary organic aerosol budget, Atmospheric Chemistry and Physics, 11, 12 109–12 136, doi:10.5194/acp-11-12109-2011, 2011.

Stelson, A. W. and Seinfeld, J. H.: Relative humidity and temperature dependence of the ammonium nitrate dissociation constant, Atmospheric Environment (1967), 16, 983–992, doi:http://dx.doi.org/10.1016/0004-6981(82)90184-6, 1982.

Strader, R., Lurmann, F., and Pandis, S. N.: Evaluation of secondary organic aerosol formation in winter, Atmospheric Environment, 33, 4849–4863, doi:http://dx.doi.org/10.1016/S1352-2310(99)00310-6, 1999.

Sun, Y., Wang, Z., Dong, H., Yang, T., Li, J., Pan, X., Chen, P., and Jayne, J. T.: Characterization of summer organic and inorganic aerosols in Beijing, China with an Aerosol Chemical Speciation Monitor, Atmospheric Environment, 51, 250–259, doi:http://dx.doi.org/10.1016/j.atmosenv.2012.01.013, 2012.

Sun, Y.-L., Zhang, Q., Schwab, J. J., Demerjian, K. L., Chen, W.-N., Bae, M.-S., Hung, H.-M., Hogrefe, O., Frank, B., Rattigan, O. V., and Lin, Y.-C.: Characterization of the sources and processes of organic and inorganic aerosols in New York city with a high-resolution time-of-flight aerosol mass spectrometer, Atmospheric Chemistry and Physics, 11, 1581–1602, doi:10.5194/acp-11-1581-2011, 2011.

Sun, Y. L., Wang, Z. F., Fu, P. Q., Yang, T., Jiang, Q., Dong, H. B., Li, J., and Jia, J. J.: Aerosol composition, sources and processes during wintertime in Beijing, China, Atmospheric Chemistry and Physics, 13, 4577–4592, doi:10.5194/acp-13-4577-2013, 2013.

Sutton, M. A., Dragosits, U., Tang, Y. S., and Fowler, D.: Ammonia emissions from non-agricultural sources in the UK, Atmospheric Environment, 34, 855 – 869, doi:http://dx.doi.org/10.1016/S1352-2310(99)00362-3, 2000.

Szidat, S., Jenk, T. M., Synal, H.-A., Kalberer, M., Wacker, L., Hajdas, I., Kasper-Giebl, A., and Baltensperger, U.: Contributions of fossil fuel, biomass-burning, and

biogenic emissions to carbonaceous aerosols in Zurich as traced by ^{14}C, Journal of Geophysical Research: Atmospheres, 111, D07 206, doi:10.1029/2005JD006590, 2006.

Tao, J., Gao, J., Zhang, L., Zhang, R., Che, H., Zhang, Z., Lin, Z., Jing, J., Cao, J., and Hsu, S.-C.: $PM_{2.5}$ pollution in a megacity of southwest China: source apportionment and implication, Atmospheric Chemistry and Physics, 14, 8679–8699, doi:10.5194/acp-14-8679-2014, 2014.

Thorpe, A. and Harrison, R. M.: Sources and properties of non-exhaust particulate matter from road traffic: A review, Science of The Total Environment, 400, 270–282, doi:http://dx.doi.org/10.1016/j.scitotenv.2008.06.007, 2008.

Trivitayanurak, W. and Adams, P. J.: Does the POA-SOA split matter for global CCN formation?, Atmospheric Chemistry and Physics, 14, 995–1010, doi:10.5194/acp-14-995-2014, 2014.

Tsigaridis, K. and Kanakidou, M.: Global modelling of secondary organic aerosol in the troposphere: a sensitivity analysis, Atmospheric Chemistry and Physics, 3, 1849–1869, doi:10.5194/acp-3-1849-2003, 2003.

Turpin, B. J. and Huntzicker, J. J.: Secondary formation of organic aerosol in the Los Angeles basin: A descriptive analysis of organic and elemental carbon concentrations, Atmospheric Environment. Part A. General Topics, 25, 207–215, doi:http://dx.doi.org/10.1016/0960-1686(91)90291-E, 1991.

Ulbrich, I. M., Canagaratna, M. R., Zhang, Q., Worsnop, D. R., and Jimenez, J. L.: Interpretation of organic components from Positive Matrix Factorization of aerosol mass spectrometric data, Atmospheric Chemistry and Physics, 9, 2891–2918, doi:10.5194/acp-9-2891-2009, 2009.

Van Krevelen, D. W.: Graphical-statistical method for the study of structure and reaction processes of coal, Fuel, 24, 269–284, 1950.

Volkamer, R., Jimenez, J. L., San Martini, F., Dzepina, K., Zhang, Q., Salcedo, D., Molina, L. T., Worsnop, D. R., and Molina, M. J.: Secondary organic aerosol formation from anthropogenic air pollution: Rapid and higher than expected, Geophysical Research Letters, 33, 1–4, doi:10.1029/2006GL026899, 2006.

Wagener, S., Langner, M., Hansen, U., Moriske, H.-J., and Endlicher, W. R.: Source apportionment of organic compounds in Berlin using positive matrix factorization Assessing the impact of biogenic aerosol and biomass burning on urban particulate matter, Science of The Total Environment, 435436, 392–401, doi:http://dx.doi.org/10.1016/j.scitotenv.2012.07.039, 2012a.

Wagener, S., Langner, M., Hansen, U., Moriske, H.-J., and Endlicher, W. R.: Spatial and seasonal variations of biogenic tracer compounds in ambient PM_{10} and PM_1 samples in Berlin, Germany, Atmospheric Environment, 47, 33–42, doi:http://dx.doi.org/10.1016/j.atmosenv.2011.11.044, 2012b.

Waked, A., Favez, O., Alleman, L. Y., Piot, C., Petit, J.-E., Delaunay, T., Verlinden, E., Golly, B., Besombes, J.-L., Jaffrezo, J.-L., and Leoz-Garziandia, E.: Source apportionment of PM_{10} in a north-western Europe regional urban background site (Lens, France) using positive matrix factorization and including primary biogenic emissions, Atmospheric Chemistry and Physics, 14, 3325–3346, doi:10.5194/acp-14-3325-2014, 2014.

Wang, S. C. and Flagan, R. C.: Scanning Electrical Mobility Spectrometer, Aerosol Science and Technology, 13, 230–240, doi:10.1080/02786829008959441, 1990.

Watson, J. G.: Visibility: Science and Regulation, Journal of the Air & Waste Management Association, 52, 628–713, doi:10.1080/10473289.2002.10470813, 2002.

Watson, J. G., Cooper, J. A., and Huntzicker, J. J.: The effective variance weighting for least squares calculations applied to the mass balance receptor model, Atmospheric Environment (1967), 18, 1347–1355, doi:http://dx.doi.org/10.1016/0004-6981(84)90043-X, 1984.

Weber, R. J., Sullivan, A. P., Peltier, R. E., Russell, A., Yan, B., Zheng, M., de Gouw, J., Warneke, C., Brock, C., Holloway, J. S., Atlas, E. L., and Edgerton, E.: A study of secondary organic aerosol formation in the anthropogenic-influenced southeastern United States, Journal of Geophysical Research: Atmospheres, 112, 1–13, doi:10.1029/2007JD008408, 2007.

Weimer, S., Drewnick, F., Hogrefe, O., Schwab, J. J., Rhoads, K., Orsini, D., Canagaratna, M., Worsnop, D. R., and Demerjian, K. L.: Size-selective nonrefractory ambient aerosol measurements during the Particulate Matter Technology Assessment and Characterization StudyNew York 2004 Winter Intensive in New

York City, Journal of Geophysical Research: Atmospheres, 111, D18 305, doi: 10.1029/2006JD007215, 2006.

Weimer, S., Alfarra, M. R., Schreiber, D., Mohr, M., Prévôt, A. S. H., and Baltensperger, U.: Organic aerosol mass spectral signatures from wood-burning emissions: Influence of burning conditions and wood type, Journal of Geophysical Research: Atmospheres, 113, D10 304, doi:10.1029/2007JD009309, 2008.

WHO: Air Quality Guidelines, Global update 2005, Particulate matter, ozone, nitrogen dioxide and sulphur dioxide, World Health Organization European Office, Copenhagen, 2005.

WHO: Urbanization and health, Bulletin of the World Health Organization, 88, 245–246, doi:10.2471/BLT.10.010410, 2010.

WHO: World Health Statistics 2014, World Health Organization, 2014.

Wichmann, H.-E. and Peters, A.: Epidemiological evidence of the effects of ultrafine particle exposure, Philosophical Transactions of the Royal Society of London. Series A: Mathematical, Physical and Engineering Sciences, 358, 2751–2769, doi:10.1098/rsta.2000.0682, 2000.

Wiedensohlet, A., Orsini, D., Covert, D. S., Coffmann, D., Cantrell, W., Havlicek, M., Brechtel, F. J., Russell, L. M., Weber, R. J., Gras, J., Hudson, J. G., and Litchy, M.: Intercomparison Study of the Size-Dependent Counting Efficiency of 26 Condensation Particle Counters, Aerosol Science and Technology, 27, 224–242, doi: 10.1080/02786829708965469, 1997.

Williams, P. I.: Construction and validation of a DMPS for aerosol characterisation, Ph.D. thesis, University of Manchester, 1999.

Williams, P. I., McFiggans, G., and Gallagher, M. W.: Latitudinal aerosol size distribution variation in the Eastern Atlantic Ocean measured aboard the FS-Polarstern, Atmospheric Chemistry and Physics, 7, 2563–2573, doi:10.5194/acp-7-2563-2007, 2007.

Wilson, W. E. and Suh, H. H.: Fine Particles and Coarse Particles: Concentration Relationships Relevant to Epidemiologic Studies, Journal of the Air & Waste Management Association, 47, 1238–1249, doi:10.1080/10473289.1997.10464074, 1997.

Winklmayr, W., Reischl, G., Lindner, A., and Berner, A.: A new electromobility spectrometer for the measurement of aerosol size distributions in the size range from 1 to 1000 nm, Journal of Aerosol Science, 22, 289–296, doi:http://dx.doi.org/10.1016/S0021-8502(05)80007-2, 1991.

Yin, J., Harrison, R. M., Chen, Q., Rutter, A., and Schauer, J. J.: Source apportionment of fine particles at urban background and rural sites in the UK atmosphere, Atmospheric Environment, 44, 841–851, doi:http://dx.doi.org/10.1016/j.atmosenv.2009.11.026, 2010.

Yin, J., Cumberland, S. A., Harrison, R. M., Allan, J., Young, D. E., Williams, P. I., and Coe, H.: Receptor modelling of fine particles in Southern England using CMB including comparison with AMS-PMF factors, Atmospheric Chemistry and Physics Discussions, 14, 24 523–24 572, doi:10.5194/acpd-14-24523-2014, 2014.

Zahardis, J. and Petrucci, G. A.: The oleic acid-ozone heterogeneous reaction system: products, kinetics, secondary chemistry, and atmospheric implications of a model system - a review, Atmospheric Chemistry and Physics, 7, 1237–1274, doi:10.5194/acp-7-1237-2007, 2007.

Zhang, J. K., Sun, Y., Liu, Z. R., Ji, D. S., Hu, B., Liu, Q., and Wang, Y. S.: Characterization of submicron aerosols during a month of serious pollution in Beijing, 2013, Atmospheric Chemistry and Physics, 14, 2887–2903, doi:10.5194/acp-14-2887-2014, 2014.

Zhang, Q., Alfarra, M. R., Worsnop, D. R., Allan, J. D., Coe, H., Canagaratna, M. R., and Jimenez, J. L.: Deconvolution and Quantification of Hydrocarbon-like and Oxygenated Organic Aerosols Based on Aerosol Mass Spectrometry, Environmental Science Technology, 39, 4938–4952, doi:10.1021/es048568l, 2005a.

Zhang, Q., Worsnop, D. R., Canagaratna, M. R., and Jimenez, J. L.: Hydrocarbon-like and oxygenated organic aerosols in Pittsburgh: insights into sources and processes of organic aerosols, Atmospheric Chemistry and Physics, 5, 3289–3311, doi:10.5194/acp-5-3289-2005, 2005b.

Zhang, Q., Jimenez, J. L., Canagaratna, M. R., Allan, J. D., Coe, H., Ulbrich, I., Alfarra, M. R., Takami, A., Middlebrook, A. M., Sun, Y. L., Dzepina, K., Dunlea, E., Docherty, K., DeCarlo, P. F., Salcedo, D., Onasch, T., Jayne, J. T., Miyoshi, T., Shimono, A., Hatakeyama, S., Takegawa, N., Kondo, Y., Schneider, J., Drewnick,

F., Borrmann, S., Weimer, S., Demerjian, K., Williams, P., Bower, K., Bahreini, R., Cottrell, L., Griffin, R. J., Rautiainen, J., Sun, J. Y., Zhang, Y. M., and Worsnop, D. R.: Ubiquity and dominance of oxygenated species in organic aerosols in anthropogenically-influenced Northern Hemisphere midlatitudes, Geophysical Research Letters, 34, L13 801, doi:10.1029/2007GL029979, 2007.

Zhang, Q., Gangupomu, R. H., Ramirez, D., and Zhu, Y.: Measurement of ultrafine particles and other air pollutants emitted by cooking activities, International journal of environmental research and public health, 7, 1744–1759, doi:10.3390/ijerph7041744, 2010.

Zhang, X., Smith, K. A., Worsnop, D. R., Jimenez, J., Jayne, J. T., and Kolb, C. E.: A Numerical Characterization of Particle Beam Collimation by an Aerodynamic Lens-Nozzle System: Part I. An Individual Lens or Nozzle, Aerosol Science and Technology, 36, 617–631, doi:10.1080/02786820252883856, 2002.

Zhang, X., Smith, K. A., Worsnop, D. R., Jimenez, J. L., Jayne, J. T., Kolb, C. E., Morris, J., and Davidovits, P.: Numerical Characterization of Particle Beam Collimation: Part II Integrated Aerodynamic-LensNozzle System, Aerosol Science and Technology, 38, 619–638, doi:10.1080/02786820490479833, 2004.

Zheng, M., Cass, G. R., Schauer, J. J., and Edgerton, E. S.: Source Apportionment of $PM_{2.5}$ in the Southeastern United States Using Solvent-Extractable Organic Compounds as Tracers, Environmental Science & Technology, 36, 2361–2371, doi:10.1021/es011275x, 2002.